

A Nuclear Magnetic Resonance Study of the
Methoxy Group Conformation in Some 2-Fluoroanisoles and
of the Acetyl Group Conformation in Some 2-Fluoroacetophenones

by

Timothy A. Wildman

A Thesis Submitted to
The Faculty of Graduate Studies
of the University of Manitoba
in partial fulfillment of
the requirements of the degree
Doctor of Philosophy

Winnipeg, Manitoba

July, 1982

A NUCLEAR MAGNETIC RESONANCE STUDY OF THE
METHOXY GROUP CONFORMATION IN SOME 2-FLUORANISOLES AND
OF THE ACETYL GROUP CONFORMATION IN SOME 2-FLUOROACETOPHENONES

BY

TIMOTHY A. WILDMAN

A thesis submitted to the Faculty of Graduate Studies of
the University of Manitoba in partial fulfillment of the requirements
of the degree of

DOCTOR OF PHILOSOPHY

© 1982

Permission has been granted to the LIBRARY OF THE UNIVER-
SITY OF MANITOBA to lend or sell copies of this thesis, to
the NATIONAL LIBRARY OF CANADA to microfilm this
thesis and to lend or sell copies of the film, and UNIVERSITY
MICROFILMS to publish an abstract of this thesis.

The author reserves other publication rights, and neither the
thesis nor extensive extracts from it may be printed or other-
wise reproduced without the author's written permission.

Abstract

Proton, carbon, and fluorine nuclear magnetic resonance spectroscopy have been used to investigate the conformational preferences of the methoxy group in anisole, 2-fluoroanisole, 4-bromo-2-fluoroanisole, 4,6-dibromo-2-fluoroanisole, and 2,3,5,6-tetrafluoroanisole, and of the acetyl group in 2-fluoroacetophenone and 2,6-difluoroacetophenone, all in isotropic solution. Ab initio molecular orbital calculations with partial geometry optimization at the STO-3G level and INDO MO FPT calculations have been performed for anisole, 2-fluoroanisole, and 2-fluoroacetophenone.

On the basis of the molecular orbital calculations, spin-spin coupling constants, chemical shifts, and methyl carbon spin-lattice relaxation times, those compounds with only one or no substituent ortho to the side chain prefer coplanarity of all heavy atoms. The interdependence of internal motions makes barrier determinations difficult. Calculations suggest that the two-fold component of the barrier to methoxy group rotation is about $5.7 \text{ kJ}\cdot\text{mol}^{-1}$ in anisole, and that the four-fold component is not negligible. There is a strong preference for the trans conformation of 2-fluoroanisole and this increases somewhat upon 4-bromination. These tendencies reflect the degree of conjugation between the aromatic ring

and the methoxy group, and the steric interaction of the methyl group with ortho substituents. The two-fold component of the barrier to acetyl group rotation is high in 2-fluoroacetophenone, which prefers the 0-anti conformation.

When halogens occupy both positions ortho to the side chain, non-planar conformations are populated appreciably. This is particularly evident for 4,6-dibromo-2-fluoroanisole.

Long-range spin-spin coupling constants between the methyl carbon and ring carbons or ring protons provide qualitative conformational information, but suggest that quantitative relationships similar to those for analogous proton-proton coupling constants may be realized. The relative signs of ${}^5J_m^{C\alpha,H3}$ and ${}^5J_m^{C\alpha,H5}$ in 4,6-dibromo-2-fluoroanisole and of ${}^4J_o^{C\alpha,H6}$ in 2-fluoroacetophenone are positive according to weak irradiation (tickling) experiments.

An investigation of the nature of the proximate couplings ${}^5J_o^{CH_3,F}$ and ${}^4J_o^{C\alpha,F}$, which carry positive signs, suggests that both depend principally on the interactions between the methyl hydrogens and fluorine and between the methyl carbon and fluorine. Attempts are made to describe the angle dependence of these proximate coupling constants by INDO MO FPT calculations and by analyzing the temperature dependence of ${}^5J_o^{CH_3,F}$ and of ${}^4J_o^{C\alpha,F}$ in 2-fluoroacetophenone.

To my mother,
M. June Wildman

Acknowledgements

I thank Professor Ted Schaefer for his help, encouragement, and criticism. Over the course of this work he has guided me and allowed me the freedom to pursue answers to some questions of my own. I am grateful for the time I have spent in his laboratory.

I thank Professor Frank Hruska for access to the Bruker WH-90 DS spectrometer, without which this work could not have been performed. I also appreciate the technical artistry of Kirk Marat, who has helped me a great deal. Dr. Reino Laatikainen very kindly provided the computer programs TERMO and FINDO, which were used in part of this work. I thank Professor Rod Wasylshen for some useful criticisms of a draft of this thesis, and for allowing me access to the Varian CFT-20 spectrometer for two proton relaxation experiments at the Department of Chemistry, University of Winnipeg.

I am grateful for many helpful and engaging conversations with Rudy Sebastian, Dr. Reino Laatikainen, Kirk Marat, Professor Frank Hruska, Wayne Blonski, Professor Rod Wasylshen, and (by no means least) Kathleen Gough.

The love and understanding of my mother has been a great help to me in the course of my studies. I thank her affectionately.

I thank Kathy for her support and understanding, particularly during the writing of this thesis.

I am grateful to Donna Harris for her skillful typing of these pages, and to Kathy for help with proof-reading.

Finally, the financial support of the Natural Sciences and Engineering Research Council of Canada and of the University of Manitoba is much appreciated.

List of Publications

1. H. D. Gesser, T. A. Wildman, and Y. B. Tewari (1977)
"Photooxidation of n-hexadecane sensitized by xanthone."
Environ. Sci. Techn. 11, 605.
2. T. Schaefer and T. A. Wildman (1979) "Comparison of the
intramolecular hydrogen bonds and of the internal barrier
to rotation of the hydroxyl and sulfhydryl groups in 2-
methoxyphenol and 2-methoxythiophenol." Can. J. Chem.
57, 1881.
3. T. Schaefer, W. Niemczura, W. Danchura, and T. A. Wildman
(1979) "Derivatives of diphenylmethane. Preferred con-
formations and barriers to internal rotation by the J
method." Can. J. Chem. 57, 1881.
4. T. Schaefer, S. R. Salman, and T. A. Wildman (1979) "An
example of the tilt effect in homonuclear double reson-
ance. Interference with relative sign determination in
weak irradiation experiments." J. Magn. Reson. 36, 435.
5. T. Schaefer, R. Sebastian, and T. A. Wildman (1979) "The
allyl and benzyl groups as hydrogen bond acceptors in
derivatives of 2-allylphenol and 2-benzylphenol." Can.
J. Chem. 57, 3005.
6. T. Schaefer, T. A. Wildman, and S. R. Salman (1980) "The
perpendicular conformation of 2-hydroxythiophenol.
Intramolecular hydrogen bonding to a specific lone pair."
J. Am. Chem. Soc. 102, 107.

7. T. Schaefer, S. R. Salman, and T. A. Wildman (1980) "Theoretical and experimental conformational preferences of the aldehyde and fluoroaldehyde groups in 2-methylbenzaldehyde, 2-trifluoromethylbenzaldehyde, and 4-chloro-2-methylbenzoyl fluoride." *Can. J. Chem.* 58, 2364.
8. T. A. Wildman (1980) "Conformational analysis and the quantum mechanical picture of internal rotation in molecules." *Chem. Phys. Lett.* 75, 383; erratum 80, 210.
9. T. Schaefer, B. A. Addison, R. Sebastian, and T. A. Wildman (1981) "Orientations of the hydroxyl and isopropyl groups in cis and trans conformers of 2-isopropylphenol and 2-isopropyl-6-methylphenol." *Can. J. Chem.* 59, 1656.
10. T. Schaefer and T. A. Wildman (1981) "The sulfhydryl groups in 4-amino and 4-methoxythiophenol prefer the plane normal to the molecular frame." *Chem. Phys. Lett.* 80, 280.
11. T. Schaefer, R. Sebastian, and T. A. Wildman (1981) "Information from stereospecific spin-spin couplings about the relative absorptivities of the hydroxyl stretching bands in 2-iodophenol solutions." *Can. J. Chem.* 59, 3021.
12. T. Schaefer, S. R. Salman, T. A. Wildman, and P. D. Clark (1982) "Conformational consequences of intramolecular hydrogen bonding by OH to the directional lone-pair of the sulfur in derivatives of methyl phenyl sulfide, diphenyl sulfide, and diphenyl disulfide." *Can. J. Chem.* 60, 342.

13. T. Schaefer, T. A. Wildman, and R. Sebastian (1982)
"STO-3G MO calculations on structures and internal rotational barrier of phenol, benzoyl X (X = H, F, CH₃, CN, OCH₃), acetyl fluoride, acetyl cyanide, and carbonyl cyanide." J. Mol. Struct. (Theochem) in press.
14. T. Schaefer, T. A. Wildman, and R. Sebastian (1982) "The rotational angle dependence of $^5J_{m}^{H,SH}$ in benzenethiol." Can. J. Chem. 60, 1924.
15. T. Schaefer, R. Sebastian, T. A. Wildman and H. Dettman (1982) "Spin-spin coupling constants as indicators of non-planarity of anthrone in solution." Can. J. Chem. in press.

Timothy A. Wildman attended the sixth Waterloo Summer School on Nuclear Magnetic Resonance in Biology, Physical Chemistry and Physics in June of 1979.

But as for certain truth, no man has known it,
Nor will he know it; neither of the gods,
Nor yet of all the things of which I speak.
And even if by chance he were to utter
The final truth, he would himself not know it:
For all is but a woven web of guesses.

Xenophanes

I cannot give any scientist of any age better advice than this:
the intensity of the conviction that a hypothesis is true has
no bearing on whether it is true or not.

Sir Peter Medawar

Experience is the name every one gives to their mistakes.

Oscar Wilde

Our whole problem is to make the mistakes as fast as possible.

John Archibald Wheeler

Table of Contents

	Page
List of Figures	xvii
List of Tables	xxiii
Chapter	
1 Introduction	1
A. Conformational Analysis of Phenol and Thiophenol	3
B. Anisole	5
i) near-ultraviolet absorption spectroscopy	6
ii) dipole moments, Kerr constants, and dielectric relaxation	8
iii) microwave spectroscopy	11
iv) infrared and Raman spectroscopy	13
v) diffraction techniques	18
vi) photoelectron spectroscopy	21
vii) electron spin resonance	25
viii) nuclear magnetic resonance	27
a) carbon chemical shifts	28
b) carbon and hydrogen spin-lattice relaxation	36
c) molecules oriented in a nematic phase	39
d) proton chemical shifts	41

Chapter	Page
e) long-range proton-proton spin-spin coupling to methoxy protons	43
C. Acetophenone	46
i) near-ultraviolet absorption spectroscopy	47
ii) dipole moments, Kerr constants, and dielectric relaxation	49
iii) infrared absorption spectroscopy	52
iv) X-ray diffraction	54
v) electron spin resonance	55
vi) nuclear magnetic resonance	56
a) carbon chemical shifts	57
b) proton chemical shifts	59
c) molecules oriented in a nematic phase	60
d) long-range proton-proton spin-spin coupling to acetyl protons	61
D. Proximate Proton-Proton and Proton-Fluorine Spin-Spin Coupling	62
2 Introduction to the Problem	67
3 Experimental Method	69
A. Materials	70
i) bromination of 2-fluorophenol	71
ii) methylation of phenolic hydroxyl groups	72

Chapter	Page
iii) preparation of 2-fluoroacetophenone	73
B. Sample Preparation	74
C. Spectroscopic Method	75
i) low temperature experiments	77
ii) nuclear spin-lattice relaxation experiments	78
iii) methyl carbon nuclear Overhauser enhancement experiments	79
D. Computations	80
4 Experimental Results	81
A. High-resolution Spectra	81
i) anisole	84
ii) 2-fluoroanisole	88
iii) 4-bromo-2-fluoroanisole	97
a) determination of the relative sign of $^5J_{\text{O}}^{\text{CH}_3, \text{F}}$ by weak irradiation experiments	107
b) the relative sign of $^4J_{\text{O}}^{\text{C}\alpha, \text{F}}$	110
iv) 4,6-dibromo-2-fluoroanisole	113
a) determination of the relative sign of $^4J_{\text{O}}^{\text{C}\alpha, \text{F}}$	125
b) determination of the relative sign of $^5J_{\text{O}}^{\text{CH}_3, \text{F}}$ by weak irradiation experiments	125

Chapter	Page
<ul style="list-style-type: none"> c) determination of the relative signs of $^5J_{\text{m}}^{\text{C}\alpha,\text{H}3}$ and $^5J_{\text{m}}^{\text{C}\alpha,\text{H}5}$ by weak irradiation experiments 	130
v) 2,3,5,6-tetrafluoroanisole	133
vi) 2-fluoroacetophenone	142
<ul style="list-style-type: none"> a) determination of the relative sign of $^4J_{\text{O}}^{\text{C}\alpha,\text{F}}$ by weak irradiation experiments 	149
<ul style="list-style-type: none"> b) determination of the relative sign of $^5J_{\text{O}}^{\text{CH}_3,\text{F}}$ by weak irradiation experiments 	149
<ul style="list-style-type: none"> c) determination of the relative sign of $^4J_{\text{O}}^{\text{C}\alpha,\text{H}6}$ by weak irradiation experiments 	149
vii) 2,6-difluoroacetophenone	157
viii) α,α,α -trifluoroacetophenone	162
B. Low Temperature Spectra	166
<ul style="list-style-type: none"> i) 4,6-dibromo-2-fluoroanisole 	167
<ul style="list-style-type: none"> ii) 2,3,5,6-tetrafluoroanisole 	169
<ul style="list-style-type: none"> iii) 2-fluoroacetophenone 	171
<ul style="list-style-type: none"> iv) 2,6-difluoroacetophenone 	173
<ul style="list-style-type: none"> v) α,α,α-trifluoroacetophenone 	175
C. Nuclear Spin-Lattice Relaxation Experiments	177
<ul style="list-style-type: none"> i) methyl carbon nuclei 	178

Chapter		Page
	ii) fluorine nuclei	182
5	Discussion	184
	A. Anisole	
	i) ab initio molecular orbital calculations	186
	ii) semi-empirical molecular orbital calculations	198
	iii) carbon chemical shifts	214
	iv) coupling constants	218
	B. 2-Fluoroanisole	
	i) ab initio molecular orbital calculations	219
	ii) semi-empirical molecular orbital calculations	226
	iii) carbon spectrum	243
	iv) long-range coupling to methyl protons	245
	C. 4-Bromo-2-fluoroanisole	
	i) proton spectrum	246
	ii) carbon spectrum	248
	D. 4,6-Dibromo-2-fluoroanisole	
	i) proton spectrum	250
	ii) carbon spectrum	252
	iii) fluorine spectrum	257
	E. 2,3,5,6-Tetrafluoroanisole	
	i) proton spectrum	258

Chapter	Page
ii) fluorine spectrum	260
iii) methyl proton chemical shifts	261
F. 2-Fluoroacetophenone	
i) ab initio molecular orbital calculations	262
ii) semi-empirical molecular orbital calculations	268
iii) proton spectrum	277
iv) carbon spectrum	279
G. 2,6-Difluoroacetophenone	284
H. α,α,α -Trifluoroacetophenone	285
I. Temperature Dependences of ${}^5J_{\text{O}}^{\text{CH}_3,\text{F}}$ and ${}^4J_{\text{O}}^{\text{C}\alpha,\text{F}}$	286
i) 4,6-dibromo-2-fluoroanisole	289
ii) 2,3,5,6-tetrafluoroanisole	292
iii) 2-fluoroacetophenone	295
iv) 2,6-difluoroacetophenone	308
v) α,α,α -trifluoroacetophenone	312
J. Methyl Carbon Chemical Shifts	315
K. Methyl Carbon Spin-Lattice Relaxation Times	
i) theoretical considerations	317
ii) measured relaxation times	319

Chapter		Page
6	Summary and Conclusions	322
	References	329
	Appendix	351

List of Figures

Figure		Page
1	Methoxy substituent-induced chemical shifts for anisole, 2-methylanisole, and 1,2-dimethoxybenzene.	31
2	A conformation of <i>o</i> -xylene in which the methyl protons in the ring plane are coupled substantially over 320 pm.	64
3	Spectrum of the ring protons of a 4.83 mole % solution of 2-fluoroanisole in acetone-d ₆ .	90
4	Spectrum of the methyl protons of a 4.83 mole % solution of 2-fluoroanisole in acetone-d ₆ .	92
5	Spectrum of the ring protons of a 2.96 mole % solution of 4-bromo-2-fluoroanisole- α - ¹³ C in acetone-d ₆ .	99
6	Spectrum of the ring carbons of a 14.0 mole % solution of 4-bromo-2-fluoroanisole- α - ¹³ C in acetone-d ₆ .	104
7	A first-order representation of the line spectrum of the methyl protons, of the methyl carbon, and of parts of the multiplets due to H6 of 4-bromo-2-fluoroanisole.	109
8	Spectrum of H6 and of the low-field multiplet of the methyl protons of 4-bromo-2-fluoroanisole.	112

Figure		Page
9	Spectrum of the ring protons of a 15.5 mole % solution of 4,6-dibromo-2-fluoroanisole- α - ^{13}C in acetone- d_6 at 100 MHz.	117
10	Fluorine spectrum of a 15.5 mole % solution of 4,6-dibromo-2-fluoroanisole- α - ^{13}C in acetone- d_6	119
11	Spectrum of the ring carbons of a 15.5 mole % solution of 4,6-dibromo-2-fluoroanisole- α - ^{13}C in acetone- d_6 in the presence of strong irradiation (decoupling) of protons.	124
12	A first-order representation of the line spectrum of the methyl protons, of the fluorine and of the methyl carbon of 4,6-dibromo-2-fluoroanisole.	127
13	Spectra of the methyl carbon of a 15.5 mole % solution of 4,6-dibromo-2-fluoroanisole- α - ^{13}C in acetone- d_6 .	129
14	A first-order representation of the line spectrum of H3 and H5 of 4,6-dibromo-2-fluoroanisole.	132
15	Proton spectrum of a 4.70 mole % solution of 2,3,5,6-tetrafluoroanisole in acetone- d_6 .	135
16	Fluorine spectrum of a 4.70 mole % solution of 2,3,5,6-tetrafluoroanisole in acetone- d_6 .	138
17	Spectrum of the ring of a 5.35 mole % solution of 2-fluoroacetophenone in acetone- d_6 .	146

Figure		Page
18	A first-order representation of the line spectrum of the methyl protons, of the fluorine, and of the methyl carbon of 2-fluoroacetophenone.	151
19	Spectra of the methyl carbon of a 4.94 mole % solution of 2-fluoroacetophenone- α - ^{13}C in acetone- d_6 .	153
20	A first-order representation of the line spectrum of H5 and H6 of 2-fluoroacetophenone.	156
21	Spectrum of the ring protons of a solution of ca 3 mole % 2,6-difluoroacetophenone in acetone- d_6 .	159
22	Spectrum of the methyl fluorines of a 47.6 mole % solution of α,α,α -trifluoromethylacetophenone in acetone- d_6 .	164
23	A planar conformation of anisole.	190
24	A plot of the relative energies of some conformations of anisole from partially-optimized molecular orbital calculations at the STO-3G level.	193
25	A plot of the relative energies of some conformations of anisole from INDO molecular orbital calculations.	201
26	A plot of the angle dependence of $n_{\text{J}}^{\text{C}\alpha,\text{C}\text{i}}$ ($n = 2-5$; $i = 1-4$) for anisole from INDO MO FPT	206

Figure		Page
	calculations.	
27	A plot of the angle dependence of ${}^5J_{\text{C}\alpha,\text{H}i}$ ($n = 4-6$; $i = 2-4$) for anisole from INDO MO FPT calculations	208
28	A plot of the angle dependence of ${}^5J_{\text{O}}^{\text{H},\text{CH}_3}$ and the contributions of certain interactions to it according to INDO MO FPT calculations	212
29	A plot of chemical shift for ring carbons versus atomic charges calculated at the STO- 3G level	215
30	A plot of the relative energies of some confor- mations of 2-fluoroanisole from partially- optimized molecular orbital calculations at the STO-3G level and from INDO molecular orbital calculations	223
31	A plot of the angle dependence of ${}^nJ_{\text{C}\alpha,\text{C}i}$ ($n =$ $2-5$; $i = 1-6$) for 2-fluoroanisole from INDO MO FPT calculations	232
32	A plot of the angle dependence of ${}^nJ_{\text{C}\alpha,\text{H}i}$ ($n =$ $4-6$; $i = 3-6$) for 2-fluoroanisole from INDO MO FPT calculations	234
33	A plot of the angle dependence of ${}^5J_{\text{O}}^{\text{CH}_3,\text{F}}$ in 2-fluoroanisole when certain Fock elements are	

Figure		Page
	kept zero throughout the INDO MO FPT calculations	238
34	A plot of the angle dependence of ${}^4J_{\text{O}}^{\text{C}\alpha,\text{F}}$ in 2-fluoroanisole when certain Fock elements are kept zero throughout the INDO MO FPT calculations	240
35	An <u>0-anti</u> conformation of 2-fluoroacetophenone	265
36	A plot of the angle dependence of ${}^5J_{\text{O}}^{\text{CH}_3,\text{F}}$ in 2-fluoroacetophenone when certain Fock elements are kept zero throughout the INDO MO FPT calculations	273
37	A plot of the angle dependence of ${}^4J_{\text{O}}^{\text{C}\alpha,\text{F}}$ in 2-fluoroacetophenone when certain Fock elements are kept zero throughout the INDO MO FPT calculations	275
38	A plot of chemical shift for ring carbons versus π -charges calculated at the STO-3G level	281
39	A plot of the temperature dependence of ${}^5J_{\text{O}}^{\text{CH}_3,\text{F}}$ and of ν_{CH_3} for 2,4-dibromo-6- fluoroanisole- α - ${}^{13}\text{C}$	291
40	A plot of the temperature dependence of ${}^5J_{\text{O}}^{\text{CH}_3,\text{F}}$ and of ν_{CH_3} for 2,3,5,6-tetra- fluoroanisole	294

Figure		Page
41	A plot of the temperature dependence of $^5J_{\text{O}}^{\text{CH}_3, \text{F}}$ for 2-fluoroacetophenone- α - ^{13}C	297
42	A plot of the angle dependence of the methyl proton-fluorine spin-spin coupling constant inferred from the temperature dependence of $^5J_{\text{O}}^{\text{CH}_3, \text{F}}$ for 2-fluoroacetophenone	301
43	A plot of the temperature dependence of $^4J_{\text{O}}^{\text{C}\alpha, \text{F}}$ for 2-fluoroacetophenone- α - ^{13}C	305
44	A plot of the angle dependence of the methyl carbon-fluorine spin-spin coupling constant inferred from the temperature dependence of $^4J_{\text{O}}^{\text{C}\alpha, \text{F}}$ for 2-fluoroacetophenone	307
45	A plot of the temperature dependence of $^5J_{\text{O}}^{\text{CH}_3, \text{F}}$ and of ν_{CH_3} for 2,6-difluoroacetophenone	310
46	A plot of the temperature dependence of $^5J_{\text{O}}^{\text{CF}_3, \text{H}}$ for α, α, α -trifluoroacetophenone	313

List of Tables

Table		Page
1	Carbon Chemical Shifts and Coupling Constants for Anisole in Acetone-d ₆	85
2	Parameters from the Proton Spectrum of 2- Fluoroanisole	93
3	Carbon Chemical Shifts and Carbon-Fluorine Coupling Constants for 2-Fluoroanisole in Acetone-d ₆	96
4	Parameters from the Proton Spectrum of 4- Bromo-2-fluoroanisole	100
5	Carbon Chemical Shifts and Coupling Constants for 4-Bromo-2-fluoroanisole	105
6	Parameters from the Proton Spectrum of 4,6- Dibromo-2-fluoroanisole	114
7	Carbon Chemical Shifts and Coupling Constants for 4,6-Dibromo-2-fluoroanisole in Acetone-d ₆	121
8	Parameters from the Proton Spectrum of 2,3,5,6-Tetrafluoroanisole in Acetone-d ₆	136
9	Parameters from the Fluorine Spectrum of 2,3,5,6-Tetrafluoroanisole in Acetone-d ₆	140
10	Parameters from the Proton Spectrum of 2- Fluoroacetophenone in Acetone-d ₆	143
11	Carbon Chemical Shifts and Some Coupling Constants	

Table	Page
	147
12	160
13	165
14	168
15	170
16	172
17	174
18	176
19	179

Table		Page
20	Fluorine Chemical Shifts and Relaxation Rate Parameters for Some Anisoles and Acetophenones	183
21	Some Results of Partial Geometry Optimization in STO-3G Calculations for Anisole	187
22	Atomic and π -Charges for Anisole from STO-3G Calculations with Partial Geometry Optimization	197
23	Carbon-Carbon Spin-Spin Coupling Constants Relative Energy, and Dipole Moment for Some Conformations of Anisole from INDO MO FPT Calculations	199
24	Carbon-Proton Spin-Spin Coupling Constants for Some Conformations of Anisole from INDO MO FPT Calculations	202
25	Spin-Spin Coupling Constants Involving Methyl Protons and Ring Nuclei for Planar Anisole from Semi-empirical Molecular Orbital Calculations	204
26	Some Results of Partial Geometry Optimization in STO-3G Calculations for 2-Fluoroanisole	220
27	Atomic and π -Charges for 2-Fluoroanisole from STO-3G Calculations with Partial Geometry Optimization	225
28	Carbon-Carbon Spin-Spin Coupling Constants, Relative Energy, and Dipole Moment for Some	

Table	Page
Conformations of 2-Fluoroanisole from INDO MO FPT Calculations	227
29 Carbon-Proton Spin-Spin Coupling Constants for Some Conformations of 2-Fluoroanisole from INDO MO FPT Calculations	229
30 Some Spin-Spin Coupling Constants for 2-Fluoro- anisole from INDO MO FPT Calculations	236
31 Some Carbon-Proton Spin-Spin Coupling Constants Between Ring Nuclei for Benzene and Some Anisoles	254
32 Some Results of Partial Geometry Optimization in STO-3G Calculations for 2-Fluoroacetophenone	263
33 Atomic and π -Charges for 2-Fluoroacetophenone from STO-3G Calculations with Partial Geometry Optimization	267
34 Some Spin-Spin Coupling Constants, Relative Energy, and Dipole Moment for Some Conformations of 2- Fluoroacetophenone from INDO MO FPT Calculations	269
35 Some Spin-Spin Coupling Constants for 2-Fluoro- acetophenone from INDO MO FPT Calculations	270

Chapter 1
Introduction

Conformational analysis of anisoles and acetophenones has received much attention. Physical methods which relate bulk properties to molecular properties usually provide only qualitative information. Spectroscopic techniques yield molecular parameters, albeit average properties of the ensemble.

Nuclear magnetic resonance spectroscopy (nmr) has been applied to the study of anisoles and acetophenones, but most of these studies have been concerned with the interpretation of chemical shifts. Spin-spin coupling constants have not been used widely since the numbers are usually small and the form and mechanism of the coupling is not well understood. For other molecules and functional groups, coupling constants have been useful conformational indicators.

This thesis describes nuclear magnetic resonance studies of some fluoroanisoles and fluoroacetophenones concerned with the conformational behaviour of the methoxy and acetyl groups, and with the reflection of this behaviour in the nuclear magnetic resonance parameters.

The reader is referred to standard monographs for a description of the theory of the nmr experiment and spectral analysis¹⁻⁸.

The present chapter contains some brief, introductory remarks on the conformation of phenol and thiophenol, which are structurally more simple than, but similar to, anisole; a review of the conformational studies on anisole and acetophenone; and an introduction to proximate spin-spin coupling.

A. Conformational Analysis of Phenol and Thiophenol

Hermans has written that conformational analysis began with van't Hoff shortly after the enunciation of the van't Hoff-Le Bel hypothesis in 1874⁹. According to Orville-Thomas the word "conformation", meaning one of the manifold shapes which a molecule may adopt by rotation about single bonds, was introduced by Haworth in 1929¹⁰. Conformational analysis began in earnest after seminal papers by Hassel¹¹ and Barton¹² appeared. "The basic premise underlying conformational analysis is that the chemical and physical properties of compounds are closely related to preferred conformations."¹⁰ The relative orientations about a given bond are described usually by specifying a torsion (dihedral, or twist) angle ϕ ¹³. Klyne and Prelog made suggestions to make such descriptions systematic¹⁴.

In at least some circumstances the dihedral angle concept is limited by the fact that the conformational behaviour results in an average^{15,16,89}. Apparently this average may be treated classically in many cases, without recognition of a dependence on the reduced moment of inertia about the rotation axis^{17,18}.

The following example provides an illustration of this picture. The hydroxyl group in phenol prefers to lie in the plane of the aromatic ring¹⁹⁻²³. The two-fold barrier to internal rotation is $14.5 \text{ kJ}\cdot\text{mol}^{-1}$ for a potential of the form

$$V(\phi) = V_2 \sin^2 \phi \quad \text{Eq. (1)}$$

which reflects the change in conjugation between oxygen and the ring π -system. Two-fold barriers in thiophenol ($3.4 \text{ kJ}\cdot\text{mol}^{-1}$)^{24,25} and selenophenol ($1.5 \pm 1.0 \text{ kJ}\cdot\text{mol}^{-1}$)²⁶ are estimated by the J method²⁷. The relatively low barrier in thiophenol allowed study of its dependence on substitution at the para position^{24,25,28,29}. These numbers decrease in the order $\text{NO}_2 > \text{Br} > \text{Cl} > \text{H} > \text{CH}_3 > \text{F} > \text{OCH}_3 > \text{NH}_2$ with the latter two compounds preferring the sulphydryl group in the plane perpendicular to the ring plane. Evidently, the decreasing importance of conjugation between sulphur and the ring π -system is related to the electron demand of the para substituent. The nature of the sulphur 3p lone-pair is such that an ortho hydroxyl group will form a hydrogen bond with it specifically and twist the sulphydryl group out of the ring plane^{30,31}.

B. Anisole

This section contains a summary of experimental investigations of the methoxy group conformation in anisole and some of its derivatives. The conformational behaviour is adduced and, thereby, the factors which control conformation are illustrated.

i) near-ultraviolet absorption spectroscopy

From comparison of the spectra of near-ultraviolet absorptions of solutions of ortho-, meta-, and para-substituted phenols and the corresponding anisoles in ethanol, Burawoy and Chamberlain deduced that comparable hypsochromic shifts of the π - π^* band maximum occur upon O-methylation³². However, when both ortho positions were occupied much larger hypsochromic shifts were observed, presumably the result of decreased conjugation between the oxygen lone pairs and the π -system. It was proposed that while the methoxy group may evade steric interactions with a single ortho substituent by adopting the trans conformation, substitution at both positions forces the methoxy group to lie preferentially out of the plane of the aromatic ring.

Hart and Wagner supported this conclusion by reporting a marked hypsochromic shift between band maxima for anisole and t-butoxybenzene³³. Consistent also was the bathochromic shift between anisole and 2-methylcoumaran, in which the rotation about the ring carbon-oxygen bond is constrained. A monotonic decrease in the wavelength of the absorption maximum was observed for a series of heterocycles in which increasing pucker forces the aliphatic carbon bound to oxygen out of the plane of the aromatic ring.

Dearden and Forbes³⁴ and Frolen and Goodman³⁵ adhered to

this view. The latter indicated that the effective twist angle of the methoxy group increases in the following series: anisole; 2-methylanisole; 2,6-dimethylanisole; and 2,3,5,6-tetramethylanisole.

While these analyses can not provide more than a qualitative description of the conformational preference of the methoxy group, consistent behaviour is observed.

ii) dipole moments, Kerr constants, and dielectric relaxation

From comparisons of measured and calculated dipole moments, several authors have indicated that either the methoxy substituent on an aromatic ring does not lie in the ring plane or is not fixed rigidly therein³⁶⁻³⁸. LeFèvre and co-workers inferred from dipole moment and molar Kerr constant measurements that the effective conformation of anisole in carbon tetrachloride solution has a methoxy group twists angle of about 20°, possibly due to steric interactions with ortho hydrogens³⁹. Similar results were obtained if a chlorine, bromine, iodine, or methyl substituent occupied the para position, but 4-nitroanisole and 4-cyanoanisole were virtually planar⁴⁰. Bredikhin, Kostin, Vul'fson, and Vereshchagin obtained agreement between the measured Kerr constants for anisole, 4-chloroanisole, and 4-bromoanisole and the numbers calculated for planar conformers⁴¹.

In the dielectric relaxation behaviour of anisole, Smith and co-workers,^{42,43} and Klages and Kraus,⁴⁴ found evidence of two contributions to the total orientation polarization: one from molecular reorientation and a small one from hindered methoxy group rotation. According to the temperature dependence of the latter relaxation time, the enthalpy of activation for the rotation was about 6 kJ·mol⁻¹ in solution⁴³. Mazid, Shukla, and Walker stated that the relaxation for 1,3-dimethoxybenzene

dispersed in a polystyrene matrix is due principally to methoxy group rotation, the activation enthalpy being about $10 \text{ kJ}\cdot\text{mol}^{-1}$ as for 3,3'-dimethylbiphenyl; 1,7-dimethoxynaphthalene; and 3,5-dimethylanisole⁴⁵. For 2,4,6-tribromoanisole the enthalpy increased to $16 \text{ kJ}\cdot\text{mol}^{-1}$ due to steric or conjugative effects of the bromine substituents.

Dipole moment comparisons for ortho-haloanisoles led Anzilotti and Curran to conclude that methoxy groups prefer to lie entirely trans to bromine, chlorine, and (likely) fluorine substituents⁴⁶. Similar comparisons convinced Lumbroso, Curé, and Andrieu that 2-chloroanisole, 2,4-dichloroanisole, and the sulphur analogues exist predominantly as the trans conformation and to the exclusion of the hindered cis form⁴⁷. The methoxy group lies trans in 2-t-butyl-5-bromoanisole, but may be rotated out of the ring plane by 29° according to the dipole moments measurements of Allinger, Maul, and Hickey⁴⁸.

Molar Kerr constants indicated that the methoxy group prefers to lie effectively perpendicular to the ring plane when methyl, chlorine, or bromine occupies the 2,4, and 6 positions⁴⁰.

These techniques put forward a consistent picture of conjugational and steric influences on methoxy group conformation, but lend themselves to situations in which a clear distinction exists between possible outcomes. For example, since the dipole

moment of the unpopular cis form of 2-haloanisoles is less than that of the trans, small populations of the cis form may be concealed. Or the preference for a planar conformation may be masked by rotations which yield an effective twist angle which is non-zero³⁷. Consequently this may be interpreted as a preference for a non-planar conformation^{39,48} (see the preceding section A).

iii) microwave spectroscopy

Lister has made extensive studies of the microwave spectrum of 4-fluoroanisole, which was chosen because the a-component of the electric dipole moment is larger than that of anisole itself^{49,50}. The interpretation of the spectrum of the ground and first excited torsional states favoured an exactly planar preferred conformation and a fairly high barrier to rotation of the methoxy group, but Lister and Owen could not exclude the possibility of non-planar relative minima. The three-fold barrier to methyl group rotation was at least $7 \text{ kJ}\cdot\text{mol}^{-1}$, in rough agreement with the values for cis-methyl nitrite⁵¹ ($8.7 \text{ kJ}\cdot\text{mol}^{-1}$) and methyl vinyl ether⁵² ($16.1 \text{ kJ}\cdot\text{mol}^{-1}$).

In a study which included the six lowest torsional states, Lister concluded that the barrier to methoxy group rotation is at least $4.6 \text{ kJ}\cdot\text{mol}^{-1}$ ⁵⁰. Since the concentration of a second rotamer is less than 20% at 273 K the energy difference between the planar form and a hypothetical second minimum in the rotational potential was shown to be greater than $3.6 \text{ kJ}\cdot\text{mol}^{-1}$.

A function of the form

$$V(\phi) = \frac{V_2}{2} (1 - \cos 2\phi) + \frac{V_4}{2} (1 - \cos 4\phi) \quad \text{Eq. (2)}$$

with a reasonably large value for V_4 was proposed to describe the rotation.

Steinmetz interpreted the low-resolution microwave spectrum

of 4-methoxybenzaldehyde as indicative of planar and non-planar conformations, but found only planar forms for 3-methoxybenzaldehyde⁵³. No explanation for the apparent difference in behaviour was provided. Bohn and coworkers reinterpreted low-resolution microwave spectra as providing direct observation of free rotator states^{54,55}. Barriers to methoxy group rotation for 4-methoxybenzaldehyde, 4-methoxybenzoyl fluoride, and 4-methoxybenzoyl chloride were found to be $2.1 \pm 0.8 \text{ kJ}\cdot\text{mol}^{-1}$, a value which was also proposed for anisole and 4-fluoroanisole⁵⁵. Lister termed these results incompatible with the microwave spectrum⁵⁰.

The relative intensities of two band series in the low-resolution microwave spectrum of 4-fluorothioanisole suggested an energy difference of $3.0 \pm 1.0 \text{ kJ}\cdot\text{mol}^{-1}$ between conformations described as nearly planar and nearly perpendicular⁵⁶.

Thus it seems that lower limits on the barriers to methyl and methoxy group rotation for 4-fluoroanisole are set, but actual values are not known. If the para fluorine substituent reduces the two-fold barrier²⁸, these limits apply to anisole as well. Results of low-resolution microwave studies should be viewed with some circumspection since the validity of the present interpretations of the intensity of band series apparently remains in question.

iv) infrared and Raman spectroscopy

The analysis of vibrational spectra of anisoles received much attention before conformational deductions were attempted⁵⁷.

Horák, Lippencott, and Khanna suggested that, because conjugation favours the planar conformation while steric interactions favour the perpendicular, anisole probably exists in some intermediate conformation⁵⁸. Spectra and Raman polarizations were explained under the assumption of weak interaction between the characteristic vibrations of effective C_{2v} symmetry for the phenyl moiety and effective C_s symmetry for the methoxy moiety.

Infrared and Raman spectra of anisole, fluoroanisole, chloroanisole, and bromoanisole were compared by Owen and Hester⁵⁹. Except for 3-fluoroanisole, the preponderance of a single, planar heavy atom structure was inferred, as for methyl vinyl ether^{60,61}, and assigned to the trans conformer. The methyl group torsional vibration was not observed, but the barrier height was assumed to be near that for methyl vinyl ether: $16 \text{ kJ}\cdot\text{mol}^{-1}$ ⁵⁹. Two-fold torsional barriers were calculated from torsional frequencies for pure liquids, which yielded a value of $25 \text{ kJ}\cdot\text{mol}^{-1}$ for anisole⁵⁹ and $22 \text{ kJ}\cdot\text{mol}^{-1}$ for methyl vinyl ether⁶¹. For a given halogen, the barrier increases as the substituent was moved from the para (25 $\text{kJ}\cdot\text{mol}^{-1}$) to the meta (30 $\text{kJ}\cdot\text{mol}^{-1}$) position and from the

meta to the ortho ($38 \text{ kJ}\cdot\text{mol}^{-1}$) position. The barrier for 2-fluoroanisole was exceptionally low, $26 \text{ kJ}\cdot\text{mol}^{-1}$. The pattern was explained as the result of competition between the mesomeric effect of halogen substituents⁶², which is ineffective at meta positions, and the steric interaction between the methoxy group and a bulky halogen situated ortho to it.

An equilibrium between cis and trans conformers was found for 3-fluoroanisole⁵⁹. A van't Hoff plot of the ratio of intensities of unidentified vibrational lines corresponding to cis and trans conformers over the range 296 to 373 K indicated that the trans conformers is favoured by $2.4 \pm 0.6 \text{ kJ}\cdot\text{mol}^{-1}$ ⁵⁹, comparable to $2.5 \pm 0.8 \text{ kJ}\cdot\text{mol}^{-1}$ for methyl nitrite⁶⁰ and less than $6.3 \pm 0.8 \text{ kJ mol}^{-1}$ for methyl vinyl ether⁶⁰, which prefers the cis conformation. Josefi, Drahorádová, and Horák found evidence of both planar conformations of the four common 3-haloanisoles in the liquid and in solution, but not in crystalline samples at 93 K⁶³.

Enthalpy differences determined from van't Hoff plots of intensity ratios should be viewed with considered caution if not skepticism⁶⁴.

Allen and Fewster have discussed the connection between the analysis of torsional vibrations and rotational isomerism⁶⁵. From the torsional vibration frequency of the methoxy

group in the far infrared spectrum of the gas phase, the following barrier heights were determined: anisole ($15.1 \text{ kJ}\cdot\text{mol}^{-1}$), anisole- d_3 ($17.1 \text{ kJ}\cdot\text{mol}^{-1}$), and anisole- d_5 ($15.1 \text{ kJ}\cdot\text{mol}^{-1}$). Inclusion of coupling between the deuterated methyl and phenyl tops, which is expected to be small since one top is much lighter than the other, did not lower the apparent barrier for anisole- d_3 . Therefore, coupling between the methoxy group torsion and out-of-plane ring vibrations was presumed to be considerable.

Torsional frequencies implied barriers of $12.3 \text{ kJ}\cdot\text{mol}^{-1}$ for 4-fluoroanisole, $12.5 \text{ kJ}\cdot\text{mol}^{-1}$ for 4-chloroanisole, and $12.8 \text{ kJ}\cdot\text{mol}^{-1}$ for 4-methylanisole, but the apparent constancy of these results was not explained⁶⁵. Goulon, Canet, Evans, and Davies proposed that the two-fold barrier in 1,4-dimethoxybenzene is $22 \pm 3 \text{ kJ}\cdot\text{mol}^{-1}$ in the liquid⁶⁶.

Methoxy group torsions for 2,6-difluoroanisole and 2,3,4,5,6-pentafluoroanisole were consistent with a barrier height of $3.6 \text{ kJ}\cdot\text{mol}^{-1}$ ⁶⁵. This relatively low value was attributed to weakening of the ring carbon-oxygen bond by electronegative fluorine substituents, and to steric interactions between the methoxy group and fluorine at ortho positions.

Recently Tylli, Konschin, and Grundfelt-Forsius studied the Raman spectra of solid anisole, anisole- d_3 , anisole- d_5 , and anisole- d_8 at 130 K ⁶⁷⁻⁶⁹. Apparent barriers to methyl

group rotation were 22.1 ± 0.2 , 17.5 ± 0.2 , 21.8 ± 0.2 , and 17.0 ± 0.2 $\text{kJ}\cdot\text{mol}^{-1}$, respectively. The lower values for tri-deuteriomethyl groups led to the proposal of coupling between the methyl torsion and a low frequency carbon-carbon stretching mode of the ring. Barriers to methoxy group rotation were 48.2 ± 1.3 $\text{kJ}\cdot\text{mol}^{-1}$ for anisole, 49.0 ± 1.5 $\text{kJ}\cdot\text{mol}^{-1}$ for anisole- d_3 , and 46.6 ± 1.0 $\text{kJ}\cdot\text{mol}^{-1}$ for anisole- d_5 , in contradistinction to Allen and Fewster's conclusions drawn from gas phase spectra.

While the methyl group barrier for methyl vinyl ether in the gas phase and the apparent barrier for anisole in the solid phase seem to lie in rough agreement, the two-fold barrier to methoxy group rotation triples on passing from the gas to the solid. Possibly Allen and Fewster's suggestion that the difference between the torsional frequencies from the gas and the liquid should be attributed to intermolecular contributions to the barrier, perhaps as a result of some ordering of the phenyl moieties in the liquid, can be extended to the crystal. The difference concerning the coupling of the methyl group torsion to another mode is removed by postulating a change in dynamics⁶⁷.

Although the steric influence of halogens located ortho to the methoxy group seems reasonable, the electronic contribution to the weakening of the ring carbon-oxygen bond in 2,6-difluoroanisole is probably a manifestation of the mesomeric

effect rather than the inductive one. Since the same two-fold barrier is found for 2,3,4,5,6-pentafluoroanisole the steric effect appears dominant.

Barriers for the para-substituted anisoles likely lie within the experimental errors so no substituent effects are visible. However, the cause of a higher apparent barrier in anisole than in any of the para-substituted anisoles is not clear.

Cunliffe provides a discussion of the calculation of internal rotational barriers from torsional frequencies⁷⁰. The potential energy expression in the absence of coupling is usually assumed to have a simple form, either quadratic or a single $\cos n\phi$ term. Naively, the harmonic oscillator approximation yields

$$\frac{v_t^2}{F} = \sum_{n=1}^{\infty} n^2 V_n \quad \text{Eq. (3)}$$

where v_t is the torsional frequency, F is the reduced rotational constant, and V_n is the n -fold barrier height. If only one V_n is present and the molecular geometry, hence F , is known, then the torsional frequency yields an approximate barrier directly. However, if more terms are to be included, as Lister proposed for anisole, the frequencies of hot torsional bands are required. These remain unobserved. From Equation (3) and an estimate of $3.6 \text{ kJ}\cdot\text{mol}^{-1}$ for V_2 , Lister inferred a four-fold barrier height of about $2.2 \text{ kJ}\cdot\text{mol}^{-1}$ for 4-fluoroanisole⁵⁰.

v) diffraction techniques

No X-ray crystallographic studies of solid anisole have been reported, but Seip and Seip have performed an electron diffraction study of gaseous anisole⁷¹. At 328 K a model having all heavy atoms coplanar was consistent with the observed radial distribution function. However, a very slight improvement of calculated features was noticed when the methoxy group was set 10° out of the ring plane. At 523 K the planar structure was unsatisfactory and comparison of the observed and calculated intensity distributions suggested a dihedral angle of about 40° . Attempts at determination of the barrier by comparison with classical intensity distributions for a two-fold barrier failed. The existence of a second minimum in the methoxy group rotational potential was proposed to explain the large dihedral angle at high temperature.

Goodwin, Przybylska, and Robertson determined the crystal structure of 1,4-dimethoxybenzene and found no evidence of either methyl group rotation or methoxy group rotation⁷².

All heavy atoms lay in the ring plane.

Kollman, Houk, and coworkers surveyed X-ray crystallographic studies of thirty unhindered methoxy groups on aromatic rings and found an average dihedral angle of $6 \pm 6^\circ$ ⁷³. In fifty-eight of sixty cases two methoxy groups ortho to one another preferred a dihedral angle of $7 \pm 6^\circ$, but the remaining two

structures had angles of about 110° . At least one of these was attributed to crystal packing forces⁷⁴.

An inelastic neutron scattering study of 2,6-dimethyl-1,4-dimethoxybenzene concluded that the 4-methoxy group prefers the ring plane, but the 1-methoxy group makes a dihedral angle somewhat smaller than 90° ⁹⁵. Barriers for the three-fold cosine-shaped potential were obtained from the torsional transition for the methyl group of the 1-methoxy ($7.5 \text{ kJ}\cdot\text{mol}^{-1}$) and 4-methoxy ($15.0 \text{ kJ}\cdot\text{mol}^{-1}$) groups, and for the methyl groups themselves ($7.5 \text{ kJ}\cdot\text{mol}^{-1}$). No significant difference was observed between the solid and the liquid phases.

Recent X-ray crystallographic studies demonstrated that the methoxy group makes a dihedral angle of about 8° in 4-methoxyphenol, 25° in 2,6-di-t-butyl-4-methoxyphenol, and 89° in 2,3,5,6-tetramethyl-4-methoxyphenol^{76,77}. In six trimethoxy aromatics with methoxy groups at both positions ortho to the first, the outer groups preferred average dihedral angles of 5° , but the inner group was nearly perpendicular.

Anisole is expected to be planar in the crystal since a para methoxy substituent should reduce the two-fold barrier. Crystal packing forces may enforce strict planarity for 1,4-dimethoxybenzene, but the gas phase structure of anisole is convincing if an effective dihedral angle is ascribed to torsions. In most cases a single ortho substituent seems to demand

that the methoxy group lie trans. Substituents at both ortho positions lead to nearly perpendicular conformations. The low barrier to methyl group rotation for the 1-methoxy group of 2,6-dimethyl-1,4-dimethoxybenzene is consistent with reorientation in a region where steric interaction with the ortho substituents (including ortho hydrogens) is reduced⁷⁵.

vi) photoelectron spectroscopy

Baker, May, and Turner explained the splitting of the lowest ionization energy band of the photoelectron spectrum of a monosubstituted benzene as an indication of the removal of the degeneracy of the ${}^2E_{1g}$ ground state⁷⁸. The donation of electrons from the hydroxyl group to the B_1 -type orbital, which has a maximum at the position of substitution and at the para position, but not to the A_2 -type orbital, which has nodes at these positions, resulted in a 0.70 eV splitting for phenol. The 0.83 eV splitting was seen as a reflection of electron donation from the methyl group to oxygen, which facilitates mesomeric release into the phenyl ring. Therefore, the 0.5(8) eV splitting for t-butoxybenzene was attributed to a reduction of the mesomeric interaction in a non-planar conformation. No splitting was observed for trifluoromethoxybenzene or for pentafluoroethylbenzene, in which the electronegative fluorines make conjugation ineffective.

Vertical ionization potentials (IP) for the oxygen lone-pairs were estimated to be 11.3 eV for phenol and 11.2 eV for anisole⁷⁸. The value for t-butoxybenzene was 9.80 eV. A sharp band at 10.24 eV was assigned for 1,4-dimethoxybenzene, the decrease being due to the interaction between electron-donating para substituents.

While the ionization energies of the π -orbitals increased

monotonically from phenol to 2-methylphenol, and again to 2,6-dimethylphenol, decreases were observed for the corresponding anisoles, which suggests that the phenols retain conjugation while the anisoles lose it⁷⁹. The conformation of 2,3,4,5,6-pentafluoroanisole was not indicated clearly since the energies of all π -orbitals fall relative to anisole, but the energies of the π -orbitals of 2,3,4,5,6-pentafluorophenol were found below those of phenol.

Corresponding π -orbital ionization energies were similar for anisole, ethoxybenzene, and isopropoxybenzene, but lower for t-butoxybenzene⁸⁰. Methyl substitution at both ortho positions decreased the IPs except for phenyl, which remains planar, and for t-butoxybenzene, which remains near-perpendicular.

Since the highest occupied molecular orbital (HOMO) of anisole contains a mixture of ring π -orbital and oxygen lone-pair characters⁸⁰⁻⁸⁴, the first ionization energy of para-substituted anisoles was expected to be sensitive to the effect of the substituent on the degree of conjugation between the methoxy group and the ring. The order of ionization energies was⁸⁴ $\text{NO}_2 > \text{H} > \text{CH}_3 > \text{SCH}_3 > \text{OCH}_3 > \text{NH}_2 > \text{N}(\text{CH}_3)_2$.

Kollman, Houk, and coworkers compared ionization energies with values derived from molecular orbital calculations at the STO-3G level and concluded that 1,3-dimethoxybenzene and 1,4-

dimethoxybenzene are preferentially planar, but 1,2-dimethoxybenzene prefers a nearly perpendicular orientation for one methoxy group⁸⁵. From the ionization energy of the oxygen lone-pair (9.86 eV) the 2-methoxy group of 1,2,3-trimethoxybenzene was supposed to lie nearly perpendicular to the ring plane, although the methoxy groups at both ortho positions were nearly in the plane⁸⁵.

Friege and Klessinger found that sterically hindered alkyl aryl ethers prefer the perpendicular conformation⁸⁷. Anisole and other unhindered ethers preferred the planar conformation, but the existence of a less stable perpendicular conformer was established. The energy difference between these conformers was estimated from the photoelectron spectrum at high temperatures to be $5.7 \pm 0.6 \text{ kJ}\cdot\text{mol}^{-1}$ for anisole, $7.3 \pm 1.5 \text{ kJ}\cdot\text{mol}^{-1}$ for 2-methylanisole, $4.0 \pm 0.9 \text{ kJ}\cdot\text{mol}^{-1}$ for ethoxybenzene, and $5.3 \pm 0.4 \text{ kJ}\cdot\text{mol}^{-1}$ for 2-methylisopropoxybenzene.

The spectrum of thioanisole was explained by Bock, Wagner, and Kroner without resort to unoccupied d-orbitals on sulphur^{81,82}. Conformational equilibrium between the planar and the less stable perpendicular conformers was reported for methyl, ethyl, isopropyl, and t-butyl phenyl sulphides⁸⁰. Since the HOMO is almost entirely sulphur lone-pair⁸¹⁻⁸⁴, the first ionization energies of para-substituted thioanisoles were not affected as greatly as for the anisoles, but the trend was the same⁸⁴.

Schweig and Thon estimated the conformation equilibrium constant for thioanisole between 293 and 773 K⁸⁸. A two-state model implied an energy difference of $3.5 \pm 0.3 \text{ kJ}\cdot\text{mol}^{-1}$, but Honegger and Heilbronner demonstrated that a more careful analysis, which accounts for all conformations, is required⁸⁹.

All evidence from photoelectron spectra favours the planar conformation of anisole over the perpendicular one. Relatively little information about the form of the rotational potential of the methoxy group is obtained, but the perpendicular conformer appears to represent a local energy minimum^{80,87,88}. The electronic effect of para substituents is reflected in the first ionization energy and in the two-fold barrier⁸⁴, as for para substituted thiophenols²⁸. The degree of non-planarity may increase when substituents are placed at one or both ortho positions, but the origin of this effect is uncertain. Kollman, Houk, and coworkers suggest that it is entirely electronic⁸⁵, but the combined data seem to require steric interactions for a complete explanation. For example, a 2-methyl substituent is expected to reduce the energy difference between planar and perpendicular conformations of anisole, but an increase is observed⁸⁷.

vii) electron spin resonance

The use of the hyperfine coupling constant of the methoxy protons in methoxyphenoxy radicals as a conformational probe was investigated by Rabold and coworkers, who concluded that there must be overlap between the ring π -orbitals and an oxygen lone-pair, which is a maximum in the planar conformer and a minimum when the methoxy group lies in a plane perpendicular to the ring plane, and there must be sufficient spin density on the oxygen⁹⁰. The methoxy proton hyperfine coupling constant in 4-methoxyphenoxy radical was 0.21 mT⁹¹, and tabulated values for 2,6-dialkyl derivatives and compounds with only one alkyl group ortho to the 4-methoxy group lay in the 0.15 to 0.21 mT range⁹².

From the temperature dependence of the esr linewidth between 193 and 273K the activation energy of the methoxy group rotation in 2,6-dimethyl-4-methoxyphenoxy radical was estimated to be 32.6 kJ·mol⁻¹⁹³. Atherton and coworkers found no temperature dependence of the couplings in the electron-nuclear double resonance (ENDOR) spectra of 2,6-di-t-butyl-4-methoxyphenoxy radical, but a marked dependence was observed for the corresponding ethyl ether⁹⁴. In fact, the sharpness of the lines suggested rapid rotation, which was enhanced presumably by the steric interactions of the ethyl group in the planar conformer.

Methoxy proton hyperfine coupling constants in 2,3,5,6-

tetramethyl-4-methoxyphenoxy radical⁹⁵ and in 2,3,5,6-tetramethyl-4-ethoxyphenoxy radical⁹⁶ were surprisingly low, 0.000 and 0.032 mT respectively, and were attributed to the inhibition of conjugation by steric interaction with the ortho methyl groups. As expected, the coupling constant in 2,3,5,6-tetramethyl-1,4-dimethoxybenzene radical cation was found to be large, 0.2955 ± 0.0010 mT at 193K, but even larger in 1,4-dimethoxybenzene radical cation, 0.336 ± 0.01 mT at 200 K^{97,98}.

Inhibition of conjugation by steric interaction was forwarded recently by Ingold and coworkers in connection with a study of the reactivity of tocopherols towards peroxy radicals^{76,77}.

Without attempting a quantitative description of the methoxy proton hyperfine coupling, it seems clear that small coupling constants result from conformations in which conjugation between the π -orbitals and the oxygen lone-pair is not favoured sterically. Electronic effects of alkyl substituents on the aromatic ring are small by comparison.

viii) nuclear magnetic resonance

Several techniques of nuclear magnetic resonance spectroscopy have been applied to the study of methoxy group conformation in anisoles. A summary of some investigations appears in this subsection.

a) carbon chemical shifts

The carbon chemical shifts for anisole were obtained first by Lauterbur⁹⁹ and by Spiess and Schneider¹⁰⁰, who proposed that the shifts of ring carbons correlate with π -electron density. The order of increasing shielding was $C1 < C3 < C4 < C2$. Dhami and Stothers attributed the pronounced shielding of the para carbon to conjugative electron release by the methoxy group, which requires a substantial population of the planar conformer in the liquid¹⁰¹. Kitching, Adcock, and coworkers determined a 0.25 ± 0.03 ppm increase in the substituent-induced chemical shift (SCS) at C4 of 2-methylanisole, relative to anisole, but observed a 3.23 ppm decrease for 2,6-dimethylanisole¹⁰². Similar effects were seen by Dhami and Stothers, who interpreted the decrease as evidence of inhibition of conjugation. Similarly, the increase was seen as an indication of increased preference for the planar conformation of the methoxy group — enhancement of conjugation¹⁰².

For 2-alkylanisoles Dhami and Stothers found an upfield shift of C6, and a downfield shift of C2, beyond the value expected on the basis of additivity of substituent-induced chemical shifts. More recently the methoxy group of 2-methoxyanisole was found to shield C6 by an additional 4.3 ppm relative to the methoxy group in anisole, but to deshield C2 by 3.4 ppm¹⁰².

As a reflection of the conformational preference the shielding was attributed to crowding of the 6-position by the methyl of the methoxy group¹⁰¹. Such crowding was alleviated at the 2-position, relative to anisole, and therefore deshielding was observed.

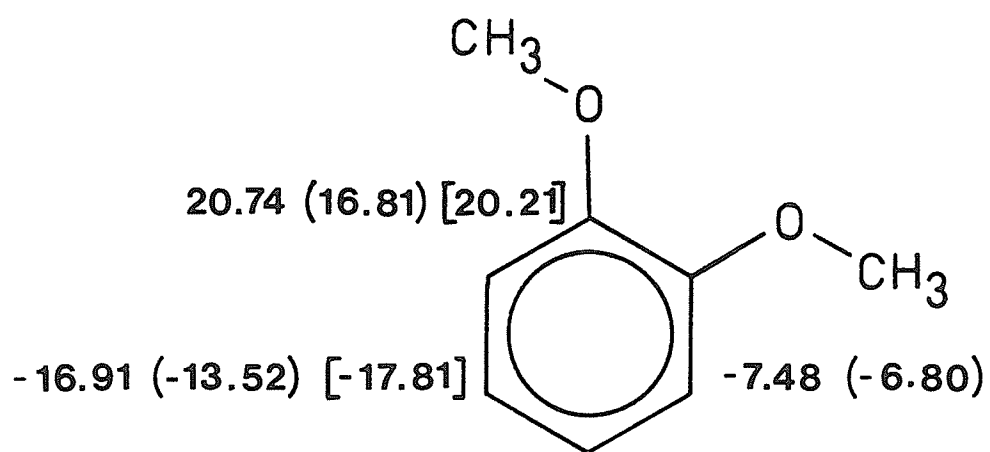
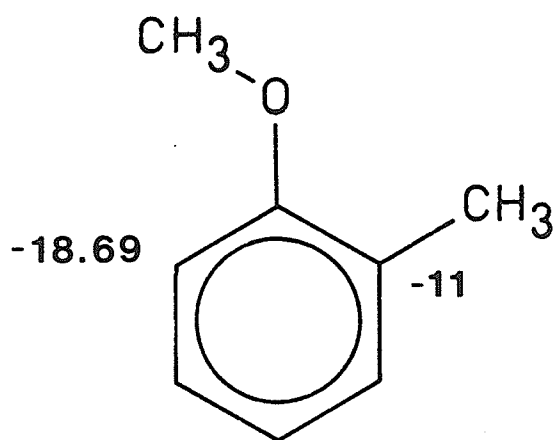
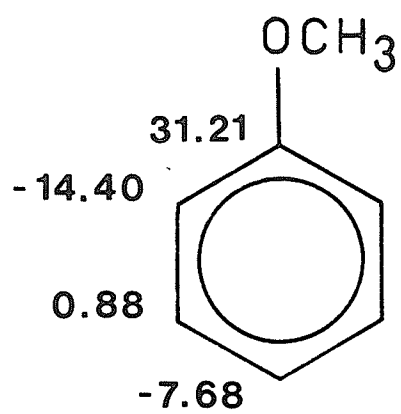
Additivity of methoxy substituent-induced chemical shifts is not particularly good for any of the dimethoxybenzenes, but it is especially poor for the ortho isomer¹⁰². (see Figure 1) While this may be evidence in favour of non-planar conformations, the discussion of 2-methylanisole suggests that separate values which account for the distinction between the two ortho positions are required. If such values (which could be called stereospecific substituent-induced chemical shifts) are approximately the same as those derived for C2 and C6 of 2-methylanisole, the agreement between additivity and observation is improved significantly. Similar considerations apply to the meta positions.

Dhami and Stothers observed that the methyl carbon chemical shift is dependent on the size of the ortho substituent, being within experimental error for anisole and 2-methylanisole, 3.9 ppm downfield for 2,6-dimethylanisole, and 9.7 ppm downfield for 2,6-di-t-butylanisole¹⁰¹. The origin of this effect remained a puzzle: a decrease in conjugative electron release by oxygen or a change in orbital hybridization on oxygen from sp^2 to

Figure 1

Methoxy substituent-induced chemical shifts for anisole, 2-methylanisole, and 1,2-dimethoxybenzene.

Carbon chemical shifts relative to internal benzene are from reference 102. Values based on additivity appear in parentheses. Values based on additivity of distinct contributions at C2 and C6 in 2-methylanisole appear in brackets.



sp^3 , or crowding of the methyl by the ortho substituents should increase the shielding of the carbon. Stothers has attributed the deshielding to an increase in the polarization of the oxygen-methyl carbon bond upon a decrease in conjugative electron release from the phenyl ring¹⁰³.

The chemical shifts from spectra of solid 1,4-dimethoxybenzene and of solid 1,4-diethoxybenzene indicated that the aromatic carbon nuclei form chemically-inequivalent pairs¹⁰⁴⁻¹⁰⁶. Although these resonances were attributed to a single planar conformer, the assignment to either the syn or the anti form was not possible on the basis of shifts alone. The spectrum of solid 1,3,5-trimethoxybenzene was consistent with the anti-symmetric planar conformation, the three protonated aromatic carbons being chemically-inequivalent¹⁰⁷.

Buchanon and coworkers found that the spectrum of thioanisole behaves much like that of anisole when substituents are placed at one or both ortho positions or at the para position¹⁰⁸. However, the order of aromatic carbon chemical shifts was $C1 < C3 < C2 < C4$, that is, C4 was most shielded. The thiomethyl carbon was shielded by about 39 ppm relative to the methoxy carbon of anisole. However, the thiomethyl carbon in 4-methoxythioanisole was deshielded by about 2 ppm relative to thioanisole, and the thiomethyl carbon in 4-nitrothioanisole was shielded by about 1 ppm. This trend opposed

that for the corresponding anisoles, for which an electron-withdrawing nitro group at the para position deshielded the methoxy carbon¹⁰¹. The lack of sensitivity of the thiomethyl carbon shift to electron donation or withdrawal by the para substituent, relative to the magnitudes for the corresponding anisoles, suggested that there is little conjugation between the sulphur lone-pair and the π -orbitals.

Kalabin and coworkers found that the trends begun in the spectra of substituted thioanisoles continue in the selenoanisoles¹⁰⁹. The trends were extended down Group VI A to tellurium by Baiwir and collaborators¹¹⁰. Monotonic downfield shifts of ortho and para carbons kept the latter to high field. While the shifts of the meta carbons changed little, those of the heteromethyl carbon and Cl moved upfield on passing down Group VIA.

As the energy of the highest occupied molecular orbital rises upon descending Group VIA, the character of the orbital approaches that of the heteroatom lone-pair⁸³. That is, conjugation between the lone-pair and the π -orbitals decreases. However, the dependence of the conjugative interaction on the dihedral angle, that is, on conformation, is supposed to become more pronounced because the hybridization of orbitals of the heteroatom changes¹⁰⁹.

Thus, as conjugation decreased, the shielding of the ortho

and para carbons decreased. Additional shielding of the ortho carbons was ascribed to steric crowding, which also affects the heteromethyl carbon chemical shift. The decrease in electronegativity upon descending Group VIA was seen to increase the shielding of Cl and the heteromethyl carbon. No evidence for participation of d-orbitals was found¹⁰⁸⁻¹¹⁰.

The deshielding of the thiomethyl carbon in 4-nitrothioanisole suggests that thioanisole itself is not effectively planar, but an electron-withdrawing para substituent can increase the degree of conjugation. For anisole the highest occupied molecular orbital has both oxygen lone-pair and π -orbital character⁸⁰⁻⁸³. Therefore, the electron withdrawal by a para nitro group may extend to the methoxy carbon.

The change in hybridization of the heteroatom upon descending Group VIA involves an increase in the s-character of one lone-pair and an increase in the p-character of the other^{30,31}. This may be accompanied by a decrease in the bond angle at the heteroatom and a concomitant increase in steric crowding in the planar conformation, which is expected to further shield the heteromethyl and ortho carbons. Such an effect might be masked by the inductive effect of the heteroatom or by the deshielding effect of the proximate, mainly p-character lone-pair¹²⁶, which may be responsible for low-field shifts of the ortho carbons of selenoanisole and telluroanisole¹¹⁰.

In summary, carbon chemical shifts can be useful probes of heteromethyl group conformation in liquid and solid phases. However, additivity of substituent-induced shifts is only approximate and may lead to mistaken interpretations of deviant behaviour. The influence of crystal packing forces on molecular conformation is not clear from spectra of solid samples.

b) carbon and hydrogen spin-lattice relaxation

In an examination of carbon spin-lattice relaxation times (T_1) Levy, Cargioli, and Anet suggested that the value for the outer methoxy groups of 3,4,5-trimethoxyphenethylamine hydrochloride (mescaline) is smaller than the value for the 4-methoxy group because rotation about the oxygen-methyl carbon bond is hindered¹¹⁰, which causes an increase in the effective correlation time for methyl group rotation^{2,5,112-114}.

Bovée and Smidt made proton relaxation time measurements for 2,6-dimethyl-1,4-dimethoxybenzene in deuteriochloroform and calculated activation enthalpies for methyl group reorientation of $12.6 \pm 0.4 \text{ kJ}\cdot\text{mol}^{-1}$ for the 4-methoxy group, $9.6 \pm 0.4 \text{ kJ}\cdot\text{mol}^{-1}$ for the 1-methoxy group, and $9.2 \pm 0.4 \text{ kJ}\cdot\text{mol}^{-1}$ for the methyl substituents¹¹⁵. Similar values were obtained from carbon disulphide solutions which suggested that the difference between the two methoxy groups is not a solvent effect. Further, these workers proposed that the dipolar mechanism dominates proton relaxation in this case and that methoxy group rotation is slow enough to be negligible when one or both ortho positions are occupied by hydrogens. With this model the activation enthalpies of the methoxy groups at positions 1 and 4 of 2,3,5-trimethyl-1,4-dimethoxybenzene were 12.6 ± 0.8 and $2.1 \pm 1.7 \text{ kJ}\cdot\text{mol}^{-1}$, respectively¹¹⁶. A similar value was obtained for 2,3,5-trimethylanisole ($15.1 \pm 1.3 \text{ kJ}\cdot\text{mol}^{-1}$).

The activation enthalpy for methyl group rotation was $15.1 \pm 0.4 \text{ kJ}\cdot\text{mol}^{-1}$ from proton relaxation times¹¹⁷ and $7.5 \pm 1.3 \text{ kJ}\cdot\text{mol}^{-1}$ from carbon relaxation times⁶⁶ for polycrystalline 1,4-dimethoxybenzene. Appreciable coupling between the methyl and methoxy group rotations was suggested by Goulon and coworkers, who found an activation enthalpy of $9.5 \text{ kJ}\cdot\text{mol}^{-1}$ for methoxy group reorientation⁶⁶. In a study of solid 2,6-dimethyl-1,4-dimethoxybenzene Wind and collaborators determined an activation enthalpy of $7.7 \text{ kJ}\cdot\text{mol}^{-1}$ for methyl group rotation in the 1-methoxy substituent, $15.0 \text{ kJ}\cdot\text{mol}^{-1}$ in the 4-methoxy substituent, and $9.0 \text{ kJ}\cdot\text{mol}^{-1}$ for the methyl substituents from the temperature dependence of carbon relaxation times⁷⁵. No evidence of methoxy group reorientation was found, which indicated that the correlation time for this motion was much longer than the correlation time for the methyl group reorientation. Discrepancies between the solution¹¹⁵ and solid phase results were attributed to uncertainties in the molecular geometry or to the difference between states.

Makriyannis and Knittel have used differences in carbon spin-lattice relaxation times among methoxy carbons in a given molecule as a relative measure of the rate of methyl group rotation under the assumption that the dipolar mechanism dominates^{118,119}. A methoxy group located ortho to a single formyl, acetyl, or methoxy substituent had a relaxation time similar to

that found when no ortho substituent was present. However, when both ortho positions were occupied by substituents the relaxation time was much longer, and the carbon resonance was shifted downfield (see the preceding subsection a).

c) molecules oriented in a nematic phase

Diehl and coworkers failed to reproduce the spectrum of anisole in a nematic phase from classical averages of the dipolar coupling constants over a two-fold potential for the methoxy group rotation and a three-fold potential for the methyl group rotation¹²⁰. A satisfactory fit was obtained with a planar methoxy group, a two-fold barrier much greater than $25 \text{ kJ}\cdot\text{mol}^{-1}$, the staggered orientation of the methyl group, and a three-fold barrier much greater than $7.5 \text{ kJ}\cdot\text{mol}^{-1}$.

Emsley and coworkers examined the spectrum of 3,5-dichloroanisole and of 3,5-dichloroanisole- α - ^{13}C and favoured a model with a high barrier (ca $12 \text{ kJ}\cdot\text{mol}^{-1}$) to interconversion between planar conformers and rapid reorientation of the methyl group^{121,122}. The spectrum of 2,6-dichloroanisole- α - ^{13}C was consistent with a high barrier to interconversion between conformers with the methoxy group in the plane perpendicular to the ring plane¹²². Free rotation of the methoxy group or interconversion of planar conformers was unacceptable.

Essentially free rotation of the methoxy group, or interconversion between 2^{n+1} equivalent positions ($n=1,2,3,\dots$), was found for 2,3,5,6-tetrafluoroanisole¹²³. The spectrum did not yield the barrier to methyl group rotation.

Certainly the approach of Diehl and coworkers¹²⁰ is preferable to the interpretation in terms of a few conformations

although the former is more difficult. Possibly the spectrum of anisole could be reproduced from averages over a non-separable energy surface composed of a two-component rotational potential for the methoxy group and a three-fold potential for the methyl group rotation. Even a brief consideration suggests that two separate, single-component potentials are insufficient and that the analysis is doomed to failure; steric interactions between the methyl of the methoxy group and the ortho hydrogens are reduced when the methoxy group lies in the plane perpendicular to the ring plane. While it may be impractical to employ this approach in the deduction of an energy surface from the spectrum, that is, to solve the so-called inverse problem, it may be useful to simulate the spectrum when the potential is known approximately from other sources. Rejection of the approximate, classical approach may be premature.

d) proton chemical shifts

Castellano, Sun, and Kostelnik found that the order of chemical shifts in the proton spectrum of anisole, whether from the neat liquid or a 10 weight % solution in carbon tetrachloride, is $H_3 > H_4 \approx H_2$ ¹²⁴. This reflected conjugative electron release by the methoxy substituent. Hutton and Schaefer observed that although the actual shifts varied considerably with solvent, the order was preserved for 4-nitroanisole¹²⁵.

Baiwir and collaborators found the order of proton chemical shifts was $H_2 > H_3 > H_4$ for thioanisole and selenoanisole, but $H_2 > H_4 > H_3$ for telluroanisole¹¹⁰. The methyl proton resonance moved upfield as Group VIA was descended. In a study which included 2-hydroxythioanisole Schaefer and coworkers¹²⁶ concluded that the thiomethyl group lies in a plane nearly perpendicular to the ring plane and, although additivity of substituent-induced proton chemical shifts is only approximate^{127,128}, the ring and methyl proton shifts are consistent with this preference. A marked downfield shift of H6, a so-called "heavy atom" effect, was attributed to the proximity of the mainly 3p lone-pair on sulphur.

Hofer investigated the conformational behaviour of the methoxy group in 6-methoxy-1-indanol, and in the 5-methyl and 7-methyl derivatives, by comparison of lanthanide-induced shifts of the methoxy protons with calculated values^{129,130}.

Essentially the methoxy groups remained in the plane of the aromatic ring, but preferred to lie trans with respect to the methyl substituent. Support came from nuclear Overhauser enhancements¹³⁰.

e) long-range proton-proton spin-spin coupling to methoxy protons

Long-range proton-proton spin-spin coupling constants involving methoxy groups in aromatic compounds were first reported by Martin and Dailey¹³¹, and by Forsén and coworkers^{132,133}. Coupling over five formal bonds between the methoxy protons and the ortho ring proton, ${}^5J_{\text{OCH}_3, \text{H6}}$, was between 0.24 and 0.31 Hz in magnitude for some 2-substituted anisoles, but no coupling to other ring protons was detected¹³³. The suggestion that the coupled protons must be proximate was supported by the small or non-existent coupling to methylene protons of 1,3-benzodioxole. The spectrum of anisole did not yield any coupling constants between methoxy and ring protons¹²⁴.

Angad Gaur and collaborators determined ${}^5J_{\text{OCH}_3, \text{H6}}$ to be -0.33 Hz in 2,4-dibromoanisole¹³⁵. This first determination of the sign was accomplished by performing double resonance experiments. The magnitude of ${}^6J_{\text{m OCH}_3, \text{H5}}$ was 0.1 Hz or less. The magnitude of ${}^5J_{\text{OCH}_3, \text{H2}}$ in 4-bromoanisole was estimated to be 0.18 ± 0.03 Hz from strong irradiation (decoupling) experiments. A number of monosubstituted anisoles were studied by Creceley, McCracken, and Goldstein, but splitting due to coupling to the methoxy protons were resolved for only a few 2-substituted anisoles¹³⁵. The magnitudes of the coupling constants clustered about 0.31 Hz. The full width of the methoxy

proton resonance was 0.45 Hz at half height, but no splitting was resolved. Schaefer, Gesser, and Rowbotham found that the analogous coupling constant, ${}^5J_{\text{cis}}^{\text{OCH}_3, \text{H}}$, was -0.32 Hz in methyl vinyl ether, -0.27 Hz in 4-methoxy-trans-3-buten-2-one, and -0.29 Hz in 1-methoxy-trans-1,3-butadiene, which prefer the cis-planar methoxy group¹³⁶. In 2-methoxyphenol and 2-methoxythiophenol the magnitude of ${}^5J_{\text{O}}^{\text{OCH}_3, \text{H}3}$ was 0.29 Hz¹³⁷. The former was found to contain a strong hydrogen bond between the phenolic hydrogen and the methoxy oxygen. Similar values were reported by de Kowalewski and collaborators for some substituted anisoles¹³⁸. Rather peculiar results were obtained when an amino substituent occupied one ortho position. For example, the methoxy protons coupled to all ring protons in 2,4-diaminoanisole, which was suggested as a reflection of a particular methoxy group conformation and electronic effects involving σ , π , and proximate coupling mechanisms.

In 3,4-dimethoxybenzaldehyde ${}^5J_{\text{O}}^{\text{OCH}_3, \text{H}2}$ and ${}^5J_{\text{O}}^{\text{OCH}_3, \text{H}5}$ were 0.25 Hz and 0.27 Hz, respectively, in magnitude¹³⁸.

In a study of 1,2-dimethoxybenzene Schaefer and Laatikainen suggest that such values indicate that both methoxy groups prefer to lie in the ring plane¹³⁹.

Lunazzi and Macciantelli proposed that ${}^5J_{\text{O}}^{\text{SCH}_3, \text{H}6}$ is dependent on the size (van der Waals radius) of the substituent for 2-substituted thioanisoles¹⁴⁰. However,

Schaefer, Sebastian, and Salman performed a careful analysis of the spectrum of 2,5-dichlorothioanisole and found that ${}^5J_{\text{O}}^{\text{SCH}_3, \text{H6}}$ was -0.35 Hz^{141} , about twice the reported value for 2-chlorothioanisole¹⁴⁰. When the thiomethyl group preferred to lie near the plane perpendicular to the ring plane, as for 2-hydroxythioanisole, the magnitude of ${}^5J_{\text{O}}^{\text{SCH}_3, \text{H6}}$ was less than 0.02 Hz^{126} . Therefore, the magnitude of this type of coupling constant did seem to depend on the proximity of the protons involved. The mechanism of other long-range couplings in 2,5-dichlorothioanisole was not examined, but ${}^6J_{\text{m}}^{\text{SCH}_3, \text{H3}}$ and ${}^7J_{\text{p}}^{\text{SCH}_3, \text{H4}}$ were $0.05 \pm 0.02 \text{ Hz}$ and $-0.03 \pm 0.02 \text{ Hz}$, respectively¹⁴¹.

C. Acetophenone

Experimental investigations of the conformational behaviour of acetophenone and some of its derivatives are summarized in this section. Some criticisms of the techniques mentioned here appeared in the preceding section on anisoles.

i) near-ultraviolet absorption spectroscopy

Braude and Sondheimer inferred conformational preferences of acetophenone and some derivatives from the intensity of the K-band absorption, due to an allowed transition of the benzoyl chromophore near 240 nm¹⁴². Alkylation at a meta or para position caused a bathochromic shift and an increase in intensity through enhancement of conjugation between the electron-withdrawing acetyl group and the ring π -system. Methylation at one ortho position caused a marked hypsochromic shift and a reduction in intensity, and a further reduction was found for 2,6-dimethylacetophenone. With the equation

$$\cos^2 \phi = \frac{\epsilon}{\epsilon_0} \quad \text{Eq. (4)}$$

where ϵ is the K-band intensity and ϵ_0 is the intensity when the acetyl group and ring are coplanar, and the assumption that acetophenone has all heavy atoms coplanar, effective twist angles ϕ about the ring-carbonyl carbon-carbon bond were calculated for 2-methylacetophenone (40°); 2,6-dimethylacetophenone (55°); and 2,4,6-trimethylacetophenone (63°). Surprisingly, the K-bands of benzaldehyde and acetophenone were nearly identical, presumably because the steric interaction between the methyl and ortho hydrogens is unimportant.

While these results are internally consistent, the assumptions underlying the use of Eq. (4) are unproven. Also, the argument leads to the erroneous conclusion that 2-methyl-

benzaldehyde does not prefer the 0-syn conformer¹⁴³.

ii) dipole moments, Kerr constants, and dielectric relaxation

A number of studies of the conformation of acetophenone derivatives have involved dipole moments, molar Kerr constants, or dielectric relaxation. Bentley and collaborators explained that steric hinderance reduces the opportunity for conjugation in 2,4,6-trimethylacetophenone relative to acetophenones with one or no ortho substituent¹⁴⁴. The conclusion that 2-methylacetophenone prefers the 0-syn conformer¹⁴⁴ was challenged by Braude and Sondheimer¹⁴².

Pinkus and Custard found that the dipole moments of methyl, ethyl, and isopropyl phenyl ketones are greater than those of the corresponding alkyl methyl ketones, possibly through greater charge separation upon conjugation¹⁴⁵. However, the dipole moment of t-butyl phenyl ketone (2.58 D) was smaller than that for t-butyl methyl ketone (2.70 D) because steric interactions between the t-butyl group and the ring favour non-planarity. Dipole moments of alkyl 2,4,6-trimethylphenyl ketones supported the proposal.

Assuming that acetophenone is planar, Bock and coworkers interpreted the dipole moment of 4-fluoroacetophenone as indicative of the planar conformation¹⁴⁶. An equilibrium mixture of planar conformers of 2-fluoroacetophenone favoured the 0-anti conformer by about $5.6 \text{ kJ}\cdot\text{mol}^{-1}$ at 298 K. In contrast, the acetyl group of 2-trifluoromethylacetophenone preferred to lie near the plane perpendicular to the ring plane.

From comparison of calculated and observed molar Kerr constants Aroney, Corfield, and LeFèvre concluded that acetophenone prefers planarity of the heavy atoms, but 2,4,6-trimethylacetophenone and 2,3,5,6-tetramethylacetophenone prefer the acetyl group in the plane perpendicular to the ring plane¹⁴⁷. Later work affirmed the result for acetophenone^{148,149}. An effective twist angle of about 20° was inferred for acetophenones with a fluorine, chlorine, bromine, nitro, or acetyl substituent at the 4-position¹⁴⁸⁻¹⁵¹. Mirarchi and Ritchie have found that the molar Kerr constants for the three 4-haloacetophenones and for the 4-nitro and 4-cyano derivatives are not consistent with strictly planar conformations¹⁴⁹. They proposed that 4-methylacetophenone is planar and that 4-t-butylacetophenone may be planar.

The dielectric relaxation time of acetophenone was consistent with a planar average conformation, but could not be conclusive¹⁵². The value was nearly doubled for 2,4,6-trimethylacetophenone, possibly because the acetyl group can not achieve coplanarity with the ring for steric reasons, or because the barrier is low in acetophenone, but rises when methyl groups on the phenyl ring enhance conjugation by electron release.

None of these studies suggest that acetophenone itself prefers a conformation with non-coplanar heavy atoms. The effective twist angles of 4-substituted acetophenones may result from torsions about the planar, minimum energy

conformation. However, it is clear that steric interactions may be important in 2,6-disubstituted acetophenones.

iii) infrared absorption spectroscopy

The infrared absorption spectrum of acetophenone is consistent with a preferred planar conformation in the liquid phase¹⁵³.

Jones, Forbes, and Mueller observed that the fundamental carbonyl stretching band is sensitive to ring substitution¹⁵⁴. The frequency for 4-substituted acetophenones is highest for 4-nitroacetophenone (1700 cm^{-1}), lowest for 4-aminoacetophenone (1677 cm^{-1}), and about $1692 \pm 1\text{ cm}^{-1}$ for acetophenone and four 4-haloacetophenones, which reflects the sum of mesomeric and inductive effects. Hydrogen bonding to the carbonyl oxygen made 2-aminoacetophenone prefer the 0-syn conformation, as does 2-methylacetophenone. A single band was found for 2-fluoroacetophenone, but two maxima were observed for the 2-chloro-, 2-bromo-, and 2-nitro-acetophenones. The alignment of carbonyl carbon-oxygen and carbon-substituent bond dipoles in the 0-syn form was expected to shift the carbonyl stretching band to higher frequency. Thus, the bands were assigned and the temperature dependence of the integrated intensity ratio suggested that 2-bromo- and 2-nitro-acetophenone prefer the 0-syn conformation, but 2-chloro- and 2-fluoro-acetophenone prefer 0-anti.

Two-fold barriers to acetyl group rotation in acetophenone ($13\text{ kJ}\cdot\text{mol}^{-1}$) and 4-fluoroacetophenone ($15\text{ kJ}\cdot\text{mol}^{-1}$) were deduced from the torsional frequency of the acetyl group of the molecule in the vapour phase by Miller,

Fateley, and Witkowski¹⁵⁵. Only one torsion was observed for 2-fluoroacetophenone so only one component of the rotational potential could be determined from Eq. (3), but neglect of the one-fold barrier yielded an effective two-fold component of 12 kJ mol^{-1} .

The effect of ring substitution on the normal modes of acetophenone might be expected to appear in the carbonyl stretching frequency, but the utility of this observation for more than qualitative characterization is uncertain. With regard to torsional frequencies, Miller and coworkers emphasize that liquids may yield barriers quite different from the intrinsic rotational barriers obtained from the gas¹⁵⁵.

iv) X-ray diffraction

The crystal structure of acetophenone was solved by Tanimoto and collaborators, who found that the acetyl group was twisted by about 4° with respect to the ring plane at 154 K¹⁵⁶. The molecules were packed by van der Waals forces.

According to Kim, Boyko, and Carpenter, the acetyl group was twisted by about 3° in the crystal structure of 4-nitroacetophenone¹⁵⁷. The nitro group was twisted by about 4° in the opposite sense.

The implication of these results for the conformational behaviour in other phases need not be obvious. However, since no specific intermolecular interactions determine the conformation in the crystal, it seems that the preferred conformation may be planar, or nearly so, in all phases.

v) electron spin resonance

Magnetic non-equivalence of meta and of ortho hydrogens in the electron spin resonance spectrum of the anion radical from 4-nitroacetophenone was reported by Kaminski and Möbius¹⁵⁸. From complete lineshape analysis at various temperatures the Arrhenius activation energy for acetyl group rotation was thought to be $37 \pm 2 \text{ kJ}\cdot\text{mol}^{-1}$. Lower bounds were set for acetophenone ($51 \text{ kJ}\cdot\text{mol}^{-1}$), 4-bromoacetophenone¹⁵⁹ ($49 \text{ kJ}\cdot\text{mol}^{-1}$), 4-methoxyacetophenone ($46 \text{ kJ}\cdot\text{mol}^{-1}$), and 4-methylacetophenone ($45 \text{ kJ}\cdot\text{mol}^{-1}$).

vi) nuclear magnetic resonance

This subsection presents a summary of some of the investigations of acetyl group conformation in acetophenone derivatives.

a) carbon chemical shifts

Spiesecke and Schneider tabulated substituent-induced chemical shifts for the acetyl group which reflect the conjugative withdrawal of electron density from the ring π -system in the order $C1 < C4 < C2 = C3$ ¹⁰⁰.

Dhami and Stothers noticed that the carbonyl and methyl carbon chemical shifts were relatively insensitive to meta or para substituent polarity while the shifts of ring carbons may be approximated by additivity of substituent-induced shifts¹⁶⁰. Apart from C4, trends in ring carbon shifts upon ortho substitution were difficult to ascertain since additivity fails¹⁶¹. As the size or number of ortho substituents increased the C4 resonance moved upfield by as much as 4 ppm. Carbonyl and methyl carbon resonances moved downfield concurrently, although the latter were less sensitive to substitution.

Ortho effects on the carbonyl carbon shift were attributed to neighbouring group anisotropy, steric effects, and other effects of unknown origin¹⁶⁰. Nevertheless, these shifts δ_{CO}^X with respect to internal carbon disulphide were used to estimate acetyl group twist angles ϕ from the formula¹⁶²

$$\cos^2 \phi = \frac{\delta_{CO}^X - \delta_{CO}^{90}}{\delta_{CO}^0 - \delta_{CO}^{90}} = \frac{\delta_{CO}^X - 23.2}{20} \quad \text{Eq. (5)}$$

where δ_{CO}^0 is the shift of the coplanar acetyl group and $\delta_{CO}^0 - \delta_{CO}^{90}$ is the expected maximal downfield shift. Acetophenone was

assumed to be planar.

Equation (5) led to consistent values for similar ortho substituents, but comparison of different substituents was rather unconvincing. For example, the twist angles derived for 2,6-dimethylacetophenone (50°) and 2,6-dichloroacetophenone (28°) are not reconciled easily.

Makriyannis and Knittel have proposed that the downfield shift of the carbonyl carbon indicates a decrease in conjugation, which may be attributed to non-coplanarity of the heavy atoms¹¹⁸. Support was drawn from the corresponding increase in the relaxation time of the methyl carbon nucleus, but not from its relatively insensitive chemical shift.

Drakenberg, Sommer, and Jost compared experimental and calculated bandshapes of ring carbon resonances from solutions of 4-substituted acetophenones at a few low temperatures^{163,164}. A free energy of activation of $22.4 \text{ kJ}\cdot\text{mol}^{-1}$ was derived for acetyl group rotation in acetophenone. For the O-protonated species in which conjugation is enhanced, a value of $48 \text{ kJ}\cdot\text{mol}^{-1}$ was determined¹⁶⁵.

b) proton chemical shifts

The order of chemical shifts in the proton magnetic resonance spectrum of acetophenone was found to be $H_2 < H_4 < H_3$, as expected for conjugative withdrawal by the acetyl group^{166,167}. Smith, Deavenport, and Ihrig have investigated the relationship of substituent effects and acetyl group conformation to the proton spectrum of several 2-substituted acetophenones and benzaldehydes¹⁶⁸. The acetyl group was more sensitive to steric factors than was the formyl group, as was evident from the shift of H_6 .

Klinck, Marr, and Stothers assumed that the acetyl group prefers to lie in the ring plane in 4-methoxyacetophenone and in 4-N,N-dimethylaminoacetophenone¹⁶⁹. From the temperature dependence of the proton spectra of these compounds in toluene- d_8 free energies of activation at the coalescence temperature were $35 \text{ kJ}\cdot\text{mol}^{-1}$ at 181 K and at most $31 \text{ kJ}\cdot\text{mol}^{-1}$ at 157 K, respectively. (cf. $28 \text{ kJ}\cdot\text{mol}^{-1}$ and $34 \text{ kJ}\cdot\text{mol}^{-1}$, respectively, from the carbon spectra^{163,164})

Lanthanide-induced chemical shifts for 2-methylacetophenone were interpreted in terms of an equilibrium mixture of planar or non-planar conformers with 0-syn favoured by $2\text{-}4 \text{ kJ}\cdot\text{mol}^{-1}$ ^{170,171}.

c) molecules oriented in a nematic phase

Solutions of acetophenone in a nematic solvent yielded spectra which were consistent with planar heavy atom structures, although Emsley and coworkers indicated that molecular reorientation is faster than the internal rotation¹⁷² while Diehl and coworkers suggested the converse¹²⁰. The attempt to determine the two-fold barrier in the latter investigation failed. Both studies concluded that one methyl carbon-hydrogen bond lies trans to the ring carbon-oxygen bond. The same geometry was preferred by 3,5-dibromoacetophenone¹²¹.

d) long-range proton-proton spin-spin coupling to acetyl protons

No coupling between the methyl and ring protons of acetophenone has been reported^{166,167}. No coupling was resolved for 2-hydroxyacetophenone, in which an intramolecular hydrogen bond fixes the acetyl group conformation¹³³. Smith and coworkers resolved no coupling to the acetyl group protons for a number of 2-substituted acetophenones¹⁶⁸. Wasylishen, Rowbotham, Ernst, and Schaefer found, however, that the magnitude of ${}^5J_{OCH_3, H6}$ is 0.19 Hz in 2-aminoacetophenone, which prefers the 0-syn, hydrogen bonded conformation¹⁷³.

D. Proximate Proton-Proton and Proton-Fluorine Spin-Spin Coupling

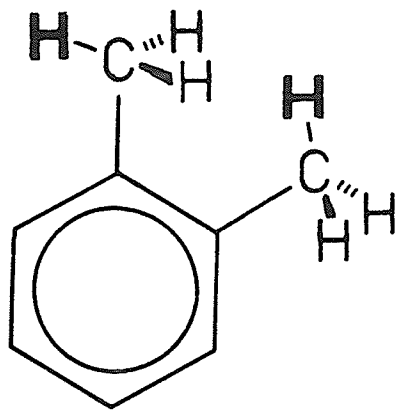
So-called "proximate", "through-space", or "direct" spin-spin coupling occurs between spatially-proximate nuclei, and necessarily along a path or paths other than the intervening framework of formal bonds. After the report of proximate coupling by Davis, Lutz, and Roberts¹⁷⁴, many examples appeared¹⁷⁵. Some provide compelling evidence if not proof of the nature of the coupling.

Semi-empirical CNDO and INDO MO FPT calculations of proximate proton-proton coupling constants were first presented by Wasylishen and Schaefer¹⁷⁶. Calculated signs were negative and the magnitudes decreased with increasing spatial separation of the spins. Unpublished results indicated that no coupling would occur over distances greater than about 220 pm, roughly twice the van der Waals radius of hydrogen. Some exceptions to these rules have been recognized. For example, in the conformation of *o*-xylene depicted in Figure 2 the protons which lie in the ring plane couple significantly over about 320 pm¹⁷⁶, possibly through the intervening rear lobe of the carbon-hydrogen bond¹⁷⁵.

Meinwald and Lewis propose that proton-proton coupling may occur when the rear lobes of antiparallel carbon-hydrogen bonds interact¹⁷⁷. Another mechanism involves transmission through

Figure 2

A conformation of o-xylene in which the methyl protons in the ring plane (which appear in bold-face) are coupled substantially over 320 pm.



an intervening third atom, as Anet, Brown, Carter, and Winston suggest¹⁷⁸. Although the prototypical third atom is oxygen, this mechanism may apply to cases in which a lone-pair on the intervening atom is essential. The example of the conformation of *o*-xylene in Figure 2 does not fit this category, since the largest coupling occurs between the protons in the ring plane specifically, and perhaps represents a separate mechanism.

Proximate proton-fluorine coupling constants are usually larger than corresponding proton-proton numbers. In the absence of specific interactions, the coupling may become unimportant over distances greater than 250 pm^{179,180}. The experimentally-observed orientational dependence of the coupling between methyl protons and a fluorine nucleus was described by the "converging vector rule", which states that it is necessary, but not sufficient, that a vector in the carbon-fluorine bond direction converge upon and intersect a vector in the carbon-hydrogen bond direction^{181,182}. This rule is of limited use¹⁷⁵.

Calculation in the INDO MO FPT approximation by Wasylshen and Barfield indicate that the sign of the coupling between proton and fluorine is usually negative when the spins are proximate¹⁸³. Bond orientation effects are important, however, and a substantial positive contribution arises from interaction between the fluorine and the rear lobe of a carbon-hydrogen bond.

In view of the complexity of proximate proton-fluorine coupling and the inadequacies of the approximate treatment these authors felt that non-contact mechanisms should not be invoked prematurely.

Chapter 2

Introduction to the Problem

Experimental studies of anisole, acetophenone, and of their 4-substituted derivatives suggest that the electron-releasing methoxy group and the electron-withdrawing acetyl group prefer to lie in the plane of the aromatic ring. Effective twist angles which are non-zero may be attributed to averaging over the rotational motion about the bond to the ring carbon. Whether a single ortho substituent enhances or inhibits conjugation is uncertain, but the methoxy group tends to lie trans to the substituent. Specific interactions between the acetyl methyl group and oxygen and the ortho substituent determine the 0-syn:0-anti equilibrium. Non-planar conformations are strongly favoured when substituents occupy both ortho positions. This seems quite clearly a steric requirement and less significantly an electronic effect.

The intent of this study was towards the description of the conformational behaviour of some 2-fluoroanisoles and 2-fluoroacetophenones in solution and towards the understanding of the reflection of this behaviour in the nuclear magnetic resonance parameters, particularly spin-spin coupling constants. Naturally, the conformational and substitutional dependences of these parameters are important in an analysis of this kind. Principal mechanisms of spin-spin coupling may be indicated.

Chapter 3
Experimental Method

A. Materials

Anisole (Baker Chemical Company); 2-fluoroanisole (Pfaltz and Bauer, Inc.); 2,3,5,6-tetrafluoroanisole (PCR, Inc.); acetophenone (Chem Service); 2,6-difluoroacetophenone (Maybridge Chemical Company); 2,3,4,5,6-pentafluoroacetophenone (Fairfield Chemical Company); and α,α,α -trifluoroacetophenone (PCR) were commercially available. Other compounds were synthesized from zone-refined phenol (Aldrich Chemical Company), from 2-fluorophenol (Pierce Chemical Company), or from 2-fluorobenzaldehyde (Aldrich). Methyl iodide was obtained from Fisher Scientific Company, from Stohler Isotope Chemicals (95 atom% ^{13}C), and from Merck, Sharp and Dohme Canada Limited (90 atom% ^{13}C). Pyridinium chlorochromate was from Aldrich.

Acetone- d_6 (99.5 atom% D) from Aldrich was used as a solvent and an internal deuterium lock signal. Solvent carbon tetrachloride was from Fisher. Tetramethylsilane from Aldrich (Diaprep) or from Merck, Sharp, and Dohme was used as an internal proton and carbon reference, and as a proton lock signal. Hexafluorobenzene from Pierce was used as an internal fluorine reference.

i) bromination of 2-fluorophenol

The bromination of 2-fluorophenol was accomplished by the standard method of adding bromine dropwise with stirring to a solution of 2-fluorophenol in tetrahydrofuran or dilute aqueous sodium hydroxide. Substitution of one or two equivalents of bromine yielded 4-bromo-2-fluorophenol and 4,6-dibromo-2-fluorophenol, which were identified by pmr and mass spectrometry.

Addition of bromine in acetic acid to a solution of 2-fluoroanisole in methanol and acetic acid yielded 4-bromo-2-fluoroanisole according to pmr and mass spectrometry.

ii) methylation of phenolic hydroxyl groups

Methylation of the hydroxyl groups of phenol, of 2-fluorophenol, of 4-bromo-2-fluorophenol, and of 4,6-dibromo-2-fluorophenol was accomplished by the standard method of adding methyl iodide to a mixture of the phenol and anhydrous potassium carbonate in acetone¹⁸⁴. Both unlabelled and methyl-¹³C-enriched compounds, except 2-fluoroanisole- α -¹³C, were obtained and identified by pmr and mass spectrometry.

An initial attempt at reaction of sodium 4,6-dibromo-2-fluorophenoxide with methyl iodide in absolute ethanol yielded the corresponding anisole, but this procedure was not preferred.

iii) preparation of 2-fluoroacetophenone

Unlabelled and methyl-¹³C-enriched 2-fluoroacetophenone were obtained as follows¹⁸⁵. Addition of 2-fluorobenzaldehyde to ethereal methyl magnesium iodide yielded 1-(2-fluorophenyl) ethanol, which was identified by pmr and mass spectrometry. A solution of the crude alcohol in methylene chloride was added to a mixture of pyridinium chlorochromate¹⁸⁶ in methylene chloride to obtain 2-fluoroacetophenone. The dark crude product was chromatographed on silica gel plates with hexanes containing a small amount of ether. The pmr spectrum of the resulting clear, pale yellow solution suggested that this material was a mixture of about 3:2 2-fluoroacetophenone and 2-fluorobenzaldehyde.

B. Sample Preparation

Solutions were prepared by weight to consist of no more than 15 mole % of the compound of interest in carbon tetrachloride or acetone- d_6 . Each was transferred to a precision-bore 5 or 10 mm nmr tube fitted with a ground glass joint through a pipette containing a filtering wad of tissue or cotton wool. Samples were degassed by at least eight freeze-pump-thaw cycles before the tube was sealed with a torch. The sample depth in either tube lay between three and five centimetres approximately.

C. Spectroscopic Method

Proton magnetic resonance spectra were recorded on a Varian Associates HA-100-D spectrometer operated in the frequency sweep mode. A Hewlett-Packard 4204A oscillator was used as the external manual oscillator. The probe temperature was maintained at 305 ± 1 K. Peak positions were determined as follows. Spectral regions of interest were divided into intervals no greater than about five Hertz wide. Each interval was recorded at least four times from low to high field. Calibration lines were placed at the beginning and the end of each interval. The corresponding frequencies were found by the difference between the manual oscillator and sweep oscillator frequencies. The average frequency of each peak and its standard deviation were calculated from peak positions obtained by interpolation between calibration lines. The typical standard deviation was less than 0.015 Hz.

Strong (decoupling) and weak¹⁸⁷ (tickling) irradiation experiments were performed with a second HP4204A oscillator which was adjusted to irradiate at the desired frequency. The amplitude of the irradiating field was adjusted to perturb at the intended frequency while avoiding proximate transitions.

Proton, fluorine, and carbon magnetic resonance free induction decays were recorded on a Bruker WH-90-DS spectrometer. The probe temperature was maintained by a Bruker B-ST100/700 temperature controller at 305 ± 1 K unless otherwise specified. Quadrature phase detection and automatic baseline correction were used.

Proton and fluorine pulse lengths produced 70° flip angles, approximately, with equilibrium delays of about five seconds. Digital resolution was typically 0.07 Hz/real point or better. Carbon flip angles were about 40° with typical equilibrium delays of ten seconds. Typical digital resolution for the carbon spectra was about 0.2 Hz/real point. Exponential multiplication of the free induction decay with the line broadening equal to the reciprocal of the acquisition time was performed in most cases.

i) low temperature experiments

Proton, fluorine, and carbon spectra at temperatures between 180 K and 305 K were acquired as above. Digital resolution was typically about 0.05 Hz/real point for proton and fluorine spectra and about 0.1 Hz/real point for carbon spectra. Samples equilibrated for at least fifteen minutes at each temperature. Some trials after only eight minutes suggested that this period was sufficient.

The temperature controller was calibrated as the temperature was raised from 170 K to 305 K. An nmr tube containing a copper-constantan thermocouple immersed in methylene chloride was placed in the probe and the reference junction was placed in an ice-water bath. Temperature readings were equal over most of the range, but the temperature controller read 2 K lower than the thermocouple at 200 K and below. Reported temperatures have been corrected.

ii) nuclear spin-lattice relaxation experiments

Carbon and fluorine spin-lattice relaxation experiments were performed at 305 K with the samples described above. Broadband proton decoupling was used in every case. Selective fluorine decoupling was accomplished in some cases with the aid of a Bruker B-SV3B decoupler and the spectrometer's frequency synthesizer.

The inversion-recovery cycle consisted of two $180-\tau-90$ sequences with a 180° phase shift of the second 180° pulse, that is, inversion-recovery with alternating phases. The 180° pulse length for carbon was set at 28 microseconds on the basis of a determination of the null for anisole- α - ^{13}C . For fluorine a pulse length of 8.4 microseconds was found for (unlabelled) 4,6-dibromo-2-fluoroanisole. The 90° pulse lengths were set at one-half of the 180° pulse length. Digital resolution was usually 0.39 Hz/real point. An equilibrium delay of 60 to 100 seconds provided at least four T_1 's before another sequence. The cycle was repeated at least four times.

Calculations of relaxation time were based usually on Lorentzian peak heights picked automatically by the Nicolet software. Occasionally, peak integrals were chosen. Data were fitted to two- and three-parameter functions with the assumption of single exponential decay. Between thirteen and fifteen data points were used in each determination.

iii) methyl carbon nuclear Overhauser enhancement experiments

Enhancement of the methyl carbon resonance intensity by strong irradiation of coupled protons was determined as follows. Spectra were acquired as for the relaxation experiments. A spectrum with broadband proton decoupling was compared to one in which the decoupler was gated on at acquisition. The comparison was by peak height and by peak integral as calculated by the Nicolet software.

D. Computations

Spectral simulations were performed with the program LAME,^{188,189} or a version accommodating eight magnetically non-equivalent spins, LAME8, in iterative and non-iterative modes and coupled to a plotting routine.

Ab initio molecular orbital calculations were performed at the STO-3G level¹⁹⁰ with the program GAUSSIAN70¹⁹¹. Semi-empirical calculations¹⁹² were performed with INDO or CNDO/2 usually using standard geometries^{192,193} or the optimum geometry from the ab initio calculations. Coupling constants were calculated using Laatikainen's FINDO program,¹⁹⁴ usually by FPT^{195,196}.

Computations were performed on an Amdahl 470/V7 or an IBM 370/168. Calculated spectra were plotted by a Versatec plotter.

Chapter 4

Experimental Results

The observations and numerical results which follow represent analyses of proton, fluorine, and carbon nmr spectra of the anisole and acetophenone derivatives studied. Some methyl carbon and ring fluorine relaxation experiments are included.

Spectral parameter values from proton or fluorine spectra are those calculated by LAME unless otherwise stated. Linewidths are roughly 0.1 to 0.2 Hz and only transitions with relative intensity greater than 0.05 are considered in most cases. Useful confidence limits^{197,198} on the parameter values are given probably by three times the standard deviation calculated by LAME, which appears in parentheses after the value.

In most cases coupling constants involving carbon nuclei are set equal to the observed splitting of the spectral lines under the assumption of first-order behaviour¹⁹⁹⁻²⁰¹. Similarly, carbon chemical shifts are those read directly from the spectra. A measure of the reproducibility of the chemical shifts is given by the root-mean-square deviation of the line positions from proton-decoupled spectra. The rms deviation of the magnitude of the observed splitting for a number of spectra is taken as an indication of the reliability of the parameter value.

Parameter values and errors deduced by other means are mentioned specifically. All quoted values are compatible with the magnitudes of calibration error, digital resolution, and linewidth.

Signs of proton-proton^{134,202}, proton-carbon^{203,204}
proton-fluorine²⁰⁵, carbon-carbon^{203,206-209}, and carbon-fluo-
rine²⁰⁵⁻²⁰⁷ spin-spin coupling constants were assumed from the
literature, unless otherwise stated.

A. High-resolution Spectra

i) anisole

Carbon spectra of a 4.39 mole % solution of anisole and of a 4.62 mole % solution of anisole- α - ^{13}C in acetone- d_6 yielded the results in Table 1. The rms deviation from the average line positions for three proton-decoupled spectra of the 4.62 mole % sample was about 0.07 Hz (0.003 ppm). This and the difference in concentration between the samples precluded any attempt to determine ^{13}C -induced ^{13}C -isotope shifts.

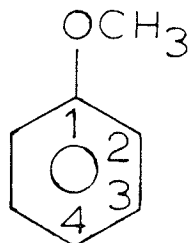
According to a comparison of linewidths the magnitude of coupling constants over four or five bonds between $\text{C}\alpha$ and $\text{C}3$ or $\text{C}4$ cannot be greater than about 0.2 Hz. The sign of $^3J_{\text{O}}^{\text{C}\alpha, \text{C}2}$ is tentatively assumed positive, but the sign of $^2J^{\text{C}\alpha, \text{C}1}$ is unknown²⁰⁹.

Only a few carbon-hydrogen coupling constants could be ascertained due to the complexity of the spectra of the coupled system. One-bond coupling constants are quite safely assumed positive also, but the sign over two bonds is unknown²⁰⁴. The widths of the resonances of $\text{C}3$ were able to accommodate small two- and four-bond couplings to $\text{H}2$, $\text{H}4$ and $\text{H}6$ if the sum was about 2.5 Hz.

Although the proton spectra of these samples were not analyzed, the centers of the methyl proton resonances were at

Table 1

Carbon Chemical Shifts^a and Coupling Constants^b for Anisole in Acetone-d₆.



	4.39 mole %	4.62 mole % (methyl ¹³ C enriched)
$\delta_{C\alpha}$	c	55.27
δ_{C1}	160.65	160.64
δ_{C2}	114.63	114.62
δ_{C3}	130.11	130.10
δ_{C4}	121.17	121.16
$2J_{C\alpha, C1}$	$\pm 2.33 \pm 0.13$	$1J_{C\alpha, H}$ 143.60 ± 0.03
$3J_{C\alpha C2}$	4.18 ± 0.09	$1J_{C2, H}$ 159.9 e
$4J_{C\alpha, C3}$	d	$1J_{C3, H}$ 159.2 e
$5J_{C\alpha, C4}$	d	$1J_{C4, H}$ 161.4 e
		$3J_{C3, H5}$ 8.0 ± 0.5
		$3J_{C4, H2}$ 7.5 ± 0.1
		$2J_{C4, H3}$ $\pm 1.3 \pm 0.1$

a In ppm downfield from internal TMS. Probably ± 0.01 ppm.

b In Hertz.

...Table 1 continued...

Table 1...

c Not observed.

d Not resolved and less than 0.2 Hz.

e $^1J_{C2,H} = 158.52$ Hz, $^1J_{C3,H} = 158.35$ Hz, $^1J_{C4,H} = 160.43$ Hz

by selective proton decoupling (ref. 229).

3.761 ppm for the 4.39 mole % solution, 3.762 ppm for the residual unlabelled compound, and 3.760 ppm for the labelled anisole in the 4.62 mole % solution.

ii) 2-fluoroanisole

The 100 MHz spectrum of the ring protons of a 4.83 mole % solution of 2-fluoroanisole in acetone-d₆ appears as Figure 3. The methyl proton resonance is included in Figure 4.

Analysis yielded the parameters in Table 2. Six- and seven-bond coupling constants between methyl protons and the meta and para ring protons were fixed at zero. Strong coupling was found between H3, H5 and H6, the three shifts occurring within about 0.5 Hz. Consequently, some large correlation coefficients were found between $^5J_p^{F,H5}$ and $^3J_o^{H4,H5}$ (0.5869), $^5J_p^{F,H5}$ and $^3J_o^{H5,H6}$ (0.5789), $^4J_m^{H3,H5}$ and $^5J_p^{H3,H6}$ (-0.5351), and $^3J_o^{H4,H5}$ and $^5J_m^{H4,H6}$ (-0.6817); and between ν_3 and $^3J_o^{H3,H4}$ (-0.5263), and ν_4 and $^3J_o^{H4,H5}$ (0.5398).

The magnitude of $^5J_o^{CH_3,H6}$ was not well-determined for this acetone solution: the near degeneracy of the proton chemical shifts ν_5 and ν_6 causes "virtual coupling"⁴ between the methyl protons and H5. For a benzene-d₆ solution which was not analyzed completely, the splittings of the resonances of H6 are about 0.25 Hz. This estimate of $^5J_o^{CH_3,H6}$ is preferred. The negative sign is assumed.¹³⁴

In accord with the determinations of the sign of $^5J_o^{CH_3,F}$ in the brominated 2-fluoroanisoles, it was set positive.

The center of the proton-decoupled fluorine resonance lay about 27.016 ppm downfield of internal hexafluorobenzene.

Figure 3

Spectrum of the ring protons of a 4.83 mole % solution of 2-fluoroanisole in acetone-d₆.

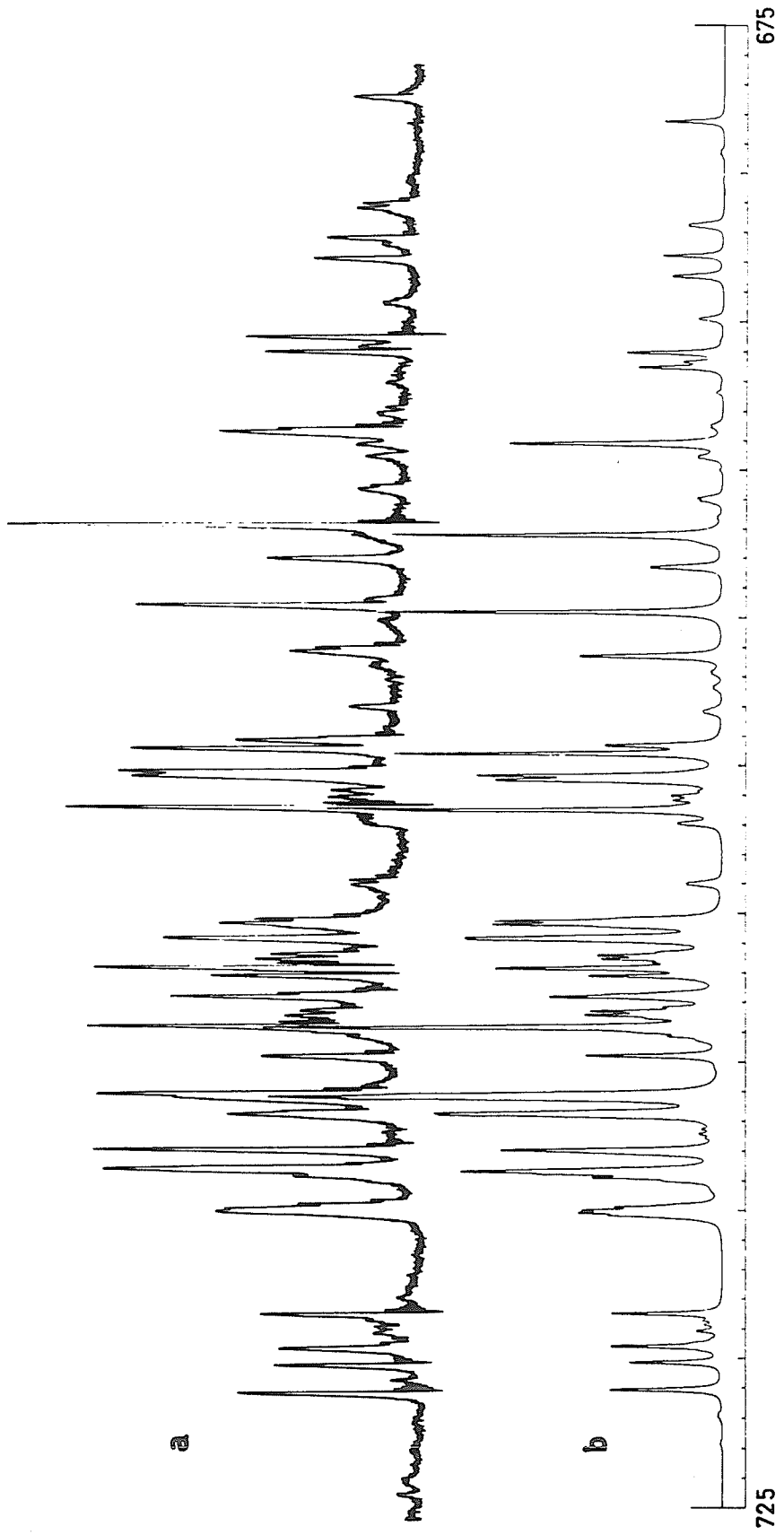


Figure 4

Spectrum of the methyl protons of a 4.83 mole % solution of 2-fluoroanisole in acetone-d₆.

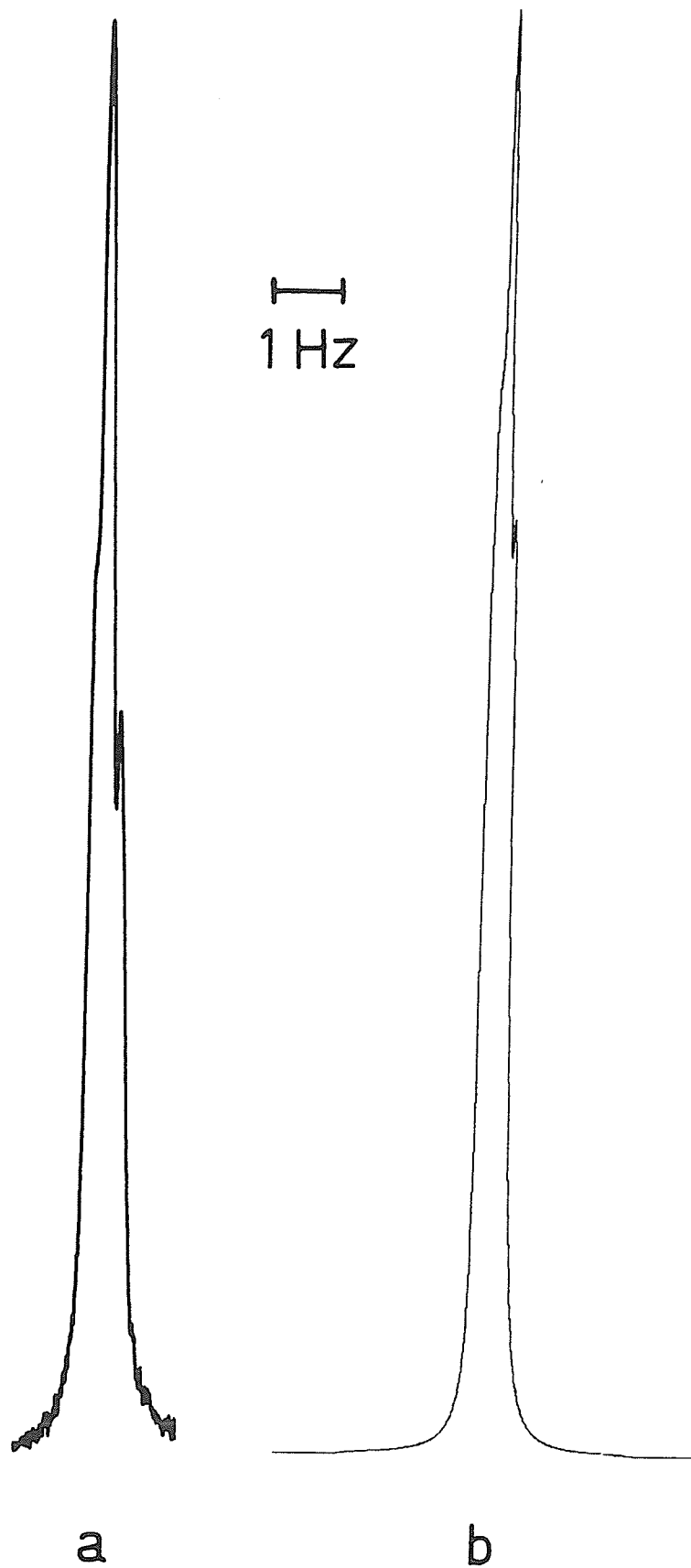
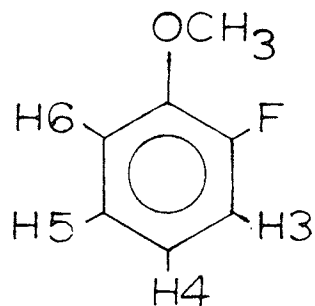


Table 2

Parameters from the Proton Spectrum of 2-Fluoroanisole^a.

ν_{CH_3}		385.959(2)	
ν_{F}		1500 ^b	
ν_3		709.369(3)	
ν_4		690.503(3)	
ν_5		709.663(4)	
ν_6		709.868(5)	
$5J_{\text{O}}^{\text{CH}_3, \text{F}}$	0.181(4)	$4J_{\text{m}}^{\text{F}, \text{H6}}$	8.697(11)
$6J_{\text{m}}^{\text{CH}_3, \text{H3}}$	0	$3J_{\text{O}}^{\text{H3}, \text{H4}}$	8.108(4)
$7J_{\text{p}}^{\text{CH}_3, \text{H4}}$	0	$4J_{\text{m}}^{\text{H3}, \text{H5}}$	1.564(6)
$6J_{\text{m}}^{\text{CH}_3, \text{H5}}$	0	$5J_{\text{p}}^{\text{H3}, \text{H6}}$	0.243(4)
$5J_{\text{O}}^{\text{CH}_3, \text{H6}}$	-0.179 ^c (4)	$3J_{\text{O}}^{\text{H4}, \text{H5}}$	7.599(6)
$3J_{\text{O}}^{\text{F}, \text{H3}}$	11.800(5)	$4J_{\text{m}}^{\text{H4}, \text{H6}}$	1.540(8)
$4J_{\text{m}}^{\text{F}, \text{H4}}$	4.555(4)	$3J_{\text{O}}^{\text{H5}, \text{H6}}$	8.202(5)
$5J_{\text{p}}^{\text{F}, \text{H5}}$	-1.178(10)		

...table 2 continued...

Table 2...

rms deviation 0.0163
largest difference 0.038
peaks observed 47
transitions assigned 283
transitions calculated 492

a At 100.001 MHz for a 4.83 mole % solution in acetone-d₆.
Chemical shifts and coupling constants are in Hertz with
internal TMS as reference. Numbers in parentheses are
standard deviations in the last decimal place, calculated
by LAME.

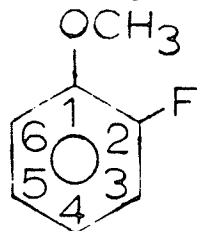
b Treated in the X approximation with no transitions assigned.

c $^5J_{O-CH_3, H6}$ is not well-determined because the near degeneracy
of the proton chemical shifts ν_5 and ν_6 causes virtual
coupling of the methyl protons and H5. See text.

Although fluorine transitions were not assigned in the spectral analysis, the simulated fluorine spectrum was consistent with observation.

The proton-decoupled carbon spectrum of this sample was assigned with reference to the assignments for the brominated 2-fluoroanisoles. Chemical shifts and carbon-fluorine coupling constants appear in Table 3, but no attempt was made to obtain carbon-hydrogen coupling constants. The signs of the carbon-fluorine coupling constants were taken from determinations for fluorobenzene^{207,250}.

Table 3

Carbon Chemical Shifts^a and Carbon-Fluorine Coupling Constants^bfor 2-Fluoroanisole in Acetone-d₆.

δ_{C1}	148.67
δ_{C2}	153.23
δ_{C3}	116.52
δ_{C4}	121.57
δ_{C5}	125.34
δ_{C6}	114.61
$1J_{C2,F}$	(-)243.98
$2J_{O,C1,F}$	10.34
$2J_{O,C3,F}$	18.04
$3J_{m,C4,F}$	6.82
$3J_{m,C6,F}$	1.98
$4J_{p,C5,F}$	3.96

a In ppm downfield from internal TMS. Probably ± 0.03 ppm.

b In Hertz.

iii) 4-bromo-2-fluoroanisole

The 100 MHz spectrum of the ring protons of a 2.96 mole % solution of 4-bromo-2-fluoroanisole- α - ^{13}C in acetone- d_6 appears as Figure 5. Results from the analysis of this spectrum and of a spectrum of the unlabelled compound at 4.52 mole % in carbon tetrachloride are presented in Table 4.

Only proton transitions were assigned in the iterative refinement of the calculated spectrum. The sign of $^5J_{\text{O}}^{\text{CH}_3, \text{H6}}$ was assumed negative¹⁴³. Calculated spectra were insensitive to the relative sign of $^5J_{\text{O}}^{\text{CH}_3, \text{F}}$ which was determined by weak irradiation experiments described below. The magnitude of $^4J_{\text{O}}^{\text{C}\alpha, \text{F}}$ should not have perturbed the other values in Table 4, but an estimate was included in the calculations. The relative sign of $^5J_{\text{m}}^{\text{C}\alpha, \text{H3}}$ was assumed from 4,6-dibromo-2-fluoroanisole- α - ^{13}C (vide infra). By comparison of the observed spectrum with calculated spectra, the effect of a non-zero $^5J_{\text{m}}^{\text{C}\alpha, \text{H5}}$ was decided: the magnitude of a small splitting in some multiplets increased. Certainly the magnitude of $^5J_{\text{m}}^{\text{C}\alpha, \text{H5}}$ was less than 0.05 Hz, if not zero (see Figure 5).

The center of the proton-decoupled fluorine resonance was found 31.063 ppm downfield from hexafluorobenzene.

Coupled and proton-decoupled carbon spectra of a 14.0 mole %

Figure 5

Spectrum of the ring protons of a 2.96 mole % solution of
4-bromo-2-fluoroanisole- α - ^{13}C in acetone- d_6 .

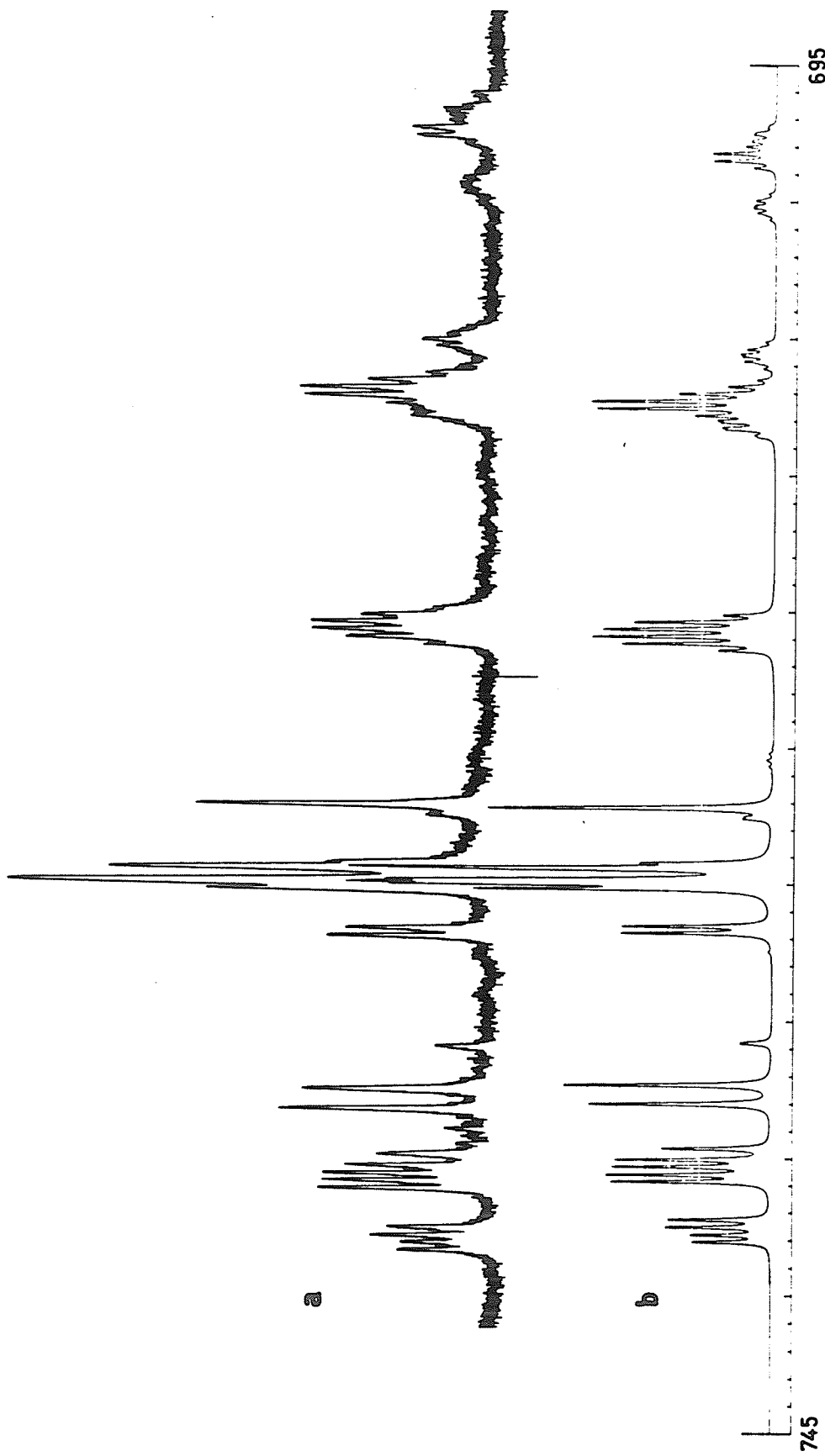
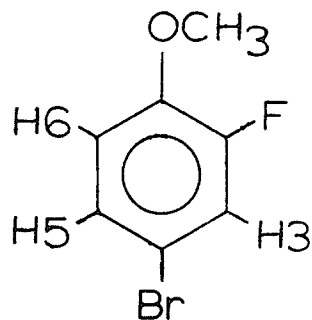


Table 4

Parameters from the Proton Spectrum of 4-Bromo-2-fluoroanisole^a.

	2.96 mole % in acetone-d ₆ (methyl ¹³ C enriched)	4.52 mole % in CCl ₄
ν_{CH_3}	387.656(1)	382.176(2)
ν_{F}	1200 ^b	1500 ^b
ν_3	730.947(3)	716.651(2)
ν_5	727.310(2)	710.361(2)
ν_6	708.200(2)	675.104(3)
$\nu_{\text{C}\alpha}$	1800 ^b	c
$^5J_{\text{OCH}_3, \text{F}}$	+ 0.173 (3)	0.340 (4)
$^5J_{\text{OCH}_3, \text{H6}}$	- 0.271 (2)	- 0.281 (3)
$^1J_{\text{CH}_3, \text{C}\alpha}$	145.132 (3)	c
$^3J_{\text{F}, \text{H3}}$	10.826 (5)	10.401 (4)
$^5J_{\text{P}, \text{H5}}$	- 1.657 (4)	- 1.659 (4)
$^4J_{\text{m}, \text{F}, \text{H6}}$	9.094 (4)	8.734 (6)
$^4J_{\text{O}, \text{F}, \text{C}\alpha}$	0.23	c
$^4J_{\text{m}, \text{H3}, \text{H5}}$	2.382 (3)	2.358 (3)

...Table 4 continued...

$5 J_{\text{p}}^{\text{H3,H6}}$	0.209 (4)	0.205 (4)
$5 J_{\text{m}}^{\text{H3,C}\alpha}$	0.264 (4)	c
$3 J_{\text{o}}^{\text{H5,H6}}$	8.783 (3)	8.689 (4)
$5 J_{\text{m}}^{\text{H5,C}\alpha}$	< 0.05	c
rms deviation	0.0133	0.0134
largest difference	0.034	0.040
peaks observed	44	36
transitions assigned	284	174
transitions calculated	442	220

a At 100.001 MHz. Chemical shifts and coupling constants are in Hertz with internal TMS as reference. Numbers in parentheses are standard deviations in the last decimal place, calculated by LAME.

b Treated in the X approximation with no transitions assigned.

c Not included in this analysis.

solution of 4-bromo-2-fluoroanisole- α - ^{13}C yielded the parameters in Table 5. The rms deviation from the average line positions for two decoupled spectra was about 0.36 Hz (0.013 ppm). Linewidths of 1 Hz or less were obtained when 0.3 Hz line broadening was applied.

Resonances were assigned with reference to the spectrum of 4,6-dibromo-2-fluoroanisole- α - ^{13}C . The C4 multiplet did not exhibit a large nuclear Overhauser enhancement.

Coupling between C α and C5 was observable, but splittings were not resolvable. Inspection of linewidths led to estimates near 0.2 Hz. Lines due to C3 or C5 had widths similar to those of multiplets in which the splittings were resolved clearly (see Figure 6).

Average carbon-hydrogen coupling constants in Table 5 were obtained from three spectra. The complexity of the C1 and C2 multiplets and the close proximity of the C1 resonances to the high-field multiplet of C2 did not allow estimation of the coupling constants between those nuclei and protons. Of the two-bond couplings involving C4 the larger was associated with H3, tentatively (see Discussion). The linewidth of the resonances of C6 suggested coupling to H5, H3, or the methyl protons, but no couplings could be resolved. The full width of each multiplet is about 1.5 Hz at half height.

Figure 6

Spectrum of the ring carbons of a 14.0 mole % solution of
4-bromo-2-fluoroanisole- α - ^{13}C in acetone- d_6 .

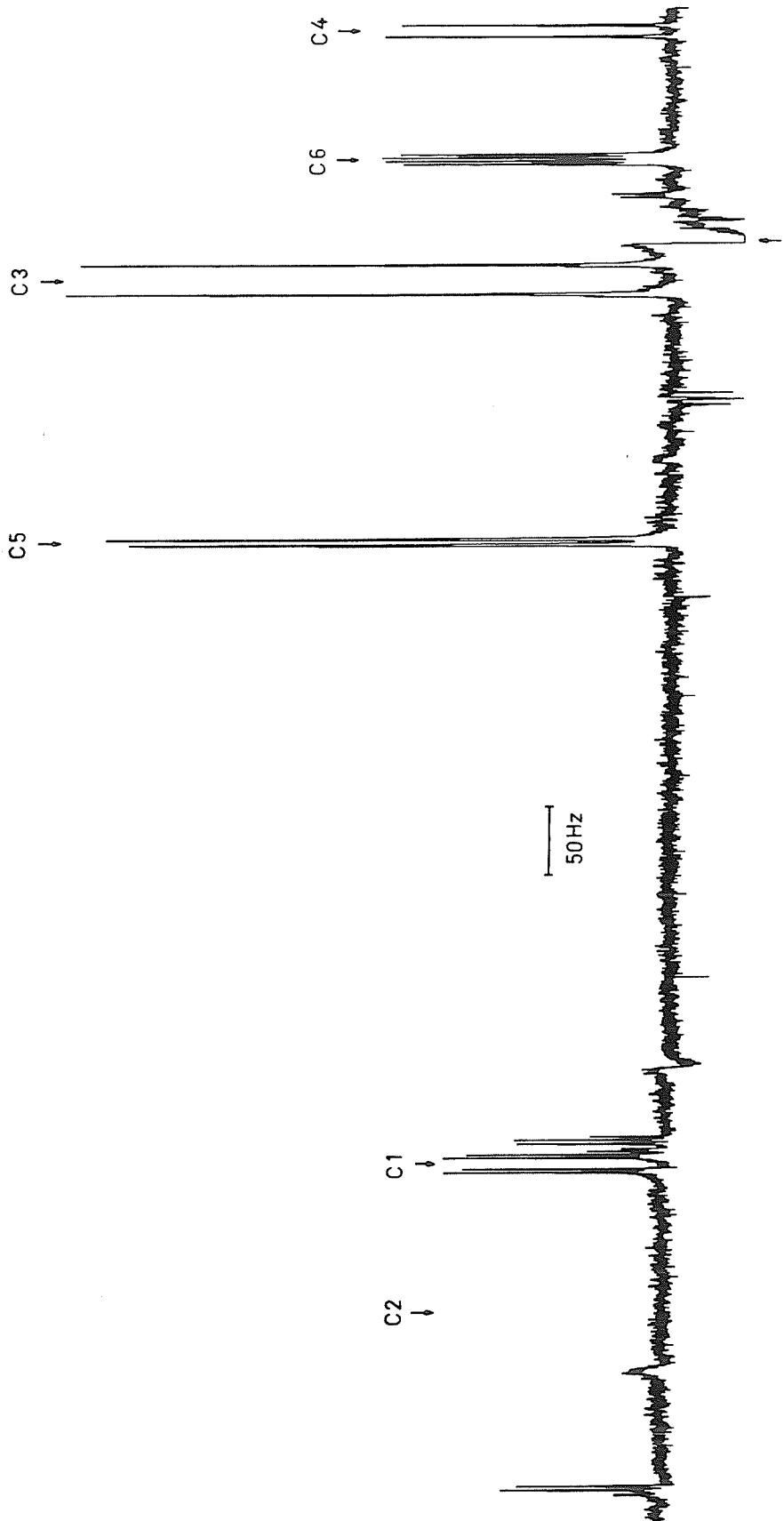
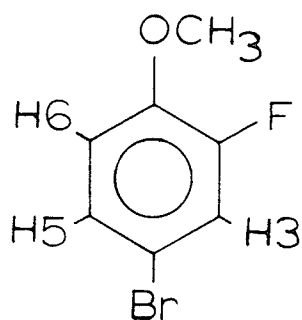


Table 5

Carbon Chemical Shifts^a and Coupling Constants^b for 4-Bromo-2-fluoroanisole in Acetone-d₆.



	$\delta_{C\alpha}$	56.95		
	δ_{C1}	148.13		
	δ_{C2}	152.97		
	δ_{C3}	119.93		
	δ_{C4}	112.05		
	δ_{C5}	128.31		
	δ_{C6}	116.11		
$2_{J_{O}}C\alpha, C1$	$\pm 2.15 \pm 0.03$		$2_{J_{O}}C1, F$	10.37 ± 0.01
$3_{J_{O}}C\alpha, C2$	2.73 ± 0.02		$1_{J}C2, F$	(-249.87 ± 0.10)
$4_{J_{m}}C\alpha, C3$	c		$2_{J_{O}}C3, F$	21.26 ± 0.01
$5_{J_{p}}C\alpha, C4$	c		$3_{J_{m}}C4, F$	8.23 ± 0.01
$4_{J_{m}}C\alpha, C5$	0.2 ± 0.1^d		$4_{J_{p}}C5, F$	4.00 ± 0.01
$3_{J_{O}}C\alpha, C6$	2.31 ± 0.01		$3_{J_{m}}C6, F$	4.75 ± 0.01
			$4_{J_{O}}C\alpha, F$	$+ 0.24 \pm 0.01$

..Table 5 continued...

Table 5...

1_{J}C3,H	167.53 ± 0.17	1_{J}C5,H	168.51 ± 0.33
$3_{\text{J}_m}\text{C3,H5}$	6.15 ± 0.01	$3_{\text{J}_m}\text{C5,H3}$	6.35 ± 0.26
$4_{\text{J}_p}\text{C3,H6}$	$(-)\text{0.87} \pm 0.05$	$2_{\text{J}_o}\text{C5,H6}$	$\pm 1.23 \pm 0.05$
$2_{\text{J}_o}\text{C4,H3}$	$\pm 4.66 \pm 0.14^e$	1_{J}C6,H	163.59 ± 0.05
$2_{\text{J}_o}\text{C4,H5}$	$\pm 3.40 \pm 0.20^e$	$4_{\text{J}_p}\text{C6,H3}$	f
$3_{\text{J}_m}\text{C4,H6}$	7.96 ± 0.14	$2_{\text{J}_o}\text{C6,H5}$	f
		$1_{\text{J}}\text{C}\alpha,\text{H}$	145.13 ± 0.05

- a In ppm downfield from internal TMS. Probably ± 0.04 ppm.
- b In Hertz.
- c Unobserved
- d Unresolved, but estimated from the linewidth.
- e Tentative assignment (see Discussion).
- f Unresolved. FWHH is about 1.5 Hz for the resonances of C6.

- a) determination of relative sign of $^5J_{\text{O}}^{\text{CH}_3, \text{F}}$ by weak irradiation experiments

If a nuclear spin couples weakly to other spins, transitions between energy levels can be assigned to particular nuclei. The position of a transition within a resonance multiplet reflects the magnetic environment of the nucleus; each position is associated with a specific orientation for each spin which is coupled to the nucleus undergoing the transition. However, the high-resolution nmr hamiltonian is symmetric with respect to reversal of all signs. If spin states are designated by + and -, and if the low-field transition is designated + when the coupling constant is positive, the relative signs may be deduced by weak irradiation experiments.

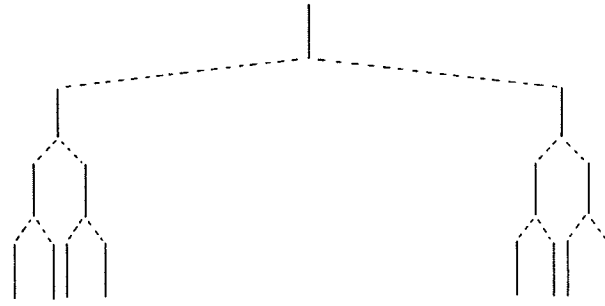
Weak irradiation of a transition within the resonance multiplet of a nuclear spin affects transitions within the multiplets of coupled nuclei. The signs of the coupling constants determine which transitions have energy levels in common and perturbation of one such transition will affect the others such that relative signs can be ascertained by multiple resonance.

A first-order representation of the line spectrum of the methyl protons, of the methyl carbon, and of parts of the multiplets due to H6 is depicted in Figure 7. It follows the relative signs from Table 4 and an extension of the conventions described above. The observed spectrum of H6 and of the low-field multiplet

Figure 7

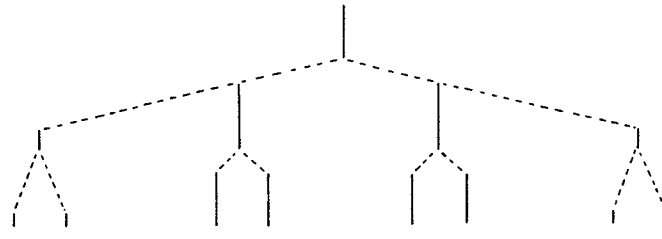
A first-order representation of the line spectrum of the methyl proton, of the methyl carbon, and of parts of the multiplets due to H6 of 4-bromo-2-fluoroanisole.

CH₃



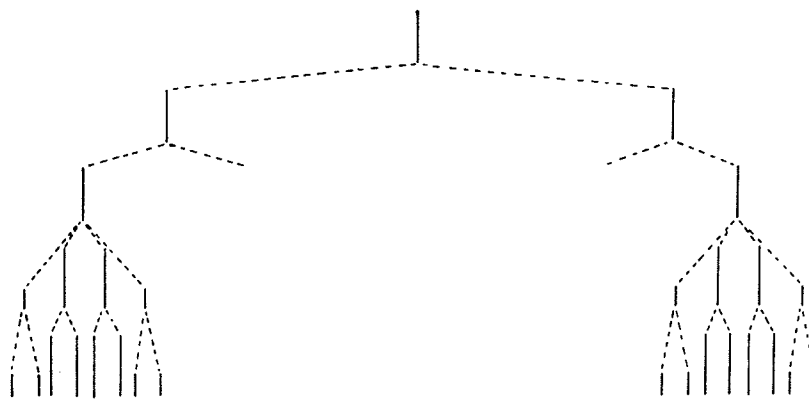
C	+	++	+	-	--	-
F	+	+-	-	+	+-	-
H6	-	+-	+	-	+-	+
	1	2 3	4	5	6 7	8

C



CH ₃	+3/2		+1/2		-1/2		-3/2	
F	+	-	+	-	+	-	+	-
	1	2	3	4	5	6	7	8

H6



F	+	-				
H5	+	-				
CH ₃	$-\frac{3}{2}$	$-\frac{1}{2}$	$+\frac{1}{2}$	$+\frac{3}{2}$		
H3	+	--	+-	+-	-	
	1			8	25	32

of the methyl protons appears in Figure 8.

Weak irradiation of line 1 or line 8 caused a reduction in the intensity of the low-field part of the methyl proton resonance (see Figure 8). These lines were associated with the + designation for the fluorine nucleus since the sign of ${}^4J_{\text{m}}^{\text{F,H6}}$ is positive. Therefore, the effected methyl resonances also had this designation and the positive sign of ${}^5J_{\text{O}}^{\text{CH}_3,\text{F}}$ was realized. As a further check on this assignment the second field was moved to the midst of the high-field member of the H6 resonance. Weak irradiation of these lines, designated F-, produced a decrease in the intensity on the high-field side of the methyl resonance, as predicted.

b) the relative sign of ${}^4J_{\text{O}}^{\text{C}\alpha,\text{F}}$

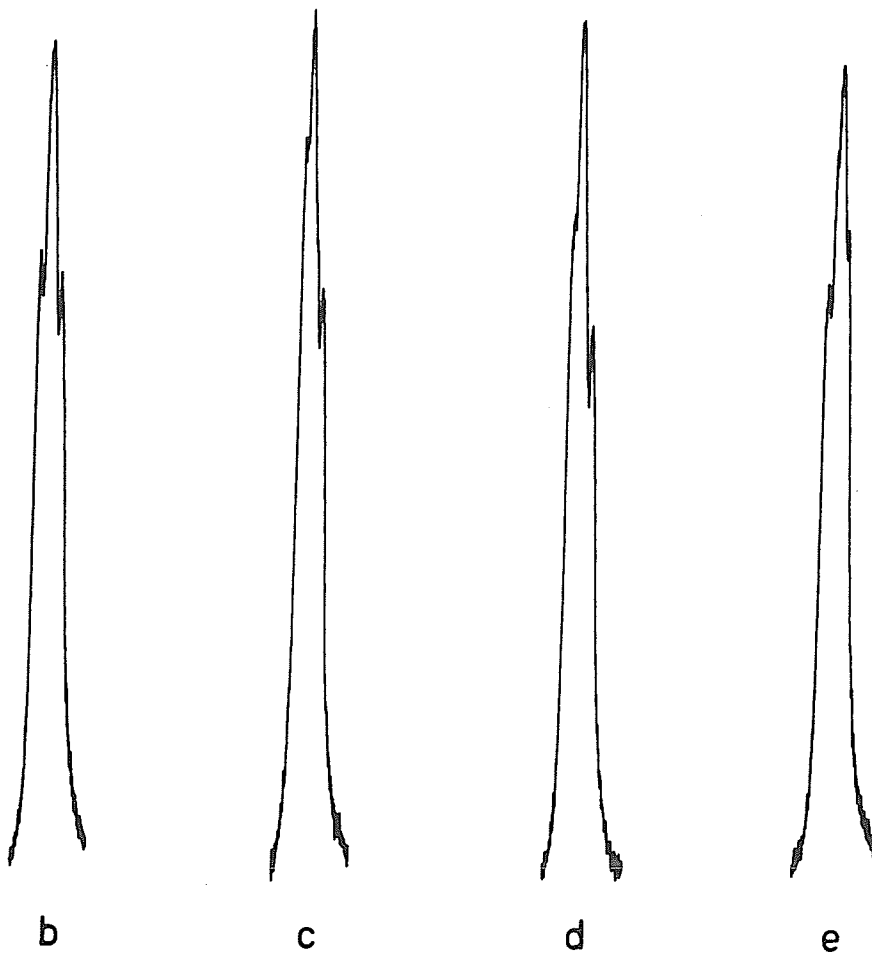
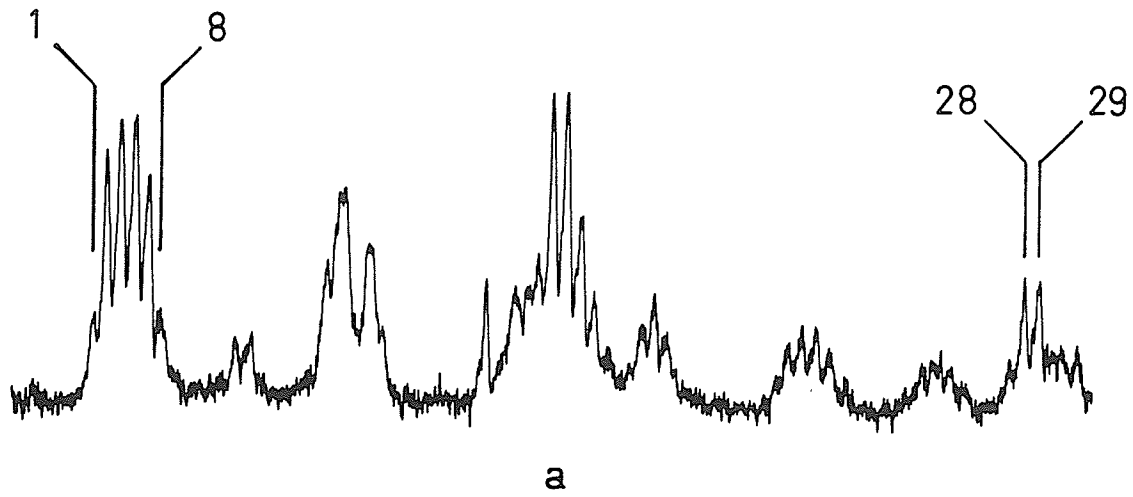
An attempt was made to determine the relative sign of ${}^4J_{\text{O}}^{\text{C}\alpha,\text{F}}$, but the small magnitude of this coupling was a hindrance. The spectrum of the methyl carbon nucleus in a 14.0 mole % solution was observed while the low-field line of the low-field methyl proton multiplet was irradiated weakly. Since the irradiated line corresponded to the + designation for the fluorine nucleus, the altered lines shared this designation. The observed reduction of intensity for the line at lowest field in the methyl carbon spectrum suggested the positive sign for ${}^4J_{\text{O}}^{\text{C}\alpha,\text{F}}$.

Figure 8

Spectrum of H6 and of the low-field multiplet of the methyl protons of 4-bromo-2-fluoroanisole.

- a the multiplet of H6 with the irradiated lines numbered according to the scheme introduced in Figure 7
- b the low-field multiplet of the methyl protons in the absence of weak irradiation
- c in the presence of weak irradiation of the line numbered 1
- d in the presence of weak irradiation of the line numbered 8
- e in the presence of weak irradiation between the lines numbered 28 and 29

1 Hz
┌───┐



iv) 4,6-dibromo-2-fluoroanisole

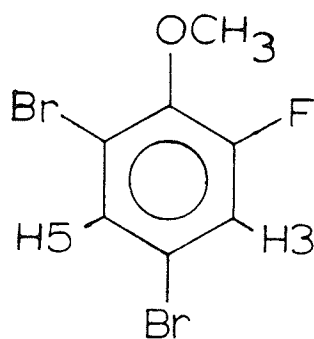
Results of the analysis of proton spectra of a 3.79 mole % solution of 4,6-dibromo-2-fluoroanisole in carbon tetrachloride and of a 15.5 mole % solution of 4,6-dibromo-2-fluoroanisole- α - ^{13}C in acetone- d_6 appear in Table 6. The ring proton resonances can be assigned unequivocally on the basis of the large downfield shift of H5, due to two bromines at ortho positions, and the large splitting of H3, due to coupling over three bonds to the fluorine nucleus. A spectrum appears as Figure 9. Of course the chemical shifts are solvent dependent^{3,215}.

Lack of discernable sharpening of these resonances when one of the methyl proton multiplets is irradiated strongly precludes coupling between methyl and ring protons. However, coupling between the methyl protons and the fluorine is obvious in the proton spectrum and in the fluorine spectrum, which appears in Figure 10. And the methyl carbon certainly couples with both ring protons and with the fluorine. The relative signs of $^5\text{J}_{\text{O}}^{\text{CH}_3,\text{F}}$, $^4\text{J}_{\text{O}}^{\text{C}\alpha,\text{F}}$, $^5\text{J}_{\text{m}}^{\text{C}\alpha,\text{H3}}$, and $^5\text{J}_{\text{m}}^{\text{C}\alpha,\text{H5}}$ can all be determined by weak irradiation experiments described below.

The increase in $^3\text{J}_{\text{O}}^{\text{F},\text{H3}}$ with solvent polarity was not unexpected²¹⁰. $^4\text{J}_{\text{m}}^{\text{F},\text{H}}$ has been shown to depend on the solvent, although $^5\text{J}_{\text{p}}^{\text{F},\text{H}}$ was invariant.

The center of the ^{12}C -methyl proton resonance lay 0.215 Hz downfield from the center of the ^{13}C -methyl resonance at

Table 6

Parameters from the Proton Spectrum of 4,6-Dibromo-2-fluoroanisole^a.

	3.79 mole % in CCl ₄ at 100.001 MHz	15.5 mole % in acetone-d ₆ at 90.0234 MHz (methyl ¹³ C enriched)
ν_{CH_3}	390.420 (0)	354.295 (1)
ν_{F}	1500 ^b	1000.199 ^c (1)
ν_3	717.432 (0)	666.397 (1)
ν_5	743.175 (0)	679.186 (1)
$\nu_{\text{C}\alpha}$	d	1500 ^b
$^5J_{\text{O}}^{\text{CH}_3, \text{F}}$	1.569 (1)	+1.484 (1)
$^3J_{\text{O}}^{\text{F}, \text{H}3}$	10.187 (1)	10.424 (1) ^e
$^5J_{\text{P}}^{\text{F}, \text{H}5}$	-1.898 (1)	-1.904 (1)
$^4J_{\text{m}}^{\text{H}3, \text{H}5}$	2.302 (1)	2.313 (1)
$^1J_{\text{C}\alpha, \text{H}}$	d	146.190 (2)
$^4J_{\text{O}}^{\text{C}\alpha, \text{F}}$	d	4.874 (2)
$^5J_{\text{m}}^{\text{C}\alpha, \text{H}3}$	d	+0.216 (2)
$^5J_{\text{m}}^{\text{C}\alpha, \text{H}5}$	d	+0.279 (2)

...Table 6 continued...

rms deviation	0.0021	0.0065
largest difference	0.005	0.017
peaks observed	10	49
transitions assigned	80	202
transitions calculated	80	208

- a In Hertz. Numbers in parentheses are standard deviations in the last decimal place, calculated by LAME.
- b Treated in the X approximation with no transitions assigned.
- c Treated in the X approximation. The numerical value is not significant.
- d Not included in this analysis.
- e Usual solvent effect on magnitude of $^3J_{H,F}$ (ref. 210)

Figure 9

Spectrum of the ring protons of a 15.5 mole % solution of
4,6-dibromo-2-fluoroanisole- α - ^{13}C in acetone- d_6 at 100 MHz.

a observed spectrum

b calculated spectrum

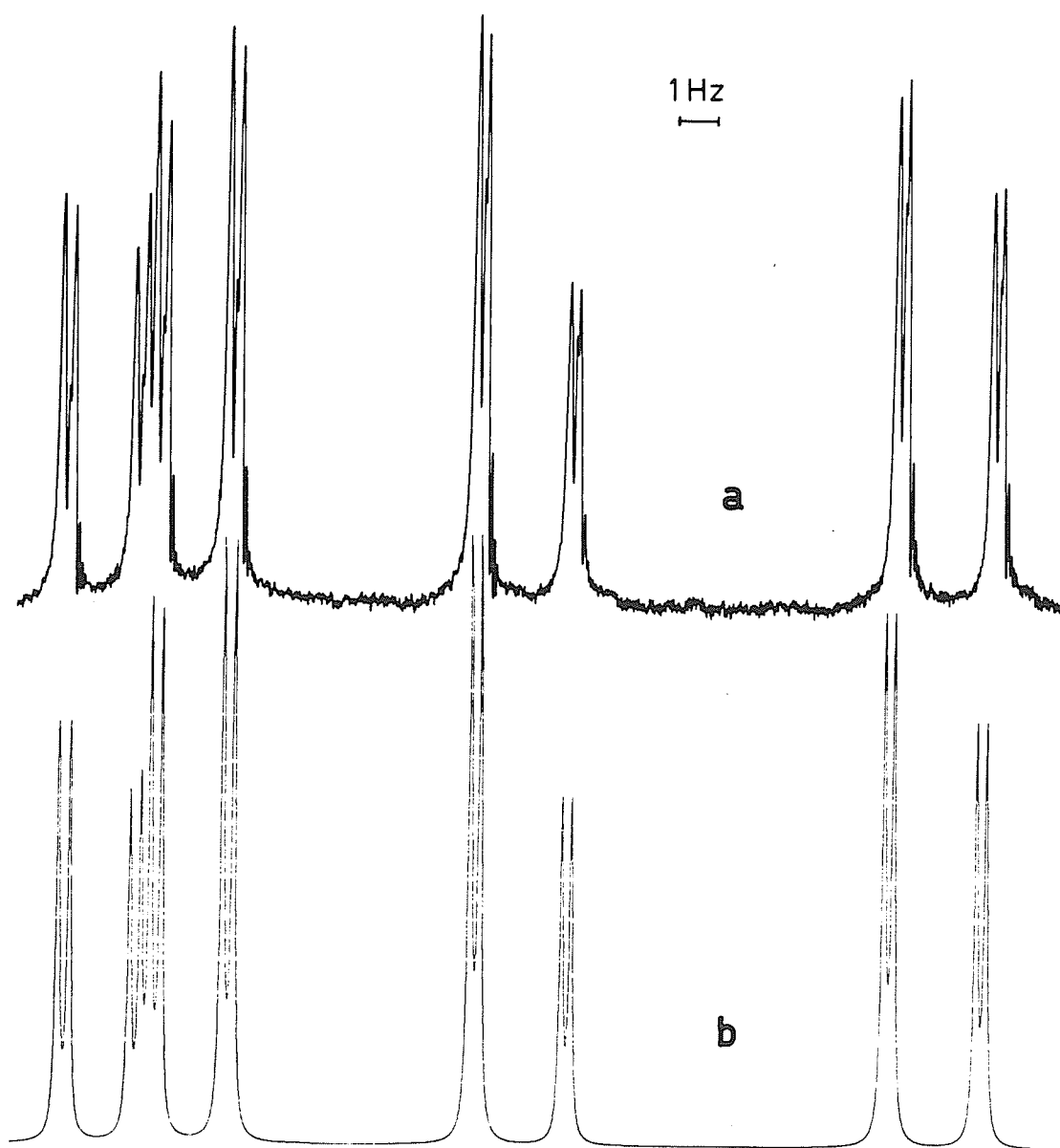
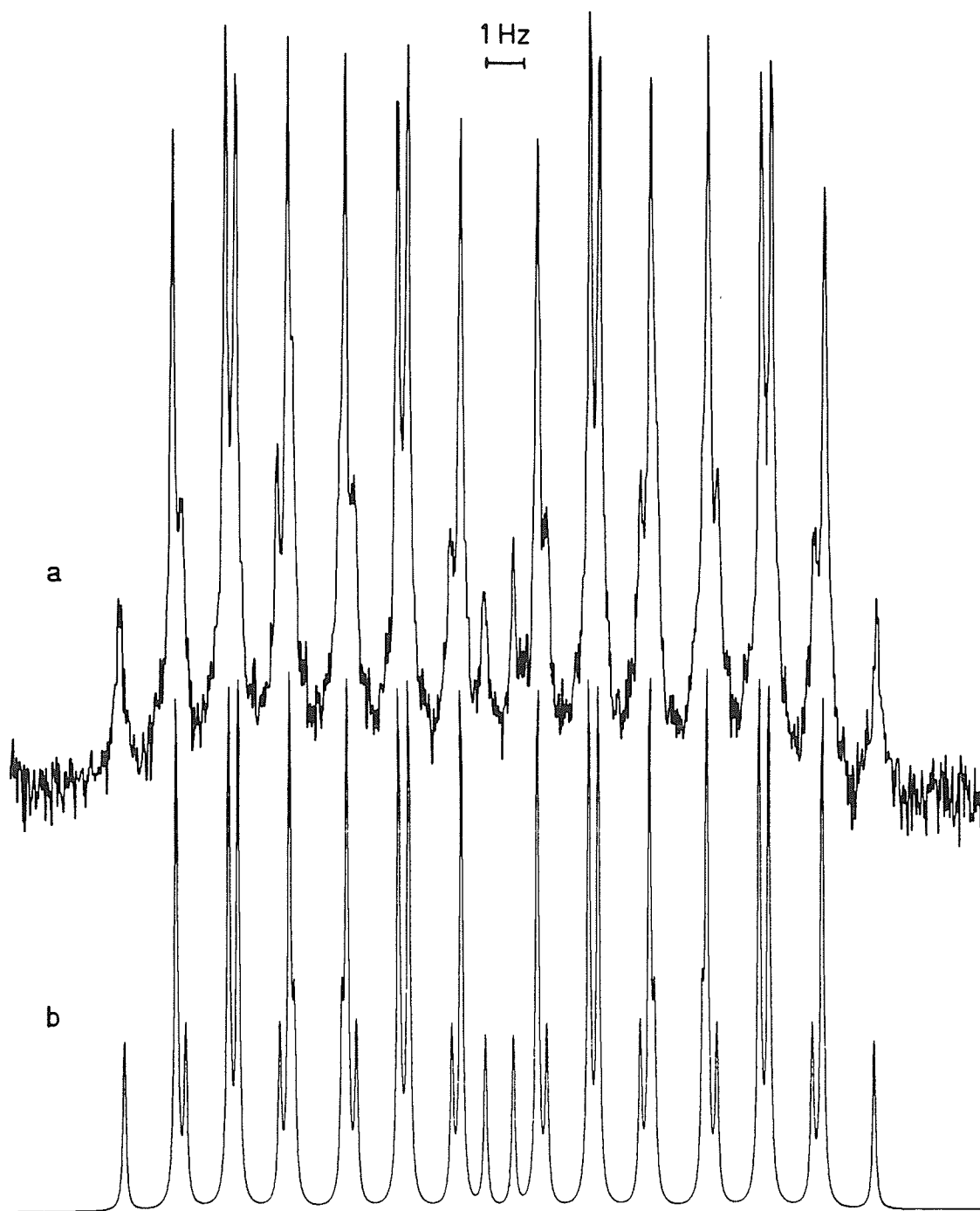


Figure 10

Fluorine spectrum of a 15.5 mole % solution of 4,6-dibromo-2-fluoroanisole- α - ^{13}C in acetone- d_6 .

a observed

b calculated



90.0234 MHz which implied an isotope shift of about -0.0024 ppm. A linewidth of about 0.2 Hz was typical. The digital resolution was 0.049 Hz/real point.

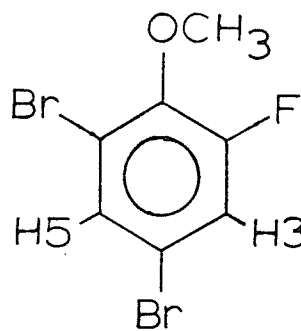
The fluorine spectrum of the 15.5 mole % solution was acquired with 0.024 Hz/real point. The linewidth for the spectrum in Figure 10 was about 0.15 Hz. The center of the proton-decoupled fluorine resonance occurred at 38.471 ppm downfield from hexafluorobenzene.

Table 7 presents the chemical shifts and coupling constants determined for carbon spectra of a 9.47 mole % solution of 4,6-dibromo-2-fluoroanisole, a 1.83 mole % solution of 4,6-dibromo-2-fluoroanisole- α - ^{13}C , and a 15.5 mole % solution of the methyl- ^{13}C -enriched compound in acetone- d_6 . Chemical shifts are derived from at least three proton-decoupled spectra of the 15.5 mole % solution. The rms deviation from the average line positions is about 0.24 Hz (0.011 ppm). As indicated by the well-resolved small splittings in Figure 11, linewidths are 0.8 Hz or less when 0.1 Hz line broadening is applied.

Coupling constants between carbon nuclei and protons were estimated from spectra of the 9.47 mole % and 1.83 mole % solutions. Proton couplings to C1 were not obtained because the peak intensity was too low under the experimental conditions. Similarly, the couplings to C2 were not well-defined. The difference between the two-bond couplings involving C4 was not discerned.

Table 7

Carbon Chemical Shifts^a and Coupling Constants^b for 4,6-Dibromo-2-fluoroanisole in Acetone-d₆.



	$\delta_{C\alpha}$	61.88		
	δ_{C1}	145.81		
	δ_{C2}	156.45		
	δ_{C3}	120.76		
	δ_{C4}	116.16		
	δ_{C5}	131.74		
	δ_{C6}	118.93		
$^2J_{C\alpha, C1}$	$\pm 3.23 \pm 0.01$		$^2J_{C1, F}$	12.87 ± 0.04
$^3J_{C\alpha, C2}$	1.51 ± 0.01		$^1J_{C2, F}$	(-253.82 ± 0.01)
$^4J_{C\alpha, C3}$	0.66 ± 0.04		$^2J_{C3, F}$	22.99 ± 0.02
$^5J_{C\alpha, C4}$	0.94 ± 0.02		$^3J_{C4, F}$	10.01 ± 0.01
$^4J_{C\alpha, C5}$	0.55 ± 0.04		$^4J_{C5, F}$	3.61 ± 0.01
$^3J_{C\alpha, C6}$	1.90 ± 0.03		$^3J_{C6, F}$	3.55 ± 0.01
			$^4J_{C\alpha, F}$	$+4.82 \pm 0.09$

...Table 7 continued...

Table 7...

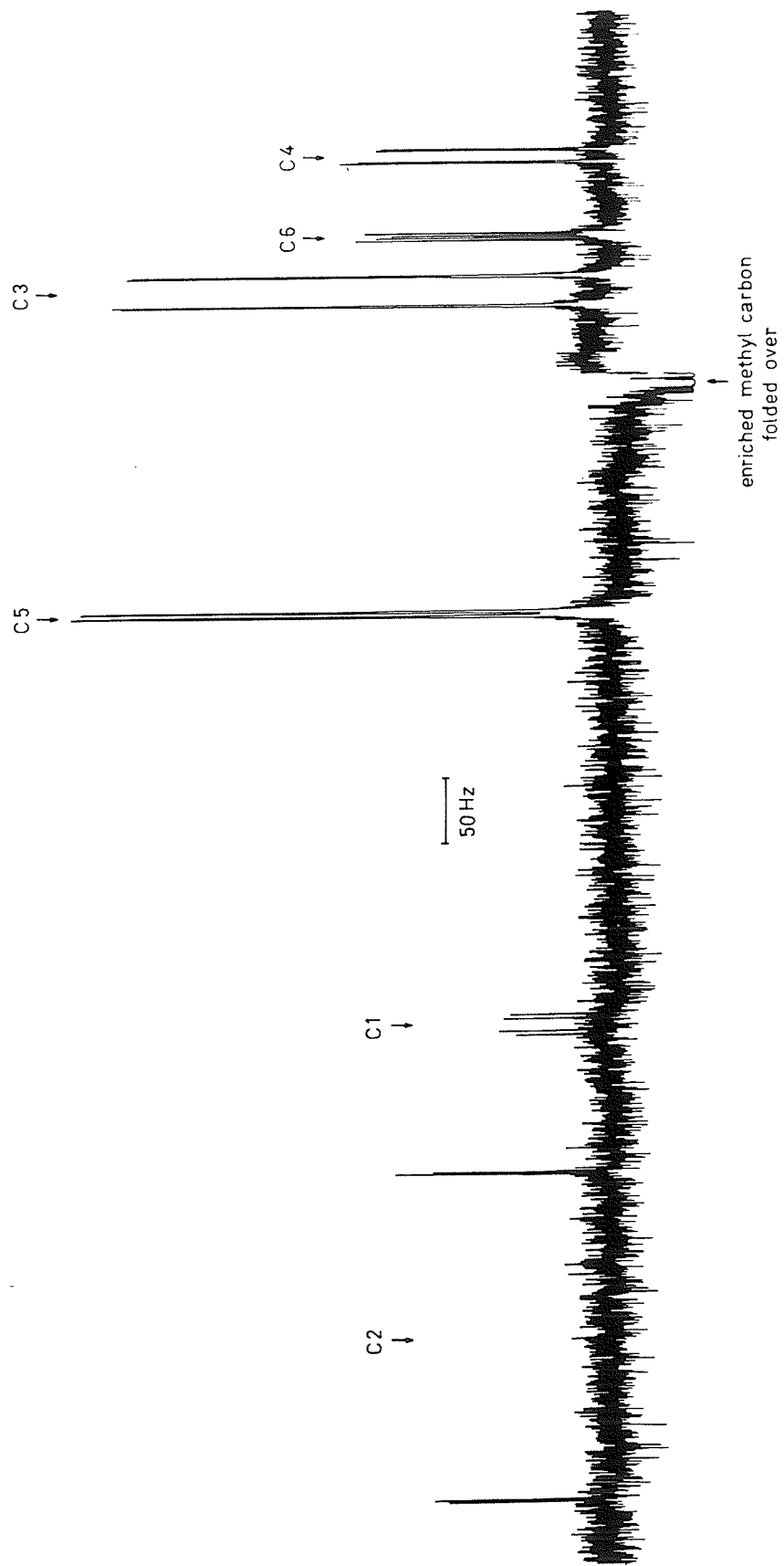
$^2_{\text{J}_o} \text{C2,H3}$	$\pm 6.1 \pm 0.4$	$^1_{\text{J}} \text{C5,H}$	173.94 ± 0.09
$^4_{\text{J}_p} \text{C2,H5}$	$(-) 2.0 \pm 0.2$	$^3_{\text{J}_m} \text{C5,H3}$	6.54 ± 0.06
$^1_{\text{J}} \text{C3,H}$	170.7 ± 0.1	$^4_{\text{J}_p} \text{C6,H3}$	$(-) 1.90 \pm 0.07$
$^3_{\text{J}_m} \text{C3,H5}$	6.5 ± 0.1	$^2_{\text{J}_o} \text{C6,H5}$	$\pm 3.89 \pm 0.06$
$^2_{\text{J}_o} \text{C4,H3}$	$\pm 4.3 \pm 0.1$	$^1_{\text{J}} \text{C}\alpha,\text{H}$	146.24 ± 0.04
$^2_{\text{J}_o} \text{C4,H5}$	$\pm 4.3 \pm 0.1$		

a In ppm downfield from internal TMS. Probably ± 0.03 ppm.

b In Hertz.

Figure 11

Spectrum of the ring carbons of a 15.5 mole % solution of 4,6-dibromo-2-fluoroanisole- α - ^{13}C in acetone- d_6 in the presence of strong irradiation (decoupling) of protons.



- a) determination of the relative sign of ${}^4J_{\text{O}}^{\text{C}\alpha,\text{F}}$ by weak irradiation experiments

First-order diagrams for the line spectrum of the methyl protons, of the fluorine, and of the methyl carbon appear in Figure 12. Signs are from Table 6.

While observing the fluorine spectrum, the methyl proton line 1 was irradiated weakly. This line was designated + for the carbon nucleus and the effected transitions must have shared this orientation. By comparison of the spectrum with Figure 12 the sign of ${}^4J_{\text{O}}^{\text{C}\alpha,\text{F}}$ was found to be positive. Weak irradiation of line 3 of the methyl proton spectrum led to reduced intensity for the fluorine transitions designated - for the carbon nucleus, which is consistent with a positive relative sign for ${}^4J_{\text{O}}^{\text{C}\alpha,\text{F}}$.

- b) determination of the relative sign of ${}^5J_{\text{O}}^{\text{CH}_3,\text{F}}$ by weak irradiation experiments

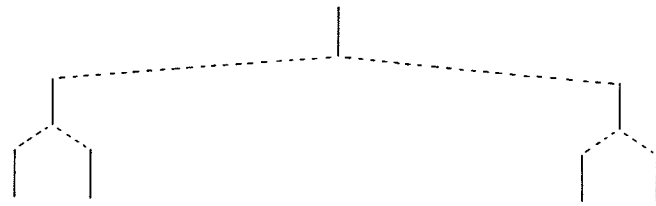
Spectra of the methyl carbon nucleus were acquired while irradiating line 1, line 3, or line 4 of the methyl proton spectrum. These transitions were associated with the fluorine nuclear orientations +, +, and - respectively, the relative sign of ${}^4J_{\text{O}}^{\text{C}\alpha,\text{F}}$ having been determined. By comparison of the carbon spectra with Figure 12, the relative sign of ${}^5J_{\text{O}}^{\text{CH}_3,\text{F}}$ was found to be positive.

Spectra are displayed in Figure 13.

Figure 12

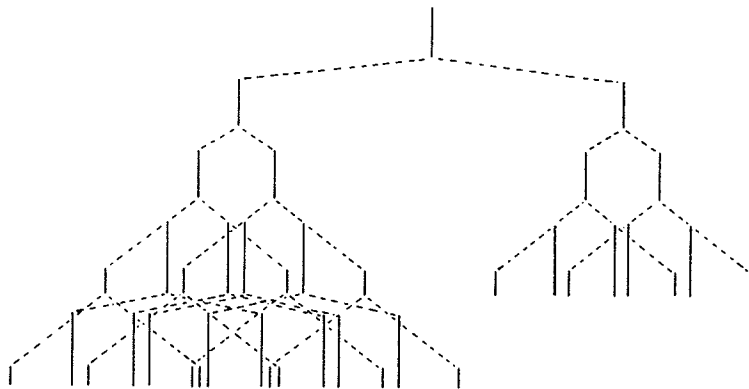
A first-order representation of the line spectrum of the methyl protons, of the fluorine, and of the methyl carbon of 4,6-dibromo-2-fluoroanisole.

CH₃



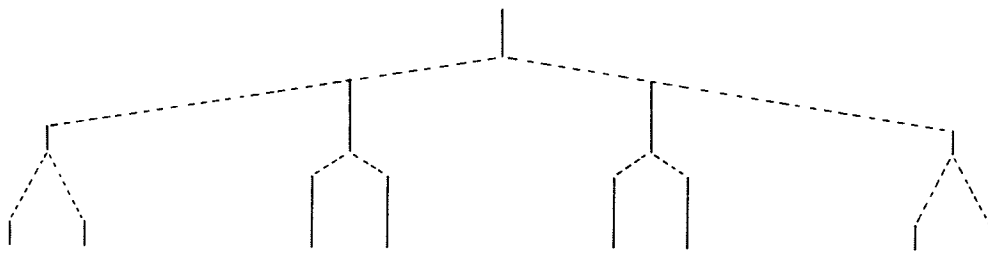
C	+	+			-	-
F	+	-			+	-
	1	2			3	4

F



H3				+											
H5	-	-	+	-	+	-	+	-	+	-	+	-	+	-	-
CH ₃	+ ^{3/2}	+ ^{1/2}	+ ^{3/2}												- ^{3/2}
C	+	++	++	+++				---	---	---	---	---	---	---	-
	1	2	3	4	5					12	13	14	15	16	

C

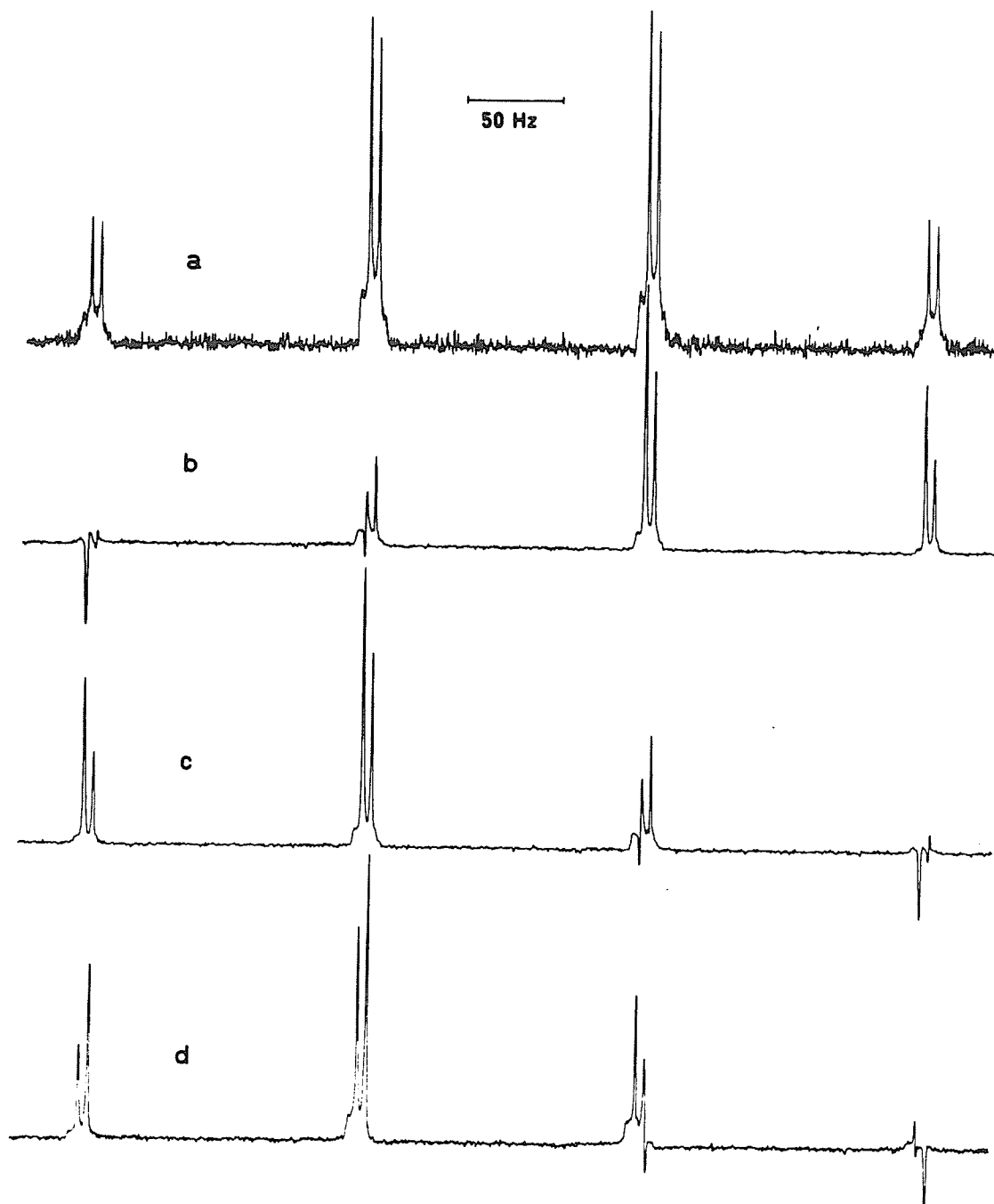


CH ₃		+ ^{3/2}		+ ^{1/2}		- ^{1/2}		- ^{3/2}	
F	+	-		+	-	+	-	+	-
	1	2		3	4	5	6	7	8

Figure 13

Spectra of the methyl carbon of a 15.5 mole % solution of 4,6-dibromo-2-fluoroanisole- α - ^{13}C in acetone- d_6 .

- a the methyl carbon multiplet in the absence of weak irradiation
- b in the presence of weak irradiation of the line numbered 1 in the methyl proton spectrum in Figure 12
- c in the presence of weak irradiation of the line numbered 3
- d in the presence of weak irradiation of the line numbered 4



- c) determination of relative signs of ${}^5J_m^{C\alpha,H3}$ and ${}^5J_m^{C\alpha,H5}$ by weak irradiation experiments

First-order representations of the line spectra of H3 and H5 appear in Figure 14.

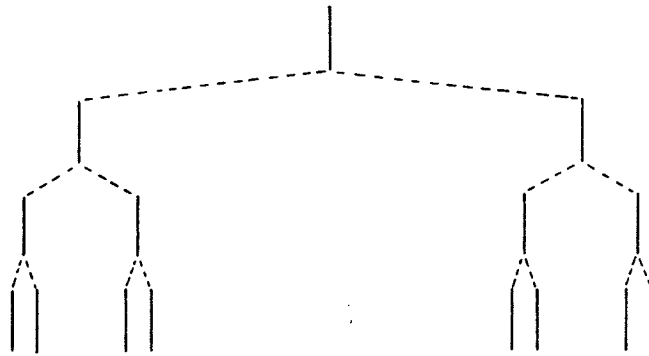
Weak irradiation of the fluorine transition corresponding to line 2 in Figure 12, and designated + for H3, - for H5, and + for C α , reduced the intensity of lines 3 and 7 in the H3 resonance and of line 1 and 3 in the H5 resonance. Since ${}^4J_o^{C\alpha,F}$ was determined to be positive, it was inferred from Figure 14 that both ${}^5J_m^{C\alpha,H3}$ and ${}^5J_m^{C\alpha,H5}$ are positive.

Moreover, weak irradiation of line 7 or line 8 of the resonance of H3 decreased the intensity of line 1 or line 2, respectively, in the resonance of H5. From Figure 14 this result implied that both ${}^5J_m^{C\alpha,H}$ have the same sign.

Figure 14

A first-order representation of the line spectrum of H3 and H5 of 4,6-dibromo-2-fluoroanisole.

H3



F

++ ++

-- --

H5

++ --

++ --

C

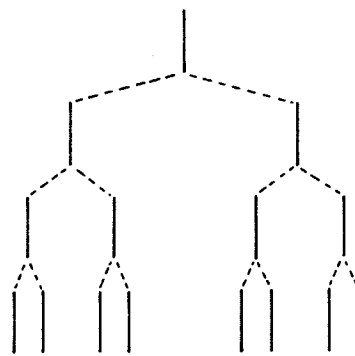
+- +-

+- +-

1 2 3 4

5 6 7 8

H5



H3

++ ++

-- --

F

-- ++

-- ++

C

+- +-

+- +-

1 2 3 4

5 6 7 8

v) 2,3,5,6-tetrafluoroanisole

The 100 MHz proton spectrum of a 4.70 mole % solution of 2,3,5,6-tetrafluoroanisole in acetone- d_6 appears in Figure 15.

Analyses of the 90.02 and 100 MHz spectra, with all fluorine-fluorine coupling constants kept zero, yielded the parameters in Table 8. No coupling between the methyl protons and the meta fluorines or H4 was observed. Linewidths of about 0.2 Hz were obtained at 90.02 MHz and a digital resolution of 0.073 Hz/real point was used.

The fluorine spectrum appearing in Figure 16 was analyzed as an $A_3BXX'YY'$ spin system with proton chemical shifts from the 90.02 MHz spectrum. The linewidth was 0.2 Hz with 0.02 Hz line broadening and 0.024 Hz/real point. Only fluorine transitions were assigned.

Fluorine nuclei F2 and F6, which resonate 5.044 ppm downfield from hexafluorobenzene, and F3 and F5, which resonate 21.843 ppm downfield from hexafluorobenzene, form isochronous but magnetically non-equivalent pairs. It is doubtless that $^4J_m^{F2,F6}$ and $^4J_m^{F3,F5}$ have the same sign; the spectrum of F2 and F6 changes dramatically if the signs are opposite. This region is also sensitive to the signs of these coupling constants relative to the other ring couplings, but the changes in calculated spectra are not sufficient to decide the sign by comparison with observed spectra. Tentatively the negative

Figure 15

Proton spectrum of a 4.70 mole % solution of 2,3,5,6-tetrafluoroanisole in acetone- d_6 .

a the methyl proton multiplet

b the ring proton multiplet

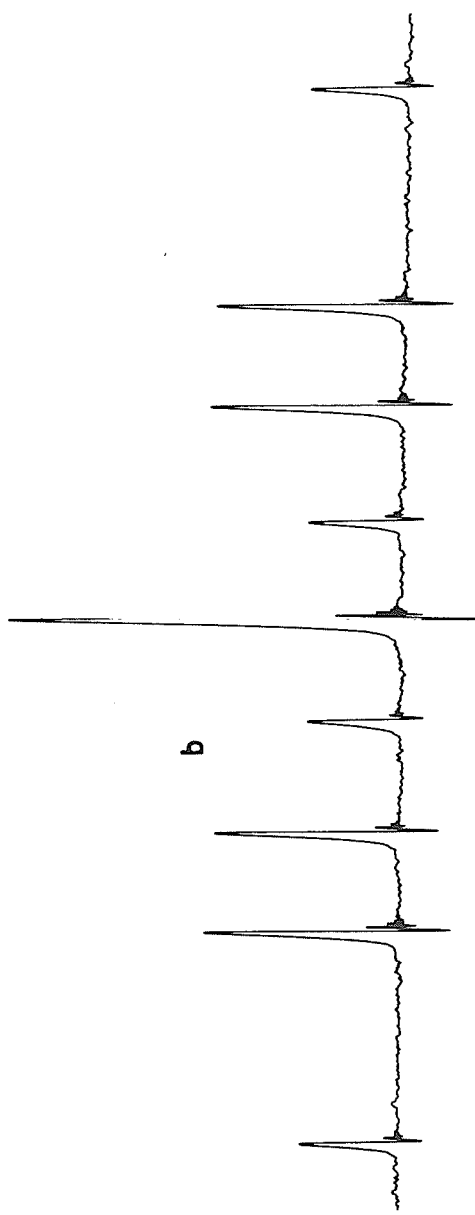
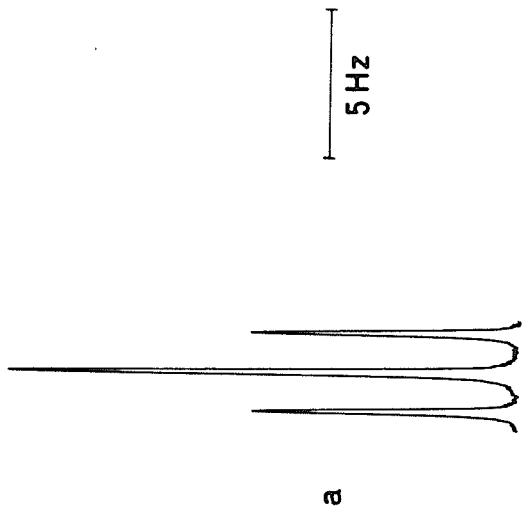
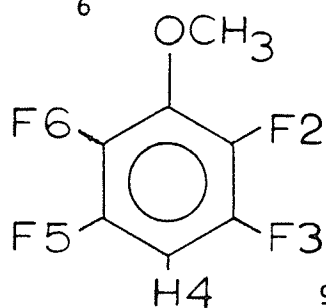


Table 8

Parameters from the Proton Spectrum of 2,3,5,6-Tetrafluoroanisole^a
in Acetone-d₆.



	90.0234 MHz	100.001 MHz
ν_{CH_3}	368.980 (0)	409.828 (0)
$\nu_{\text{F2}} = \nu_{\text{F6}}$	1500 ^b	1500 ^b
$\nu_{\text{F3}} = \nu_{\text{F5}}$	1500 ^b	1500 ^b
ν_4	643.654 (0)	714.470 (0)
${}^5J_{\text{O}} \text{CH}_3, \text{F2} = {}^5J_{\text{O}} \text{CH}_3, \text{F6}$	1.340 (0)	1.349 (0)
${}^4J_{\text{m}} \text{F2, H4} = {}^4J_{\text{m}} \text{F6, H4}$	7.205 (0)	7.204 (0)
${}^3J_{\text{O}} \text{F3, H4} = {}^3J_{\text{O}} \text{F5, H4}$	10.575 (0)	10.579 (0)
rms deviation	0.0022	0.0029
largest difference	0.006	0.013
peaks observed	12	12
transitions assigned	224	224
transitions calculated	224	224

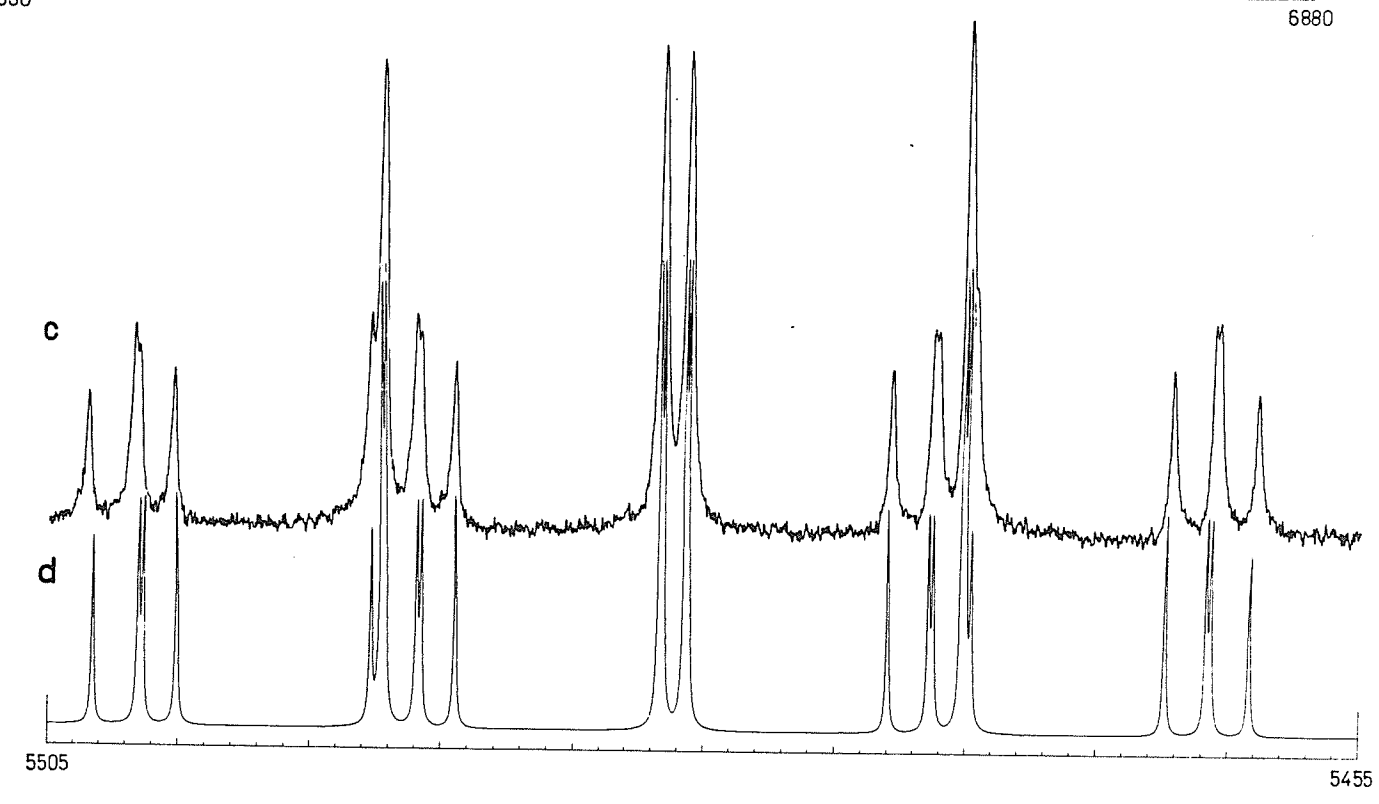
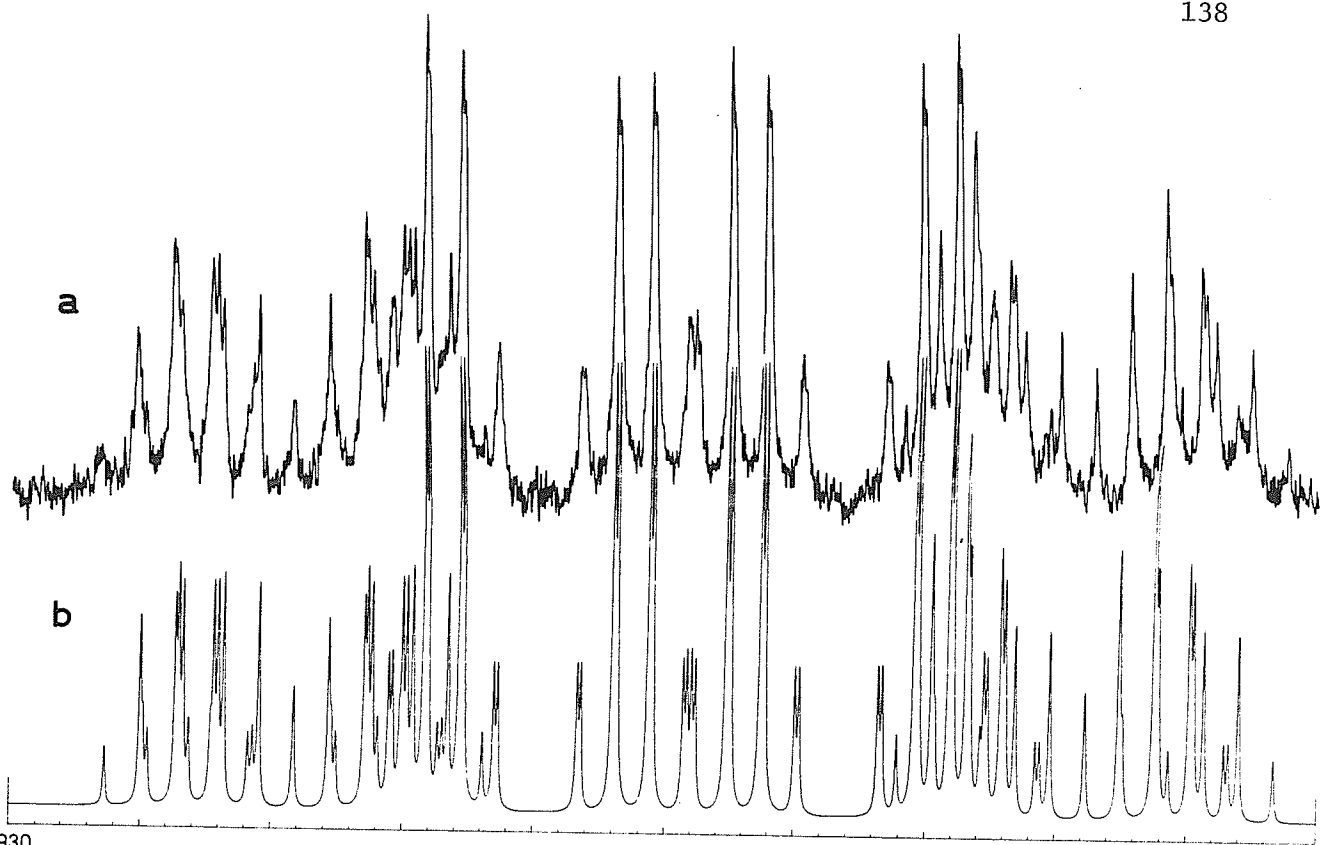
a In Hertz. Numbers in parentheses are standard deviations in last decimal place, calculated by LAME.

b Treated in the X approximation with no transitions assigned and all fluorine-fluorine spin-spin coupling constants kept zero.

Figure 16

Fluorine spectrum of a 4.70 mole % solution of 2,3,5,6-tetrafluoroanisole in acetone-d₆.

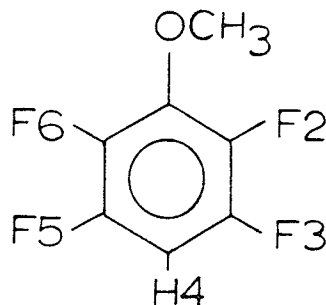
- a observed spectrum of F2 and F6
- b calculated spectrum of F2 and F6
- c observed spectrum of F3 and F5
- d calculated spectrum of F3 and F5



sign is preferred (see Discussion). The results of the analysis appear in Table 9. A correlation coefficient of 0.6667 exists between ${}^3J_{\text{O}}^{\text{F2,F3}}$ and ${}^5J_{\text{p}}^{\text{F2,F5}}$.

Table 9

Parameters from the Fluorine Spectrum of 2,3,5,6-Tetrafluoro-
anisole^a in Acetone-d₆.



ν_{CH_3}	368.980 ^b
$\nu_{\text{F2}} = \nu_{\text{F6}}$	6904.000 ^c (2)
$\nu_{\text{F3}} = \nu_{\text{F5}}$	5481.261 ^c (2)
ν_4	643.654 ^b
$^5J_{\text{o}}^{\text{CH}_3, \text{F}}$	1.345 (2)
$^3J_{\text{o}}^{\text{F2, F3}} = ^3J_{\text{o}}^{\text{F5, F6}}$	-20.832 (3)
$^4J_{\text{m}}^{\text{F2, H4}} = ^4J_{\text{m}}^{\text{F6, H4}}$	7.204 (3)
$^5J_{\text{p}}^{\text{F2, F5}} = ^5J_{\text{p}}^{\text{F3, F6}}$	9.280 (3)
$^4J_{\text{m}}^{\text{F2, F6}}$	-1.684 ^d (2)
$^3J_{\text{o}}^{\text{F3, H4}} = ^3J_{\text{o}}^{\text{F5, H4}}$	10.590 (3)
$^4J_{\text{m}}^{\text{F3, F5}}$	-1.516 ^d (2)

... Table 9 continued...

Table 9...

rms deviation	0.0147
largest difference	0.029
peaks observed	85
transitions assigned	187
transitions calculated	294

- a In Hertz. Numbers in parentheses are standard deviations in the last decimal place, calculated by LAME.
- b Treated in the X approximation with chemical shifts taken from the 90.02 MHz spectrum.
- c Absolute frequency is not significant.
- d These coupling constants have the same sign, but the sign relative to other values has not been determined experimentally.

vi) 2-fluoroacetophenone

Proton spectra of a 5.35 mole % solution of 2-fluoroacetophenone at 90.02 MHz and of a 4.94 mole % solution of 2-fluoroacetophenone- α - ^{13}C at 100 MHz, both in acetone- d_6 , yielded to analysis and some results appear in Table 10. The 90.02 MHz spectrum of the ring protons appears as Figure 17.

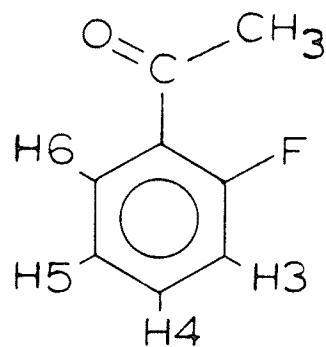
The methyl protons did not couple observably to any ring protons. However, splitting of the resonances of H6 by the methyl carbon was clear in the 100 MHz spectrum. The sign was deduced from weak irradiation experiments. Similarly, the sign of $^5\text{J}_{\text{O}}^{\text{CH}_3, \text{F}}$ was determined as described below. No coupling between the methyl carbon and H3 was observed. Parenthetically, the proton spectrum of a 5.35 mole % solution of acetophenone in acetone- d_6 was not analyzed, but the center of the methyl proton resonance occurred at 2.5644 ppm.

The fluorine resonance of the unlabelled compound occurred 52.922 ppm downfield from hexafluorobenzene.

Splittings from the proton-decoupled carbon spectra appear in Table 11. The rms deviation from the average line positions is 0.25 Hz (0.011 ppm). Linewidths of 0.8 Hz include 0.1 Hz line broadening. The spectrum of the labelled compound is complicated by the presence of impurities. Resonance assignments correspond to line positions in the clean spectrum of 2-fluoroacetophenone. Proton-carbon couplings can not be extracted under the circumstances.

Table 10

Parameters from the Proton Spectrum of 2-Fluoroacetophenone^a in Acetone-d₆.



	4.94 mole % 100.001 MHz (methyl ¹³ C enriched)	5.35 mole % 90.0234 MHz
ν_{CH_3}	258.145 (1)	323.465 (1)
ν_{F}	1000 ^b	1500 ^b
ν_3	723.876 (1)	651.772 (1)
ν_4	761.886 (1)	686.040 (1)
ν_5	729.353 (1)	656.582 (2)
ν_6	783.522 (1)	705.222 (1)
$\nu_{\text{C}\alpha}$	1500 ^b	c
$^5J_{\text{O}} \text{CH}_3, \text{F}$	+4.484 (2)	4.510 (1)
$^3J_{\text{O}} \text{F}, \text{H3}$	11.470 (2)	11.460 (2)
$^4J_{\text{m}} \text{F}, \text{H4}$	5.072 (2)	5.072 (2)
$^5J_{\text{p}} \text{F}, \text{H5}$	0.154 (3)	0.198 (5)
$^4J_{\text{m}} \text{F}, \text{H6}$	7.646 (2)	7.631 (2)
$^3J_{\text{O}} \text{H3}, \text{H4}$	8.344 (1)	8.333 (1)
$^4J_{\text{m}} \text{H3}, \text{H5}$	1.077 (1)	1.076 (2)
$^5J_{\text{p}} \text{H3}, \text{H6}$	0.367 (2)	0.362 (2)

...Table 10 continued...

Table 10...

$^3J_{\text{O}}$ H4,H5	7.336 (2)	7.344 (2)
$^4J_{\text{m}}$ H4,H6	1.880 (2)	1.887 (2)
$^3J_{\text{O}}$ H5,H6	7.792 (2)	7.775 (2)
$^1J_{\text{C}\alpha,\text{H}}$	128.246 (2)	c
$^5J_{\text{m}}$ C α ,H5	0.399 ^d (2)	c
$^4J_{\text{O}}$ C α ,H6	0.105 ^d (2)	c
rms deviation	0.0130	0.0081
largest difference	0.042	0.032
peaks observed	71	52
transitions assigned	873	373
transitions calculated	1064	540

a In Hertz. Both samples are acetone-d₆ solutions.

b Treated in the X approximation with respect to other nuclear species. No transitions were assigned.

c Not included in this analysis.

d These couplings are of the same sign, which is assumed positive.

Figure 17

Spectrum of the ring protons of a 5.35 mole % solution of
2-fluoroacetophenone in acetone-d₆.

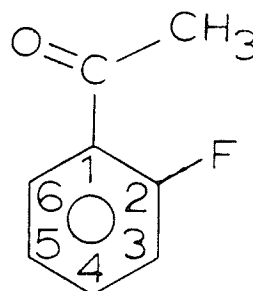
a observed. The peak indicated by x is due to an impurity.

b calculated



Table 11

Carbon Chemical Shifts^a and Some Coupling Constants^b for 2-Fluoroacetophenone in Acetone-d₆.



	$\delta_{C\alpha}$	31.19		
	δ_{C0}	195.36		
	δ_{C1}	126.65		
	δ_{C2}	162.79		
	δ_{C3}	117.40		
	δ_{C4}	135.55		
	δ_{C5}	125.29		
	δ_{C6}	131.13		
$1_{J_{C\alpha C0}}$	43.233 ± 0.089		$3_{J_{F,C0}}$	3.203 ± 0.041
$2_{J_{C\alpha,C1}}$	$\pm 13.785^c$		$2_{J_{F,C1}}$	12.927 ± 0.016
$3_{J_{C\alpha,C2}}$	d		$1_{J_{F,C2}}$	$(-)\ 253.124 \pm 0.098$
$4_{J_{C\alpha,C3}}$	d		$2_{J_{F,C3}}$	23.828 ± 0.056
$5_{J_{C\alpha,C4}}$	d		$3_{J_{F,C4}}$	9.085 ± 0.026
$4_{J_{C\alpha,C5}}$	d		$4_{J_{F,C5}}$	3.515 ± 0.013
$3_{J_{C\alpha,C6}}$	0.633 ± 0.019		$3_{J_{F,C6}}$	2.582 ± 0.033
			$4_{J_{F,C\alpha}}$	$+6.831 \pm 0.009$

...Table 11 continued...

Table 11....

a In ppm downfield from internal TMS. Probably ± 0.03 ppm.

b In Hertz.

c Due to low intensity, this value was determined only once.

d Unobserved.

- a) determination of the relative spin of ${}^4J_{\text{O}}^{\text{C}\alpha,\text{F}}$ by weak irradiation experiments

First-order diagrams for the line spectrum of the methyl protons, of the fluorine, and of the methyl carbon appear in Figure 18.

Weak irradiation of line 1 of the methyl proton spectrum during acquisition of the fluorine spectrum reduced the intensity of the low-field resonances. Since line 1 corresponds to the carbon designation + and affected lines must bear that sign, ${}^4J_{\text{O}}^{\text{C}\alpha,\text{F}}$ was found to be positive.

- b) determination of the relative sign of ${}^5J_{\text{O}}^{\text{CH}_3,\text{F}}$ by weak irradiation experiments

While observing the methyl carbon spectrum the methyl proton line 1 was irradiated weakly and line 1 of the carbon multiplet was inverted, as in Figure 19. Line 2 was inverted when the second radiofrequency was moved to line 2 of the proton spectrum. Both observations suggested the positive sign for ${}^5J_{\text{O}}^{\text{CH}_3,\text{F}}$ since ${}^4J_{\text{O}}^{\text{C}\alpha,\text{F}}$ was determined to be positive.

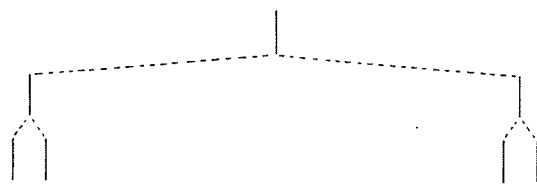
- c) determination of the relative sign of ${}^4J_{\text{O}}^{\text{C}\alpha,\text{H}6}$ by weak irradiation experiments

The proton spectrum of the labelled compound is complicated by the presence of impurity peaks, but can be analyzed reliably

Figure 18

A first-order representation of the line spectrum of the methyl proton, of the fluorine, and of the methyl carbon of 2-fluoroacetophenone.

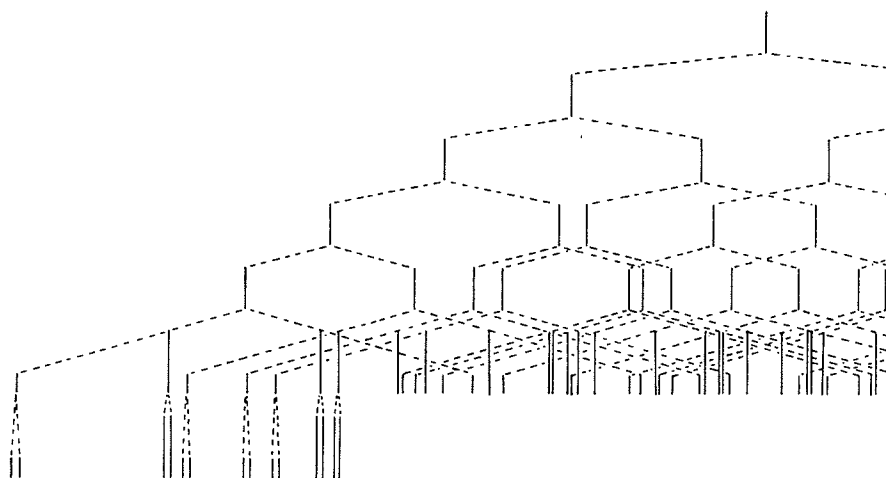
CH₃



C + +
 F + -
 1 2

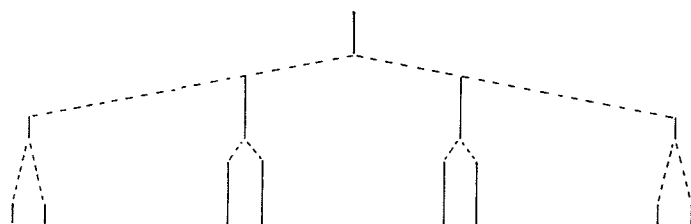
- -
 + -
 3 4

F



H3	++	++++	+++	++++
H6	++	++++	++--	++++
C	++	++++	--++	++++
H4	++	++-	+++	+-
CH ₃	+ ³ / ₂	+ ¹ / ₂ + ³ / ₂ + ³ / ₂ + ³ / ₂ - ¹ / ₂ + ¹ / ₂		
H5	+ -	++-	+-	+-
	1 2	3 6 7	10 11 14	

C

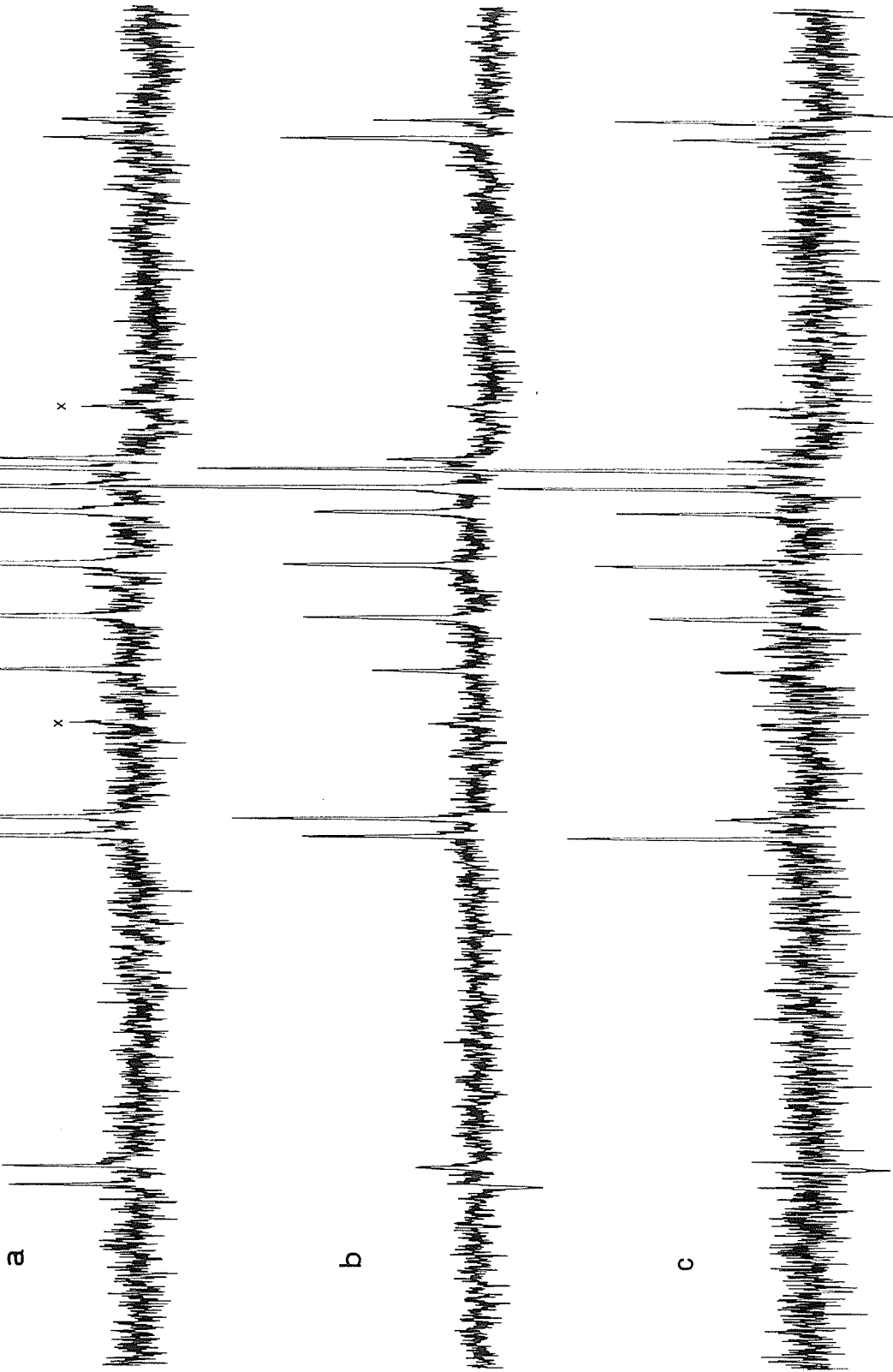


CH ₃	+ 3/2	+ 1/2	- 1/2	- 3/2
F	+ -	+ -	+ -	+ -
	1 2	3 4	5 6	7 8

Figure 19

Spectra of the methyl carbon of 4.94 mole % solution of 2-fluoroacetophenone- α - ^{13}C in acetone- d_6 .

- a the multiplet of the methyl carbon in the absence of weak irradiation. The septet indicated by x's is due to the methyl carbons of solvent acetone- d_6 .
- b in the presence of weak irradiation of the line numbered 1 in the methyl proton spectrum in Figure 18
- c in the presence of weak irradiation of the line numbered 2



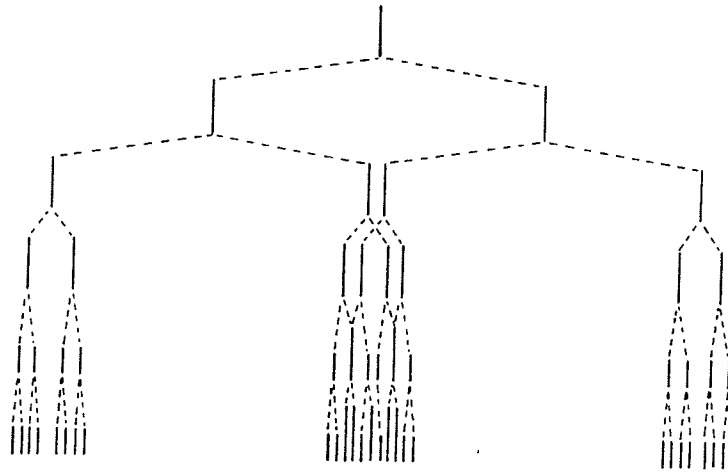
with reference to the spectrum of 2-fluoroacetophenone. The line spectra of H5 and H6 appear in Figure 20.

Weak irradiation of line 32 in the high-field multiplet of H5 decreased the intensity of line 32 in the high-field multiplet of H6. Irradiation of line 30 inverted line 30 in the H6 resonance. Therefore, ${}^5J_m^{C\alpha,H5}$ and ${}^4J_o^{C\alpha,H6}$ seemed to be of the same sign. The former was assumed to be positive, as in 4,6-dibromo-2-fluoroanisole (vide supra).

Figure 20

A first-order representation of the line spectrum of
H5 and H6 of 2-fluoroacetophenone.

H5



H6

+

-

H4

+

-

H3

+ -

+ -

C

+ - + -

+ - + -

F

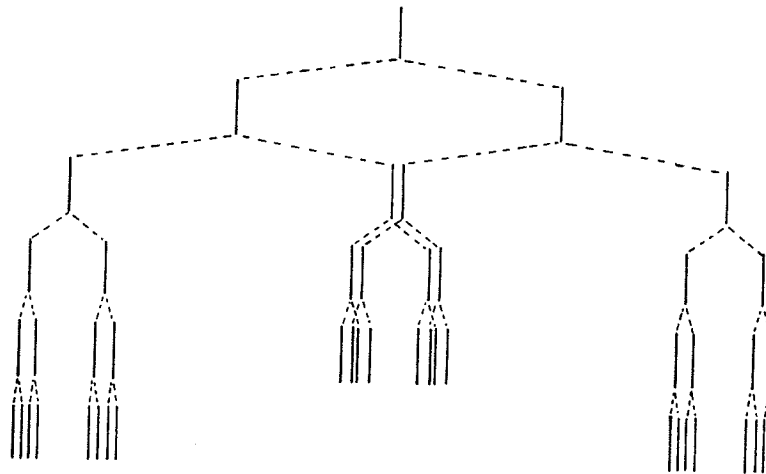
+ + + + -

+ + + + -

1 8

25 32

H6



H5

+

-

F

+

-

H4

+ -

+ -

H3

+ - + -

+ - + -

C

+ + - - + + - -

+ + - - + + - -

1 8

25 32

vii) 2,6-difluoroacetophenone

Commercially obtained 2,6-difluoroacetophenone contained a significant amount of impurity and, therefore, the actual concentration of the sample was not known precisely, but was between 2.5 and 3.5 mole % in acetone-d₆.

The 90.02 MHz spectrum of the ring protons appears in Figure 21. The linewidth is about 0.2 Hz with 0.073 Hz/real point. Linewidths in the fluorine spectrum are 0.3 Hz with 0.024 Hz/real points. Table 12 presents the results of iterative refinement of the A₃BB'CXX' spin system.

Impurity peaks did not interfere with the determination of line positions. The sign of $^5J_{\text{O}}^{\text{CH}_3, \text{F}}$ was assumed from 2-fluoroacetophenone (vide supra). No coupling was observed between the methyl and ring protons.

The proton-decoupled fluorine resonance occurred 50.151 ppm downfield from hexafluorobenzene.

Parenthetically, the methyl proton resonance of a 4.66 mole % solution of 2,3,4,5,6-pentafluoroacetophenone was centered at 2.61819 ppm. The spectrum was not analyzed, but the triplet splitting read from it is 1.822 ± 0.005 Hz. The 0.2 Hz linewidth gave no indication of coupling between the methyl protons and fluorine nuclei at meta or para positions.

Figure 21

Spectrum of the ring protons of a solution of ca 3 mole %
2,6-difluoroacetophenone in acetone-d₆.

a calculated spectrum

b observed spectrum

c calculated spectrum of an unidentified impurity

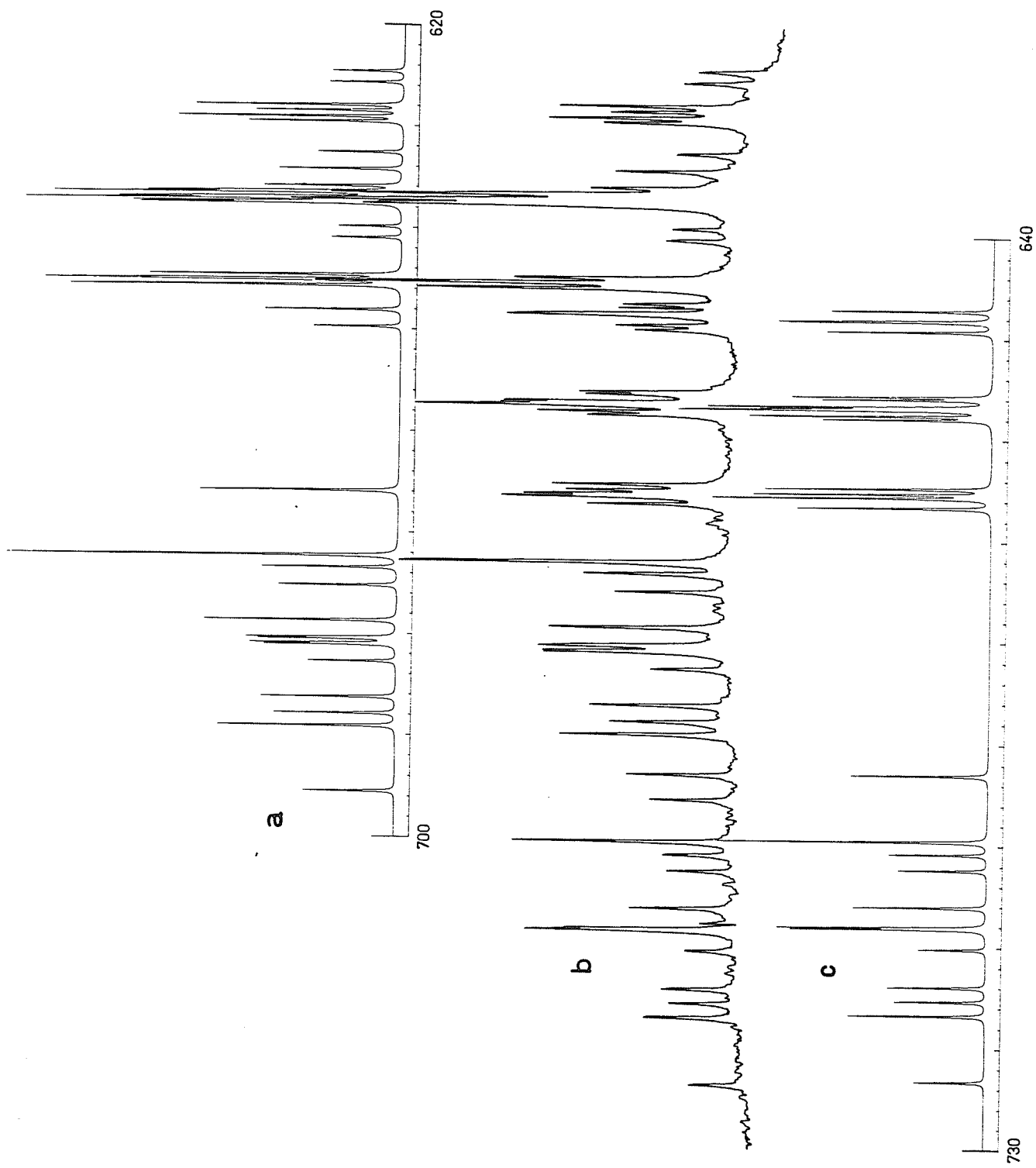
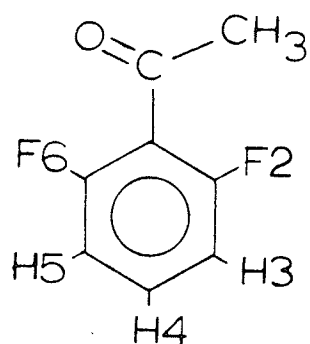


Table 12

Parameters from the Proton and Fluorine Spectra of 2,6-Difluoroacetophenone^a in Acetone d-6.



ν_{CH_3}	229.658 (1)
$\nu_{\text{F2}} = \nu_{\text{F6}}$	1528.099 ^b (1)
$\nu_3 = \nu_5$	637.417 (1)
ν_4	679.889 (1)
$5J_{\text{O}} \text{CH}_3, \text{F2} = 5J_{\text{O}} \text{CH}_3, \text{F6}$	1.564 (1)
$3J_{\text{O}} \text{F2}, \text{H3} = 3J_{\text{O}} \text{H5}, \text{F6}$	9.612 (2)
$4J_{\text{m}} \text{F2}, \text{H4} = 4J_{\text{m}} \text{H4}, \text{F6}$	6.425 (1)
$5J_{\text{p}} \text{F2}, \text{H5} = 5J_{\text{p}} \text{H3}, \text{F6}$	-1.183 (2)
$5J_{\text{m}} \text{F2}, \text{F6}$	3.938 (2)
$3J_{\text{O}} \text{H3}, \text{H4} = 3J_{\text{O}} \text{H4}, \text{H5}$	8.488 (1)
$4J_{\text{m}} \text{H3}, \text{H5}$	0.927 (2)
rms deviation	0.0113
largest difference	0.035
peaks observed	74
transitions assigned	474
transitions calculated	569

.....Table 12 continued...

Table 12....

a In Hertz. Numbers in parentheses are standard deviations in the last decimal place, calculated by LAME.

b Treated in the X approximation.

iii) α,α,α -trifluoroacetophenone

The proton spectrum of α,α,α -trifluoroacetophenone was not analyzed.

The fluorine spectrum of a 4.76 mole % solution in acetone- d_6 was acquired with 0.024 Hz/real point, the linewidth being about 0.4 Hz. The triplet splitting suggested that ${}^5J_{O}^{CF_3,H_2}$ was 1.116 ± 0.014 Hz, as in Figure 22.

Carbon chemical shifts and a few carbon-fluorine spin-spin coupling constants appear in Table 13.

The rms deviation from the average line positions in two proton-coupled carbon spectra was 0.072 Hz (0.003 ppm). A digital resolution of 0.293 Hz/real point was used. No coupling was observed between the fluorine nuclei and C2, C3, or C4.

Figure 22

Spectrum of the methyl fluorines of a 4.76 mole % solution of α, α, α -trifluoromethylacetophenone in acetone- d_6 .

┌───┐
1 Hz

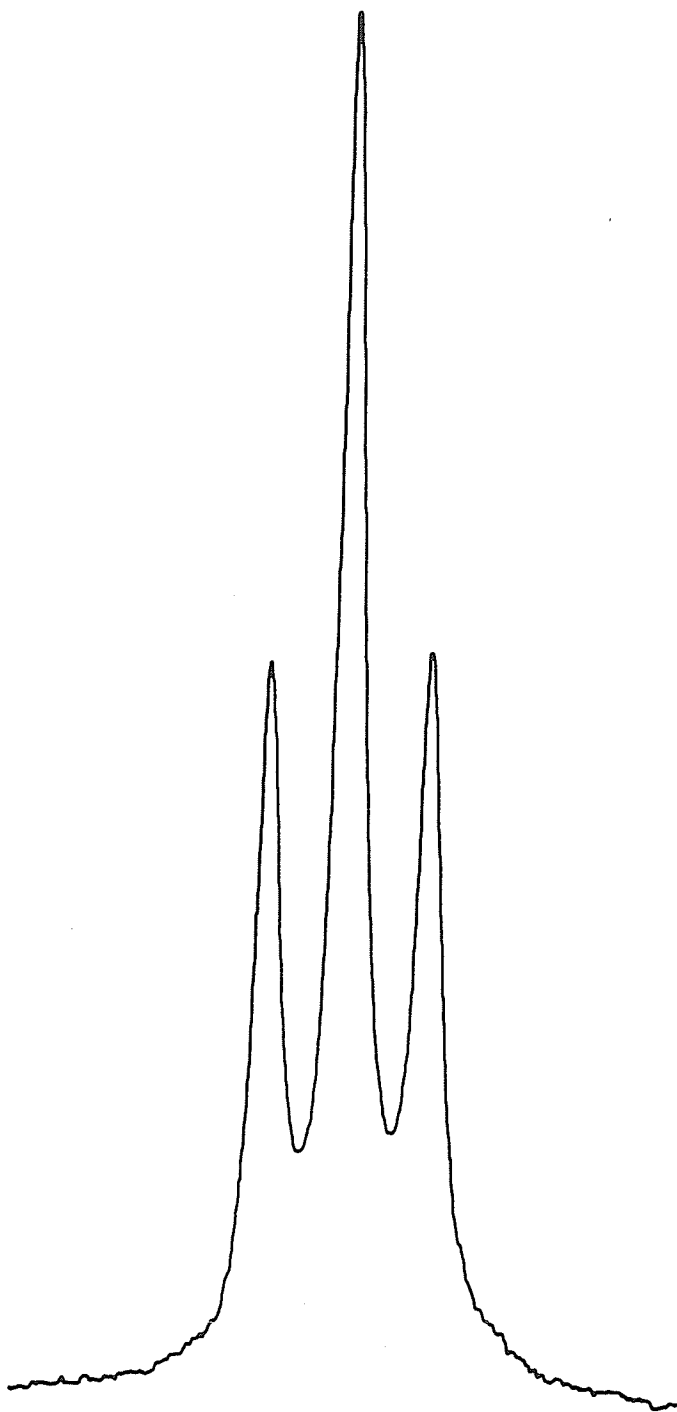
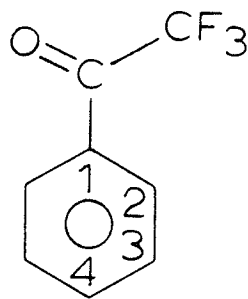


Table 13

Carbon Chemical Shifts^a and Carbon-Fluorine Coupling Constants^b
for α,α,α -Trifluoroacetophenone in Acetone- d_6 .



δ_{CF_3}	117.61
δ_{C0}	180.94
δ_{C1}	130.62
δ_{C2}	130.20
δ_{C3}	128.48
δ_{C4}	136.65
$^1J_{F,C\alpha}$	(-)290.944 \pm 0.021
$^2J_{F,C0}$	\pm 34.55 \pm 0.31
$^3J_{F,C1}$	2.183 \pm 0.028

a In ppm downfield from TMS. Probably \pm 0.01 ppm.

b In Hertz.

B. Low Temperature Spectra

Spectra of the resonances of particular nuclei in some samples were obtained at intervals below 305 K. Acetone freezes at about 177.8 K and freezing point depressions of about 2 K were expected for the sample concentrations used. In most cases the lowest temperature attained was 192 K.

Experimental data are tabulated in this section and appear graphically in the Discussion.

i) 4,6-dibromo-2-fluoroanisole

Spectra of the methyl proton resonances of a 15.5 mole % solution of 4,6-dibromo-2-fluoroanisole- α - ^{13}C in acetone- d_6 were acquired at intervals between 192 and 305 K. Usual digital resolution was 0.061 Hz/real point and the linewidth increased from 0.3 to greater than 1 Hz at 192 K. The splitting due to $^5\text{J}_{\text{O}}^{\text{CH}_3, \text{F}}$ was not resolved at 192 K.

Splittings and chemical shifts at 90.0234 MHz appear in Table 14. As the temperature decreases, $^5\text{J}_{\text{O}}^{\text{CH}_3, \text{F}}$ decreases.

Table 14

Temperature Dependence of Parameters from the Methyl Proton
Spectrum of 4,6-Dibromo-2-fluoroanisole- α - ^{13}C .

T(K)	ν_{CH_3} (Hz)	$^1\text{J}_{\text{CH}}$ (Hz)	$^5\text{J}_{\text{OCH}_3, \text{F}}$ (Hz)
305	354.132	146.191	1.491
290	354.416	146.206	1.477
280	354.558	146.207	1.466
270	354.912	146.238	1.456
260	a	146.254	1.456
250	a	146.265	1.422
240	355.775	146.248	1.211
230	356.127	146.301	1.386
220	a	146.300	1.329
211	357.078	146.314	1.293
202	357.770	146.321	1.121
192	358.483	146.249	a

a Not determined

ii) 2,3,5,6-tetrafluoroanisole

The 90.0234 MHz methyl proton spectrum of 4.70 mole % solution of 2,3,5,6-tetrafluoroanisole in acetone-d₆ was obtained at intervals between 192 and 305 K, with 0.061 Hz/real point.

The linewidth increased from 0.3 to about 1 Hz at 192 K.

Table 15 presents the chemical shifts and coupling constants. As the temperature decreases ${}^5J_{\text{OCH}_3, \text{F}}$ increases.

Table 15

Temperature Dependence of Parameters from the Methyl Proton
Spectrum of 2,3,5,6-Tetrafluoroanisole.

T(K)	ν_{CH_3} (Hz)	$^5J_{\text{OCH}_3, \text{F}}$ (Hz)
305	369.000	1.340
300	369.147	1.346
290	369.400	1.354
280	369.721	1.365
270	370.026	1.376
260	370.372	1.387
250	370.748	1.397
240	371.109	1.412
230	371.464	1.423
220	371.882	1.433
211	372.406	1.454
202	372.846	1.440
192	373.466	1.450

iii) 2-fluoroacetophenone

The 90.02 MHz methyl proton spectrum of a 4.94 mole % solution of 2-fluoroacetophenone- α - ^{13}C in acetone- d_6 was acquired at intervals between 182 and 305 K, usually with 0.049 Hz/real point. The linewidth increased from 0.3 to greater than 1 Hz at 182 K.

The proton-decoupled fluorine resonance at 51.545 ppm downfield from hexafluorobenzene had a linewidth of 1.2 Hz at 182 K.

Methyl carbon spectra were acquired with 0.098 Hz/real point. Linewidths remained near 1 Hz. The small splitting, due to $^4J_{\text{O}}^{\text{C}\alpha, \text{H}6}$, also remained constant to within experimental error.

Parameters appear in Table 16.

Table 16

Temperature Dependence of Parameters from the Methyl Proton
and Methyl Carbon Spectra of 2-Fluoroacetophenone- α - ^{13}C .

T(K)	$^1\text{J}_{\text{C}\alpha,\text{H}}$ (Hz)	$^4\text{J}_{\text{O}}^{\text{C}\alpha,\text{F}}$ (Hz)	$^5\text{J}_{\text{O}}^{\text{CH}_3,\text{F}}$ (Hz)	
	a	b		
305	128.239	128.211	6.839	4.508
290	128.245	128.238	6.888	4.648
280	128.246	128.235	6.951	4.752
270	128.250	128.240	6.999	4.858
260	128.255	128.241	7.080	4.971
250	128.276	128.262	7.122	5.088
240	128.264	128.255	7.082	5.210
230	128.281	128.303	7.228	5.330
220	128.286	128.319	7.234	5.461
211	128.309	128.301	7.296	5.583
202	128.311	128.321	7.327	5.737
192	128.312	128.370	7.368	5.878
182	128.401	c	c	5.992

a From the proton spectrum.

b From the carbon spectrum.

c Not determined.

iv) 2,6-difluoroacetophenone

The 90.0234 MHz methyl proton spectrum of a solution containing about 3 mole % 2,6-difluoroacetophenone in acetone- d_6 was acquired with 0.073 Hz/real point at intervals between 192 and 305 K. The linewidth increased from about 0.3 to 0.6 Hz at 192 K.

Chemical shifts and coupling constants appear in Table 17. As temperature decreases, $^5J_{O-CH_3, F}$ increases.

Table 17

Temperature Dependence of Parameters from the Methyl Proton
Spectrum of 2,6-Difluoroacetophenone.

T(K)	ν_{CH_3} (Hz)	$^5J_{\text{OCH}_3, \text{F}}$ (Hz)
305	229.656	1.555
290	230.496	1.581
280	231.123	1.597
270	231.730	1.612
260	232.318	1.628
250	232.975	1.646
240	233.657	1.663
230	234.385	1.684
192	237.474	1.765

v) α,α,α -trifluoroacetophenone

The fluorine spectrum of a 4.76 mole % solution of α,α,α -trifluoroacetophenone in acetone- d_6 was acquired with 0.049 Hz/real point at intervals between 211 and 305 K. Linewidths increased from about 0.4 to 1 Hz at 211 K.

The dependence of ${}^5J_{\text{O}}^{\text{CF}_3,\text{H}}$ on temperature is suggested by the values in Table 18. As temperature decreases, ${}^5J_{\text{O}}^{\text{CF}_3,\text{H}}$ increases.

Table 18

Temperature Dependence of ${}^5J_{\text{O}}^{\text{CF}_3, \text{H}}$ for α, α, α -Trifluoroacetophenone.

T(K)	${}^5J_{\text{O}}^{\text{CF}_3, \text{H}}$ (Hz)
305	1.108
300	1.115
290	1.129
280	1.116
270	1.129
260	1.148
250	1.140
240	1.158
230	1.172
220	1.143
211	1.172

C. Nuclear Spin-Lattice Relaxation Experiments

Relaxation rate parameters are obtained by least-squares fitting of the peak heights, or peak integrals, from the inversion-recovery experiment as a function of time, $S(t)$, to the expression

$$S(t) = S_0 \{1 - [1 + W(1 - \exp(-\frac{D}{T_1}))] \exp(-\frac{t}{T_1})\} \quad \text{Eq. (6)}$$

where S_0 is the equilibrium peak height, $S_0 W$ is the peak height immediately after the 180° pulse, D is the delay time before the 180° pulse, and T_1 is the spin-lattice relaxation time²¹¹.

Of the three parameters in this equation, the value of S_0 is not significant. The value of W is unity for a perfect 180° pulse and lesser values indicate pulse imperfection. Values between 0.8 and 0.9 are common.

Standard deviation in the relaxation time was calculated from the deviations of ordinate values, $S(t)$, from the curve. Experimental data were also fitted while W was held equal to unity.

i) methyl carbon nuclei

Methyl carbon chemical shifts, nuclear Overhauser enhancements²¹², and relaxation rate parameters for solutions of anisole- α - ^{13}C ; 4-bromo-2-fluoroanisole- α - ^{13}C ; 4,6-dibromo-2-fluoroanisole- α - ^{13}C ; 2,3,5,6-tetrafluoroanisole; acetophenone; 2-fluoroacetophenone- α - ^{13}C ; and 2,6-difluoroacetophenone in acetone- d_6 are listed in Table 19. The experimental method appears in the preceding chapter.

Concerning the data for 4-bromo-2-fluoroanisole, the more dilute solution was clear, pale yellow in colour while the other was dark brown. It was not apparent whether the difference in observed relaxation times was due to impurities or to the influence of concentration. The more dilute solution was preferred for comparisons with the other compounds since the 4-bromo-2-fluoroanisole had been chromatographed to remove impurities and since the concentration is closer to that of the other solutions.

Fluorine decoupling was performed in one determination of the relaxation parameters for 4,6-dibromo-2-fluoroanisole. Differences between relaxation times were within the experimental errors.

Relaxation data for 2,6-difluoroacetophenone were particularly difficult to obtain since the resonances lay very near to the low-field member of the acetone- d_6 septet. This

Table 19

Methyl Carbon Chemical Shifts, Nuclear Overhauser Enhancements,
and Relaxation Rate Parameters for Some Anisoles and Acetophenones.

	δ (ppm)	η^a	T_1 (s)		W
			b	c	
anisole- α - ^{13}C 4.62 mole %	55.27	1.6-1.7	8.5 ± 0.3	9.93 ± 0.06	0.85
4-bromo-2-fluoroanisole- α - ^{13}C 2.96 mole %	56.95	1.6-1.7	5.0 ± 0.4	6.7 ± 0.2	0.74
14.0 mole %		1.8-1.9	2.77 ± 0.09	3.13 ± 0.05	0.86
4,6-dibromo-2-fluoroanisole- α - ^{13}C 1.83 mole %	61.88	1.3-1.5	15.02 ± 0.06	15.2 ± 0.1	0.89
	d	1.3-1.5	14.1 ± 0.3	15.4 ± 0.1	0.92
2,3,5,6-tetrafluoroanisole 4.70 mole %	62.70	e	18 ± 1	22 ± 1	0.79
acetophenone 5.35 mole %	27.57	1.8-1.9	12.9 ± 0.5	15.4 ± 0.2	0.84
2-fluoroacetophenone- α - ^{13}C 4.94 mole %	31.19	1.5-1.7	12.6 ± 0.4	14.6 ± 0.2	0.86
2,6-difluoroacetophenone about 3 mole %	33.24	f	17 ± 3	32 ± 3	0.53

a Nuclear Overhauser enhancement in the presence of strong irradiation of coupled protons. The theoretical maximum value is 1.988.

b With W fixed at unity.

c With W as a parameter.

d With strong irradiation of coupled fluorine nuclei.

e Not determined.

....Table 19 continued...

Table 19.....

- f The intensity of the resonance without strong irradiation of coupled protons was not determined reliably because the resonance overlaps the low-field member of the acetone-d₆ septet.

interference made the results of the fitting unreliable, as the difference between the two relaxation times shows.

ii) fluorine nuclei

Fluorine chemical shifts and relaxation rate parameters for solutions of 4,6-dibromo-2-fluoroanisole; 2,3,5,6-tetrafluoroanisole; 2-fluoroacetophenone; and 2,6-difluoroacetophenone in acetone- d_6 appear in Table 20.

Relaxation parameters for 2,3,5,6-tetrafluoroanisole were calculated for particular lines in the presence of fluorine-fluorine spin-spin coupling. These entries in Table 20 must be viewed as estimates only²¹³.

Table 20

Fluorine Chemical Shifts and Relaxation Rate Parameters for
Some Anisoles and Acetophenones.

	δ (ppm downfield from internal C_6F_6)	T_1 (s)		W
		a	b	
4,6-dibromo-2-fluoroanisole 9.47 mole %	38.471	13 ± 1	21 ± 1	0.6-0.7
2,3,5,6-tetrafluoroanisole 4.70 mole %	5.044 ^c	18 ± 2	19 ± 1	0.8-1.0
	21.843 ^d	16 ± 2	21 ± 5	0.8-1.0
2-fluoroacetophenone 5.35 mole %	52.922	7.9 ± 0.5	10.0 ± 0.3	0.8
2,6-difluoroacetophenone about 3 mole %	50.151	16 ± 1	20.6 ± 0.6	0.79

a With W fixed at unity.

b With W as a parameter.

c F2 and F6.

d F3 and F5.

Chapter 5
Discussion

In this chapter the discussion of the experimental results and of some results of molecular orbital calculations is presented.

Ab initio molecular orbital calculations at the STO-3G level with partial geometry optimization have yielded conformational energies. Semi-empirical calculations in the INDO or CNDO/2 approximations gave conformational energies and, by finite perturbation theory (FPT), spin-spin coupling constants.

Coupling mechanisms are elaborated by examination of the conformational dependence of coupling constants and of the effect of elimination of certain Fock elements from the calculations, as pioneered by Barfield²³⁰.

Solvent effects may suffice to vitiate some of the conformational deductions presented here^{214,215}. For example, polar solvents may induce a preference for more polar conformers rather than less polar conformers, which may be preferred in the vapour phase or in non-polar solvents. Since most of the discussion is concerned with dilute acetone solutions, comparisons between similar compounds seem justified. These similitudes may not extend to other solvents or other phases.

A. Anisole

i) ab initio molecular orbital calculations

Molecular mechanics calculations indicate that the barrier to methoxy group rotation in anisole is essentially zero⁴⁸.

Ab initio molecular orbital calculations at the STO-3G level place the energy of the orthogonal conformation about $20 \text{ kJ}\cdot\text{mol}^{-1}$ below the planar one, but optimization of the bond angle at oxygen for each conformer reduces the difference to near zero²¹⁶.

Similar calculations with partial geometry optimization place the planar conformers of 4-fluoroanisole at energy minima and the orthogonal conformers at relative minima at $4.7 \text{ kJ}\cdot\text{mol}^{-1}$ ⁵⁶.

Approximate molecular orbital calculations at the INDO level with geometry optimization suggest that the orthogonal conformation is preferred by $15.1 \text{ kJ}\cdot\text{mol}^{-1}$ ²¹⁷.

While the present work was in progress, two groups reported results of STO-3G calculations with partial geometry optimization^{69,85}. The energy difference between the planar and orthogonal conformations was $5.61 \text{ kJ}\cdot\text{mol}^{-1}$ or $9.27 \text{ kJ}\cdot\text{mol}^{-1}$, with the planar lower.

Some results of the present partial geometry optimization appear in Table 21 with reference to Figure 23. The geometry of the aromatic ring is not optimum and the methyl group retains C_{3v} symmetry about the oxygen-methyl carbon bond axis. The total energies are lower than those previously reported for the planar and orthogonal conformations.

Table 21

Some Results of Partial Geometry Optimization in STO-3G Calculations for Anisole.

	experimental ^a		calculated ^b			
	0	0	25	45	65	90
C2C1Oα						
C ₁ O	136.1(3)	140.0	(140.7)	140.7	141.1	141.3
OCα	142.3(15)	143.4	(143.8)	143.8	144.0	144.0
COH	-	109.3	(109.3)	(109.3)	(109.3)	(109.3)
C ₁ OCα	120(2)	114.7	114.1	113.6	111.3	110.2
C ₂ C ₁ O	124	125.9	125.1	124.5	122.1	120.0
H ₂ C ₂ C ₁	-	120.9	(120.9)	(120.9)	(120.6)	120.6
OC H _α α	-	110.4	(110.4)	(110.4)	(110.4)	(110.4)
C ₁ OC H _α α	-	180.0	166.4	167.8	179.3	180.0
C ₃ C ₂ C ₁ O	-	180.0	(177.4)	177.4	176.3	177.5
dipole moment (D)	1.25 ^c	1.177	d	d	1.303	1.335
total energy (H)	-	-340.30960	-340.30876	-340.30740	-340.30724	-304.30741
relative energy (kJ·mol ⁻¹)	-	0	2.2 ₀	5.7 ₆	6.1 ₉	5.7 ₃

...Table 21 continued....

Table 21...

a From reference 71.

b Angles in degrees, bondlengths in pm. Quantities in parentheses were assumed and not optimized.

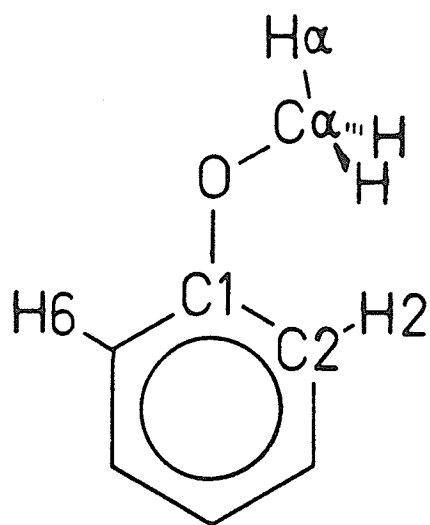
c From reference 218.

d Not calculated.

Figure 23

A planar conformation of anisole.

Some atoms used in the description of the geometry are identified.



The calculated geometry of the planar conformation agrees with the structure of anisole as determined by electron diffraction⁷¹, and with the average structural parameters of the methoxy group⁸⁵. As for the calculations for water and for phenol^{219,220}, the bond angle at oxygen seems too small.

As the twist angle $C2C10C\alpha$ increases, the degree of conjugation between oxygen and the ring π -system decreases (vide infra), which results in an increase in the bondlength $C10$. Concomitant reduction of the bond angle $C10C\alpha$ reflects the decrease in steric interaction between the methyl group and the phenyl group. Notice that the methyl group rotates to minimize interactions between methyl hydrogens and $H2$, although the dihedral angle $C10C\alpha H\alpha$ is 180° in both the planar and orthogonal conformations.

The dipole moment of anisole is midway between the numbers calculated for the planar and orthogonal conformations. The angle between the $OC\alpha$ bond and the dipole moment is 30.0° in the planar conformation and 39.7° in the orthogonal.

Relative energies from Table 21 appear graphically in Figure 24. A curve through these points approximates a path of steepest descent on a surface

$$E = f(\phi, \psi) \quad \text{Eq. (7)}$$

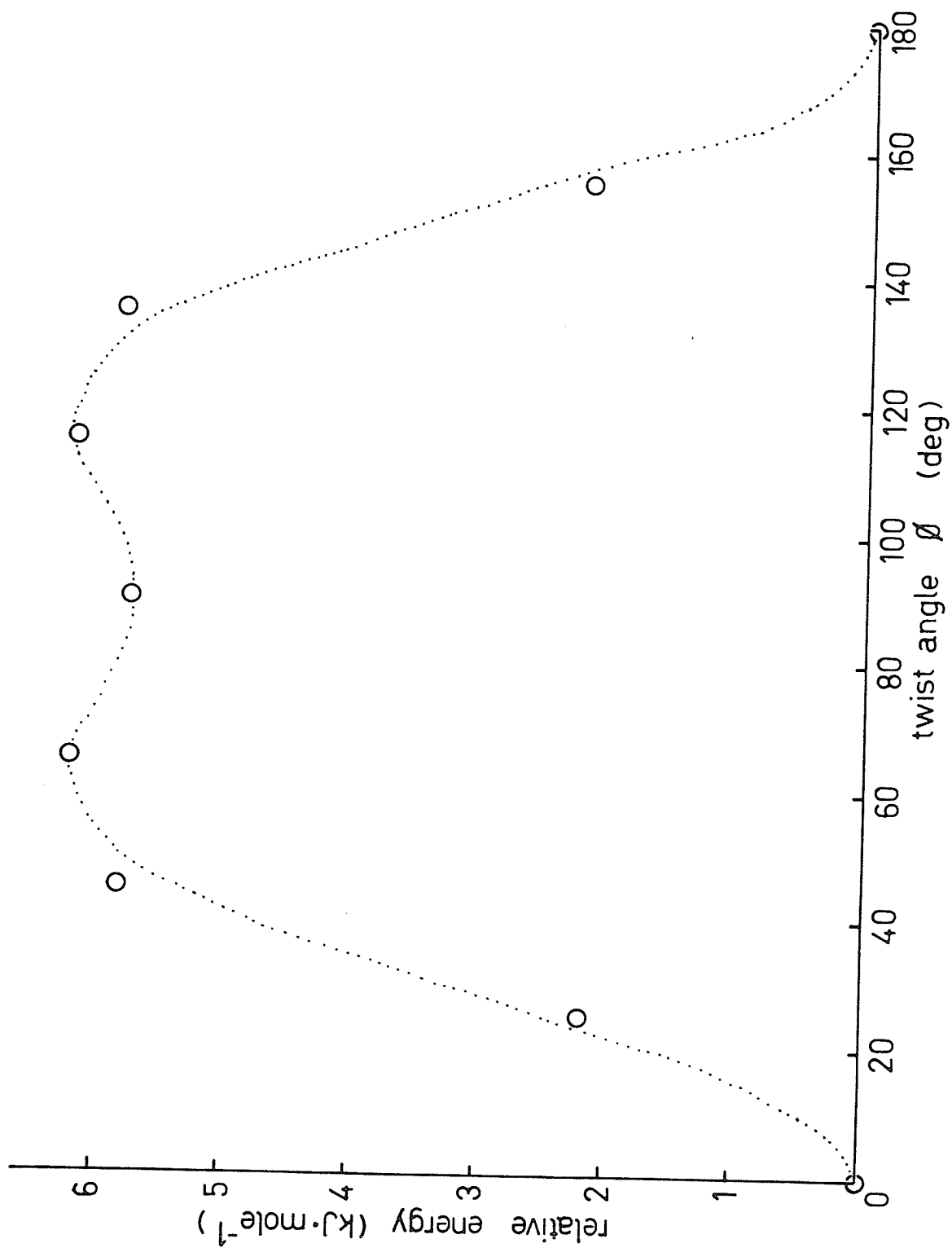
where $\phi = C2C10C\alpha$ and $\psi = C10C\alpha H\alpha$. This is the most probable path for methoxy group reorientation. The three-fold barrier to

Figure 24

A plot of the relative energies of some conformations of anisole from partially-optimized molecular orbital calculations at the STO-3G level.

○ calculated

dotted line Eq. (8)



methyl group rotation is $25.6 \text{ kJ}\cdot\text{mol}^{-1}$ for the given planar geometry and $10.5 \text{ kJ}\cdot\text{mol}^{-1}$ for the given orthogonal geometry. Clearly the magnitude and phase of the rotational potential are dependent on ϕ , that is, the rotations of the methoxy group and the methyl group are not separable.

While they recognize the importance of methyl group orientation in the methoxy group rotation, Konschin, Tylli, and Grundfelt-Forsius state that no evidence supports coupled or correlated reorientation of the methyl and methoxy groups⁶⁹. On the contrary the present results indicate most definitely that the energetically-preferred path includes both motions, but the populations of the various conformers are just as definitely given by a distribution over the surface described by Eq. (7). Notice that the steric interaction between the methyl group and ortho-carbon-hydrogen bonds of the phenyl ring is not the sole factor determining the minimum energy conformation of the methyl group. There is a strong tendency to retain the trans orientation $\text{ClOC}\alpha\text{H}\alpha$ in Figure 23 for all methoxy group twist angles $\text{C2ClOC}\alpha$. This factor is well-known for methanol²²¹.

Crudely, the path in Figure 24 can be described by a potential

$$V(\phi) = 5.7 \sin^2 \phi + 2.5 \sin^2 2\phi \quad \text{Eq. (8)}$$

where V has the units $\text{kJ}\cdot\text{mol}^{-1}$. This form is suggested by Lister⁵⁰. The two-fold barrier is in exact agreement with the

energy difference proposed on the basis of the temperature dependence of the photoelectron spectrum⁸⁷. The validity of the two-site model which yields this number is, however, doubtful⁸⁹ and indeed inconsistent with Eq. (8). The present number does exceed the minimum energy difference between the planar and orthogonal conformations which is expected for anisole on the basis of the microwave spectrum of 4-fluoroanisole⁵⁰. The four-fold component is "reasonably large", as Lister suggests.

In the harmonic oscillator approximations with a reduced rotational constant between 1.2^{50} and 1.5 cm^{-1} ⁶⁹ Eq. (3) yields torsional frequencies between 66 and 89 cm^{-1} . The observed frequency is 81.5 cm^{-1} for gaseous anisole⁶⁵.

Catalán and Yáñez are reluctant to believe that the planar conformation of anisole is preferred since the proton affinity of oxygen agrees with a prediction for the orthogonal conformation²¹⁷. On the assumption of the same linear relationship between proton affinity and theoretical $1s$ -orbital binding energy, the present calculations predict proton affinities for oxygen which are $837 \text{ kJ}\cdot\text{mol}^{-1}$ for the planar conformation and $815 \text{ kJ}\cdot\text{mol}^{-1}$ for the orthogonal one. The experimental number is $834 \text{ kJ}\cdot\text{mol}^{-1}$ ²²², which may suggest that the planar conformer is preferred, but not to the exclusion of others. The predicted proton affinity of the para carbon is $769 \text{ kJ}\cdot\text{mol}^{-1}$ for the planar conformation and $808 \text{ kJ}\cdot\text{mol}^{-1}$ for the orthogonal conformation, which runs counter

to the trend proposed by Catalán and Yáñez. Although the experimental proton affinity of the para carbon is unknown, the proton magnetic resonance spectra of some anisole derivatives in strongly acidic solutions support this contention^{223,224}. Anisole prefers protonation of the para carbon over protonation of oxygen, but protonation of oxygen is preferred by 2,6-dimethylanisole, in which conjugation between oxygen and the π -system is inhibited.

Atomic charges (gross orbital charges condensed to atoms) and π -charges are given in Table 22 for the planar and orthogonal conformations. If the atomic charge on carbon is 6.063e for benzene²¹⁶, the apparent σ -electron withdrawal of the methoxy group is 0.229e for the planar and 0.190e for the orthogonal conformation. Inhibition of conjugation drops the π -electron donation from 0.087e to 0.037e.

Table 22

Atomic and π -Charges for Anisole from ST0-3G Calculations with
Partial Geometry Optimization.

	planar		orthogonal	
	atomic	π	atomic	π
C1	5.876	0.986	5.886	1.003
C2	6.097	1.065	6.079	1.019
C3	6.053	0.984	6.058	0.993
C4	6.075	1.030	6.066	1.010
C5	6.055	0.982	6.058	0.993
C6	6.080	1.040	6.078	1.019
O	8.237		8.242	
C α	6.060		6.062	
H2	0.937		0.931	
H3	0.935		0.934	
H4	0.940		0.937	
H5	0.934		0.934	
H6	0.928		0.931	
H α	0.922		0.926	
H	0.936		0.939	
H	0.936		0.939	

ii) semi-empirical molecular orbital calculations

Semi-empirical molecular orbital calculations in the INDO MO FPT approximation yielded the relative energy and dipole moment of the conformers listed in Table 23. Standard geometries were chosen for most parameters. In particular, the bond angle at oxygen was 120° , in rough agreement with the experimental value⁷¹.

The relative energies appear graphically in Figure 25. No minimum exists at the orthogonal conformation. A different choice of geometry¹³⁹ does provide a relative minimum, indeed the energy is below the lower bound suggested by Lister⁵⁰. Dipole moments from the present calculations were higher than 1.25 D ²¹⁸.

Spin-spin coupling constants appear in Tables 23, 24, and 25. Plots of the angle dependence of these numbers comprise Figures 26 and 27. From Figure 26 it appears that ${}^5J_p^{C\alpha,C4}$ follows the form

$${}^5J_p^{C\alpha,C4}(\phi) \approx {}^5J_{90}^{C\alpha,C4} \sin^2\phi \quad \text{Eq. (9)}$$

where ${}^5J_{90}^{C\alpha,C4}$ is about 1.26 Hz. If such a relationship does hold, this coupling may be a useful conformational indicator because it follows a simple function of the twist angle ϕ . If the contribution from transmission of spin information through the σ -bond framework^{225,226} (σ -mechanism) vanishes, the coupling is probably transmitted via spin polarization of the π -electrons²²⁷

Table 23

Carbon-Carbon Spin-Spin Coupling Constants, Relative Energy, and Dipole Moment for Some Conformations of Anisole from INDO MO FPT Calculations^a.

ϕ (deg)	$J^{C\alpha, X}$ (Hz)						energy (kJ·mol ⁻¹)	μ (D)
	X=C1	C2	C3	C4	C5	C6		
0	-4.827	1.727	-0.231	-0.017	0.129	3.002	0	1.456
	(-5.095	1.901	-0.169	-0.000	0.222	3.452) ^b		
	(-2.129	1.752	0.067	-0.003	0.113	1.777) ^c		
15	-4.851	1.792	-0.296	0.079	0.044	2.924	1.32	1.462
30	-4.913	1.806	-0.487	0.335	-0.193	2.723	3.59	1.479
45	-4.995	1.626	-0.762	0.675	-0.524	2.453	5.00	1.500
60	-5.013	1.410	-1.004	0.979	-0.833	2.109	5.91	1.520
75	-4.977	1.337	-1.135	1.171	-1.045	1.742	6.63	1.534
90	-4.994	1.480	-1.167	1.255	-1.167	1.480	6.93	1.539

a From the standard geometry except C10 = 140.0 pm, OC α = 143.4 pm, and COC α = 120°.

b From the STO-3G partially-optimized geometry.

c From CNDO//STO-3G calculations.

Figure 25

A plot of the relative energies of some conformations of anisole from INDO molecular orbital calculations.

- from this work.
- from reference 139.

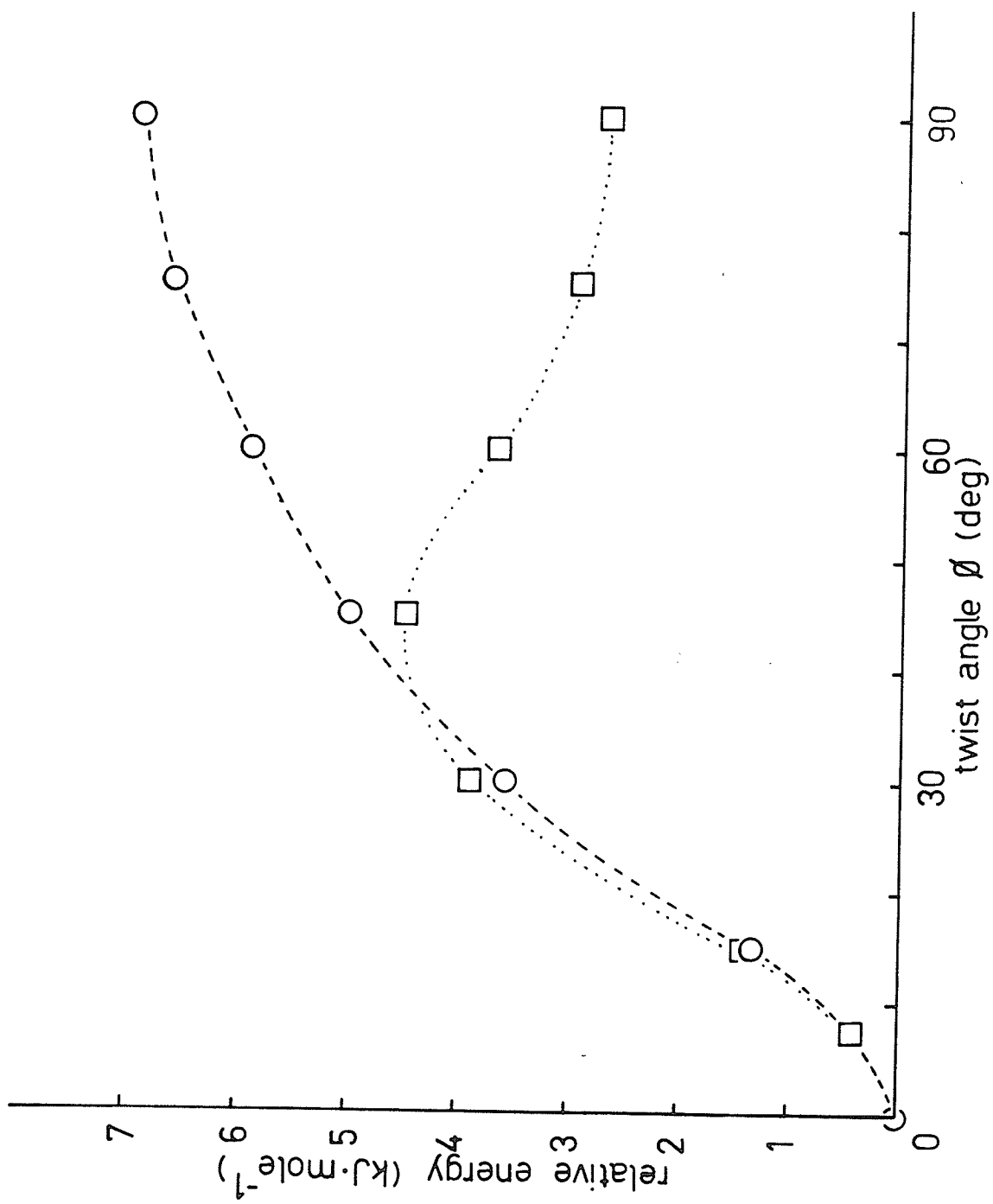


Table 24

Carbon-Proton Spin-Spin Coupling Constants for Some Conformations of Anisole from INDO MO FPT Calculations^a.

ϕ (deg)	X=H2	$J^{C\alpha, H}$ (Hz)						H	average H
		H3	H4	H5	H6	H	H		
0	-0.103	-0.134	-0.012	0.442	-0.479	139.035	133.958	133.958	135.650
	(0.005	-0.090	-0.008	0.450	-0.439	-	-	-	135.082) ^b
	(-0.012	0.029	-0.000	0.189	-0.051	-	-	-	103.461) ^c
15	-0.163	-0.118	-0.035	0.436	-0.492	139.088	133.907	133.942	135.646
30	-0.259	-0.071	-0.102	0.420	-0.528	139.270	133.677	133.752	135.566
45	-0.320	-0.001	-0.198	0.394	-0.574	139.549	133.303	133.293	135.382
60	-0.384	0.072	-0.283	0.346	-0.596	139.696	132.814	132.686	135.065
75	-0.463	0.138	-0.335	0.278	-0.580	139.704	132.336	132.218	134.753
90	-0.541	0.211	-0.359	0.211	-0.541	139.778	132.172	132.172	134.707

...Table 24 continued....

Table 24.....

- a From the standard geometry except C10 = 140.0 pm, OC α = 143.4 pm, and COC α = 120°.
- b From the STO-3G partially optimized geometry.
- c From CNDO//STO-3G calculations.

Table 25

Spin-Spin Coupling Constants Involving Methyl Protons and Ring
Nuclei for Planar Anisole from Semi-empirical Molecular
Orbital Calculations.^a

	INDO//STO-3G			CNDO//STO-3G		
	H α	H	average	H α	H	average
C1	7.518	0.833	3.061	5.282	0.855	2.331
C2	0.319	0.042	0.134	0.612	0.123	0.286
C3	0.143	-0.041	0.020	0.026	0.002	0.010
C4	-0.027	0.044	0.020	0.043	0.019	0.027
C5	0.449	-0.048	0.118	0.237	0.018	0.103
C6	0.259	-0.194	-0.043	0.419	0.013	0.148
H2	-0.124	-0.242	-0.203	-0.066	-0.178	-0.141
H3	0.037	-0.013	0.011	0.026	0.013	0.017
H4	0.025	-0.002	0.007	-0.000	0.004	0.003
H5	0.200	-0.031	0.046	0.146	0.008	0.054
H6	0.181	-0.012	0.052	0.120	0.007	0.045

a In Hertz.

Figure 26

A plot of the angle dependence of ${}^nJ^{Ca,Ci}$ ($n = 2-5$; $i = 1-4$) for anisole from INDO MO FPT calculations.

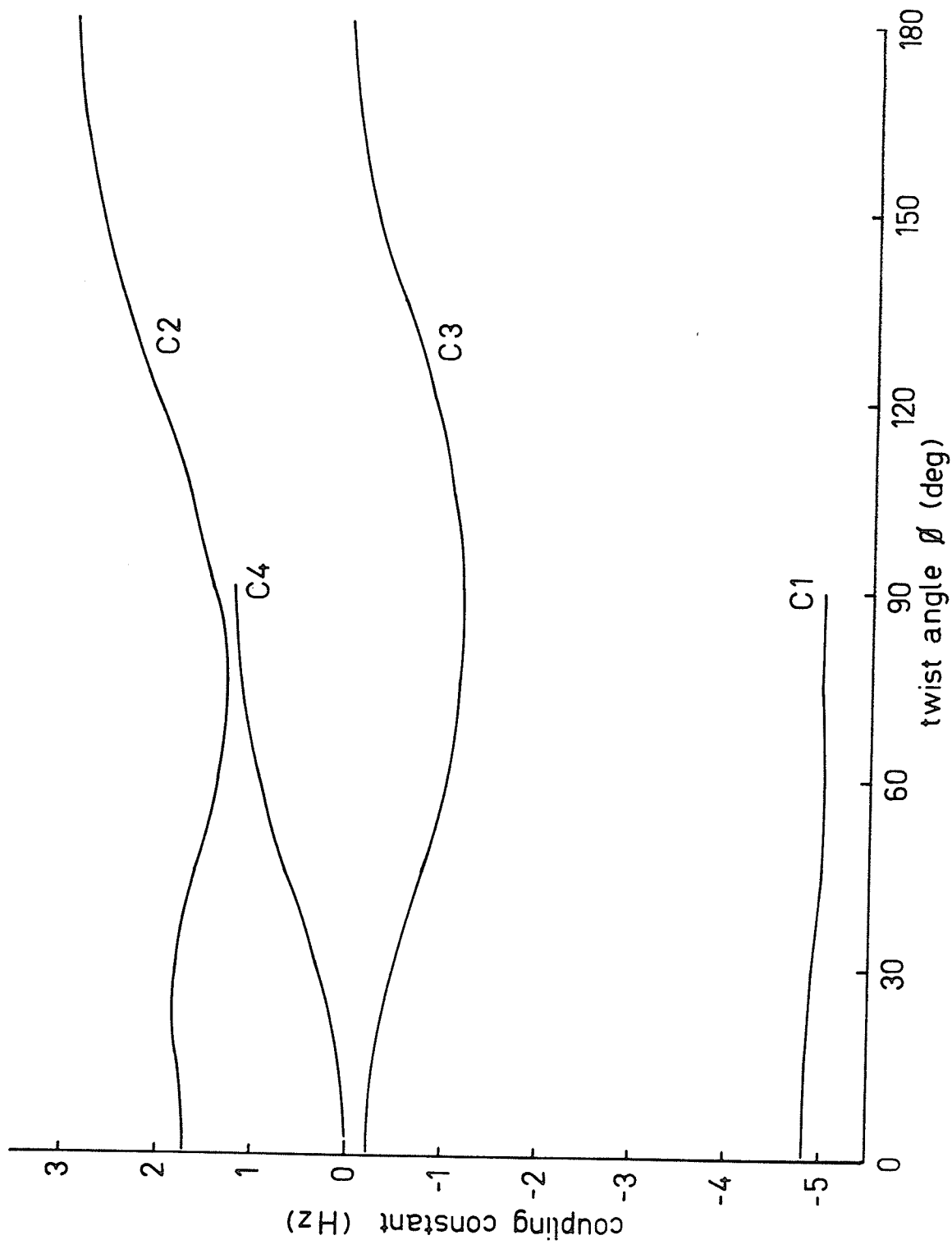
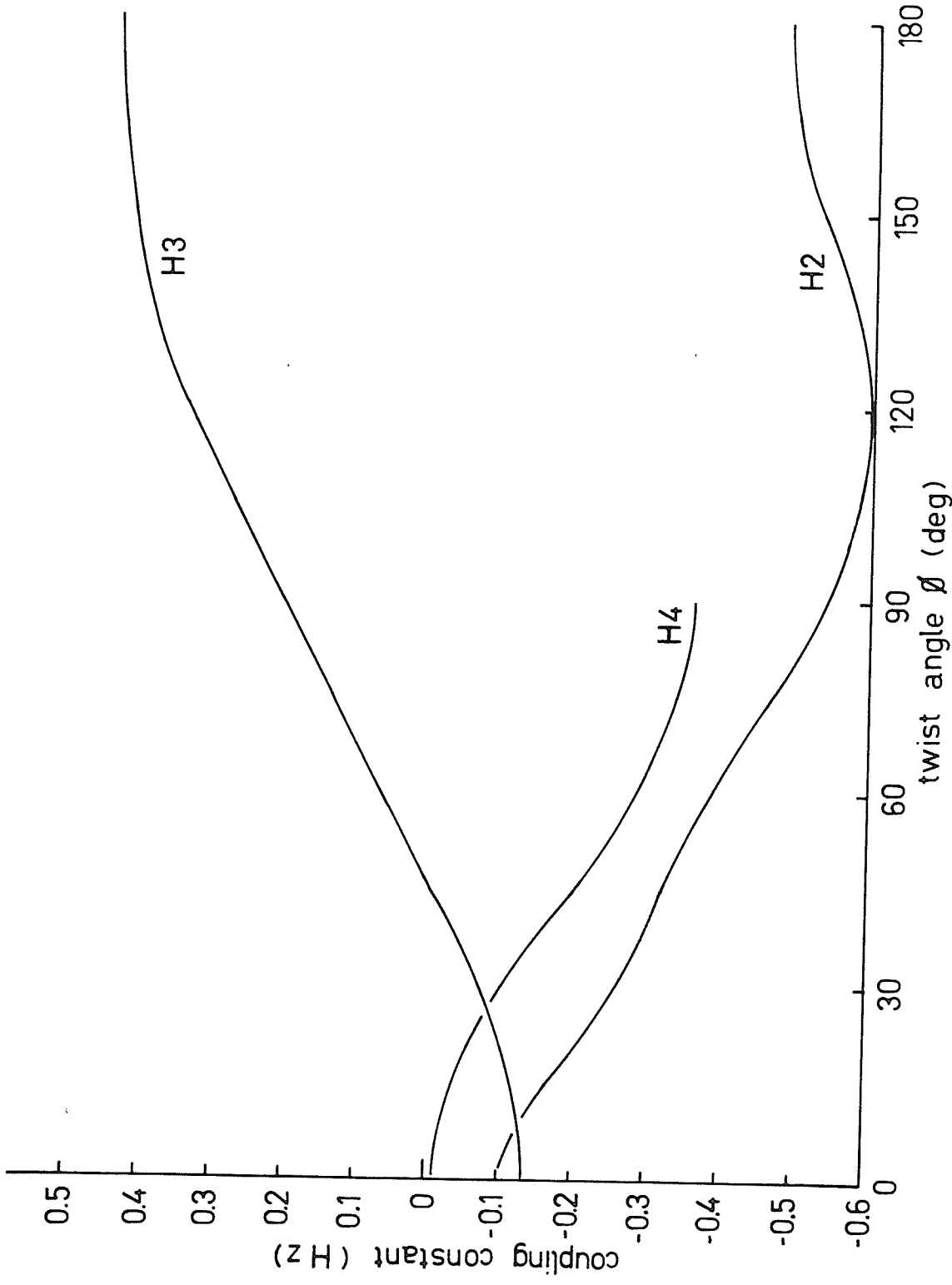


Figure 27

A plot of the angle dependence of ${}^n_J C_{\alpha, Hi}$ ($n = 4-6$; $i = 2-4$)
for anisole from INDO MO FPT calculations.



on C4 (σ - π -mechanism, or π -mechanism). Such a mechanism is responsible for the coupling over six formal bonds between alpha protons and a para proton in substituted benzenes, which is the foundation of the J method²⁷.

Of the other carbon-carbon coupling constants in Figure 26, ${}^3J_o^{C\alpha,C2}$ and ${}^4J_m^{C\alpha,C3}$ may be described by expressions of the form

$$J(\phi) = J_o + J_{90} \sin^2 \phi + J_{180} \sin^2 \frac{\phi}{2} \quad \text{Eq. (10)}$$

but the observed coupling is an average over the rotational potential²⁹. Consequently, empirical parametrization of this expression is difficult. The conformational dependence of ${}^2J^{C\alpha,C1}$ is not strong enough to be useful.

Both ${}^5J_m^{C\alpha,H3}$ and ${}^6J_p^{C\alpha,H4}$ increase monotonically in magnitude as the twist angle ϕ increases. Figure 27 shows that the latter dependence is analogous to the proton-proton coupling constant²⁷, although the form is not exact. Perhaps

$${}^6J_p^{C\alpha,H4}(\phi) \approx {}^6J_{90}^{C\alpha,H4} \sin^2 \phi \quad \text{Eq. (11)}$$

where ${}^6J_{90}^{C\alpha,H4}$ is about -0.36 Hz. Eq. (10) describes ${}^5J_m^{C\alpha,H3}$ if ${}^5J_o^{C\alpha,H3}$ is -0.13 Hz, ${}^5J_{90}^{C\alpha,H3}$ is 0.06 Hz, and ${}^5J_{180}^{C\alpha,H3}$ is 0.58 Hz. Such an equation is not easily used unless the rotational barriers are high enough to permit relatively few conformations with significant populations.

The angle dependence of ${}^4J_o^{C\alpha,H2}$ is more complicated and may

contain a contribution from proximate coupling.

Significant coupling between the methyl protons and C1, C2, and C5 occurs in the most stable conformation of anisole, as shown in Table 25. The couplings ${}^3J_{H\alpha,C1}$ and ${}^5J_{H\alpha,C5}$ occur over all-trans paths^{225,226}. On the other hand, ${}^4J_{H\alpha,C2}$ is larger than ${}^4J_{H\alpha,C6}$ which is transmitted over an all-trans arrangement of formal bonds. Some contribution from proximate coupling may be present in ${}^4J_{H\alpha,C2}$.

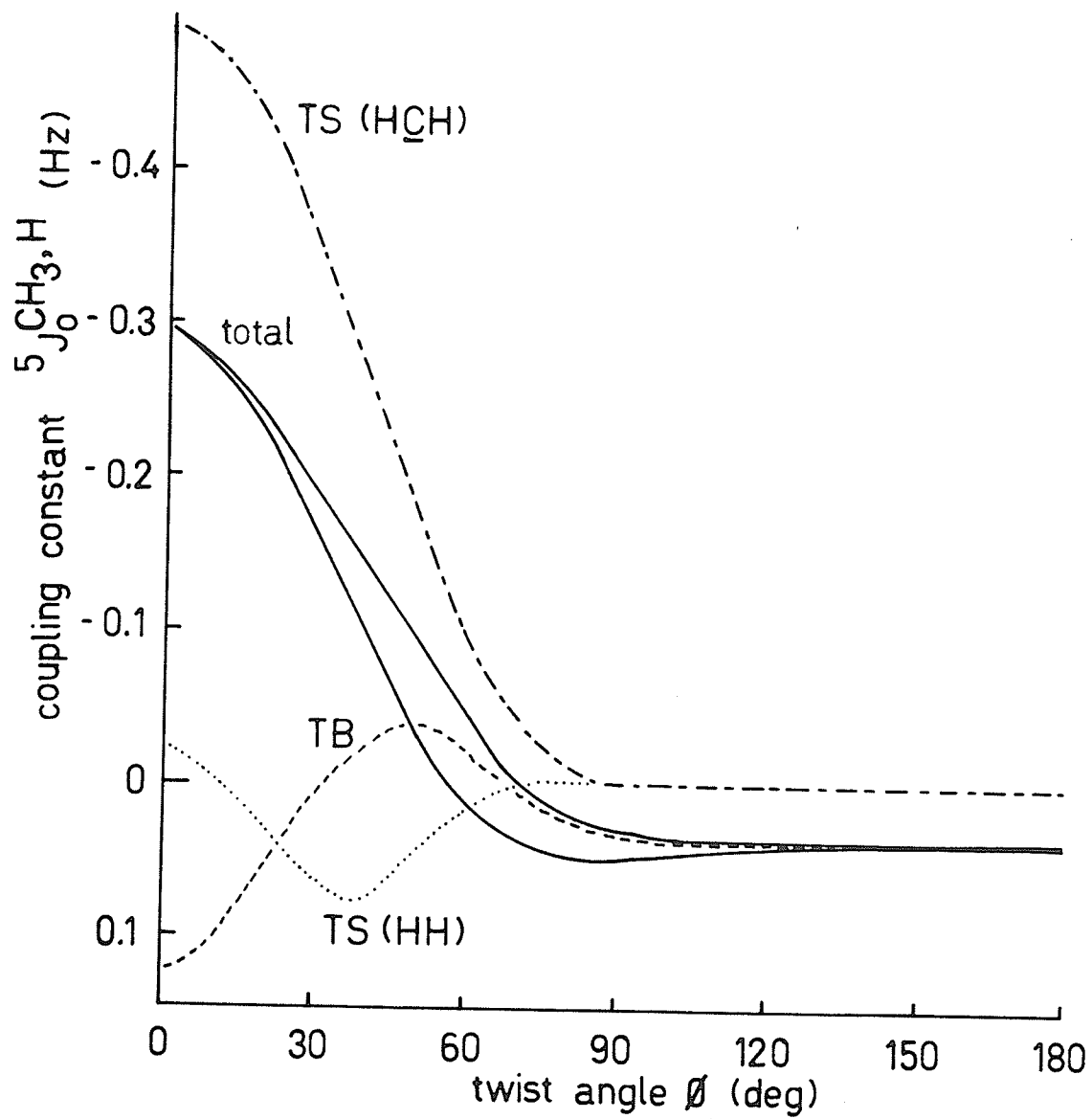
The large, negative coupling constant between the methyl protons and the proximate ring proton H2 is expected¹³⁶. A large, positive number is calculated for the all-trans path between the in-plane methyl proton H α and H5, but the average coupling constant ${}^6J_m^{CH_3,H5}$ is small. Similar remarks apply to ${}^5J_o^{CH_3,H6}$. Other couplings to ring protons are negligible.

The decomposition of ${}^5J_o^{CH_3,H2}$ by Schaefer and Laatikainen illustrates the angle dependence of coupling paths through formal bonds and through space¹³⁹. The latter encompasses direct interaction between the protons and interactions via the methyl carbon. Figure 28 depicts these contributions. The curve labelled TS(HCH) represents the difference between the coupling constant from the usual INDO FPT calculation and the coupling constant from a calculation in which the Fock elements between the ortho hydrogens and the s-orbital of the methyl carbon are set zero in each SCF cycle. Curve TS(H,H) represents the difference between the

Figure 28

A plot of the angle dependence of ${}^5J_{\text{O}}^{\text{H,CH}_3}$ and the contributions of certain interactions to it according to INDO MO FPT calculations.

From reference 139. See the text for explanation.



usual calculation and the coupling constant derived from a calculation in which all Fock elements between the ortho hydrogens and the methyl hydrogens are set at zero. Curve TB describes the difference between the coupling constant derived from the usual calculation and that from a calculation in which all Fock elements between the ortho hydrogens and the s-orbitals on the methyl carbon or on the methyl hydrogens are set at zero. These contributions are not strictly additive. Notice that the "total" coupling constant decreases quite quickly as the twist angle of the methoxy group increases. Of the two "total" curves depicted the lower corresponds to correlated motion of the methyl and methoxy groups to minimize steric interaction with the ortho hydrogen, but not necessarily to follow the minimum energy path (see the preceding subsection i).

iii) carbon chemical shifts

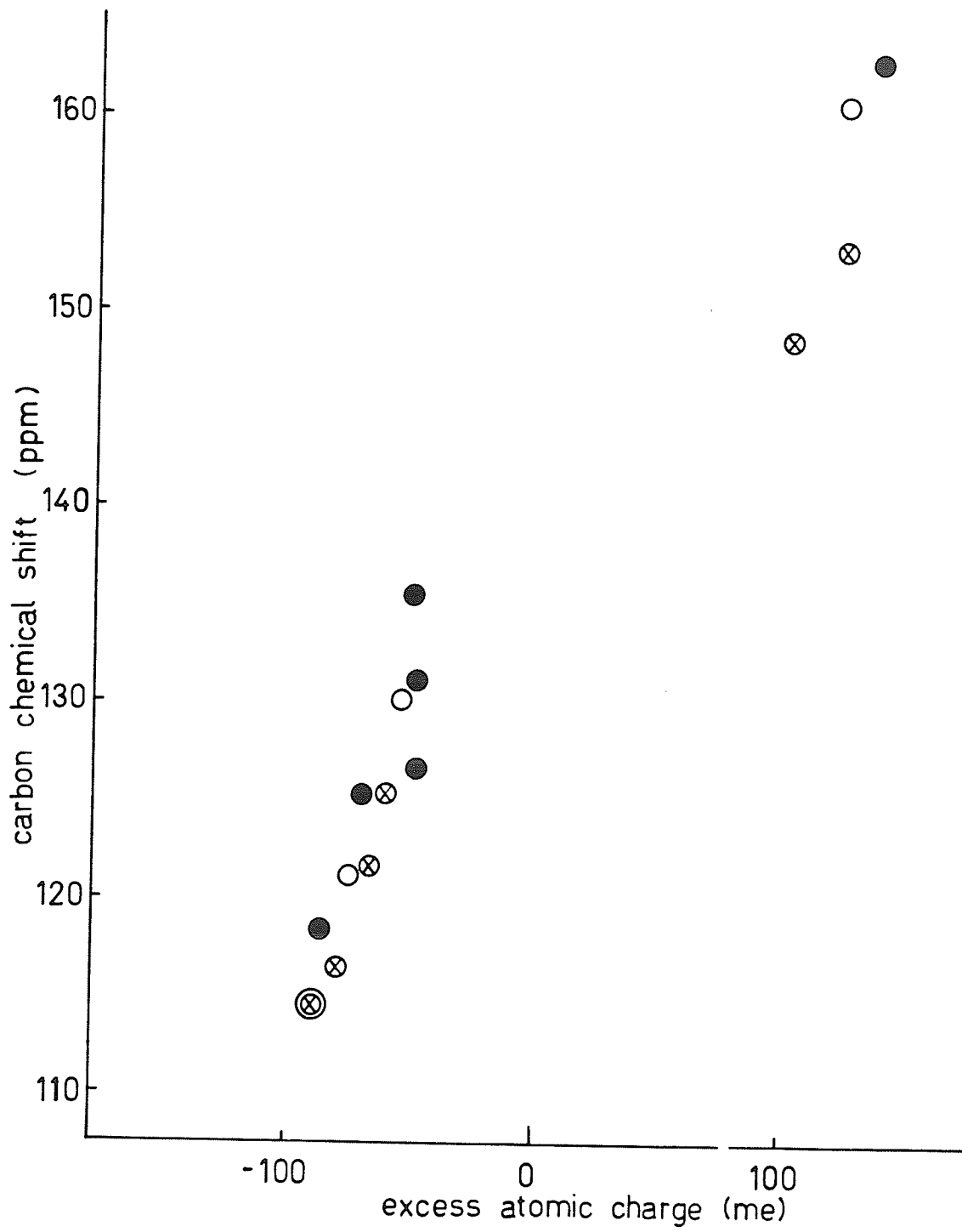
As noticed previously^{99,100}, the order of chemical shifts $C3 > C4 > C2$ opposes the order of π -electron densities in Table 22, but the downfield shift of C1 suggests that σ -electron withdrawal by the methoxy group is important. According to Henry and Fliszár, a correlation exists between net charge density and carbon chemical shift for certain ethylenic carbons²²⁸ and perhaps such a correlation exists in the present case. These authors caution that the chemical shift is a result of interaction between charge density and the magnetic environment and, therefore, a linear correlation of shift with charge is unwarranted. Ab initio calculations must be completely optimized, including orbital exponents, if the best approximation is to be expected. Also, the Mulliken population analysis is not satisfactory in half-and-half partitioning of overlap populations without regard for dissimilarity of the elements. Both of these criticisms apply to the charges in Table 22, but these numbers are used in Figure 29. With only four points the trend is not very significant.

Notice that the charge on C2 (6.097e) exceeds that on C6 (6.080). Whether this effect is transmitted through formal bonds or through space, it certainly reflects the conformation of the methoxy group and additional diamagnetic shielding of C2 is expected relative to C6. Of course this effect is not observed at temperatures which allow rapid interconversion

Figure 29

A plot of chemical shift for ring carbons versus atomic charges calculated at the STO-3G level.

- anisole
- ⊗ 2-fluoroanisole
- 2-fluoroacetophenone



between planar conformers on the nmr time-scale. If anisole did prefer the orthogonal conformation, the ortho carbons would not experience this shielding and would appear to be deshielded by a few ppm.

iv) coupling constants

Carbon-carbon coupling constants in Table 1 agree with values obtained from spectra of ^{13}C -satellites in carbon spectra²⁰⁹.

Comparison with the INDO MO FPT predictions indicates that $^2\text{J}_{\text{C}\alpha,\text{C}1}$ is negative, but over-estimated, and $^3\text{J}_{\text{C}\alpha,\text{C}2}$ is positive, but under-estimated. No conformational information can be extracted. As expected from the magnitude and angle dependence of $^4\text{J}_{\text{m}}^{\text{C}\alpha,\text{C}3}$ and the population distribution implied by Figure 24, the coupling constant is small if not zero.

Classically, the average value of $\sin^2\phi$ for the potential given by Eq. (8) is 0.212. If $^5\text{J}_{\text{p}}^{\text{C}\alpha,\text{C}4}$ is given by Eq. (9), the expected $^5\text{J}_{\text{p}}^{\text{C}\alpha,\text{C}4}$ is 0.27 Hz, not inconsistent with observation.

One-bond carbon-proton coupling constants in Table 1 are about 1 Hz larger than the numbers determined by selective decoupling of the methyl protons, which are to be preferred²²⁹. $^3\text{J}_{\text{C},\text{H}}$ values agree, but $^2\text{J}_{\text{C}4,\text{H}3}$ is only 0.85 Hz.

B. 2-Fluoroanisole

i) ab initio molecular orbital calculations

Some results of the present partial geometry optimization appear in Table 26 with reference to Figure 23. For the most part, the geometry of the aromatic ring remains standard. The methyl group retains C_{3v} symmetry about the oxygen-methyl carbon bond axis, but the methyl group twist angle $C1OC\alpha H\alpha$ is variable.

The geometry of trans-2-fluoroanisole is nearly identical to that of planar anisole. No experimental determination is available for comparison, but the bond angle at oxygen is probably too small, as for STO-3G geometries of water, phenol, and anisole.

The dipole moment of 2-fluoroanisole is $2.31 D^{46}$, larger than the number expected if the entire population is trans. The oxygen-methyl carbon bond axis and the dipole moment make an angle of 43.4° in the trans conformer, 63.6° in the orthogonal conformation, and 86.2° in the cis conformer, according to the calculations.

Relative energies from Table 26 appear in Figure 30. Description of this minimum energy path by a Fourier series is too complicated to be useful, but for small twist angles about the trans conformer the curve resembles that for anisole in Figure 24. The relative minimum near the orthogonal conformation is more pronounced than for anisole. The cis conformation

Table 26

Some Results of Partial Geometry Optimization in STO-3G Calculations for 2-Fluoroanisole^a

	0	45	90	115	135	155	180
C2C10C α							
C10	140.6	(140.6)	(140.6)	(140.4)	(140.4)	(140.4)	140.4
OC α	143.7	(143.7)	(143.7)	(143.2)	(143.2)	(143.2)	143.2
CH α	109.3	(109.3)	(109.3)	(109.3)	(109.3)	(109.3)	109.3
CF	136.1	(136.1)	(136.1)	(135.7)	(135.7)	(135.7)	135.7
C10C α	115.5	113.1	110.1	111.4	113.8	114.6	115.4
C2C10	127.6	124.3	119.9	117.5	115.1	114.8	114.0
C1C2F	122.5	121.2	119.8	(119.0) ^b	119.6	(119.6)	119.7
H6C6C1	118.3	118.6	119.0	(120.3)	120.3	(120.3)	121.0
OC α H α	110.3	(110.3)	(110.3)	(110.5)	(110.5)	(110.5)	110.5
C10C α H α	180.0	172.5	180.0	179.2 ^c	190.8	195.8	180.0
C3C2C10	180.0	177.9	177.9	177.7	177.3	179.0	180.0
dipole moment (D)	0.501	1.150	1.831	1.993	2.042	2.084	2.092
total energy (H)	-437.76329	-437.76397	-437.76438	-437.76385	-437.76369	-437.76483	-437.76552
relative energy (kJ.mol ⁻¹)	5.8 ₅	4.0 ₅	2.9 ₉	4.3 ₈	4.7 ₉	1.7 ₉	0

...Table 26 continued...

Table 26....

a Angles in degrees, bondlengths in pm.

Quantities in parentheses were assumed and not optimized.

b This angle is slightly too small due to a typographical error in the geometry input.

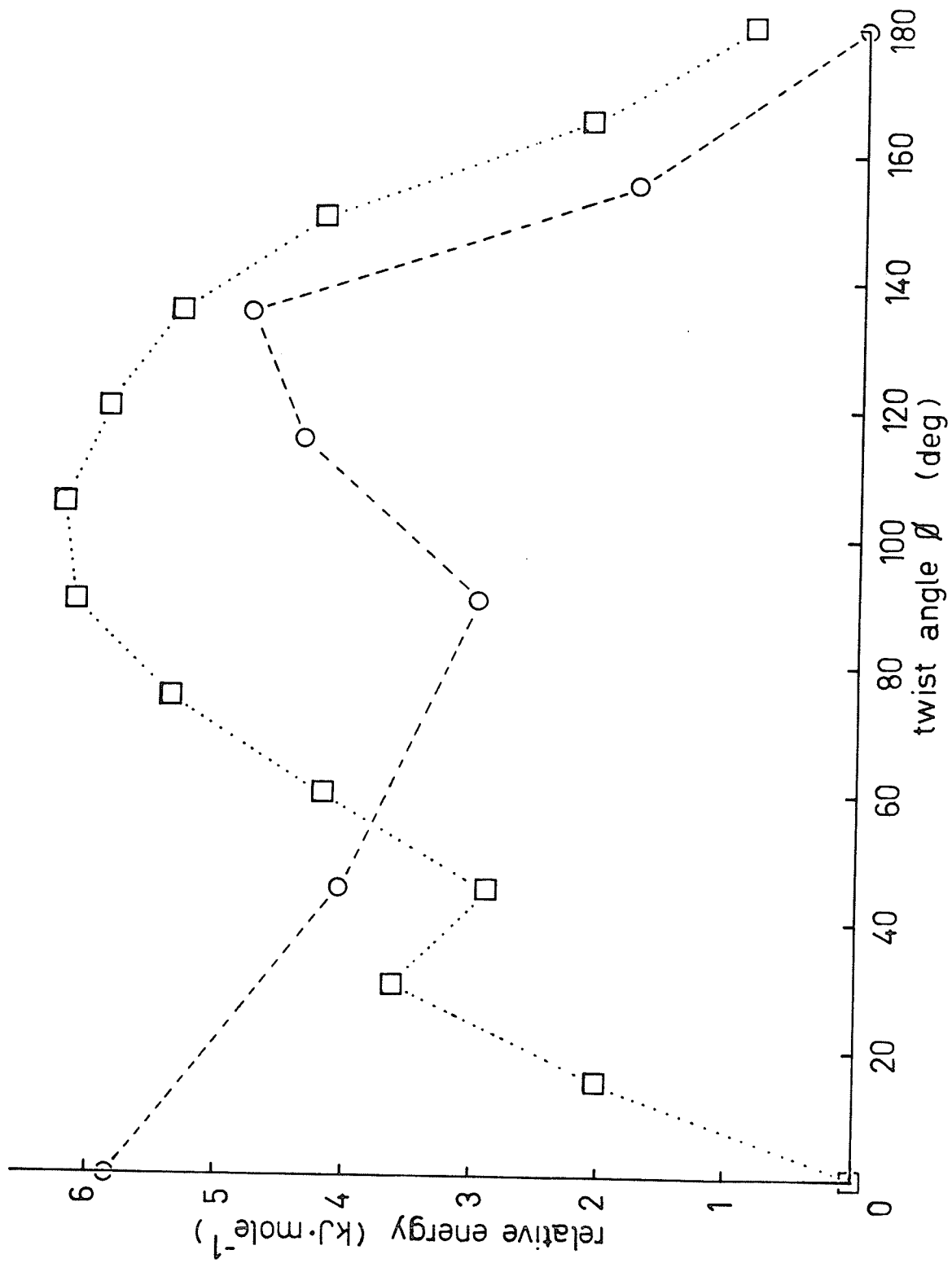
c Probably 180 deg.

Figure 30

A plot of the relative energies of some conformations of 2-fluoroanisole from partially-optimized molecular orbital calculations at the STO-3G level and from INDO molecular orbital calculations.

○ STO-3G

□ INDO



represents a relative energy maximum and is not populated significantly. This must result from proximate interaction between fluorine and the methyl group.

Atomic charges and π -charges for the trans, orthogonal, and cis conformers appear in Table 27. The total π -electron donation for these conformers is 0.151e, 0.104e, and 0.144e, respectively. If the atomic charge on carbon is 6.063 in benzene, the apparent σ -electron withdrawal by the substituents is 0.311e, 0.319e, and 0.310e. Simple additivity of π -charge differences for anisole and fluorobenzene, relative to benzene, is obeyed nearly in 2-fluoroanisole. The reduction of π -electron donation in the orthogonal conformer is then comparable to the reduction for the orthogonal conformer of anisole, 0.05e. Net atomic charges of the ring carbons are not additive.

Table 27

Atomic and π -Charges for 2-Fluoroanisole from STO-3G Calculations
with Partial Geometry Optimization

	trans		orthogonal		cis	
	atomic	π	atomic	π	atomic	π
C1	5.897	1.020	5.906	1.038	5.897	1.017
C2	5.876	1.044	5.878	1.026	5.897	1.069
C3	6.079	1.021	6.082	1.029	6.076	1.019
C4	6.066	1.015	6.058	0.996	6.066	1.016
C5	6.060	1.001	6.065	1.010	6.061	0.998
C6	6.089	1.050	6.070	1.005	6.071	1.025
O	8.234		8.239		8.234	
C α	6.058		6.061		6.063	
F	9.126		9.128		9.136	
H3	0.926		0.926		0.925	
H4	0.934		0.931		0.934	
H5	0.934		0.933		0.933	
H6	0.932		0.925		0.922	
H α	0.919		0.923		0.923	
H	0.935		0.939		0.931	
H	0.935		0.936		0.931	

ii) semi-empirical molecular orbital calculations

Semi-empirical molecular orbital calculations in the INDO MO FPT approximation were based on standard geometry unless otherwise indicated. The bond angle at oxygen was 120° , as for anisole.

Relative energies appear in Table 28 and in Figure 30. There is a relative maximum near the orthogonal conformation and the planar conformations are nearly degenerate. The relative maximum near 30° is caused by steric interaction of one methyl hydrogen-carbon bond with the fluorine.

Comparison of the dipole moments in Table 28 with 2.31 D^{46} suggests that many kinds of conformational mixture could reproduce the observed value.

Spin-spin coupling constants appear in Tables 28 and 29, and in Figures 31 and 32. Notice that the angle dependence of ${}^3J_{\text{O}} \text{C}\alpha, \text{C6}$, ${}^4J_{\text{m}} \text{C}\alpha, \text{C3}$, ${}^4J_{\text{m}} \text{C}\alpha, \text{C5}$, and ${}^5J_{\text{p}} \text{C}\alpha, \text{C4}$ resembles that for the analogous couplings in anisole. If these couplings experience only minor substituent effects, they may be useful conformational indicators, as mentioned previously. From comparison of Figures 27 and 32, couplings between the methyl carbon and ring protons are relatively insensitive to the fluorine substituent.

The angle dependence of ${}^5J_{\text{O}} \text{CH}_3, \text{F}$ and ${}^4J_{\text{O}} \text{C}\alpha, \text{F}$ is a complicated function which depends on the proximity of coupled nuclei and on

Table 28

Carbon-Carbon Spin-Spin Coupling Constants, Relative Energy, and Dipole Moment for Some Conformations of 2-Fluoroanisole from INDO MO FPT Calculations^a

ϕ (deg)	$J^{C\alpha, X}$ (Hz)						energy ($\text{kJ}\cdot\text{mol}^{-1}$)	μ (D)
	X=C1	C2	C3	C4	C5	C6		
0	-4.666	0.790	-0.262	-0.016	0.108	2.879	0	1.501
	(-4.970)	1.194	-0.211	-0.003	0.259	3.265) ^b		
	(-2.101)	0.950	-0.000	-0.002	0.115	1.784) ^c		
15	-4.736	0.777	-0.337	0.075	0.018	2.812	2.030	1.551
30	-4.893	0.850	-0.525	0.318	-0.221	2.622	3.680	1.701
45	-5.061	1.049	-0.769	0.646	-0.547	2.363	3.401	1.928
60	-5.211	1.256	-1.020	0.984	-0.889	2.089	4.167	2.191
75	-5.388	1.483	-1.240	1.275	-1.199	1.866	5.393	2.453
90	-5.450	1.698	-1.283	1.375	-1.336	1.651	6.137	2.693
105	-5.435	1.948	-1.145	1.283	-1.295	1.526	6.234	2.900
120	-5.287	2.177	-0.820	0.995	-1.060	1.518	5.891	3.070
135	-5.202	2.454	-0.460	0.661	-0.782	1.718	5.343	3.200
150	-5.112	2.701	-0.109	0.323	-0.504	1.907	4.229	3.289
165	-5.084	2.906	0.139	0.070	-0.317	1.897	2.158	3.339

Table 28.....

180	-5.027	2.971	0.236	-0.031	-0.243	1.825	0.907	3.356
	(-5.285	3.189	0.276	-0.005	-0.198	1.890) ^b		
	(-2.181	1.636	0.127	-0.003	0.054	1.673) ^c		

a From the standard geometry except C10 = 140.4 pm, OC α = 143.2 pm, and COC α = 115.4°.

b From the STO-3G partially-optimized geometry.

c From CNDO//STO-3G calculations.

Table 29

Carbon-Proton Spin-Spin Coupling Constants for Some Conformations of 2-Fluoroanisole from
INDO MO FPT Calculations^a

ϕ (deg)	$J^{C\alpha,H}$ (Hz)										average H
	X=H3	H4	H5	H6	H	H	H	H	H	H	
0	-0.113 (-0.099 (0.057	0.011 0.009 0.003	0.424 0.432 0.191	-0.455 -0.410 -0.040	136.060 - -	137.348 - -	137.348	137.348	137.348	137.348	136.919 135.676) ^b 103.925) ^c
15	-0.098	-0.013	0.423	-0.471	136.086	134.721	139.715	136.841	139.715	136.841	136.841
30	-0.061	-0.081	0.412	-0.515	136.823	132.946	139.746	136.505	139.746	136.505	136.505
45	-0.012	-0.182	0.386	-0.576	138.295	132.343	137.578	136.072	137.578	136.072	136.072
60	0.055	-0.286	0.350	-0.628	139.496	132.257	135.508	135.754	135.508	135.754	135.754
75	0.143	-0.375	0.315	-0.662	140.227	132.259	134.335	135.607	134.335	135.607	135.607
90	0.222	-0.406	0.257	-0.631	140.539	132.273	133.699	135.504	133.699	135.504	135.504
105	0.290	-0.379	0.184	-0.549	140.587	132.431	133.437	135.485	133.437	135.485	135.485
120	0.332	-0.292	0.094	-0.432	140.307	132.642	133.299	135.416	133.299	135.416	135.416
135	0.372	-0.192	0.015	-0.357	140.109	133.161	133.491	135.587	133.491	135.587	135.587
150	0.399	-0.094	-0.054	-0.296	139.892	133.627	133.749	135.756	133.749	135.756	135.756
165	0.418	-0.026	-0.102	-0.198	139.893	133.970	133.969	135.965	133.969	135.965	135.965

...Table 29 continued...

Table 29.....

180	0.421	0.001	-0.018	-0.133	139.787	133.969	133.969	135.908
	(0.457	-0.002	-0.082	0.026	-	-	-	135.113) ^b
	(0.202	0.001	0.028	-0.013	-	-	-	103.497) ^c

a From the standard geometry except $OC1 = 140.4$ pm, $OC\alpha = 143.2$ pm, and $COC\alpha = 115.4^\circ$.

b From the STO-3G partially-optimized geometry.

c From CNDO//STO-3G calculations.

Figure 31

A plot of the angle dependence of ${}^nJ^{C\alpha, C_i}$ ($n = 2-5$; $i = 1-6$)
for 2-fluoroanisole from INDO MO FPT calculations.

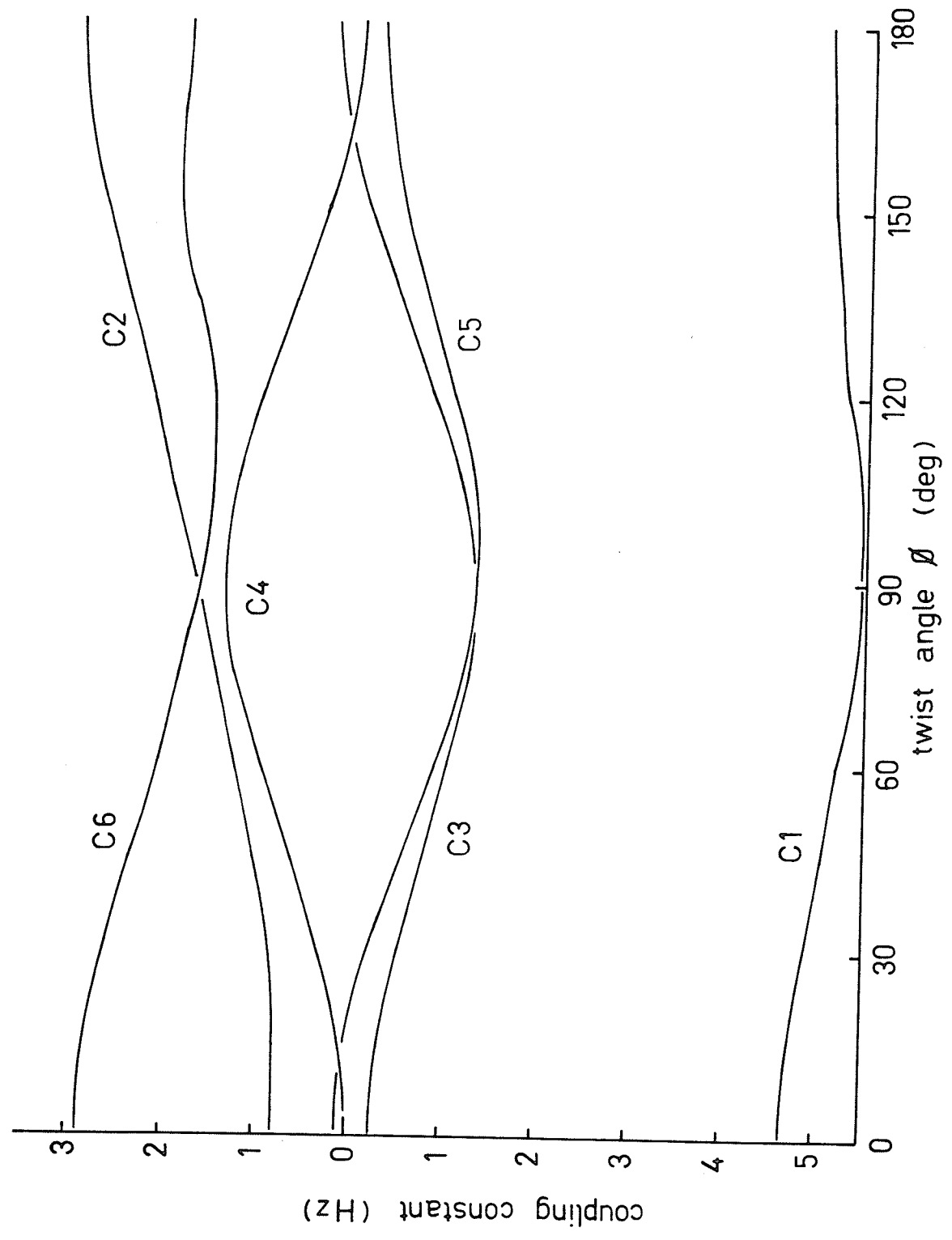
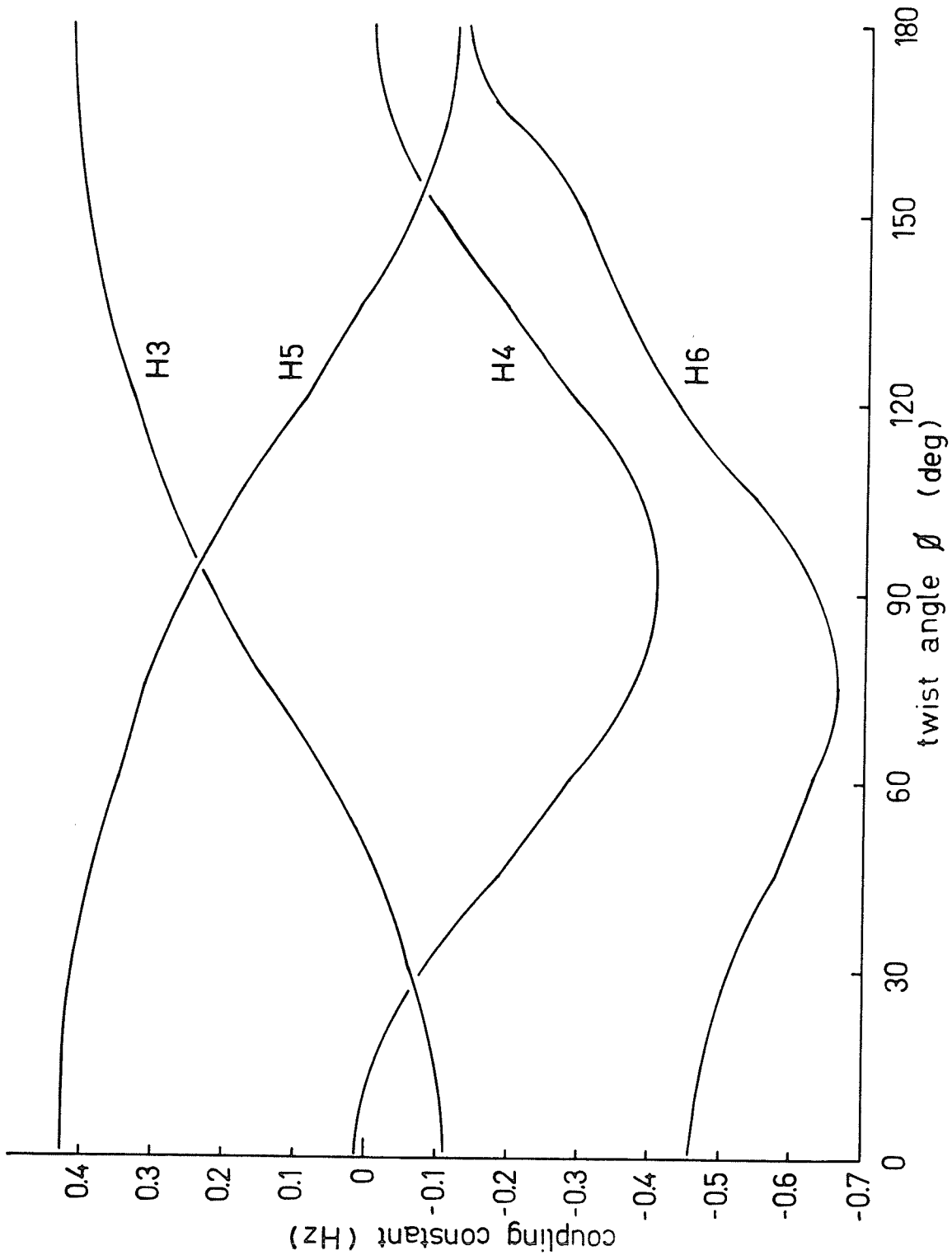


Figure 32

A plot of the angle dependence of $^5J^{C\alpha,Hi}$ ($n = 4-6$; $i = 3-6$)
for 2-fluoroanisole from INDO MO FPT calculations.



bond orientations. A description in terms of a single parameter, the methoxy group twist angle, is inadequate when a conformational average is computed. Despite this criticism, computations of the angle dependence of these coupling constants for a rigid rotator illustrate coupling mechanisms.

To estimate the importance of various coupling paths to ${}^5J_{\text{O}}^{\text{CH}_3, \text{F}}$ and ${}^4J_{\text{O}}^{\text{C}\alpha, \text{F}}$ the usual INDO MO FPT calculation is compared with calculations in which interactions between particular pairs of formally non-bonded atoms are neglected by setting the appropriate off-diagonal elements of the Fock matrix to zero in every self-consistent field (SCF) cycle²³⁰. The chosen geometry is that of the trans conformer in Table 26, but with $\text{C2C1O} = \text{C1C2F} = \text{H6C6C1} = 120^\circ$. For each conformer coupling constants appear in Table 30 and in Figures 33 and 34 to represent the usual calculation (labelled "total") and calculations which neglect interaction between the fluorine and the methyl group (labelled "TB") or just the methyl carbon (labelled "no CF") or just the methyl hydrogens (labelled "no HF"). Notice that contributions from these paths are not strictly additive since this procedure is only a means of approximation.

According to Figures 33 and 34, contributions from coupling through formal bonds are relatively unimportant. In the calculations ${}^5J_{\text{O}}^{\text{CH}_3, \text{F}}$ is dominated by the direct interaction of fluorine and hydrogens. Neglect of the fluorine-methyl carbon

Table 30

Some Spin-Spin Coupling Constants for 2-Fluoroanisole from INDO MO FPT Calculations

ϕ (deg)	$^5 J_{\text{O}}^{\text{CH}_3, \text{F}}$ (Hz)			$^4 J_{\text{O}}^{\text{C}\alpha, \text{F}}$ (Hz)			
	total	no HF	no CF	total	no HF	no CF	
0	4.165 (16.222) (-1.864)	18.783 9.014 23.667	-10.359 2.00 -16.538	19.618	-14.698	52.973	TB 1.371
15	-4.351	15.358	-15.071	31.648	-11.858	60.037	1.227
30	-12.774	8.614	-17.490	38.496	-6.317	55.507	0.879
45	-7.942	3.572	-9.711	20.346	-2.241	27.748	0.553
60	-2.303	1.260	-2.873	5.825	-0.386	8.154	0.395
75	-0.294	0.506	-0.429	1.359	0.216	1.192	0.349
90	0.153	0.306	0.137	0.480	0.324	0.560	0.306
120	0.199	0.208	0.202	-0.063	-0.071	-0.085	-0.097
150	0.181	0.185	0.179	-0.074	-0.713	-0.705	0.714
180	0.199	0.202	0.197	-0.999	-1.006	-0.988	-0.995

a Between F and H α in Figure 23

b Between F and H in Figure 23

Figure 33

A plot of the angle dependence of ${}^5J_{\text{O}}^{\text{CH}_3, \text{F}}$ in 2-fluoroanisole when certain Fock elements are kept zero throughout the INDO MO FPT calculations.

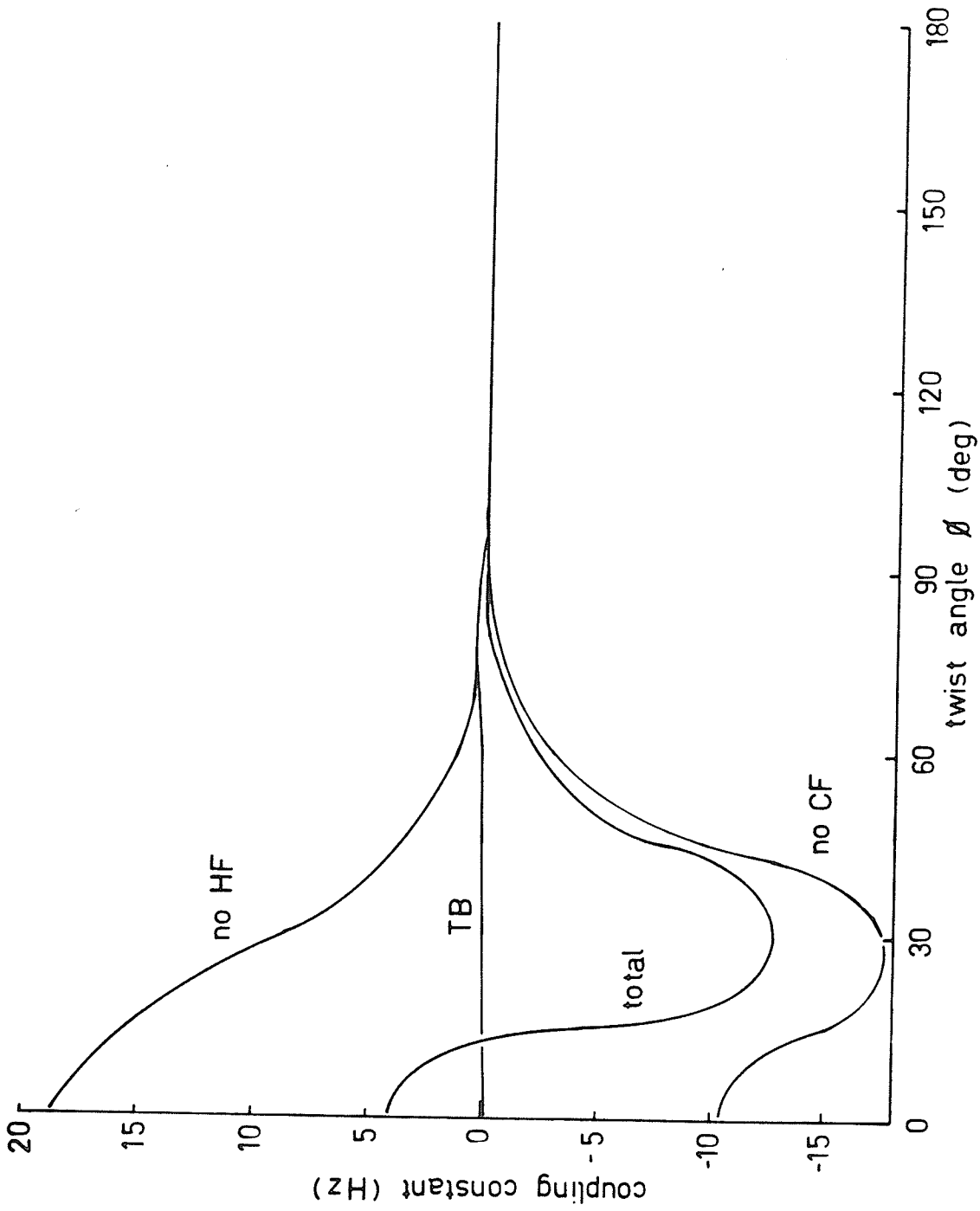
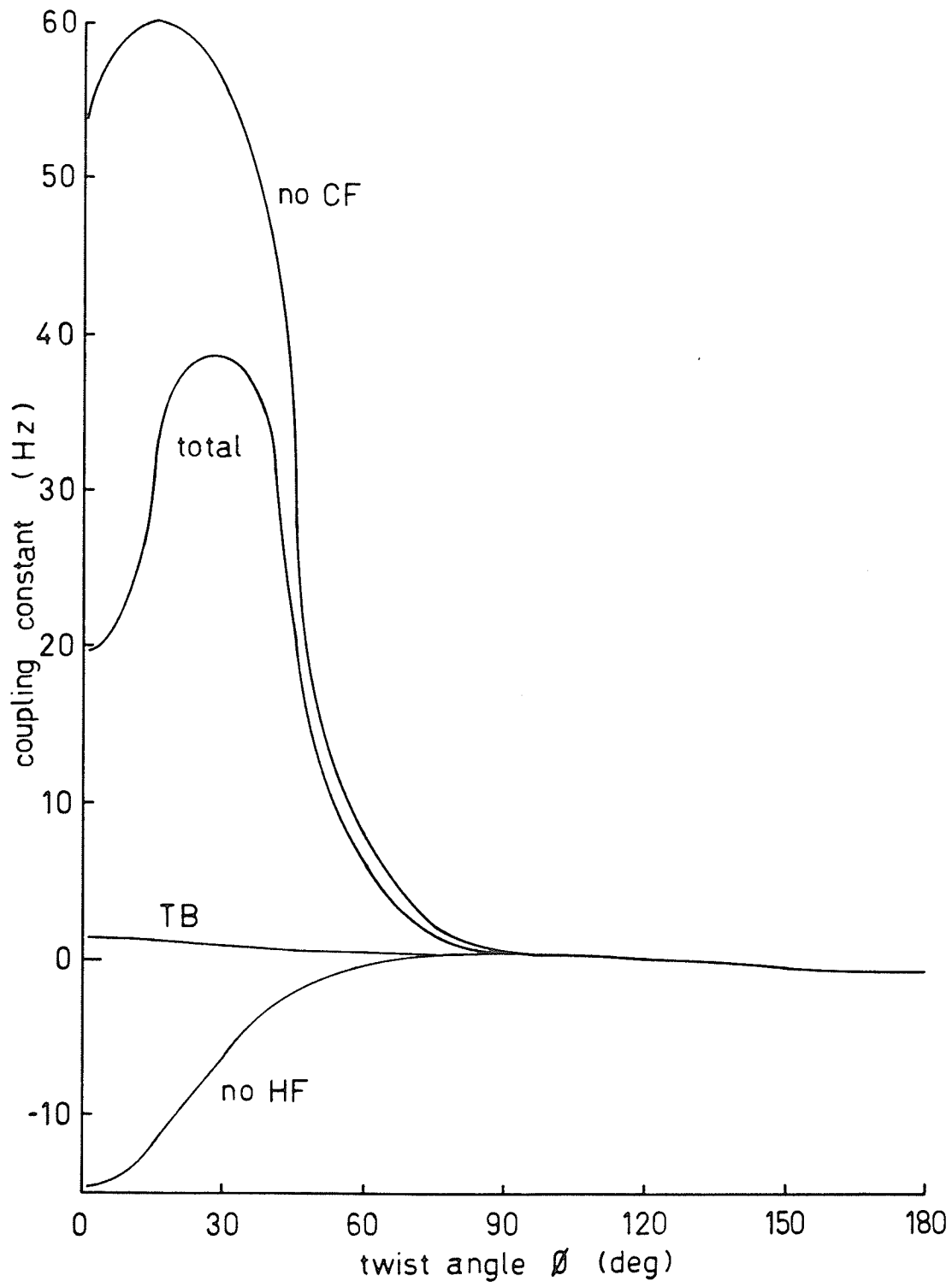


Figure 34

A plot of the angle dependence of ${}^4J_{\text{O}}^{\text{C}\alpha,\text{F}}$ in 2-fluoroanisole when certain Fock elements are kept zero throughout the INDO MO FPT calculations.



interaction produces relatively small changes in the form of the angle dependence and in the energy, relative to neglect of the fluorine-methyl hydrogen interaction. The contribution of indirect interaction via the methyl carbon to ${}^5J_{\text{O}}^{\text{CH}_3, \text{F}}$ is positive.

Indirect interaction mediated by the methyl hydrogens dominates ${}^4J_{\text{O}}^{\text{C}\alpha, \text{F}}$. The contribution of this mechanism is positive and the direct fluorine-methyl carbon interaction provides a negative contribution.

In the absence of fluorine-methyl carbon interactions, fluorine-methyl hydrogen coupling might be transmitted indirectly via another methyl hydrogen, but calculations which exclude methyl hydrogen-methyl hydrogen interactions do not implicate this mechanism.

Examination of the couplings between fluorine and individual methyl hydrogens in the cis conformer is useful. The coupling constant involving the proton directed away from fluorine ($\text{H}\alpha$ in Figure 23) is large, positive, and responsible for the positive portion of the "total" curve in Figure 33. This coupling is transmitted via the methyl carbon. The coupling constant between fluorine and the other two protons is small and negative, but when the fluorine-methyl carbon interaction is neglected both numbers decrease by about 14.5 Hz. The coupling constant between fluorine and the more proximate methyl protons contains nearly

equal contributions from direct and indirect interaction, which differ in sign.

When the fluorine-methyl hydrogen interaction is eliminated, the coupling constant between fluorine and H_α is reduced by 7.2 Hz, but the other increases by 25.5 Hz so both are positive. Since direct fluorine-methyl hydrogen interaction provides a negative contribution to the coupling constant, the latter increase is expected. Net reduction of the coupling constant between fluorine and H_α is expected because this coupling is transmitted largely via the methyl carbon. Fluorine-methyl carbon coupling is dominated by indirect interaction via the methyl hydrogens. When the fluorine-methyl hydrogen interaction is removed, the fluorine-methyl carbon coupling decreases and consequently the indirect (positive) contribution to the fluorine-methyl proton coupling constant decreases.

Since the contributions of these mechanisms are interdependent, it is not surprising that the calculated effects are not additive.

iii) carbon spectrum

Comparison does not support a simple relationship between chemical shifts of the ring carbons from Table 3 and π -charges from Table 27. Inductive withdrawal of electron density by the methoxy and fluorine substituents is evident in the downfield shifts of C1 and C2, but not in the π -charges.

Linear regression by the method of least squares for the ten points from anisole and 2-fluoroanisole yields

$$\delta_c = 0.18 q_c + 133.56, \quad r = 0.97831 \quad \text{Eq. (12)}$$

where δ_c is the ring carbon chemical shift in ppm and q_c is the net atomic charge in millielectrons. The slope of this line, the charge ratio, is similar to those found by Spiesecke and Schneider and by Olah and coworkers²³¹. Ewing notes that the slope of such lines is quite variable²³². For example, Hehre, Taft and Topsom plot meta and para carbon shifts of mono-substituted benzenes separately and find slopes of 150 ppm electron⁻¹ and 450 ppm electron⁻¹ respectively²³³. When the ipso carbon shifts are excluded the seven remaining points yield

$$\delta_c = 0.41 q_c + 150.56, \quad r = 0.96953 \quad \text{Eq. (13)}$$

which is significant at the 1% level²³⁴.

Electron withdrawal from the σ -framework by the methoxy group may be seen in the carbon-fluorine spin-spin coupling constants in Table 3. There is an alternating substituent effect on

$^3J_{C,F}$ in fluorobenzene derivatives²⁰⁶, which is expected to make $^3J_{C6,F}$ smaller than $^3J_{C4,F}$ in 2-fluoroanisole. The magnitude of $^2J_{C1,F}$ is smaller than $^2J_{C3,F}$. The signs and magnitudes of analogous coupling constants in 1,2-difluorobenzene are consistent with the numbers in Table 3²³⁵.

iv) long-range couplings to methyl protons

In comparison with the INDO MO FPT results in Table 30 and with the other experimental results (vide infra), the magnitude of ${}^5J_{\text{O}}^{\text{CH}_3, \text{F}}$ suggests that the cis conformer is not significantly populated. This is in accord with the ab initio calculations, but contrary to the INDO prediction.

The magnitude of ${}^5J_{\text{O}}^{\text{CH}_3, \text{H6}}$ (ca 0.25 Hz for a benzene solution) is larger than for anisole itself, and is consistent with a strong preference for the trans conformer.

Methyl protons are not observably coupled to any other ring protons.

C. 4-Bromo-2-fluoroanisole

i) proton spectrum

The bromine substituent causes large downfield shifts of H3 and H5 relative to 2-fluoroanisole²³⁶. The small shift of H6 to higher field may be a substituent effect or due to a conformational change such as an increased preference for the trans conformer.

According to Figure 28, ${}^5J_{\text{O}}^{\text{CH}_3, \text{H6}}$ increases as the proximity of the methyl group and H6 increases. The magnitude of ${}^5J_{\text{O}}^{\text{CH}_3, \text{H6}}$ is 0.27 Hz in 4-bromo-2-fluoroanisole, 0.30 Hz in 4-formyl-2-fluoroanisole, and about 0.25 Hz in 2-fluoroanisole. Apparently the electron-withdrawing formyl substituent, and less clearly the bromine substituent, raises the two-fold component of the rotational potential of the methoxy group, or changes in bond lengths or angles bring these nuclei into closer proximity.

According to Figure 33, ${}^5J_{\text{O}}^{\text{CH}_3, \text{F}}$ is insensitive to minor conformational or geometrical changes if the trans conformer predominates. The magnitude is 0.17 Hz in 4-bromo-2-fluoroanisole, 0.21 Hz in 4-formyl-2-fluoroanisole, and 0.18 Hz in 2-fluoroanisole. The sign is positive. Doubling of ${}^5J_{\text{O}}^{\text{CH}_3, \text{F}}$ in carbon tetrachloride solution is presumably a solvent effect on the coupling constant, or possibly on the conformational energies²¹⁴.

The absence of observable coupling between the methyl carbon and H6 suggests that the trans conformer is preferred and that

INDO FPT calculations over-estimate ${}^4J_{\text{O}}^{\text{C}\alpha,\text{H}6}$ ($\phi=180^\circ$) in Figure 32. Since ${}^5J_{\text{m}}^{\text{C}\alpha,\text{H}5}$ is at most 0.05 Hz and ${}^5J_{\text{m}}^{\text{C}\alpha,\text{H}3}$ equals 0.26 Hz, the conformers near trans are preferred, but these numbers cannot be assigned to a particular twist angle in Figure 33.

ii) carbon spectrum

Relative to 2-fluoroanisole, C1 and C4 are expected to shift to higher field while C3, C5, C2, and C6 shift to lower field on the basis of additivity of bromine substituent-induced chemical shifts¹⁰⁰. Only C2, which bears the fluorine substituent, fails to meet this expectation, possibly because these substituents interact electronically. There is no clear evidence for a significant conformational change of the methoxy group. If the shielding of C1 is interpreted as an increase in net charge, however, it may signify an increase in conjugation between oxygen and the π -system.

INDO FPT calculations over-estimate ${}^2J_{C\alpha,C1}$ in anisole and produce even larger values for conformations of 2-fluoroanisole which are near the trans conformer. In 4-bromo-2-fluoroanisole ${}^2J_{C\alpha,C1}$ equals 2.15 Hz in magnitude, smaller than for anisole (2.33 Hz), which may indicate an increased preference for the trans conformer. Calculations also support the notion that ${}^3J_{O,C\alpha,C2}$ is greater than ${}^3J_{O,C\alpha,C6}$ in those conformations (see Figure 31). The other coupling constants are not inconsistent with this picture.

The small value of ${}^4J_{O,C\alpha,F}$ corresponds to a preference for the trans conformer, but the suggested positive sign is contrary to the INDO result. The bromine substituent increases the magnitudes of ${}^2J_{C3,F}$ and ${}^3J_{C4,F}$, as expected for an alternating

substituent effect on these coupling constants²⁰⁶. $^2J_{C1,F}$ and $^4J_{C5,F}$ remain unchanged, but $^3J_{C6,F}$ is more than double the value in 2-fluoroanisole.

The discussion of ring carbon-proton coupling constants is postponed to the following section.

D. 4,6-Dibromo-2-fluoroanisole

i) proton spectrum

The bromine substituent ortho to the methoxy group shifts the resonances of H3 upfield and the resonances of H5 downfield relative to 4-bromo-2-fluoroanisole.

Since ${}^5J_{\text{O}}^{\text{CH}_3, \text{F}}$ equals 1.484 Hz for the acetone- d_6 solution and 1.569 Hz for the carbon tetrachloride solution, the coupled nuclei are more proximate than the trans conformer allows.

Evidently steric repulsions disfavour the methoxy group cis to fluorine, which suggests that non-planar conformations are abundant. The positive sign of ${}^5J_{\text{O}}^{\text{CH}_3, \text{F}}$ can be reconciled with Figure 33 if the cis conformer is preferred very strongly. These calculations are more likely to suggest that the sign is negative, possibly because the negative contribution of fluorine-methyl hydrogen interaction is over-estimated relative to the contribution from fluorine-methyl carbon interaction.

By comparison with Figure 32 both ${}^5J_{\text{m}}^{\text{C}\alpha, \text{H3}}$ and ${}^5J_{\text{m}}^{\text{C}\alpha, \text{H5}}$ imply that the methoxy group prefers to lie near the plane perpendicular to the ring plane. Since ${}^5J_{\text{m}}^{\text{C}\alpha, \text{H3}}$ equals 0.216 Hz and ${}^5J_{\text{m}}^{\text{C}\alpha, \text{H5}}$ equals 0.279 Hz, the methyl carbon prefers to lie closer to fluorine than bromine, possibly a reflection of the relative sizes of these substituents and the strength of steric interactions. Figure 33 is not compatible with a nearly rigid orthogonal conformation since the observed ${}^5J_{\text{O}}^{\text{CH}_3, \text{F}}$ is too large.

Positive signs are calculated for both $^5J_{m}^{C\alpha,H}$ and are confirmed by weak irradiation (tickling) experiments. The signs of very few long-range coupling constants between aromatic ring protons and side-chain carbons are known²⁰⁴.

ii) carbon spectrum

The substituent-induced chemical shifts of bromine at C6 are quite different from those of bromine at C4 if the methoxy group conformation is unchanged. All ring carbons except C1 shift to lower field and the magnitudes of these shifts differ significantly from 4-bromo-2-fluoroanisole. If chemical shifts reflect changes in net charge, these observations in conjunction with the charges in Tables 22 and 27 point towards a conformational change which places the methoxy group close to the plane perpendicular to the ring plane.

The methyl carbon couples with all ring carbons. Since the forms of the rotational angle dependence of the INDO FPT coupling constants in Figures 26 and 31 are not very different, they may serve as approximations to the present case.

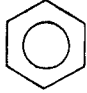
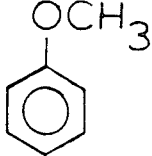
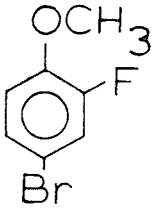
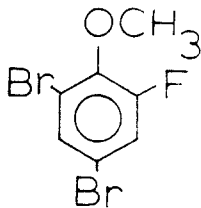
The magnitudes of ${}^2J_{C\alpha, C1}$ are 2.33 Hz in anisole, 2.15 Hz in 4-bromo-2-fluoroanisole, and 3.23 Hz in 4,6-dibromo-2-fluoroanisole. Since the calculations indicate that this coupling increases when one ortho fluorine is present, the value in 4,6-dibromo-2-fluoroanisole may be simply a substituent effect and not an indication of greater preference for non-planar conformations. By comparison with Figure 31, the relative magnitudes of ${}^3J_{O, C\alpha, C2}$ and ${}^3J_{O, C\alpha, C6}$ and of ${}^4J_{m, C\alpha, C3}$ and ${}^4J_{m, C\alpha, C5}$ are consistent with an effective twist angle ϕ of somewhat less than 90° .

Of particular interest is ${}^5J_{\text{p}}^{\text{C}\alpha,\text{C}4}$, which equals 0.94 Hz. If the form of this coupling constant is given by Eq. (9), it yields $\langle \sin^2 \phi \rangle$ if ${}^5J_{90}^{\text{C}\alpha,\text{C}4}$ is known²⁷. INDO FPT calculations imply that substituents affect ${}^5J_{90}^{\text{C}\alpha,\text{C}4}$, but the utility of this coupling constant in conformational analysis is unknown at this time. It is clear that this magnitude can be explained if the methoxy group lies near the plane perpendicular to the ring plane. Moreover, if 0.94 Hz is a lower bound on the magnitude of ${}^5J_{90}^{\text{C}\alpha,\text{C}4}$, both anisole and 4-bromo-2-fluoroanisole prefer the methoxy group near the ring plane since ${}^5J_{\text{p}}^{\text{C}\alpha,\text{C}4}$ is not observable.

The magnitude of ${}^4J_{\text{o}}^{\text{C}\alpha,\text{F}}$ is consistent with the proximity of the coupled nuclei. The sign is positive, in agreement with the calculations. As expected, the bromine substituent at C6 increases ${}^2J_{\text{C}1,\text{F}}$ and ${}^3J_{\text{C}4,\text{F}}$ relative to 4-bromo-2-fluoroanisole. Contrary to expectation, ${}^3J_{\text{C}6,\text{F}}$ decreases.

Some carbon-proton spin-spin coupling constants between ring nuclei appear in Table 31. These numbers are taken from the present and previous^{229,237} work. Solvent effects are liable to be within the experimental error, except perhaps for ${}^1J_{\text{CH}}$. As predicted on the basis of additivity of substituent effects, the 4-bromine reduces ${}^3J_{\text{C}3,\text{H}5}$ and ${}^3J_{\text{C}5,\text{H}3}$, which are both positive. Contrary to observation, the 2-fluorine is supposed to increase ${}^3J_{\text{C}3,\text{H}5}$, but to decrease ${}^3J_{\text{C}5,\text{H}3}$ slightly,

Table 31
 Some Carbon-Proton Spin-Spin Coupling Constants Between Ring Nuclei
 for Benzene^a and Some Anisoles^b

				
$^1_J C2, H2$	158.43	158.52, 159.9	-	-
$^2_J C2, H3$	1.15	1.42, c	c	$(-)6.1 \pm 0.4$
$^4_J C2, H5$	-1.31	-1.42, c	c	$(-)2.0 \pm 0.2$
$^1_J C3, H3$	158.43	158.35, 159.2	167.53 ± 0.17	170.7 ± 0.1
$^3_J C3, H5$	7.62	8.73, 8.0 ± 0.5	6.15 ± 0.01	6.5 ± 0.1
$^4_J C3, H6$	-1.31	-0.75, c	$(-)0.87 \pm 0.05$	-
$^3_J C4, H2$	7.62	7.52, 7.5 ± 0.1	-	-
$^2_J C4, H3$	1.15	0.85, 1.3 ± 0.1	$(-)4.66 \pm 0.14$	$(-)4.3 \pm 0.1$
$^1_J C4, H4$	158.43	160.43, 161.4	-	-
$^2_J C4, H5$	1.15	0.85, 1.3 ± 0.1	$(-)3.40 \pm 0.02$	$(-)4.3 \pm 0.1$
$^3_J C4, H6$	7.62	7.52, 7.5 ± 0.1	7.6 ± 0.14	-
$^3_J C5, H3$	7.62	8.73, 8.0 ± 0.5	6.35 ± 0.26	6.54 ± 0.06
$^1_J C5, H5$	158.43	158.35, 159.2	168.51 ± 0.33	173.94 ± 0.09
$^2_J C5, H6$	1.15	-0.32, c	1.23 ± 0.05	-

...Table 31 continued....

Table 31....

$^4\text{J}_{\text{C6,H3}}$	-1.31	-1.42,c	c	$(-)\text{1.90} \pm 0.07$
$^2\text{J}_{\text{C6,H5}}$	1.15	1.42,c	c	$(-)\text{3.89} \pm 0.06$
$^1\text{J}_{\text{C6,H6}}$	158.43	158.52, 159.9	163.59 ± 0.05	-

a From reference 237.

b The first number listed for anisole is from selective decoupling experiments on an 80 volume % solution with 10 volume % tetramethylsilane (reference 229). The second number is from the present work.

c Unresolved.

if simple additivity is obeyed strictly. In the same way the 6-bromine decreases ${}^3J_{C3,H5}$ and increases ${}^3J_{C5,H3}$ to 7.08 Hz and 6.89 Hz, respectively. ${}^3J_{C4,H6}$ is predicted to be 12.50 Hz in 4-bromo-2-fluoroanisole, but in fact it increases little relative to the corresponding numbers for anisole and benzene.

${}^2J_{C2,H3}$ is expected to be -4.95 Hz on the basis of additivity and, therefore, the negative sign is chosen for this coupling constant in 4,6-dibromo-2-fluoroanisole. Similarly, ${}^2J_{C4,H3}$ and ${}^2J_{C4,H5}$ are predicted to be negative in 4-bromo-2-fluoroanisole (-5.31 Hz and -3.10 Hz, respectively). A correspondence assigns the larger observed magnitude to ${}^2J_{C4,H3}$. The small ${}^2J_{C5,H6}$ in anisole has a magnitude comparable to the substituent effects, which differ in sign. ${}^2J_{C6,H5}$ is expected to be 1.21 Hz in 4-bromo-2-fluoroanisole and -3.33 Hz in 4,6-dibromo-2-fluoroanisole. The latter is 3.89 Hz in magnitude experimentally.

Predicted four-bond coupling constants ${}^4J_{C2,H5}$, ${}^4J_{C3,H6}$, and ${}^4J_{C6,H3}$ are -1.32 Hz, -0.95 Hz, and -1.17 Hz, respectively. Again simple additivity is not obeyed, but the relative ordering of the magnitudes is correct.

iii) fluorine chemical shift

Proposed relationships imply that fluorine chemical shift is more sensitive to π -electron density than carbon chemical shift²³³. Electronic effects of the bromine substituents may account for the downfield shifts from 2-fluoroanisole to 4-bromo-2-fluoroanisole (4.0 ppm) to 4,6-dibromo-2-fluoroanisole (7.4 ppm). It is not clear whether the larger shift includes the decrease in π -electron density which is predicted when the methoxy group moves from the planar to the orthogonal conformation²³⁸.

E. 2,3,5,6-Tetrafluoroanisole

i) proton spectrum

The upfield shift of H4 relative to 2-fluoroanisole is consistent with fluorine substituent-induced shifts²³⁶. Proton-fluorine coupling constants between ring nuclei are comparable to those in pentafluorobenzene²³⁹.

The magnitude of ${}^5J_{\text{O}}^{\text{CH}_3, \text{F}}$ is 1.345 Hz, about 0.14 Hz smaller than in 4,6-dibromo-2-fluoroanisole. This suggests that the conformational behaviour of the methoxy group is similar in both compounds, if the rotational angle dependence of this coupling constant is assumed to be the same in both compounds. In the simplest case tetrafluoroanisole is essentially planar, ${}^5J_{\text{O}}^{\text{CH}_3, \text{F}}$ is near the average of the coupling constants for cis and trans conformations, and if the trans value is about 0.2 Hz a cis value of 2.5 Hz is inferred.

Apparently the steric repulsion between the methoxy group and an ortho fluorine substituent is important. Non-planar conformations of 4,6-dibromo-2-fluoroanisole are populated substantially and by analogy this may be true for 2,3,5,6-tetrafluoroanisole. A rigid, orthogonal conformation could not be made consistent with proton and fluorine nmr spectra of a nematic solution¹²³. Emsley, Lindon, and Stephenson support models with free rotation of the methoxy group or exchange between 2^{n+1} equivalent and symmetrically-disposed sites ($n = 1, 2, 3, \dots$) and with free rotation of the methyl group or

exchange between equivalent sites located gauche and trans to the oxygen-ring carbon bond. It is not clear whether averaging over a rotational potential with minima at or near the plane perpendicular to the ring plane would prove adequate for simulation of spectra from the ordered liquid, but $^5J_{\text{O-CH}_3, \text{F}}$ seems consistent with significant non-planarity. A model with quite low barriers to methoxy group rotation may suffice to explain the observations. The rotational potential which was calculated at the ST0-3G level for 2-fluoroanisole may support the proposal of a little hindering in 2,3,5,6-tetrafluoroanisole. Emsley suggests that 2,3,4,5,6-pentafluoroanisole does not prefer the planar conformation on the basis of the chemical shift of the para fluorine²³⁸.

A study of 2,3,5,6-tetrafluoroanisole- α - ^{13}C is needed to determine whether the analogy with 4,6-dibromo-2-fluoroanisole is justified. Significant coupling between the methyl carbon and C4 would betray non-planar conformations.

ii) fluorine spectrum

The magnitudes of the fluorine-fluorine coupling constants are similar to those found by Bruce²⁴⁰ for a chloroform solution of 2,3,5,6-tetrafluoroanisole and to those in pentafluorobenzene²³⁹. Emsley and coworkers assume that both ${}^4J_m^{F2,F6}$ and ${}^4J_m^{F3,F5}$ are negative by comparison with signs in similar molecules¹²³. The present work indicates that both have the same sign, but the sign relative to other coupling constants between ring nuclei could not be deduced experimentally. From the substituent constants of Abraham, Macdonald, and Pepper²⁴¹, ${}^4J_m^{F2,F6}$ and ${}^4J_m^{F3,F5}$ are 2.9 Hz and -2.6 Hz in 2,3,5,6-tetrafluorophenol and -2.1 Hz and -1.9 Hz in pentafluorobenzene. From weak irradiation experiments, the latter numbers are -2.2 Hz and -1.1 Hz²³⁹. Since the spectrum of 2,3,5,6-tetrafluoroanisole is otherwise quite similar to the spectrum of pentafluorobenzene, the analogy is carried over to the signs.

iii) methyl proton chemical shifts

For acetone solutions of comparable concentration the methyl proton chemical shift moves downfield in the series: anisole (3.76 ppm), 2-fluoroanisole (3.86 ppm), 4-bromo-2-fluoroanisole (3.88 ppm), 4,6-dibromo-2-fluoroanisole (3.94 ppm), and 2,3,5,6-tetrafluoroanisole (4.10 ppm). If the latter two compounds prefer non-planar conformations, this trend is contrary to the change in ring current-induced chemical shift²⁴², by which the methyl protons of the planar conformation are deshielded by about 0.18 ppm relative to the orthogonal conformation. The expected effect appears for 2-hydroxythioanisole¹²⁶. The deshielding which is observed for the present anisoles may be explained qualitatively as due to local group anisotropy of the halogen substituents²⁴³, or to local electric fields²⁴⁴, or to substituent-induced changes in the charge on the methyl group. Decomposition of the observed trend in terms of these effects is not possible within the present study.

F. 2-Fluoroacetophenone

i) ab initio molecular orbital calculations

Optimization of the geometry of the side-chain lowers the energy difference between planar and orthogonal conformations of acetophenone by about $2 \text{ kJ}\cdot\text{mol}^{-1}$ at the STO-3G level, to make the planar form more stable by $16.1 \text{ kJ}\cdot\text{mol}^{-1}$ 216,220. Calculations at the INDO level with standard geometry indicate that the 0-anti conformer of 2-fluoroacetophenone is more stable than 0-syn by $5.65 \text{ kJ}\cdot\text{mol}^{-1}$ 146.

Some results of the present geometry optimization at the STO-3G level are present in Table 32 with reference to Figure 35. The geometry of the aromatic ring is not optimum and the methyl group retains C_{3v} symmetry about the carbonyl carbon-methyl carbon bond axis.

Although the structure of 2-fluoroacetophenone has not been determined experimentally, differences between the conformations are interesting. In particular the angle $\text{ClCC}\alpha$ is lowest for the orthogonal conformation, which minimizes steric interactions between the acetyl group and the aromatic ring.

Relative energies in Table 32 do not provide a detailed description, but will be treated as extrema on the minimum energy path for a surface given by Eq. (7). Of the two planar conformers 0-anti is more stable because electrostatic repulsion between the carbon-oxygen and carbon-fluorine bonds is minimized.

Table 32

Some Results of Partial Geometry Optimization in STO-3G Calculations
for 2-Fluoroacetophenone^a

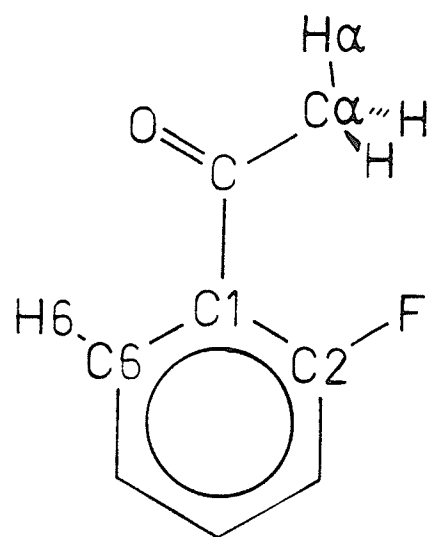
	<u>0-anti</u>	orthogonal	<u>0-syn</u>
C2C1O α	0	90	180
C1C	153.1	153.8	152.7
CC α	154.3	154.2	154.4
C α H	108.6	108.6	108.6
C0	122.3	122.1	122.4
C1C2	139.1	139.0	138.9
C1C6	139.9	139.6	140.2
C2F	135.6	135.6	135.4
C1CC α	118.8	116.6	118.5
C1C0	120.0	120.4	121.1
C2C1C	123.6	119.4	118.9
CC α H	110.1	110.0	110.2
FC2C1	121.9	119.8	120.7
H6C6C1	118.3	119.5	120.0
C1CC α H α	(180.0)	(180.0)	(180.0)
C3C2C1C	(180.0)	180.0	(180.0)
dipole moment (D)	1.687	2.323	2.827
total energy (H)	-475.16506	-475.16042	-475.16380
relative energy (kJ mol ⁻¹)	0	12.1 ₈	3.3 ₀

^a Angles in degrees, bondlengths in pm. Quantities in parentheses were assumed and not optimized.

Figure 35

An 0-anti conformation of 2-fluoroacetophenone.

Some atoms used in the description of the geometry are identified.



Furthermore, the 0-anti conformer may afford the opportunity for intramolecular hydrogen bonding between the methyl group and fluorine.

The dipole moments in Table 32 are too small to account for the measured value, 2.77 D^{146} , unless the relative energies are incorrect.

Atomic charges and π -charges for the 0-anti, orthogonal, and 0-syn conformers appear in Table 33. The total π -electron donation of the substituents is 0.045e, 0.066e, and 0.051e for each respectively. The apparent σ -electron withdrawal is 0.215e, 0.217e, and 0.221e, with the assumption that the atomic charge on carbon is 6.063e in benzene. Additivity of atomic charge and π -charge effects in acetophenone and fluorobenzene is obeyed nearly. The reduction in π -electron withdrawal by the acetyl group in the orthogonal conformation is about 0.021e relative to 0-anti.

Table 33

Atomic and π -Charges for 2-Fluoroacetophenone from STO-3G
Calculations with Partial Geometry Optimization

	<u>O-anti</u>		orthogonal		<u>O-syn</u>	
	atomic	π	atomic	π	atomic	π
C1	6.048	1.048	6.040	1.031	6.046	1.050
C2	5.862	1.004	5.863	1.014	5.852	0.991
C3	6.086	1.039	6.083	1.032	6.086	1.037
C4	6.049	0.973	6.053	0.984	6.049	0.973
C5	6.070	1.018	6.066	1.012	6.070	1.020
C6	6.048	0.963	6.056	0.993	6.054	0.980
C	5.799		5.794		5.802	
C α	6.207		6.206		6.207	
O	8.227		8.214		8.219	
F	9.131		9.133		9.119	
H3	0.926		0.926		0.925	
H4	0.929		0.930		0.929	
H5	0.932		0.932		0.933	
H6	0.914		0.931		0.929	
H α	0.925		0.922		0.922	
H	0.924		0.924		0.929	
H	0.924		0.927		0.929	

ii) semi-empirical molecular orbital calculations

Semi-empirical molecular orbital calculations in the INDO MO FPT approximation are based on a standard geometry or on the partially-optimized STO-3G geometry from Table 32. Results of some calculations based on the latter geometries appear in Table 34. Preference for the 0-anti conformer in combination with the dipole moments is consistent with the experimental value of 2.77 D^{146} . Contrary to the STO-3G results, the three energies increase monotonically from 0-anti to 0-syn.

The coupling constants in Table 34 bear some resemblance to those for 2-fluoroanisole. In particular, notice that $^3J_{C\alpha,C}$ and $^5J_{C\alpha,H}$ increase monotonically as the rotational angle increases. The magnitudes of $^5J_{C\alpha,C4}$ and $^6J_{C\alpha,H4}$ are largest at or near the orthogonal conformation.

The importance of various coupling paths between the methyl group and fluorine is illustrated in Table 35 and in Figures 36 and 37. Coupling constants represent the usual calculation (labelled "total") and calculations which neglect elements of the Fock matrix between fluorine and the methyl group (labelled "TB") or just the methyl carbon (labelled "no CF") or just the methyl hydrogens (labelled "no HF"). The geometry is that of the 0-anti conformer in Table 32 with $C1C2 = C1C6 = 140.0 \text{ pm}$ and $C2C1C = FC2C1 = H6C6C1 = 120^\circ$. Coupling through formal bonds is relatively unimportant when the nuclei are proximate.

Table 34

Some Spin-Spin Coupling Constants^a, Relative Energy, and Dipole Moment for Some Conformations of 2-Fluoroacetophenone from INDO MO FPT Calculations^b

	<u>0-anti</u>	orthogonal	<u>0-syn</u>
$J^{C\alpha,C1}$	3.756	3.475	4.117
$J^{C\alpha,C2}$	1.047	1.826	2.891
$J^{C\alpha,C3}$	-0.365	-0.535	0.306
$J^{C\alpha,C4}$	0.500	0.914	0.403
$J^{C\alpha,C5}$	0.140	-0.527	-0.267
$J^{C\alpha,C6}$	2.736	1.856	1.687
$J^{C\alpha,C}$	67.054	65.998	68.261
$J^{C\alpha,F}$	2.349	0.446	0.201
$J^{C\alpha,H3}$	0.100	0.396	0.602
$J^{C\alpha,H4}$	-0.140	-0.270	-0.110
$J^{C\alpha,H5}$	0.630	0.377	0.064
$J^{C\alpha,H6}$	-0.096	-0.190	-0.123
$J^{C\alpha,H}$	119.068	118.741	118.251
dipole moment (D)	2.547	3.758	4.565
relative energy (kJ mol ⁻¹)	0	1.32	2.36

a In Hertz

b Geometry from partially-optimized STO-3G calculations

Table 35 Some Spin-Spin Coupling Constants for 2-Fluoroacetophenone from INDO MO FPT Calculations

twist angle ϕ (deg)	${}^5J_{\text{O}}^{\text{CH}_3, \text{F}}$ (Hz)			${}^4J_{\text{O}}^{\text{C}\alpha, \text{F}}$ (Hz)				
	total	noHF	noCF	TB	total	noHF	noCF	TB
0	0.178	5.841	-4.652	-0.555	5.714	-3.234	15.682	0.323
	(4.808	3.109	-0.673	-0.948) ^a				
	(-2.137	7.207	-6.642	-0.359) ^b				
15	-2.467	4.639	-5.995	-0.483	8.448	-2.439	16.791	0.261
30	-4.786	2.359	-6.231	-0.285	9.481	-0.934	14.176	0.137
45	-2.933	0.908	-3.313	-0.018	4.763	0.021	6.457	0.081
60	-0.749	0.449	-0.801	0.229	1.181	0.398	1.510	0.181
75	0.162	0.420	0.176	0.394	0.365	0.579	0.336	0.399
90	0.407	0.452	0.421	0.457	0.508	0.731	0.450	0.633
120	0.325	0.331	0.325	0.330	0.807	0.869	0.790	0.848

Table 35

150	0.134	0.140	0.131	0.137	0.484	0.504	0.478	0.497
180	0.026	0.032	0.023	0.030	0.115	0.125	0.112	0.122

a Between F and $H\alpha$ in Figure 35.

b Between F and H in Figure 35.

Figure 36

A plot of the angle dependence of $^5J_{\text{OCH}_3, \text{F}}$ in 2-fluoroacetophenone when certain Fock elements are kept zero throughout the INDO MO FPT calculations.

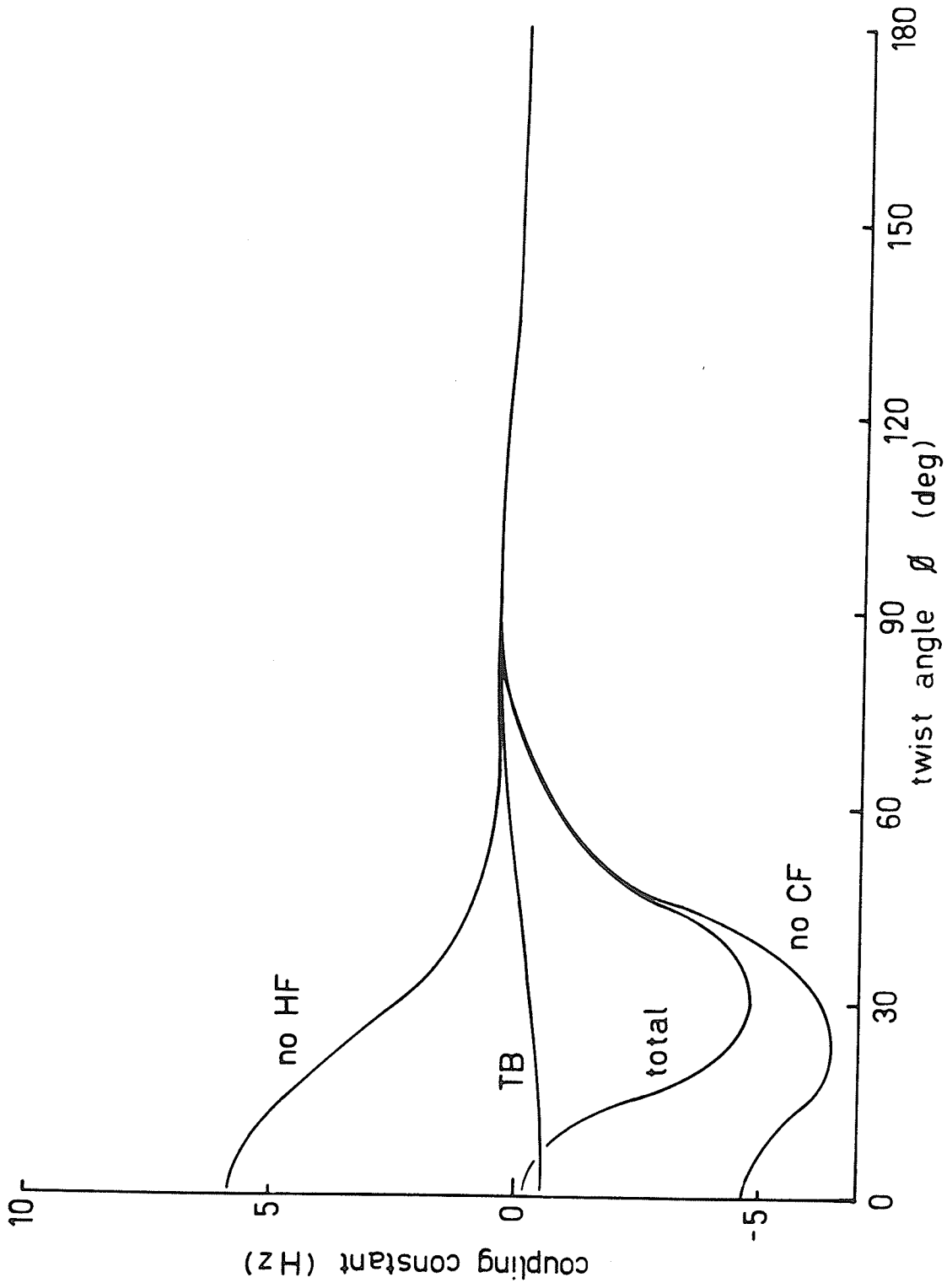
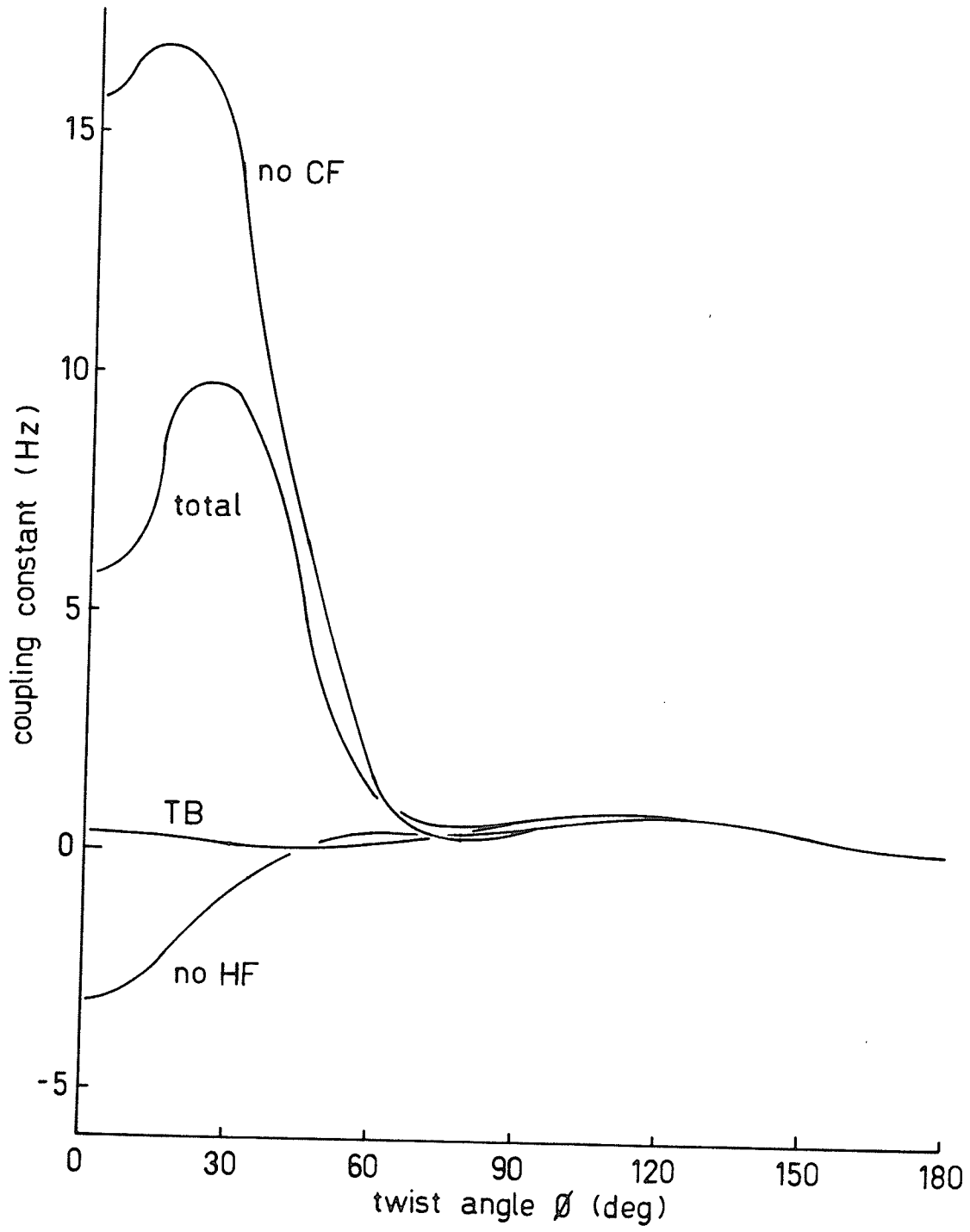


Figure 37

A plot of the angle dependence of ${}^4J_{\text{C}\alpha,\text{F}}$ in 2-fluoroacetophenone when certain Fock elements are kept zero throughout the INDO MO FPT calculations.



Rotational angle dependences of ${}^5J_{\text{O}}^{\text{CH}_3,\text{F}}$ and ${}^4J_{\text{O}}^{\text{C}\alpha,\text{F}}$ are similar to those for 2-fluoroanisole in Figures 33 and 34 and similar comments apply.

iii) proton spectrum

Chemical shifts of the ring protons of 2-fluoroacetophenone are consistent with fluorine substituent-induced shifts²³⁶. Deshielding of H4 and H6 is due in part to electron withdrawal from the aromatic ring by the acetyl group. Magnetic anisotropy of the carbonyl group also deshields H6 and the sensitivity of this shift in 2-haloacetophenones stands in contrast to the 2-halobenzaldehydes, for which steric effects are less pronounced¹⁶⁸.

As Smith and coworkers found¹⁶⁸, the methyl protons do not couple observably with any ring protons, but the magnitude of $^5J_{\text{O}}^{\text{CH}_3, \text{F}}$ is striking: 4.484 Hz, larger than for any of the anisoles studied. In conjunction with the INDO FPT calculations this observation implies a preference for conformations near 0-anti. The positive sign cannot be reconciled with Figure 36. The similarity between the rotational angle dependences of $^5J_{\text{O}}^{\text{CH}_3, \text{F}}$ and $^4J_{\text{O}}^{\text{C}\alpha, \text{F}}$ for 2-fluoroanisole and 2-fluoroacetophenone suggests that the electronic structure along the intervening path of formal bonds is unimportant relative to proximate interaction between the methyl group and fluorine. Internuclear separation and bond orientation determine the form of these coupling constants^{183,245}. Apparently the positive segment of the "total" curve in Figure 36 is under-estimated, apparently because the negative contribution from direct hydrogen-fluorine interaction is over-estimated.

The methyl carbon couples with H5 and H6, but not other ring protons. By comparison with the INDO FPT coupling constants in Table 34 these observations are consistent with a preference for the 0-anti conformer. Weak irradiation (tickling) experiments reveal that both ${}^5J_m^{C\alpha,H5}$ and ${}^4J_o^{C\alpha,H6}$ are positive. Although the latter is calculated to be -0.096 Hz, this is the smallest magnitude obtained and it may be reconciled with a small, positive value.

iv) carbon spectrum

Ring carbon chemical shifts from Table 11 and net atomic charges derived from Table 33 are plotted in Figure 29 and follow the pattern determined previously. When the sixteen points from anisole, 2-fluoroanisole, and 2-fluoroacetophenone are used the regression line is

$$\delta_c = (0.181 \pm 0.002)q_c + (135.24 \pm 0.05), r = 0.96539 \quad \text{Eq. (14)}$$

where δ_c is in ppm and q_c is in millelectrons. When only the negative net charges are used

$$\delta_c = (0.40 \pm 0.03)q_c + (150.41 \pm 1.93), r = 0.93160 \quad \text{Eq. (15)}$$

Both correlations are significant at the 0.1% level²³⁴.

A plot of chemical shift for the ring carbons of anisole, 2-fluoroanisole, and 2-fluoroacetophenone versus excess π -charge ($\Delta q_\pi = q_\pi - 1$) appears as Figure 38. As for Figure 29 the substituted carbons are easily distinguished. A regression line through the eleven points for unsubstituted carbons is

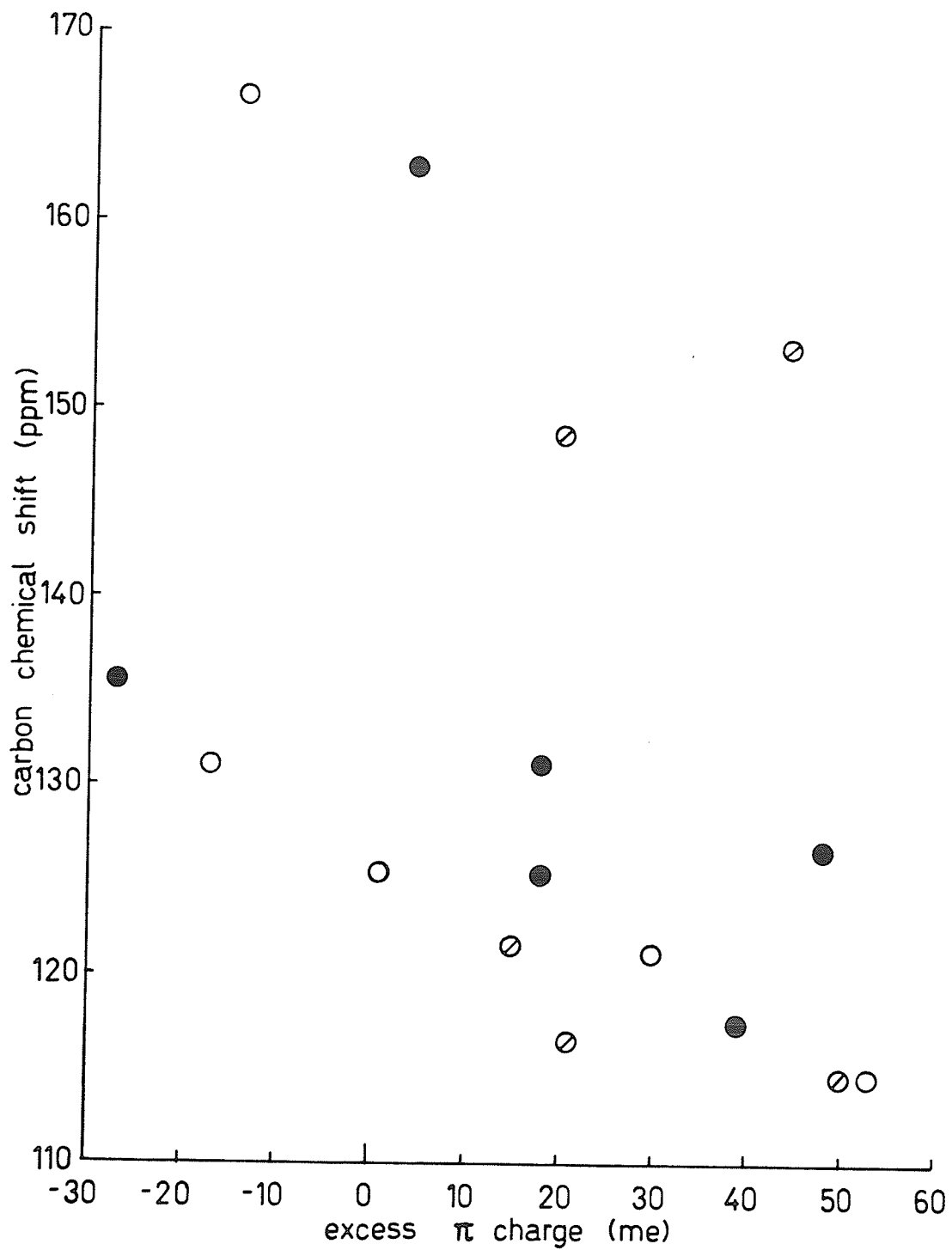
$$\delta_c = -0.25 \Delta q_\pi + 127.52, r = 0.87448 \quad \text{Eq. (16)}$$

and the correlation is significant at the 0.1% level. Hehre, Taft, and Topsom propose that the apparent correlation for all positions of carbon in the aromatic ring is an illusion²³³. When separate plots are constructed for the meta and para carbons of mono-substituted benzenes, different slopes result. Furthermore,

Figure 38

A plot of chemical shift for ring carbons versus π -charges calculated at the STO-3G level.

- anisole
- ◊ 2-fluoroanisole
- 2-fluoroacetophenone



induced σ -charge differences for para carbons are inversely proportional to induced π -charge differences at the same site. Consequently correlations of chemical shift with σ -charge, π -charge, or total charge are of the same quality. Excess π -charge is related to the chemical shift of the para carbon of 1,4-disubstituted benzenes, for which substituent-induced chemical shifts are not additive²⁴⁶.

From Table 11 the magnitudes of $^1_J^{C\alpha,C}$ and $^2_J^{C\alpha,C1}$ are 43.2 Hz and 13.8 Hz, respectively. That is, the INDO calculations over-estimate $^1_J^{C\alpha,C}$ and under-estimate $^2_J^{C\alpha,C1}$. The magnitudes of these coupling constants are 42.7 Hz and 13.7 Hz in acetophenone itself, and 45.12 Hz and 17.58 Hz in acenaphthenone, which is a model for a conformationally-frozen acetyl group²⁴⁷.

$^3_J^{C\alpha,C}$ is 8.4 Hz in acetophenone²⁴⁷. The magnitudes of $^3_J^{C\alpha,C2}$ and $^3_J^{C\alpha,C6}$ in 2-fluoroacetophenone are unexpectedly small; $^3_J^{C\alpha,C6}$ equals 0.63 Hz and $^3_J^{C\alpha,C2}$ is unobservable. This unusual result is similar to the observation that $(2+3)_J^{C\alpha,C9}$ equals 1.56 Hz in acenaphthenone, but $(3+4)_J^{C\alpha,C2}$ is unobservable. Marshall and coworkers propose that these coupling constants represent the algebraic sum of coupling over both formal bond paths²⁴⁷, but this explanation cannot apply here since only one formal bond path exists. It is possible that interactions between formally non-bonded nuclei transmit significant contributions to $^3_J^{C\alpha,C2}$ and $^3_J^{C\alpha,C6}$, and these contributions are

manifest in the preference for the 0-anti conformer. For example, when the Fock elements between the carbonyl carbon and C2 and C6 of 2-fluoroacetophenone are set at zero in INDO FPT calculations, $^3J^{C\alpha,C2}$ decreases by 0.1 Hz and $^3J^{C\alpha,C6}$ increases by 0.8 Hz. When the Fock elements between the methyl carbon and C2 are neglected, $^3J^{C\alpha,C2}$ increases by 0.8 Hz and $^3J^{C\alpha,C6}$ increases by 0.3 Hz. Somewhat similar calculations demonstrate the importance of direct interaction in $^3J^{C,C}$ for butane²³⁰ and cis-crotonaldehyde²⁴⁸. Similar small values of $^3J^{C,C}$ appear between ortho carbons of phenyl groups and β -carbons in 9,10-diphenylphenanthrene and tetraphenylcyclopentadienone²⁴⁹.

As expected when an electronegative substituent lies ortho to fluorine, the magnitude of $^2J^{F,C1}$ is less than $^2J^{F,C3}$ and $^3J^{F,C6}$ is less than $^3J^{F,C4}$. All coupling constants between fluorine and carbon, except the methyl carbon, agree with the determination of Weigert and Roberts²⁵⁰. These authors place an upper bound of 0.4 Hz on the magnitude of $^4J_o^{C\alpha,F}$. Under the conditions of the present work, this coupling constant equals 6.83 Hz. The positive sign is reproduced by the INDO FPT calculations. Transmission of the coupling is substantially through space when the methyl group and fluorine are proximate.

G. 2,6-Difluoroacetophenone

The methyl proton resonances of dilute acetone- d_6 solutions of acetophenone and 2-fluoroacetophenone occur at 2.56 ppm and 2.58 ppm respectively. For 2,6-difluoroacetophenone and 2,3,4,5,6-pentafluoroacetophenone the resonances occur at 2.55 ppm and 2.62 ppm. That is, the methyl proton resonance is either relatively insensitive or the contributions of various effects cancel approximately. Increased non-planarity of the acetyl group causes a decrease in deshielding due to the magnetic anisotropy of the aromatic ring. Local group anisotropy and local electric fields may cause shielding or deshielding^{243,244}. Electron donation by fluorine to the π -system may shield the methyl protons.

Methyl protons couple with the ortho fluorine nuclei by 1.56 Hz, but do not couple with other ring protons. Evidently the methyl group does not prefer to lie in the ring plane since $^5J_{O}CH_3,F$ is smaller than for 2-fluoroacetophenone. Interaction between the carbonyl group and the carbon-fluorine bonds makes the planar conformation unfavourable.

The observation of coupling to ortho fluorine nuclei, but not to other fluorines or protons, and the similarity of the magnitude of $^5J_{O}CH_3,F$ in 2,6-difluoroacetophenone, 2,3,5,6-tetrafluoroanisole (1.35 Hz), and 2,3,4,5,6-pentafluoroacetophenone (1.82 Hz) may betray an underlying similarity in the form and mechanism of this coupling.

H. α, α, α -Trifluoroacetophenone

The coupling constant ${}^5J_{\text{O}}^{\text{CF}_3, \text{H}}$ may be transmitted directly between the nuclei rather than via the trifluoromethyl carbon, but the mechanism and the sign are not known. The magnitude is 1.12 Hz, which is comparable to the value of ${}^5J_{\text{O}}^{\text{CH}_3, \text{F}}$ when the methyl group prefers non-planarity with the aromatic ring. This may be coincidental since ${}^5J_{\text{O}}^{\text{CF}_3, \text{CHO}}$ is 2.23 Hz in 2-trifluoromethylbenzaldehyde, for which the 0-anti conformer is at least 95% extant, and since ${}^5J_{\text{O}}^{\text{CH}_3, \text{CFO}}$ is 1.84 Hz in 2-methylbenzoyl fluoride, for which the 0-syn conformer is about 75% extant¹⁴³.

Chemical shifts of C1, C2, C3 and C4 resemble those for C1, C6, C5 and C4 of 2-fluoroacetophenone, or for acetophenone itself²⁴⁷, but downfield shifts of C2 and C4 are consistent with greater electron withdrawal by the trifluoroacetyl group than by the acetyl group.

The magnitude of ${}^1J_{\text{F}, \text{C}\alpha}$ is comparable to those in trifluoroacetic acid (-283.8 Hz)²⁰⁵ or 1,1,1-trifluoroacetone (-289 Hz)²⁵¹. ${}^2J_{\text{F}, \text{C}}$ is 41.7 Hz in trifluoroacetic acid, which is similar to the value for the present compound, 34.6 Hz. The sign is not known. ${}^3J_{\text{F}, \text{C1}}$ equals 2.18 Hz, but coupling to the ring carbons is not observable.

No conclusion can be reached as to the preferred conformation of the trifluoroacetyl group. Further discussion is deferred to the succeeding section.

I. Temperature Dependences of $^5J_{\text{O}}^{\text{CH}_3, \text{F}}$ and $^4J_{\text{O}}^{\text{C, F}}$

The temperature dependences of $^5J_{\text{O}}^{\text{CH}_3, \text{F}}$ for 4,6-dibromo-2-fluoroanisole, 2,3,5,6-tetrafluoroanisole, 2-fluoroacetophenone, 2,6-difluoroacetophenone, and α, α, α -trifluoroacetophenone appear in Figures 39, 40, 41, 44, and 45. The temperature dependence of $^4J_{\text{O}}^{\text{C, F}}$ for 2-fluoroacetophenone appears in Figure 43. The observed coupling constant represents an average over the distribution of individual conformers, which can be represented by a static (or discrete) model²⁵² or by a dynamic (or continuous) model^{253,254}.

The mathematical formalism of Gutowsky, Belford, and McMahon is based on the approximation that an nmr parameter $\langle P \rangle$ is an average of the parameters from N possible conformations, weighted by the mole fraction of the conformer, x_i .

$$\langle P \rangle = \sum_{i=1}^N x_i P_i \quad \text{Eq. (17)}$$

$$x_i = \frac{n_i}{\sum_{i=1}^N n_i} = \frac{n_i}{\sum_{i=1}^N n_i \exp[-\beta(E_i - E_1)]} \quad \text{Eq. (18)}$$

where n_i is the number of moles of the i -th conformer, $\beta = (RT)^{-1}$, and $(E_i - E_1)$ is the energy of the i -th conformer relative to the lowest energy, E_1 . Energy E is presumably a free energy. The temperature dependence of the spectrum at high temperatures yields nmr and thermodynamic parameters for the

conformers, usually by a least-squares method²⁵⁵. Govil and Bernstein warn that this technique suffers from a number of limitations in both the underlying assumptions and in the least-square method²⁵⁶.

A classical dynamic model may be developed as follows. The observable J , also denoted by $\langle J \rangle$ or $J(\beta)$, is recognized as an average over the rotational motion, thus:

$$\langle J \rangle = \frac{\int_0^{2\pi} C(\phi) \exp[-\beta E(\phi)] d\phi}{\int_0^{2\pi} \exp[-\beta E(\phi)] d\phi} \quad \text{Eq. (19)}$$

where $C(\phi)$ is the coupling constant as a function of angle, rather than temperature. Concisely

$$J(\beta) = \int_0^{2\pi} p(\beta, \phi) C(\phi) d\phi \quad \text{Eq. (20)}$$

$$\text{where } p(\beta, \phi) = \frac{\exp[-\beta E(\phi)]}{\int_0^{2\pi} \exp[-\beta E(\phi)] d\phi} \quad \text{Eq. (21)}$$

The correspondence between Eq. (17) and Eq. (20) is clear.

Equation (20) is called a Fredholm integral equation of the first kind^{257,258}. Solutions to such equations frequently pose problems and accurate results are difficult to obtain due to ill-conditioning, in the sense that many solutions will satisfy exactly an equation which is perturbed slightly from the original. A "smooth" solution, rather than an exact solution, may be obtained numerically by expressing it in terms of the dominant

singular values and the corresponding singular functions of the linear operator in Eq. (20). Small singular values correspond to highly oscillatory components and are omitted. The uniqueness of the result is achieved by preferring the minimal least-squares solution. The operator which yields this solution when applied to $J(\beta)$ is called the pseudo-inverse of the linear operator in Eq. (20). (see Appendix)

Since the barriers to internal rotation may be too low to justify the approximation of the distribution of conformer populations by relatively few fixed conformations, as Eq. (17) implies, and since the rotational angle dependence of ${}^5J_{\text{O}}^{\text{CH}_3, \text{F}}$ is not known from experiment, the discussion of the temperature dependence is confined for the most part to qualitative remarks. It is recognized, with the intent to avoid impertinent conclusions, that the temperature dependences of chemical shifts and coupling constants may contain contributions from intermolecular and intramolecular effects²¹⁵. An unambiguous distinction between these effects is not possible here.

i) 4,6-dibromo-2-fluoroanisole

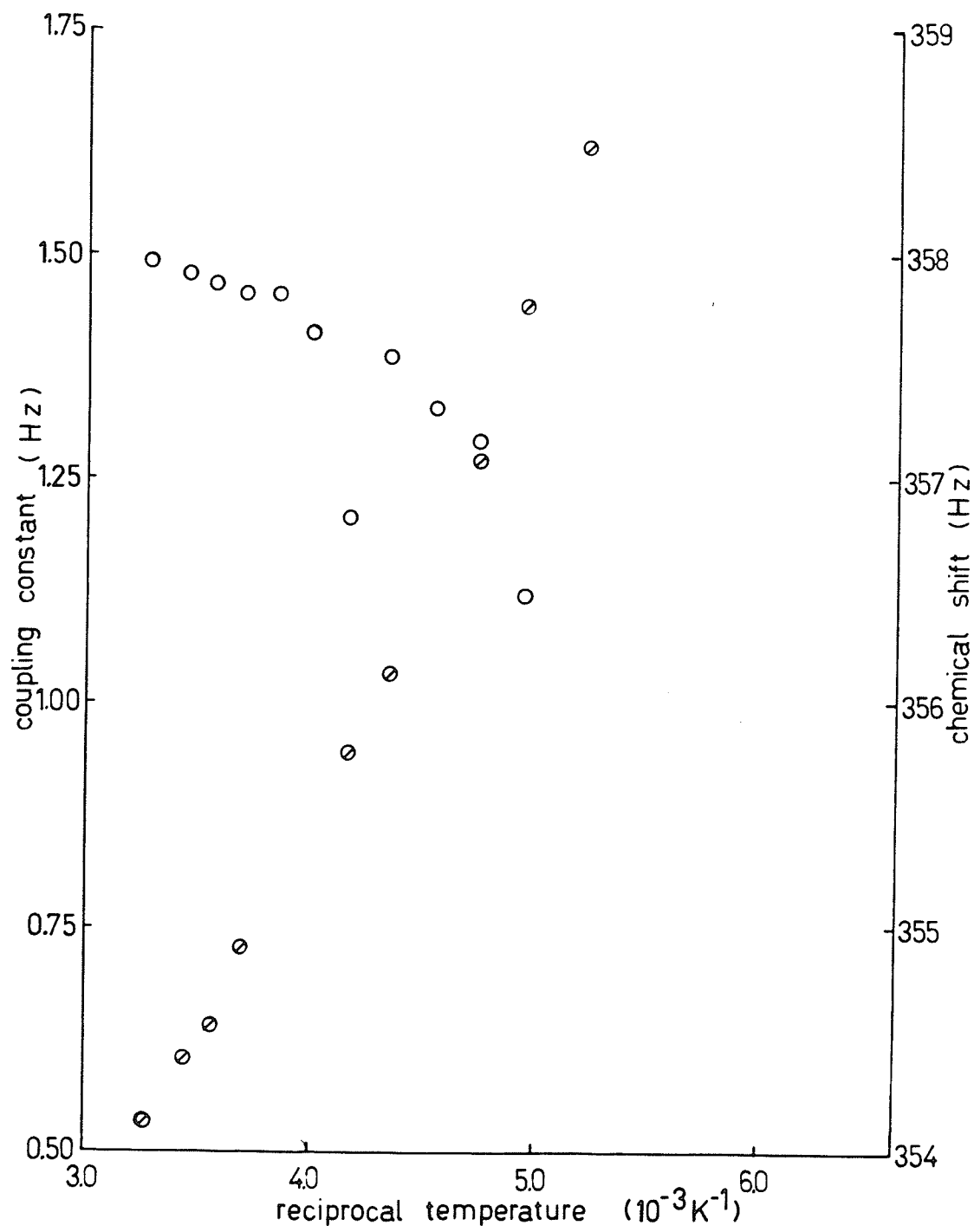
The monotonically decreasing magnitude of ${}^5J_{\text{OCH}_3, \text{F}}$ shows that the sign of this coupling constant is positive at all of the temperatures investigated. Naturally, the population of the preferred conformation increases as the temperature decreases. Since the coupling constant is only 0.17 Hz in 4-bromo-2-fluoroanisole, which prefers the methoxy group trans to fluorine, and since the value must be on the order of several Hertz in the cis conformer, the decreasing magnitude with decreasing temperature is consistent with a preference for a substantially non-planar conformer, provided that it reflects conformational change and not other factors (such as vibrational effects).

Parenthetically, $J(\beta)$ becomes linearly dependent on β as β decreases. If a line is fitted to the five points at lowest reciprocal temperature in Figure 39 the y-intercept lies at 1.70 ± 0.06 Hz. This value approximates the average coupling constant when all conformations have equal weights, presumably.

Figure 39

A plot of the temperature dependence of $^5J_{\text{OCH}_3, \text{F}}$ and of ν_{CH_3} for 4,6-dibromo-2-fluoroanisole- α - ^{13}C .

- coupling constant
- ⊙ methyl proton chemical shift



ii) 2,3,5,6-tetrafluoroanisole

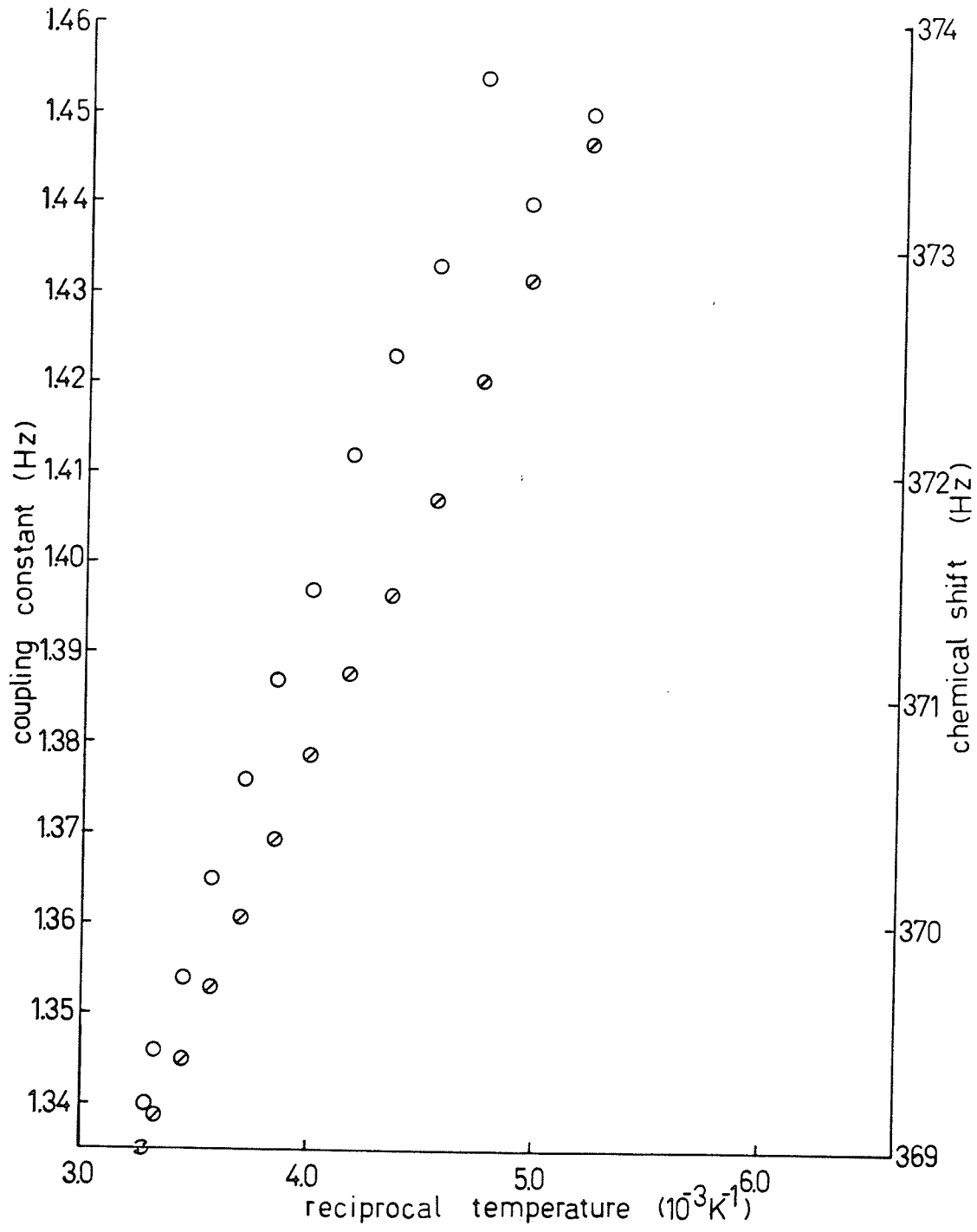
The temperature dependence of ${}^5J_{\text{O}}^{\text{CH}_3, \text{F}}$ is consistent with a preference for coplanarity of the methoxy group with the aromatic ring. If changes in ${}^5J_{\text{O}}^{\text{CH}_3, \text{F}}$ are due solely to conformational changes, the increasing magnitude suggests that the population of conformers with the methyl group and the fluorine proximate is increasing at lower temperatures. This can be reconciled with a weak preference for conformations which are nearly planar. Such a description is in accord with the conclusions of the study of a solution of 2,3,5,6-tetrafluoroanisole in a nematic liquid¹²³ and with the discussion in section E above.

A line through the six points at lowest reciprocal temperature in Figure 40 has a y-intercept at 1.07 ± 0.05 Hz.

Figure 40

A plot of the temperature dependence of ${}^5J_{\text{OCH}_3, \text{F}}$ and of ν_{CH_3} for 2,3,5,6-tetrafluoroanisole.

- coupling constant
- ⊙ methyl proton chemical shift



iii) 2-fluoroacetophenone

The temperature dependence of $^5J_{\text{OCH}_3, \text{F}}$ is striking because the coupling constant increases by 1.5 Hz between 305 K and 182 K. Qualitatively, this suggests that the methyl group prefers to lie near fluorine.

Since the two-fold component of the barrier to rotation of the acetyl group is relatively high in acetophenone itself (about 13 kJ mol^{-1} from torsional frequencies from the vapour¹⁵⁵ and about 16 kJ mol^{-1} from STO-3G calculations²²⁰), a two-state static model may be useful. The data from Table 16 can be fitted to this model by a computer program devised by Laatikainen²⁵⁹. With the assumption of no entropy difference, the 0-anti conformer lies $3.14 \pm 0.26 \text{ kJ}\cdot\text{mol}^{-1}$ below 0-syn, where the estimated error represents the 90% confidence limit. The characteristic coupling constants for these conformers are found to be $7.49 \pm 0.22 \text{ Hz}$ and $-5.82 \pm 0.34 \text{ Hz}$, respectively. Calculated numbers may be compared in Figure 41. The rms deviation of the coupling constants is 0.011 Hz from the observed values, which may well be smaller than the contribution of vibrations and solvent effects.

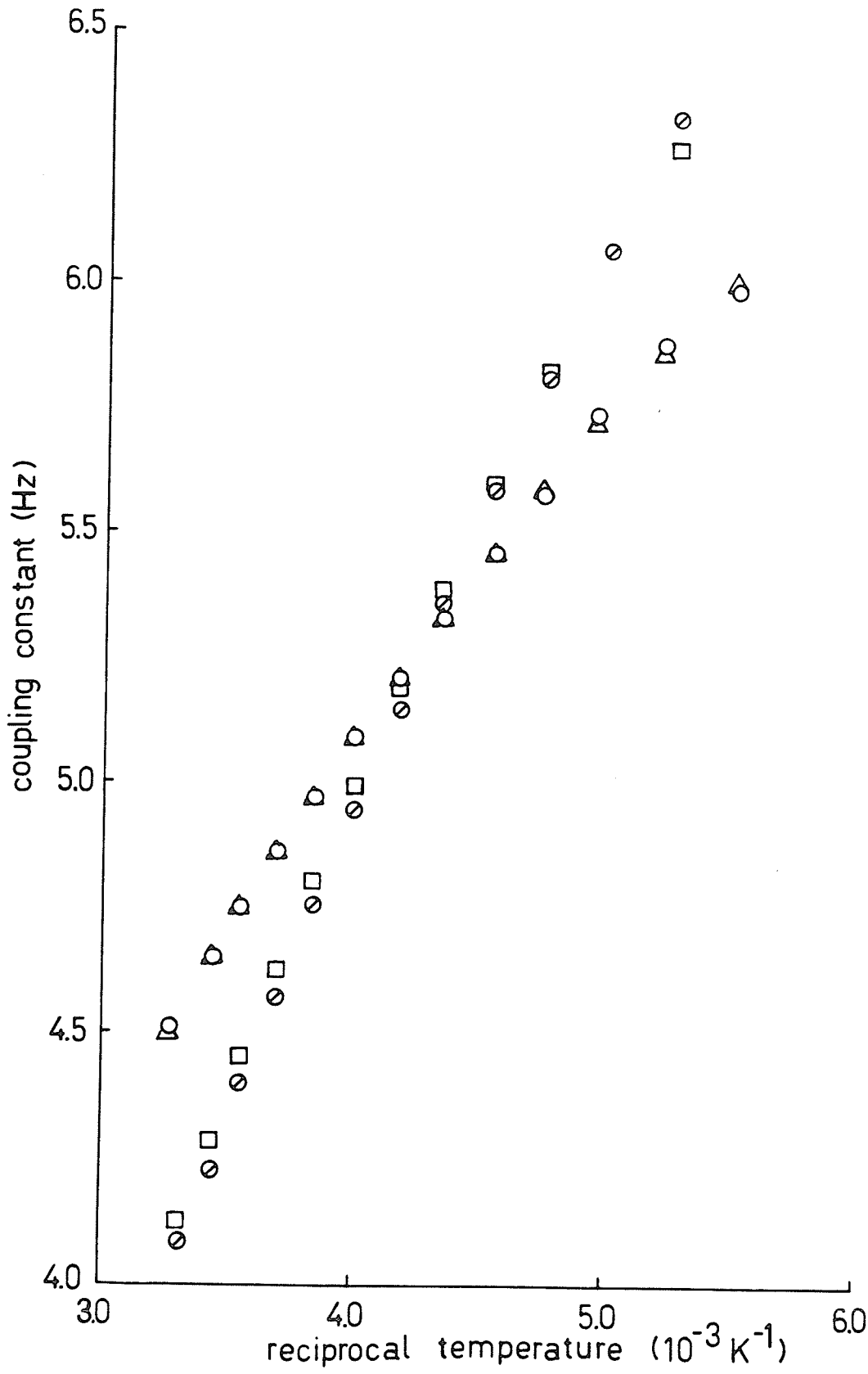
A computer program devised to invert the temperature dependence described by Eq. (20) is based on singular value decomposition^{257,260} (see Appendix). The rotational potential is described simply by

$$V(\phi) = V_1 \sin^2 \frac{\phi}{2} + V_2 \sin^2 \phi \quad \text{Eq. (22)}$$

Figure 41

A plot of the temperature dependence of ${}^5J_{\text{OCH}_3}^{\text{F}}$ for 2-fluoroacetophenone- α - ${}^{13}\text{C}$.

- observed
- △ static model
- ⊙ dynamic model with two singular values
- dynamic model with three singular values



From the preceding STO-3G results, values of $V_1 = 3.3 \text{ kJ}\cdot\text{mol}^{-1}$ and $V_2 = 10.5 \text{ kJ}\cdot\text{mol}^{-1}$ may be inferred, although a complete description of the energy surface is preferable. The resultant solution is given in terms of singular functions²⁵⁷, which are approximated by a cosine series. If a basis of ten cosine terms is used to describe the singular functions, it appears that relatively few singular functions are required to describe the temperature dependence. Unfortunately the calculations show that the most significant singular function is rather poorly approximated.

With Eq. (22) the angle dependence of the coupling constant is

$$\begin{aligned}
 C(\phi) = & 0.096 + 2.236\cos\phi + 1.139\cos2\phi + 3.016\cos3\phi \\
 & + 2.021\cos4\phi + 1.804\cos5\phi + 1.266\cos6\phi \\
 & + 0.667\cos7\phi + 0.335\cos8\phi - 0.071\cos9\phi
 \end{aligned}
 \tag{23}$$

when two singular values are retained and

$$\begin{aligned}
 C(\phi) = & -1.063 + 3.279\cos\phi + 2.496\cos2\phi + 2.787\cos3\phi \\
 & + 2.162\cos4\phi + 0.724\cos5\phi + 0.545\cos6\phi - 0.421\cos7\phi \\
 & - 0.494\cos8\phi - 0.783\cos9\phi
 \end{aligned}
 \tag{24}$$

when three singular values are kept. Temperature dependences inferred from these solutions are plotted for comparison in Figure 41. The rms deviations are 0.318 Hz and 0.274 Hz, respectively. Both are likely to be of the order of the combined effects of vibrational and intermolecular contributions²¹⁵.

Determinations of the dependence of $^5J_{\text{O}}^{\text{CH}_3, \text{F}}$ over a wider temperature range in a variety of solvents are desirable if this problem is to be treated properly.

Since populations imply and are implied by free energies, the energy function $E(\phi)$ in Eq. (19) may be approximated by an expression such as

$$A(\phi) = V(\phi) - TS(\phi) \quad \text{Eq. (25)}$$

where the entropy is given by the usual expression

$$S(\phi) = -R \sum p(\phi) \ln p(\phi) \quad \text{Eq. (26)}$$

and is implicitly a function of β since $p(\phi) \equiv p(\beta, \phi)$ in Eq. (21). This approach did not yield better results in any case.

Both Eq. (23) and Eq. (24) are plotted in Figure 42. Apparently the coupling constant decreases quickly as the twist angle increases, as the INDO MO FPT calculations suggest. The same calculations, and the spectra of compounds which prefer the trans conformer, favour a small magnitude for $C(\phi = 180^\circ)$, but these equations fail to describe this detail. It is not clear whether the present results support the INDO prediction of a ponderable, if over-estimated, negative contribution from direct hydrogen-fluorine interaction, as in Figure 36.

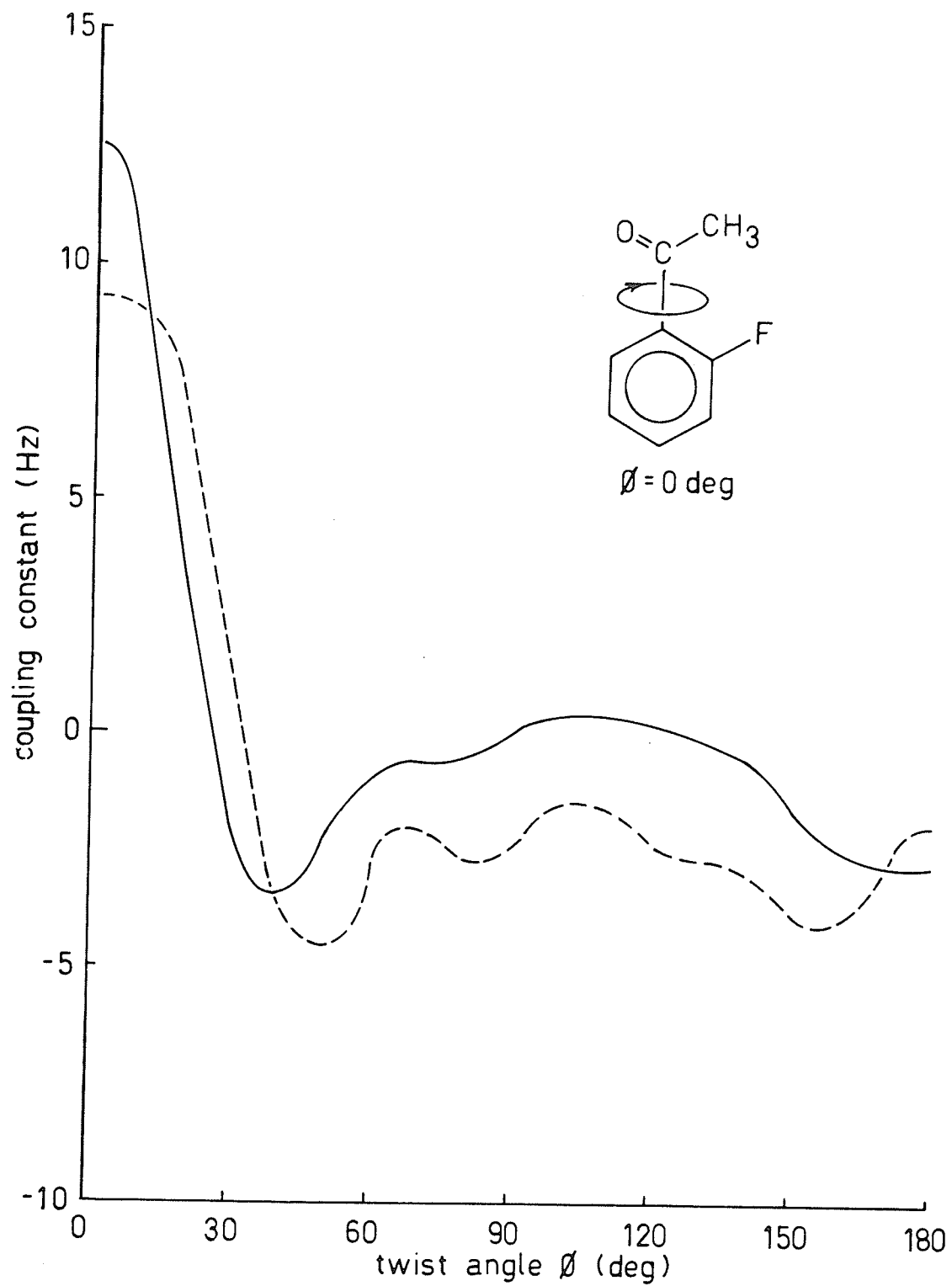
A line through the five points at lowest reciprocal temperature intercepts the ordinate at 1.83 ± 0.06 Hz. It is interesting that the corresponding number for 4,6-dibromo-2-fluoroanisole is

Figure 42

A plot of the angle dependence of the methyl proton-fluorine spin-spin coupling constant inferred from the temperature dependence of ${}^5J_{\text{O}}^{\text{CH}_3, \text{F}}$ for 2-fluoroacetophenone.

solid line two singular values

broken line three singular values



1.70 \pm 0.06 Hz. If the intercept is interpreted as the average value of $C(\phi)$ over all possible twist angles with equal probabilities, the near equality of these numbers may imply that the angle dependence of the methyl proton-fluorine coupling constant is similar for these compounds. The predictions of Eq. (23) and Eq. (24) are 0.096 Hz and -1.063 Hz, respectively.

The temperature dependence of ${}^4J_{\text{O}}^{\text{C}\alpha,\text{F}}$ in 2-fluoroacetophenone is consistent with a preference for the 0-anti conformer. The two-state model yields an energy difference of 5.2 \pm 2.2 kJ mol⁻¹ and characteristic coupling constants of 7.63 \pm 0.23 Hz for the 0-anti conformer and 0.63 \pm 3.72 Hz for the 0-syn. The rms deviation is 0.028 Hz. If the energy difference is fixed at 3.2 kJ·mol⁻¹, in agreement with the result derived from the temperature dependence of ${}^5J_{\text{O}}^{\text{CH}_3,\text{F}}$ and with the ab initio calculations, the characteristic coupling constants are 8.14 \pm 0.09 Hz and 4.62 \pm 0.22 Hz, respectively and the rms deviation is 0.032 Hz. The predicted temperature dependence appears in Figure 43 for comparison.

With Eq. (22) and the values of V_1 and V_2 suggested by the STO-3G calculations, the dynamic model yields

$$\begin{aligned}
 C(\phi) = & 2.824 + 2.613\cos\phi + 3.686\cos2\phi - 0.225\cos3\phi \\
 & + 0.768\cos4\phi - 1.278\cos5\phi - 0.550\cos6\phi - 0.927\cos7\phi \\
 & - 0.430\cos8\phi - 0.107\cos9\phi
 \end{aligned}
 \tag{27}$$

when three singular values are used and

$$\begin{aligned}
 C(\phi) = & 2.717 + 2.541\cos\phi + 4.189\cos2\phi - 0.704\cos3\phi \\
 & + 0.772\cos4\phi - 1.283\cos5\phi - 0.575\cos6\phi - 0.576\cos7\phi \\
 & - 0.161\cos8\phi + 0.295\cos9\phi
 \end{aligned}
 \tag{Eq. (28)}$$

when four singular values are kept. The rms deviations are 0.055 Hz and 0.101 Hz, respectively. Predicted temperature dependences appear in Figure 43. As noted above, the most important singular function is not well-approximated by the ten cosine terms and the resulting solutions $C(\phi)$ are not as reliable as the problem demands. Equations (27) and (28) are plotted in Figure 44.

${}^4J_{\text{O}}^{\text{C}\alpha,\text{F}}$ tends towards zero in those compounds which prefer the trans conformation (vide supra), which is inconsistent with the prediction based on either equation. It may be significant that both equations describe a maximum near $\phi = 30^\circ$, which is similar to the INDO MO FPT results in Figure 37. Further work is necessary if reliable comparisons are to be made, but these results are encouraging.

A line through the six points at lowest reciprocal temperature intercepts the ordinate at 5.48 Hz. The average over all possible twist angles with equal probability yields 2.824 Hz for Eq. (27) and 2.717 Hz for Eq. (28).

Figure 43

A plot of the temperature dependence of ${}^4J_{\text{O}}^{\text{C}\alpha,\text{F}}$ for 2-fluoroacetophenone- α - ${}^{13}\text{C}$.

- observed
- △ static model
- ⊙ dynamic model with three singular values
- dynamic model with four singular values

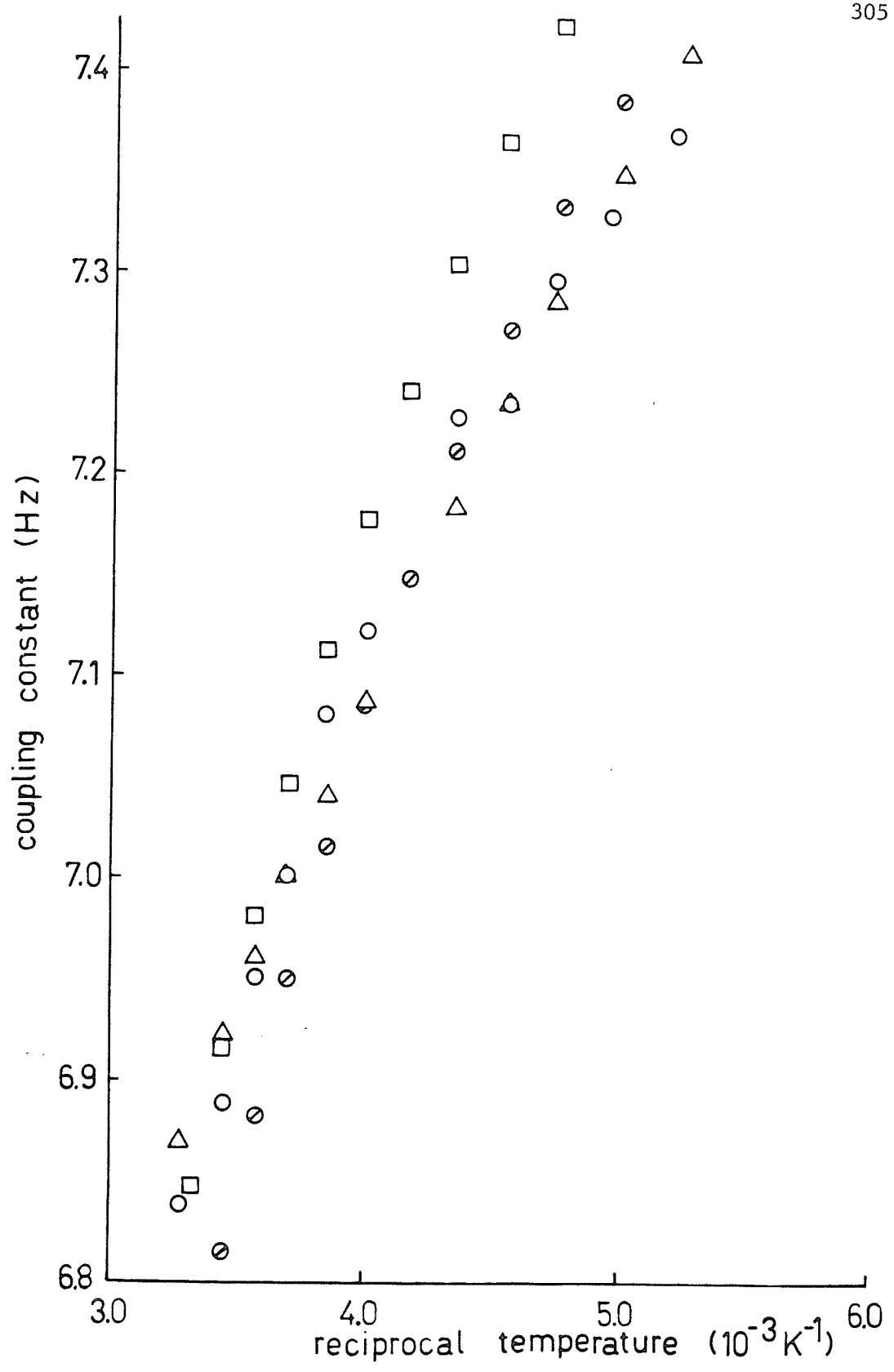
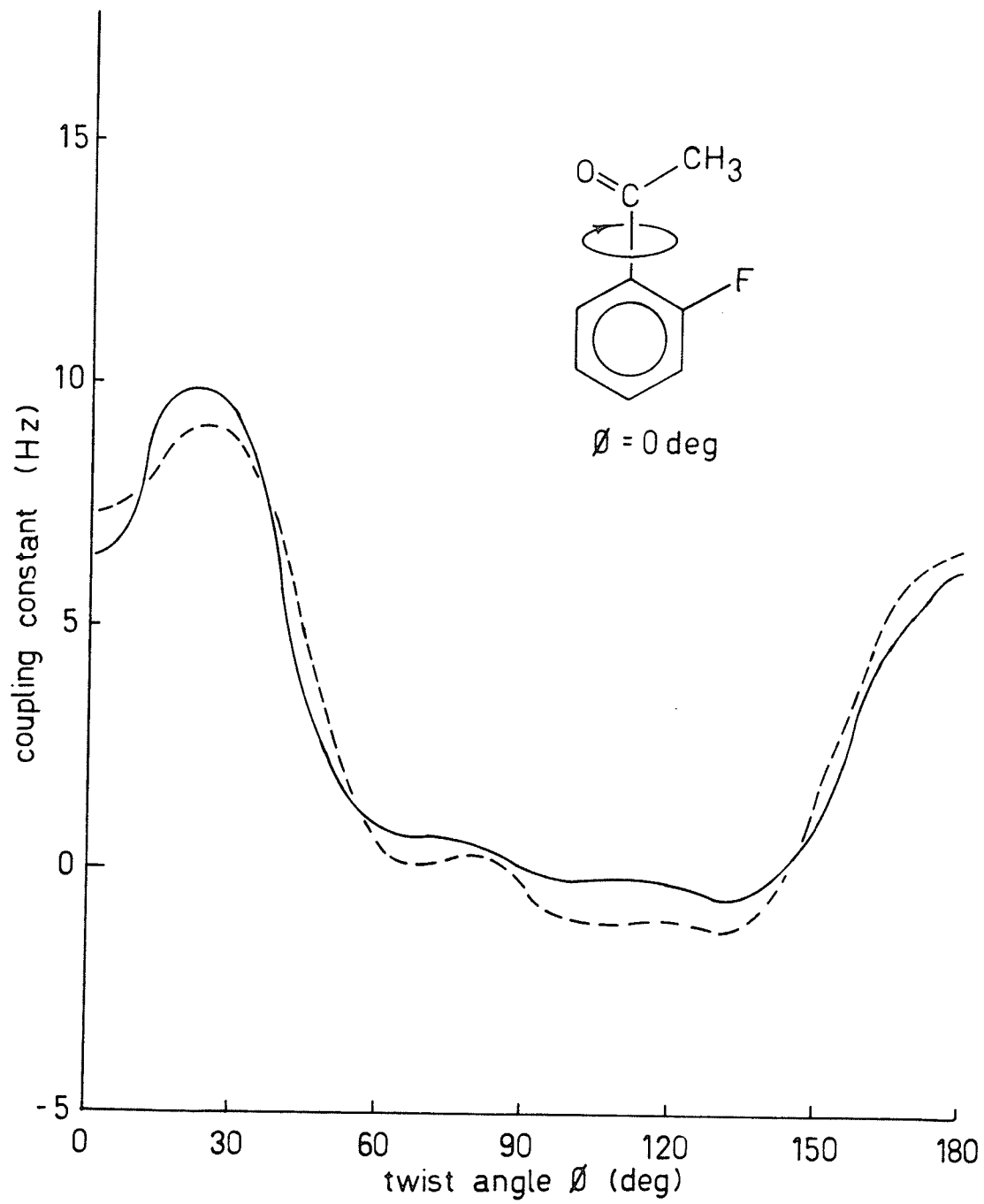


Figure 44

A plot of the angle dependence of the methyl carbon-fluorine spin-spin coupling constant inferred from the temperature dependence of ${}^4J_{\text{O}}^{\text{C}\alpha,\text{F}}$ for 2-fluoroacetophenone

solid line three singular values

broken line four singular values



iv) 2,6-difluoroacetophenone

The temperature dependence of ${}^5J_{\text{O}}^{\text{CH}_3, \text{F}}$ in Figure 45 resembles that for 2,3,5,6-tetrafluoroanisole in Figure 40. The rotational potential for the acetyl group is predominantly two-fold and non-planar conformations are populated significantly. If Eq. (22) and Eq. (23) are modified to reflect the two-fold symmetry of the aromatic ring by writing

$$V(\phi) = V_1 \left(\sin^2 \frac{2\phi}{2} + \sin^2 \frac{\phi + 180^\circ}{2} \right) + V_2 \sin^2 \phi \quad \text{Eq. (29)}$$

where V_1 and V_2 are approximated by the values used for 2-fluoroacetophenone ($3.3 \text{ kJ}\cdot\text{mol}^{-1}$ and $10.5 \text{ kJ}\cdot\text{mol}^{-1}$, respectively), and

$$C(\phi) = 0.096 + 1.139 \cos 2\phi + 2.021 \cos 4\phi + 1.266 \cos 6\phi + 0.335 \cos 8\phi \quad \text{Eq. (30)}$$

the predicted coupling constants are between 0.4 and 0.8 Hz too large over the observed temperature range.

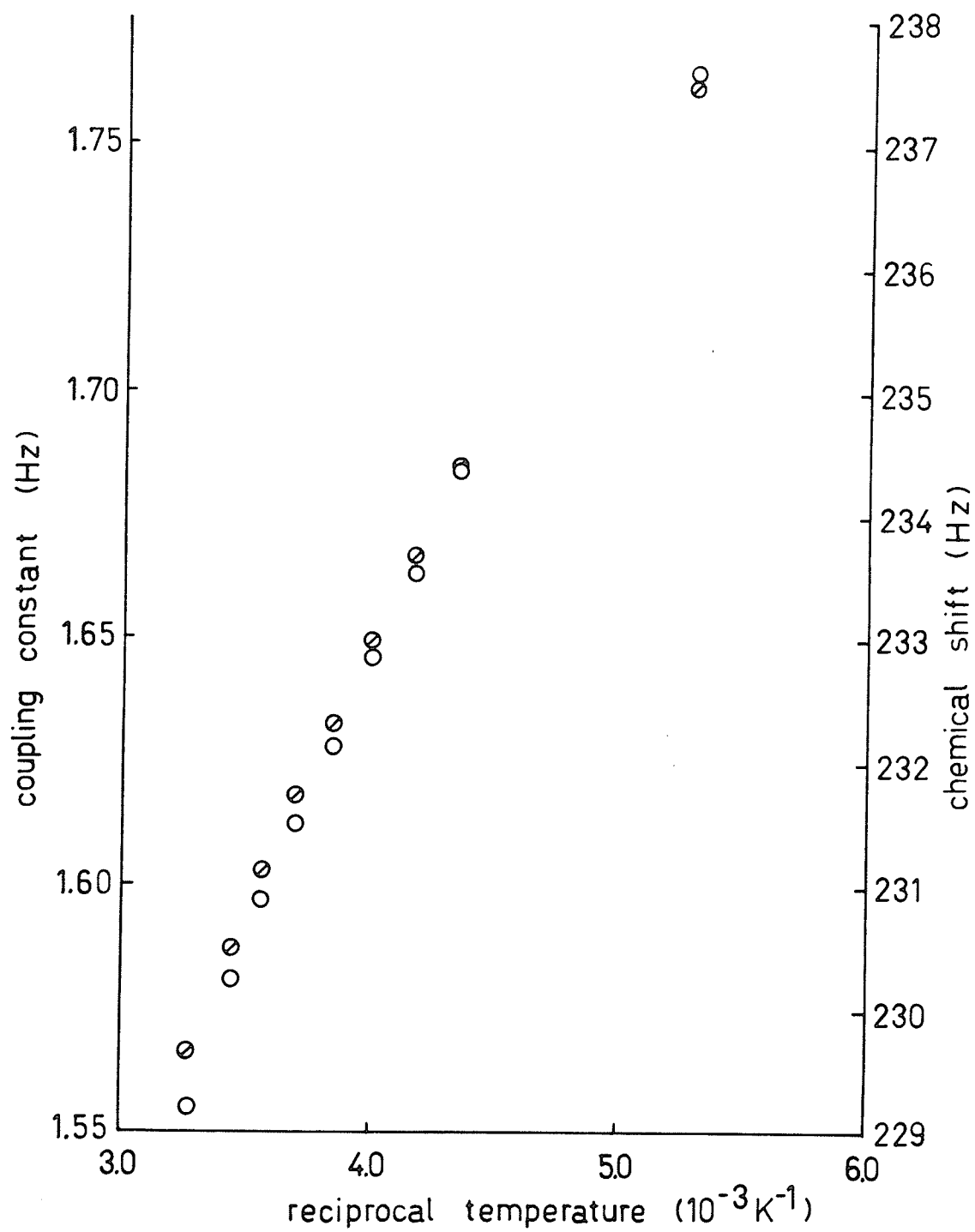
If ${}^5J_{\text{O}}^{\text{CH}_3, \text{F}}$ at 192 K approximates $({}^5J_{\text{cis}} + {}^5J_{\text{trans}})/2 \equiv [C(0^\circ) + C(180^\circ)]/2$, the observed value of 1.765 Hz is to be compared with the calculated values of 1.67 ± 0.40 Hz from the static model and 2.429 Hz from the dynamic model.

The intercept of a line through the reciprocal temperatures between 230 K and 280 K and the ordinate is 1.20 ± 0.04 Hz. This is similar to the value of 2,3,5,6-tetrafluoroanisole (1.07 ± 0.05 Hz), which again suggests that the rotational angle

Figure 45

A plot of the temperature dependence of $^5J_{\text{OCH}_3, \text{F}}$ and of ν_{CH_3} for 2,6-difluoroacetophenone

- coupling constant
- ⊙ methyl proton chemical shift



dependence of these two coupling constants is nearly the same.

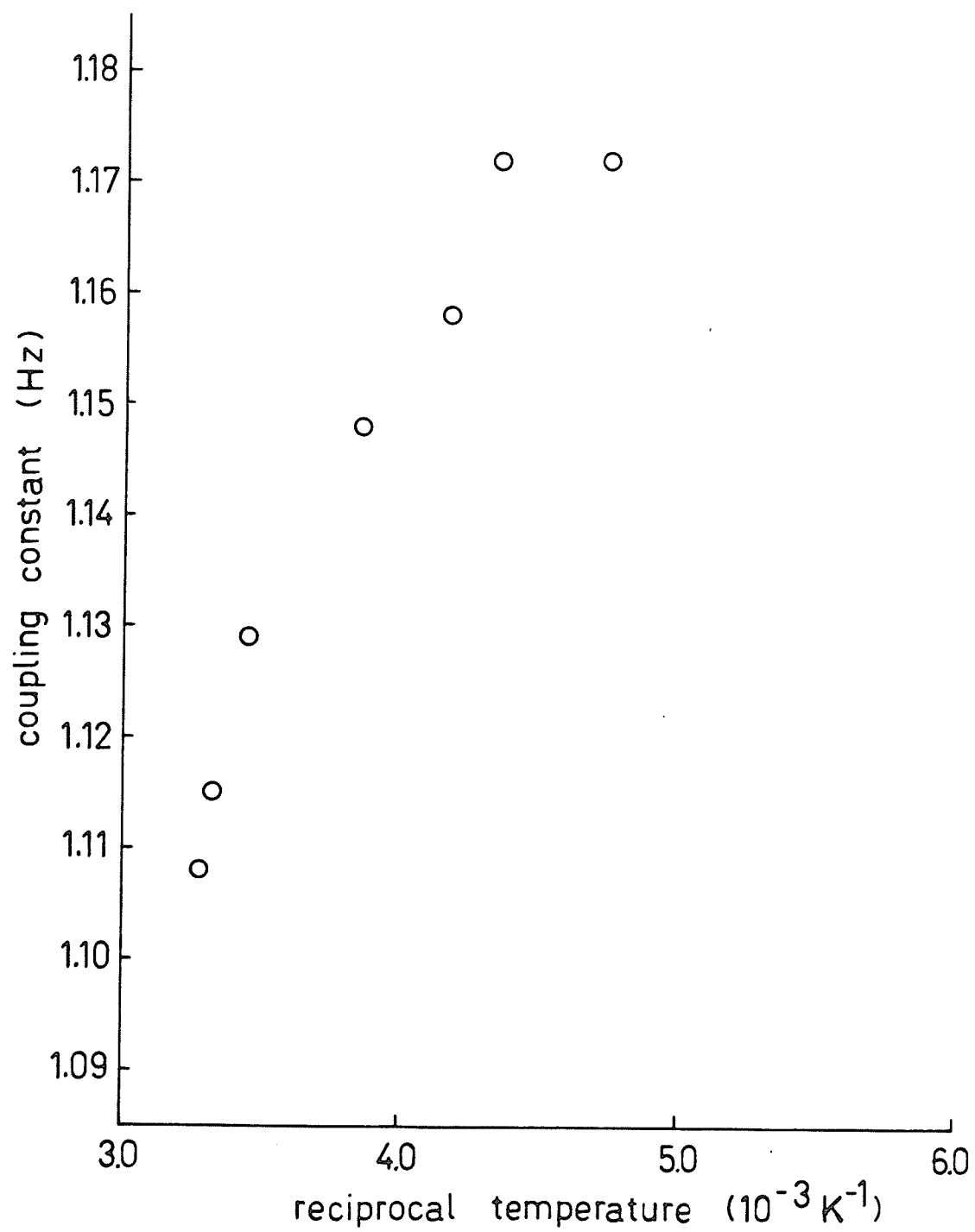
The average of Eq. (30) over all twist angles with equal probability yields 0.096 Hz.

v) α,α,α -trifluoroacetophenone

The temperature dependence of ${}^5J_{\text{O}}^{\text{CF}_3,\text{H}}$ in Figure 46 is not well-determined, but may imply that planar conformations are preferred. The rate of change of the coupling constant with reciprocal temperature is comparable to that for 2,6-difluoroacetophenone, but the significance of this observation is not apparent. The magnitude of the coupling constant is somewhat smaller in the present compound due to the differences in geometry, coupling mechanism, and rotational potential.

Figure 46

A plot of the temperature dependence of ${}^5J_{\text{O}}^{\text{CF}_3, \text{F}}$ for α, α, α -trifluoroacetophenone.



J. Methyl Carbon Chemical Shifts

The chemical shift of the methyl carbon of substituted anisoles remains a puzzle. Steric crowding and reduction of conjugation are expected to increase the electron density at the methyl carbon and, thereby, to shield this nucleus¹⁰¹. Stothers proposes that deshielding is caused by increased polarization of the oxygen-methyl carbon bond as the methoxy group twist angle increases¹⁰³.

As in Table 19, the methyl carbon chemical shift progresses to lower field in anisole, 4-bromo-2-fluoroanisole, 4,6-dibromo-2-fluoroanisole, and 2,3,5,6-tetrafluoroanisole. This observation may find an explanation in the net atomic charge on carbon. As conjugation between oxygen and the π -system is reduced, the atomic charge on the methyl carbon (indeed the electronic population of the methyl group as a whole) increases according to the *ab initio* calculations. The polarization argument is not supported. Fliszár suggests that a Mulliken population analysis is not a good approximation for polar bonds and that the carbon atoms in alkanes are, contrary to the common view, positively charged when an appropriate definition of charge is applied²⁶¹. Any decrease in the positive charge causes a decrease in shielding, which is perhaps unexpected. Pugmire and Grant propose that the local paramagnetic screening exhibits such a charge dependence²⁶².

The magnetic anisotropy of the phenyl ring should lead to a

decrease in deshielding as the methoxy group twists out of the ring plane, but this effect is masked. Local group anisotropy of substituents on the phenyl ring, local electric fields, and substituent-induced electronic effects may contribute to the chemical shift, as for the methyl proton chemical shifts.

These shifts indicate that the electronic environment of the methyl carbons in 4,6-dibromo-2-fluoroanisole and 2,3,5,6-tetrafluoroanisole is quite different from the electronic environment of the methyl carbons in anisole and 4-bromo-2-fluoroanisole. This supports the contention that the methoxy group prefers to lie in the ring plane in the latter two compounds, but non-planar conformations are preponderant for the di-ortho substituted anisoles.

A similar gradation is found for acetophenone, 2-fluoroacetophenone, and 2,6-difluoroacetophenone, but it is less marked and is not a particularly good conformation indicator.

K. Methyl Carbon Spin-Lattice Relaxation Times

i) theoretical considerations

Methyl carbon spin-lattice relaxation in the anisoles and acetophenones studied here is dominated by dipole-dipole relaxation by the methyl protons. The dipole-dipole relaxation time, $T_1(DD)$, can be determined from the measured relaxation time, T_1 , from Table 19 by the formula¹¹⁴

$$T_1(DD) = \frac{\eta_{\max}}{\eta} T_1 \quad \text{Eq. (31)}$$

where η is the nuclear Overhauser enhancement and 1.988 is the maximal value for carbon relaxed by protons. In the extreme narrowing limit, the dipole-dipole relaxation time is inversely proportional to an effective correlation time, τ_c :

$$\frac{1}{T_1(DD)} = n \hbar^2 \gamma_C^2 \gamma_H^2 r_{CH}^{-6} \tau_c \quad \text{Eq. (32)}$$

where n is the number of protons attached to the carbon, γ is the gyromagnetic ratio of the nucleus, and r_{CH} is the internuclear separation.

Molecular reorientation may be described by the tumbling of an ellipsoid at different rates about each of the three internal coordinate axes^{112,114}. Internal motions are superimposed on these rotations in a manner which depends on the overall geometry. Simplifying assumptions are required if the problem is to be tractable. For the present discussion, the

overall rotational motion is isotropic and the methoxy group rotation is prohibited. If the methyl group jumps between equivalent positions in a three-fold barrier, the effective correlation time is given by¹¹⁴

$$\tau_c = \frac{A}{6D} + \frac{B + C}{6D + (3/2)D_i} \quad \text{Eq. (33)}$$

where A, B, and C are geometrical parameters, D is the rotational diffusion coefficient, and D_i is the methyl jump rate. With these approximations and the assumption that the rotational diffusion coefficients are equal for all of the anisoles studied, an increase in $T_1(DD)$ corresponds to an increase in the methyl jump rate.

Actually the molecular tumbling is not isotropic and methoxy group reorientation should be included in the analysis. Within the analysis presented above, the constancy of the rotational diffusion coefficient, D, could be checked by determining $T_1(DD)$ for a carbon nucleus within the rigid framework.

Coupling between the methyl carbon and fluorine may cause deviations from exponential recovery through cross-relaxation²¹³. Since dipole-dipole relaxation of the methyl carbon is dominated by the methyl protons and since coupling between the methyl carbon and fluorine is weak, a negligible error is incurred if fluorine is not irradiated strongly during the relaxation experiments.

ii) measured relaxation times

The nuclear Overhauser enhancements in Table 19 demonstrate that dipole-dipole relaxation of the methyl carbon by methyl protons is dominant. Strong irradiation of fluorine in the presence of strong broadband irradiation of protons did not influence the value of relaxation parameters for 4,6-dibromo-2-fluoroanisole.

Since the nuclear Overhauser enhancements are not well-determined, relaxation times $T_1(DD)$ will not be quoted. The spin-lattice relaxation time for anisole, $9.93 \pm 0.06s$, is taken as a reference point. For 4-bromo-2-fluoroanisole the relaxation time which was found for a clean, dilute solution is $6.7 \pm 0.2s$. Qualitatively this is interpreted as a sign of more hindered methyl group reorientation than in anisole. The preference for the trans conformer results in a greater population of more hindered methyl groups. In contrast the relaxation time for 4,6-dibromo-2-fluoroanisole is $15.2 \pm 0.1s$, which implies that methyl group reorientation is less hindered than in anisole. This is expected for non-planar conformations in which the steric interaction between the methyl group and the phenyl groups is reduced. Ab initio calculations for anisole reproduce this effect. Similarly, the relaxation time is, quite roughly, $22 \pm 1s$ for 2,3,5,6-tetra-

fluoroanisole, which indicates that non-planar conformations are populated significantly.

Proton inversion-recovery experiments performed on a Varian CFT-20 spectrometer provide a measure of the correlation time for overall reorientation. Since the coupled spectra are not amenable to a proper determination of the relaxation times, the position of the null is taken for comparison of 4-bromo-2-fluoroanisole and 4,6-dibromo-2-fluoroanisole. For H3 the null occurs at 27 ± 3 s for 4-dibromo-2-fluoroanisole and at 20 ± 2 for 4,6-dibromo-2-fluoroanisole, that is, the overall reorientation of the former compound is faster than for the latter. The short spin-lattice relaxation time of the methyl carbon of 4-bromo-2-fluoroanisole is then not due to slower reorientation of the whole molecule.

Relaxation times for the methyl carbons of acetophenone and 2-fluoroacetophenone are 15.4 ± 0.2 s and 14.6 ± 0.2 s, respectively, which implies similar conformational behaviour for both. This view is consistent with a strong preference for planar conformers of both compounds. It is not clear that the relaxation time is much greater for 2,6-difluoroacetophenone and the three-parameter fit of the relaxation data is suspect. If the two-parameter fit

is preferred, the relaxation time may be somewhat longer than for the other two acetophenones, but the results are not of sufficient quality to be conclusive.

Various mechanisms, but in particular the spin-rotation²⁶³ and dipole-dipole mechanisms, contribute to relaxation of covalently-bonded fluorine in small molecules. For larger molecules the contribution from spin rotation decreases. The contribution from the dipole-dipole mechanism can be deduced from nuclear Overhauser enhancements and reaches a maximum of 0.53 for fluorine relaxed by protons. Such enhancements affirm the importance of this mechanism in fluorobenzenes²⁶⁴.

The fluorine spin-lattice relaxation times in Table 20 are essentially identical for 4,6-dibromo-2-fluoroanisole, 2,3,5,6-tetrafluoroanisole, and 2,6-difluoroacetophenone. The number for 2-fluoroacetophenone is about one-half of this common value, which is most probably an indication of the proximity of the fluorine and the methyl protons which cause dipole-dipole relaxation. (The enhancement of the fluorine signal in the presence of broadband irradiation of protons is about 0.16 for 2-fluoroacetophenone). The similarity between the two anisoles and 2,6-difluoroacetophenone supports the argument that the non-planar conformations of the latter are populated significantly.

Chapter 6
Summary and Conclusions

In this work proton, fluorine and carbon nuclear magnetic resonance spectroscopy has been used to investigate the methoxy group conformation in some 2-fluoroanisoles and the acetyl group conformation in some 2-fluoroacetophenones. Long-range spin-spin coupling constants have been the principal source of information.

A review of the literature on the conformational behaviour of the methoxy group in anisole concludes that the barrier lies between 0 and 40 kJ·mol⁻¹. Evidently the preferred conformation has all heavy atoms coplanar. The present study of anisole in solution demonstrates that the planar conformer is preferred and that a finite barrier to internal rotation exists. Ab initio molecular orbital calculations at the STO-3G level reinforce this conclusion, but indicate that a significant four-fold component creates a local minimum at the orthogonal conformation on the minimum energy path for methoxy group reorientation, at least for the isolated molecule. The methyl and methoxy group rotations are not separable. Long-range carbon-carbon and carbon-proton coupling constants have not been widely used as conformational indicators, but it appears that ${}^5J_{\text{p}}^{\text{C}\alpha, \text{C}4}$, ${}^6J_{\text{p}}^{\text{C}\alpha, \text{H}4}$, ${}^4J_{\text{m}}^{\text{C}\alpha, \text{C}}$ and ${}^5J_{\text{m}}^{\text{C}\alpha, \text{H}}$ may be important in this regard. Future research might continue to seek empirical relationships similar to those for ${}^6J_{\text{p}}^{\text{XH}, \text{H}4}$, ${}^4J_{\text{o}}^{\text{XH}, \text{H}}$ and ${}^5J_{\text{m}}^{\text{XH}, \text{H}}$.

A strong preference for trans-2-fluoroanisole is seen in the nmr parameters and is predicted from the ab initio calculations.

INDO FPT calculations of ${}^5J_{\text{O}}^{\text{CH}_3,\text{F}}$ and ${}^4J_{\text{O}}^{\text{C}\alpha,\text{F}}$ imply that transmission of both couplings relies on the proximity of the methyl group and fluorine. Direct hydrogen-fluorine interaction dominates the calculated ${}^5J_{\text{O}}^{\text{CH}_3,\text{F}}$, but the indirect interaction of carbon and fluorine, mediated by the methyl hydrogens, dominates the calculated ${}^4J_{\text{O}}^{\text{C}\alpha,\text{F}}$. Both coupling constants contain contributions from direct carbon-fluorine interaction. Apparently the INDO FPT calculations over-estimate the significance of direct hydrogen-fluorine interaction, which provides a negative contribution to ${}^5J_{\text{O}}^{\text{CH}_3,\text{F}}$, relative to the indirect interaction, which is mediated by carbon: rotational averaging over the calculated angle dependence of ${}^5J_{\text{O}}^{\text{CH}_3,\text{F}}$ is expected to yield a negative sign, but a positive sign is inferred from weak irradiation experiments.

${}^5J_{\text{O}}^{\text{CH}_3,\text{H6}}$ is large and ${}^5J_{\text{O}}^{\text{CH}_3,\text{F}}$ is small in 4-bromo-2-fluoroanisole, which strongly prefers the trans conformation. ${}^5J_{\text{m}}^{\text{C}\alpha,\text{H3}}$ is relatively large, but ${}^5J_{\text{m}}^{\text{C}\alpha,\text{H5}}$ is at most 0.05 Hz in magnitude, which is consistent with this conclusion.

The effect of the ortho bromine substituent in 4,6-dibromo-2-fluoroanisole is dramatic. The nmr parameters indicate that the methoxy group prefers to lie near the plane perpendicular to the ring plane. Coupling between the methyl carbon and all ring carbons is observable. The magnitudes of ${}^3J_{\text{O}}^{\text{C}\alpha,\text{C2}}$ and ${}^3J_{\text{O}}^{\text{C}\alpha,\text{C6}}$, and of ${}^4J_{\text{m}}^{\text{C}\alpha,\text{C3}}$ and ${}^4J_{\text{m}}^{\text{C}\alpha,\text{C5}}$, are nearly equal, which implies

that the methyl carbon lies near the plane perpendicular to the benzene ring. The large magnitude of ${}^5J_{\text{p}}^{\text{C}\alpha,\text{C}4}$ (0.94 ± 0.02 Hz) places a lower bound on ${}^5J_{90}^{\text{C}\alpha,\text{C}4}$. Signs of ${}^5J_{\text{o}}^{\text{CH}_3,\text{F}}$, ${}^4J_{\text{o}}^{\text{C}\alpha,\text{F}}$ and ${}^5J_{\text{m}}^{\text{C}\alpha,\text{H}}$ are positive. Both ${}^3J_{\text{o}}^{\text{C}\alpha,\text{C}}$ and ${}^5J_{\text{m}}^{\text{C}\alpha,\text{H}}$ suggest that the methyl group lies somewhat nearer to fluorine than to bromine, on the average. The methyl carbon spin-lattice relaxation time and the temperature dependence of ${}^5J_{\text{o}}^{\text{CH}_3,\text{F}}$ may be explained if a near-orthogonal conformation is preferred.

Similarly, significant populations of non-planar conformations of 2,3,5,6-tetrafluoroanisole exist. Rotation of the methoxy group is less hindered by an ortho fluorine substituent than by bromine. Since ${}^5J_{\text{o}}^{\text{CH}_3,\text{F}}$ increases as temperature decreases, contrary to the observations for 4,6-dibromo-2-fluoroanisole, the preferred conformation of 2,3,5,6-tetrafluoroanisole is planar, or more nearly so. However, the barrier to methoxy group rotation cannot be estimated without further information. Determinations of the coupling constants between the methyl carbon and ring carbons, fluorines, and H4 would be useful.

High resolution spectra of 2-fluoroacetophenone are consistent with a preference for the O-anti conformation over the O-syn. If only these two conformers are appreciably populated, the temperature dependences of ${}^5J_{\text{o}}^{\text{CH}_3,\text{F}}$ and ${}^4J_{\text{o}}^{\text{C}\alpha,\text{F}}$ are consistent with an energy difference of 3.1 ± 0.3 kJ·mol⁻¹. Ab initio calculations place the energy of the O-anti conformer of the isolated molecule 3.3 kJ·mol⁻¹

below that of the 0-syn. ${}^4J_{\text{O}}^{\text{C}\alpha,\text{H}6}$ and ${}^5J_{\text{m}}^{\text{C}\alpha,\text{H}5}$ are both finite and positive, but ${}^5J_{\text{m}}^{\text{C}\alpha,\text{H}3}$ is unobservable, which reinforces the conclusion that 0-anti is strongly preferred. INDO FPT calculations yield rotational angle dependences of ${}^5J_{\text{O}}^{\text{CH}_3,\text{F}}$ and ${}^4J_{\text{O}}^{\text{C}\alpha,\text{F}}$ which are quite similar to those calculated for 2-fluoroanisole. A dynamic (continuous) model of the temperature dependences of ${}^5J_{\text{O}}^{\text{CH}_3,\text{F}}$ and ${}^4J_{\text{O}}^{\text{C}\alpha,\text{F}}$ leads to forms which are similar to those calculated with INDO FPT, but which suggest that the indirect interaction dominates both couplings. Further experimental and theoretical work is needed to complete the determination of the conformational dependence and mechanism of both couplings.

The magnitude of ${}^5J_{\text{O}}^{\text{CH}_3,\text{F}}$ in 2,6-difluoroacetophenone is much smaller than in 2-fluoroacetophenone, but it is comparable to the number for 2,3,5,6-tetrafluoroanisole. If 2-fluoroacetophenone prefers the 0-anti conformation in order to minimize repulsive interactions between the carbonyl oxygen and fluorine, it may follow that these interactions create a substantial population of non-planar conformers of 2,6-difluoroacetophenone. Although the temperature dependence of ${}^5J_{\text{O}}^{\text{CH}_3,\text{F}}$ suggests that the preferred conformation is planar, the similarity of the fluorine spin-lattice relaxation times for 4,6-dibromo-2-fluoroanisole, 2,3,5,6-tetrafluoroanisole and 2,6-difluoroacetophenone is adduced for significant populations of non-planar conformers.

The magnitude and temperature dependence of ${}^5J_{\text{O}}^{\text{CF}_3,\text{H}}$ in

α,α,α -trifluoroacetophenone may indicate that the planar conformer is preferred, and that non-planar conformations are significantly populated.

A relationship exists between ring carbon charges derived from *ab initio* calculations for anisole, 2-fluoroanisole, and 2-fluoroacetophenone, and chemical shifts. With an appropriate definition of charge, the conformational dependence of methyl carbon chemical shifts for the anisoles is explicable.

Although much of this work could not have been performed without a pulsed nmr spectrometer with time averaging and some multinuclear capabilities, these studies could be performed better and more quickly, and could be extended further, if a high-field spectrometer with suitable hardware and computer support were accessible. A superconducting magnet provides the advantages of high spectral dispersion for ease of analysis, high sensitivity to reduce the time required to obtain a spectrum, and stability of field superior to an electromagnet (which is essential for lengthy experiments aimed at high resolution).

A computer with appropriate programming for pulse sequencing and data acquisition could open the possibility of performing the more recent experiments which involve considerable gymnastics on the part of the nuclear spins. Such techniques may remove much of the complexity from a spectrum to reveal otherwise inaccessible information. For example, carbon-carbon spin-spin coupling

constants may be obtained from compounds with ^{13}C in natural abundance by creating double-quantum coherence, as demonstrated by Bax, Freeman, and Kempell²⁶⁵. Long-range proton-carbon spin-spin coupling constants may be obtained by a technique proposed by Bax and Freeman²⁶⁶ which includes a selective 180° pulse applied to the isolated resonance of the proton of interest. The required spectral dispersion may be obtained readily with a high-field magnet.

References

1. J. A. Pople, W. G. Schneider, and H. J. Bernstein, High-resolution Nuclear Magnetic Resonance. (McGraw-Hill, New York, 1959).
2. A. Abragam, The Principles of Nuclear Magnetism. (Oxford University Press, Oxford, 1961).
3. J. W. Emsley, J. Feeney, and L. H. Sutcliffe, High Resolution Nuclear Magnetic Resonance Spectroscopy (Pergamon Press, London, 1965).
4. R. J. Abraham, The Analysis of High Resolution NMR Spectra (Elsevier, Amsterdam, 1971).
5. T. C. Farrar and E. D. Becker, Pulse and Fourier Transform NMR (Academic, New York, 1971).
6. D. Shaw, Fourier Transform NMR Spectroscopy. (Elsevier, Amsterdam, 1976).
7. C. P. Slichter, Principles of Magnetic Resonance. (Springer-Verlag, Berlin, 1978).
8. A. Carrington and A. D. McLachlan, Introduction to Magnetic Resonance. (Chapman and Hall, London, 1979).
9. P. H. Hermans, in: van't Hoff-Le Bel Centennial, ed. O. B. Ramsey. (American Chemical Society, Washington, 1975) pp. 123.
10. W. J. Orville-Thomas, in: Internal Rotation in Molecules, ed. W. J. Orville-Thomas. (Wiley and Sons, London, 1974) p. 7.

11. O. Hassel, *Tidsskr. Kjemi Bergvesen og Met.* 3 (1943) 32;
reprinted in English in: *Topics in Stereochemistry*,
Vol. 6, eds. N. L. Allinger and E. L. Eliel. (Wiley-
Interscience, New York, 1971) pp. 11.
12. D. H. R. Barton, *Experientia* 6 (1950) 316.
13. R. Bucourt, in: *Topics in Stereochemistry*, Vol. 8,
eds. E. L. Eliel and N. L. Allinger, (Wiley-Interscience,
New York, 1973) pp. 159.
14. W. Klyne and V. Prelog, *Experientia* 16 (1960) 521.
15. T. A. Wildman, *Chem. Phys. Lett.* 75 (1980) 383; 80 (1981)
210.
16. O. Jardetzky, *Biochim. Biophys. Acta* 621 (1980) 227.
17. A. Haaland and J. E. Nilsson, *Acta. Chem. Scand.* 22 (1968)
2653.
18. T. A. Wildman, unpublished calculations.
19. H. D. Bist, J. C. D. Brand, and D. R. Williams, *J. Mol.*
Spectrosc. 24 (1967) 402.
20. E. Mathier, D. Welte, A. Bauder, and Hs. H. Gunthard, *J.*
Mol. Spectrosc. 37 (1971) 63.
21. N. W. Larsen and F. M. Nicolaisen, *J. Mol. Struct.* 22
(1974) 29.
22. L. Radom, W. J. Hehre, J. A. Pople, G. L. Carlson, and
W. G. Fateley, *J. Chem. Soc. Chem. Commun.* (1972) 3666.
23. T. Schaefer, J. B. Rowbotham, and K. Chum, *Can. J. Chem.*

- 54 (1976) 3666.
24. W. J. E. Parr and T. Schaefer, J. Magn. Reson. 25 (1977)
171.
 25. T. Schaefer and W. J. E. Parr, Can. J. Chem. 55 (1977)
552.
 26. W. J. E. Parr and T. Schaefer, J. Mol. Spectrosc. 66 (1977)
448.
 27. W. J. E. Parr and T. Schaefer, Accounts Chem. Res. 13 (1980)
400.
 28. T. Schaefer and T. A. Wildman, Chem. Phys. Lett. 80 (1981)
280.
 29. T. Schaefer, T. A. Wildman, and R. Sebastian, Can. J. Chem.
60 (1982) 1924.
 30. T. Schaefer, T. A. Wildman, and S. R. Salman, J. Am. Chem.
Soc. 102 (1980) 107.
 31. T. Schaefer, R. P. Veregin, and D. M. McKinnon, Can. J.
Chem. 59 (1981) 3204.
 32. A. Burawoy and J. T. Chamberlain, J. Chem. Soc. (1952) 2310.
 33. H. Hart and C. R. Wagner, Proc. Chem. Soc. (1958) 284.
 34. J. C. Dearden and W. F. Forbes, Can. J. Chem. 37 (1959)
1305.
 35. L. J. Frolen and L. Goodman, J. Am. Chem. Soc. 83 (1961)
3405.
 36. P. F. Oesper, C. P. Smyth, and M. S. Kharasch, J. Am.
Chem. Soc. 64 (1942) 937.

37. K. B. Everard and L. E. Sutton, *J. Chem. Soc.* (1949) 2312.
38. H. Lumbroso, *Bull. Soc. chim. France* (1950) 812.
39. a) M. Aroney, R. J. W. LeFèvre, and S.-S. Chang, *J. Chem. Soc.* (1964) 2954.
b) M. J. Aroney, M. G. Corfield, and R. J. W. LeFèvre, *J. Chem. Soc.* (1964) 2954.
40. M. J. Aroney, R. J. W. LeFèvre, R. K. Pierens, and M. G. N. The, *J. Chem. Soc. B* (1969) 666.
41. A. A. Bredikhin, V. P. Kostin, S. G. Vul'fson, and A. N. Vereshchagin, *Bull. Acad. Sci. USSR, Div. Chem.* 30 (1981) 419.
42. D. M. Roberti and C. P. Smyth, *J. Am. Chem. Soc.* 82 (1960) 2106.
43. S. K. Garg and C. P. Smyth, *J. Chem. Phys.* 46 (1967) 373.
44. G. Klages and G. Kraus, *Z. Naturforsch.* A26 (1971) 1272.
45. M. A. Mazid, J. P. Shukla, and S. Walker, *Can. J. Chem.* 56 (1978) 1800.
46. W. F. Anzilotti and B. C. Curran, *J. Am. Chem. Soc.* 65 (1943) 607.
47. H. Lumbroso, J. Curé, and C. G. Andrieu, *J. Mol. Struct.* 43 (1978) 87.
48. N. L. Allinger, J. J. Maul, and M. J. Hickey, *J. Org. Chem.* 36 (1971) 2747.
49. D. G. Lister and N. L. Owen, *J. Chem. Soc. Faraday Trans.*

- II 69 (1973) 1304.
50. D. G. Lister, J. Mol. Struct. 68 (1980) 33.
51. P. H. Turner, M. J. Corkill, and A. P. Cox, J. Phys. Chem. 83 (1979) 1473.
52. P. Cahill, L. P. Gold, and N. L. Owen, J. Chem. Phys. 48 (1968) 1620.
53. W. E. Steinmetz, J. Am. Chem. Soc. 96 (1974) 685.
54. N. S. True and R. K. Bohn, Chem. Phys. Lett. 60 (1979) 332.
55. N. S. True, N. S. Farag, J. Radhakrishnan, and R. K. Bohn. This result remains unpublished at this writing, but appears in reference 50.
56. D. G. Lister, P. Palmieri, and C. Zauli, J. Mol. Struct. 35 (1976) 299.
57. See papers 1-13 cited in reference 67.
58. M. Horák, E. R. Lippincott, and R. K. Khanna, Spectrochim. Acta A 23 (1967) 1111.
59. N. L. Owen and R. E. Hester, Spectrochim. Acta A 25 (1969) 343.
60. N. L. Owen and N. Sheppard, Proc. Chem. Soc. (1963) 264.
61. N. L. Owen and N. Sheppard, Trans. Faraday Soc. 60 (1964) 634.
62. K. Venkateswarlu and M. Radhakrishnan, Spectrochim. Acta 18 (1962) 1433.

63. R. Josefi, E. Drahorádová, and M. Horák, Collection Czechoslov. Chem. Comm. 39 (1974) 1541.
64. T. Schaefer, R. Sebastian, and T. A. Wildman, Can. J. Chem. 59 (1981) 3021.
65. G. Allen and S. Fewster, in: Internal Rotation in Molecules, ed. W. J. Orville-Thomas. (Wiley and Sons, London, 1974) Chapter 8.
66. J. Goulon, D. Canet, M. Evans, and G. J. Davies, Mol. Phys. 30 (1975) 973.
67. H. Tylli and H. Konschin, J. Mol. Struct. 42 (1977) 7.
68. H. Tylli, H. Konschin, and C. Grundfelt-Forsius, J. Mol. Struct. 55 (1979) 157.
69. H. Konschin, H. Tylli, and C. Grundfelt-Forsius, J. Mol. Struct. 77 (1981) 51.
70. A. V. Cunliffe, in: Internal Rotation in Molecules, ed. W. J. Orville-Thomas. (Wiley and Sons, London, 1974) Chapter 7.
71. H. M. Seip and R. Seip, Acta Chem. Scand. 27 (1973) 4024.
72. T. H. Goodwin, M. Przybylska, and J. M. Robertson, Acta Cryst. 3 (1950) 279.
73. Reference 85 and references therein.
74. P. A. Luhan and A. T. McPhail, J. Chem. Soc. Perkin Trans. II (1973) 51.
75. R. A. Wind, W. M. M. J. Bovée, J. C. F. Kupers, J. Smidt,

- and Chr. Steenbergen, Z. Naturforsch. A 34 (1979) 631.
76. G. W. Burton, Y. LePage, E. J. Gabe, and K. U. Ingold, J. Am. Chem. Soc. 102 (1980) 7792.
77. G. W. Burton and K. U. Ingold, J. Am. Chem. Soc. 103 (1981) 6472.
78. A. D. Baker, D. P. May, and D. W. Turner, J. Chem. Soc. B(1968) 22.
79. J. P. Maier and D. W. Turner, J. Chem. Soc. Faraday Trans. II 69 (1973) 521.
80. P. S. Dewar, E. Ernstbrunner, J. R. Gilmore, M. Godfrey, and J. M. Mellor, Tetrahedron 30 (1974) 2455.
81. H. Bock and G. Wagner, Tetrahedron Lett. (1971) 3713.
82. H. Bock, G. Wagner, and J. Kroner, Chem. Ber. 105 (1972) 3850.
83. G. Tschmutowa and H. Bock, Z. Naturforsch. 31 B (1976) 1611.
84. F. Bernardi, G. Distefano, A. Mangini, S. Pignataro, and G. Spunta, J. Electron Spectrosc. Relat. Phenom. 7 (1975) 457.
85. G. M. Anderson III, P. A. Kollman, L. N. Domelsmith, and K. N. Houk, J. Am. Chem. Soc. 101 (1979) 2344.
86. L. N. Domelsmith and K. N. Houk, Int. J. Quantum Chem., Quantum Biol. Symp. 5 (1978) 257.
87. H. Friege and M. Klessinger, Chem. Phys. Lett. 112 (1979) 1614.
88. A. Schweig and N. Thon, Chem. Phys. Lett. 38 (1976) 482.

89. E. Honegger and E. Heilbronner, Chem. Phys. Lett. 81 (1981) 615.
90. G. P. Rabold, R. T. Ogata, M. Okamura, L. H. Piette, R. E. Moore, and P. J. Scheuer, J. Chem. Phys. 46 (1967) 1161.
91. W. T. Dixon, M. Moghimi, and D. Murphy, J. Chem. Soc. Faraday Trans. II 70 (1974) 1713.
92. W. Uber and H. B. Stegmann, in: Landolt-Börnstein, New Series, Magnetic Properties of Free Radicals. Vol. 9, eds. H. Fischer and K.-H. Hellwege. (Springer-Verlag, Berlin, 1979) Chapter 8, Part c2, pp. 29-214.
93. W. J. van den Hoek, W. G. B. Huysmans, and M. J. C. van Gemert, J. Magn. Reson. 3 (1970) 137.
94. N. M. Atherton, A. J. Blackhurst, and I. P. Cook, Trans. Faraday Soc. 67 (1971) 2510.
95. W. J. van den Hoek, J. F. Th. de Winter, and J. Smidt, J. Magn. Reson. 6 (1972) 15.
96. W. G. B. Huysmans, W. J. Mijs, J. G. Westra, W. J. van Hoek, H. Angad Gaur, and J. Smidt, Tetrahedron 25 (1969) 2249.
97. W. F. Forbes and P. D. Sullivan, J. Chem. Phys. 48 (1968) 1411.
98. P. D. Sullivan, J. Phys. Chem. 74 (1970) 2563.
99. P. C. Lauterbur, J. Am. Chem. Soc. 83 (1961) 1846.

100. H. Spiesecke and W. G. Schneider, *J. Chem. Phys.* 35 (1961) 731.
101. K. S. Dhama and J. B. Stothers, *Can. J. Chem.* 44 (1966) 2855.
102. W. Kitching, I. de Jonge, W. Adcock, and A. N. Abeywickrema, *Org. Magn. Reson.* 14 (1980) 502.
103. J. B. Stothers, *Carbon-13 NMR Spectroscopy*. (Academic Press, New York, 1972) pp. 203-204.
104. M. Maricq and J. S. Waugh, *Chem. Phys. Lett.* 47 (1977) 327.
105. E. T. Lippmaa, M. A. Alla, T. J. Pehk, and G. Engelhardt, *J. Am. Chem. Soc.* 100 (1978) 1929.
106. A. Höhener, *Chem. Phys. Lett.* 53 (1978) 97.
107. T. R. Steger, E. O. Stejskal, R. A. McKay, B. R. Stutts, and J. Schaefer, *Tetrahedron Lett.* (1979) 295.
108. G. W. Buchanan, C. Reyes-Zamora, and D. E. Clarke, *Can. J. Chem.* 52 (1974) 3895).
109. G. A. Kalabin, D. F. Kushnarev, V. M. Bzesovsky, and G. A. Tschmutova, *Org. Magn. Reson.* 12 (1979) 598.
110. G. Llabres, M. Baiwir, L. Christiaens, J. Denoel, L. Laitem, and J.-L. Piette, *Can. J. Chem.* 56 (1978) 2008.
111. G. C. Levy, J. D. Cargioli, and F. A. L. Anet, *J. Am. Chem. Soc.* 95 (1973) 1527.
112. D. E. Woessner, B. S. Snowden, Jr., and G. H. Meyer, *J. Chem. Phys.* 50 (1969) 719.

113. J. R. Lyerla, Jr., and D. M. Grant, *J. Phys. Chem.* 76 (1972) 3213.
114. J. B. Lambert, R. J. Nienhuis, and J. W. Keepers, *Angew. Chem. Int. Ed. Engl.* 20 (1981) 487.
115. W. M. M. J. Bovée and J. Smidt, *Mol. Phys.* 26 (1973) 1133.
116. W. M. M. J. Bovée and J. Smidt, *Mol. Phys.* 28 (1974) 1617.
117. J. D. Cutnell and L. Verduin, *J. Chem. Phys.* 59 (1973) 258.
118. A. Makriyannis and J. J. Knittel, *Tetrahedron Lett.* (1979) 2753.
119. J. J. Knittel and A. Makriyannis, *J. Med. Chem.* 24 (1981) 906.
120. P. Diehl, H. Huber, A. C. Kunwar, and M. Reinhold, *Org. Magn. Reson.* 9 (1977) 374.
121. J. W. Emsley, J. C. Lindon, and J. M. Street, *J. Chem. Soc. Perkin Trans II* (1976) 805.
122. J. W. Emsley, C. M. Exon, S. A. Slack, and A.-M. Giroud, *J. Chem. Soc. Perkin Trans. II* (1978) 928.
123. J. W. Emsley, J. C. Lindon, and D. S. Stephenson, *J. Chem. Soc. Perkin Trans. II* (1975) 1794.
124. S. Castellano, C. Sun, and R. Kostelnik, *Tetrahedron Lett.* (1967) 5205.
125. H. M. Hutton and T. Schaefer, *Can. J. Chem.* 43 (1965) 3116.
126. T. Schaefer, S. R. Salman, T. A. Wildman, and P. D. Clark,

- Can. J. Chem. 60 (1982) 342.
127. P. Diehl, *Helv. Chim. Acta* 44 (1961) 829.
128. J. S. Martin and B. P. Dailey, *J. Chem. Phys.* 39 (1963) 1722.
129. O. Hofer, *Tetrahedron Lett.* (1975) 3415.
130. O. Hofer, *Monatsch. Chem.* 109 (1978) 405.
131. J. Martin and B. P. Dailey, *J. Chem. Phys.* 37 (1962) 2594.
132. S. Forsén, *J. Phys. Chem.* 67 (1963) 1740.
133. S. Forsén, B. Åkermark, and T. Alm, *Acta Chem. Scand.* 18 (1964) 2313.
134. H. Angad Gaur, J. Vriend, and W. G. B. Huysmans, *Tetrahedron Lett.* (1969) 1999.
135. R. W. Creceley, K. W. McCracken, and J. H. Goldstein, *Tetrahedron* 25 (1969) 877.
136. T. Schaefer, H. D. Gesser, and J. B. Rowbotham, *Can. J. Chem.* 54 (1976) 2235.
137. T. Schaefer and T. A. Wildman, *Can. J. Chem.* 57 (1979) 450.
138. D. G. de Kowalewski, R. H. Contreras, A. R. Engelmann, J. C. Facelli, and J. C. Durán, *Org. Magn. Reson.* 17 (1981) 199.
139. T. Schaefer and R. Laatikainen, unpublished.
140. L. Lunazzi and D. Macciantelli, *J. Chem. Soc. Chem. Comm.* (1971) 933.

141. T. Schaefer, R. Sebastian, and S. R. Salman, *J. Magn. Reson.* 46 (1982) 325.
142. E. A. Braude and F. Sondheimer, *J. Chem. Soc.* (1955) 3754.
143. T. Schaefer, S. R. Salman, and T. A. Wildman, *Can. J. Chem.* 58 (1980) 2364.
144. J. B. Bentley, K. B. Everard, R. J. B. Marsden, and L. E. Sutton, *J. Chem. Soc.* (1949) 2957.
145. A. G. Pinkus and H. C. Custard, Jr., *J. Phys. Chem.* 74 (1970) 1042.
146. E. Bock, R. Wasylshen, B. E. Gaboury, and E. Tomchuk, *Can. J. Chem.* 51 (1973) 1906.
147. M. J. Aroney, M. G. Corfield, and R. J. W. LeFèvre, *J. Chem. Soc.* (1964) 648.
148. P. H. Gore, P. A. Hopkins, R. J. W. LeFèvre, L. Radom, and G. L. D. Ritchie, *J. Chem. Soc. B* (1971) 120.
149. D. Mirarchi and G. L. D. Ritchie, *Aust. J. Chem.* 34 (1981) 1443.
150. C. L. Cheng, R. J. W. LeFèvre, G. L. D. Ritchie, P. A. Goodman, and P. H. Gore, *J. Chem. Soc. B* (1971) 1198.
151. C. T. Aw, H. H. Huang, and E. L. K. Tan, *J. Chem. Soc. Perkin Trans. II* (1972) 1638.
152. R. J. W. LeFèvre, D. V. Radford, and E. P. A. Sullivan, *Aust. J. Chem.* 20 (1967) 623.
153. A. Gambi, S. Giorgianni, A. Passerini, R. Visinoni, and S. Gherseti, *Spectrochim. Acta* 36 A (1980) 871.

154. R. N. Jones, W. F. Forbes, and W. A. Mueller, *Can. J. Chem.* 53 (1957) 504.
155. F. A. Miller, W. G. Fateley, and R. E. Witkowski, *Spectrochim. Acta* 23 A (1967) 891.
156. Y. Tanimoto, H. Kobayashi, S. Nagakura, and Y. Saito, *Acta Cryst.* 29 B (1973) 1822.
157. J. K. S. Kim, E. R. Boyko, and G. B. Carpenter, *Acta Cryst.* 29 B (1973) 1141.
158. W. Kaminski and K. Möbius, *J. Magn. Reson.* 5 (1971) 182.
159. W. Kaminski, *Z. Naturforsch.* 25 A (1970) 639.
160. K. S. Dhimi and J. B. Stothers, *Can. J. Chem.* 43 (1965) 479.
161. P. C. Lauterbur, *J. Am. Chem. Soc.* 83 (1961) 1846.
162. K. S. Dhimi and J. B. Stothers, *Tetrahedron Lett.* (1964) 631.
163. T. Drakenberg, J. M. Sommer, and R. Jost, *Org. Magn. Reson.* 8 (1976) 579.
164. T. Drakenberg, J. Sommer, and R. Jost, *J. Chem. Soc. Perkin Trans. II* (1980) 363.
165. J.-F. Barthelemy, R. Jost, and J. Sommer, *Org. Magn. Reson.* 11 (1978) 438.
166. K. Hayamizu and O. Yamamoto, *J. Mol. Spectrosc.* 25 (1968) 422.
167. S. Castellano and C. Sun, in: W. Brügel, *Handbook of NMR Spectral Parameters.* (Heyden and Son, London, 1979) p.34.

168. W. B. Smith, D. L. Deavenport, and A. M. Ihrig, *J. Am. Chem. Soc.* 94 (1972) 1959.
169. R. E. Klinck, D. H. Marr, and J. B. Stothers, *J. Chem. Soc. Chem. Comm.* (1967) 409.
170. M. Grimaud and G. Pfister-Guillouzo, *Org. Magn. Reson.* 7 (1975) 386.
171. R. Benassi, D. Iarossi, U. Folli, L. Schenetti, and T. Taddei, *J. Chem. Soc. Perkin Trans. II* (1981) 228.
172. J. W. Emsley, J. C. Lindon, J. M. Street, and G. E. Hawkes, *J. Chem. Soc. Faraday Trans. II* 72 (1976) 1365.
173. R. Wasylshen, J. B. Rowbotham, L. Ernst, and T. Schaefer, *Can. J. Chem.* 50 (1972) 2575.
174. D. R. Davis, R. P. Lutz, and J. D. Roberts, *J. Am. Chem. Soc.* 83 (1961) 246.
175. J. Hilton and L. H. Sutcliffe, in: *Progress in Nuclear Magnetic Resonance Spectroscopy*, Vol. 10, ed. J. W. Emsley, J. Feeney, and L. H. Sutcliffe. (Pergamon Press, London, 1971) pp. 27 and references therein.
176. R. Wasylshen and T. Schaefer, *Can. J. Chem.* 50 (1972) 1852.
177. J. Meinwald and A. Lewis, *J. Am. Chem. Soc.* 83 (1961) 2769.
178. F. A. L. Anet, A. J. R. Brown, P. Carter, and S. Winston, *J. Am. Chem. Soc.* 87 (1965) 5249.
179. P. C. Myhre, J. W. Edmonds, and J. D. Kruger, *J. Am. Chem.*

- Soc. 88 (1966) 5249.
180. J. P. N. Brewer, H. Heaney, and B. A. Marples, J. Chem. Soc. Chem. Comm. (1967) 27.
181. A. D. Cross and P. W. Landis, J. Am. Chem. Soc. 84 (1962) 3784.
182. A. D. Cross and P. W. Landis, J. Am. Chem. Soc. 86 (1965) 4005.
183. R. E. Wasylshen and M. Barfield, J. Am. Chem. Soc. 97 (1975) 4545.
184. L. F. Fieser and M. Fieser, Reagents in Organic Synthesis (Wiley and Sons, New York, 1967) 682f.
185. J. L. Marshall, D. E. Miiller, H. C. Dorn, and G. E. Maciel, J. Am. Chem. Soc. 97 (1975) 460.
186. E. J. Corey and J. W. Suggs, Tetrahedron Lett. (1975) 2647.
187. R. Freeman and W. A. Anderson, J. Chem. Phys. 37 (1962) 2053.
188. S. M. Castellano and A. A. Bothner-By, J. Chem. Phys. 41 (1964) 3863.
189. C. W. Haigh and J. W. Williams, J. Mol. Spectrosc. 32 (1969) 398.
190. W. J. Hehre, R. F. Stewart, and J. A. Pople, J. Chem. Phys. 51 (1969) 2657.
191. W. J. Hehre, W. A. Lathan, R. Ditchfield, M. D. Newton, and J. A. Pople, Program 236, Quantum Chemistry Program

Exchange, Indiana University, Bloomington, Indiana.

192. J. A. Pople and D. L. Beveridge, *Approximate Molecular Orbital Theory*. (McGraw-Hill, New York, 1970).
193. J. A. Pople and M. Gordon, *J. Am. Chem. Soc.* 89 (1967) 4253.
194. R. Laatikainen., *FINDO*, unpublished. This modification of the QCPE C/INDO program contains numerous options incorporated by Laatikainen. In particular the facility for modifying or neglecting Fock elements throughout the SCF calculations was useful in the present work.
195. J. A. Pople, J. W. McIver, and N. S. Ostlund, *J. Chem. Phys.* 49 (1968) 2960.
196. J. A. Pople, J. W. McIver, and N. S. Ostlund, *J. Chem. Phys.* 49 (1968) 2965.
197. R. Laatikainen, *J. Magn. Reson.* 27 (1977) 169.
198. O. Manscher, K. Schaumburg, and J. P. Jacobsen, *Acta Chem. Scand. A* 35 (1981) 13.
199. M. Hansen and H. J. Jakobsen, *J. Magn. Reson.* 10 (1973) 74.
200. A. W. Douglas and M. Shapiro, *Org. Magn. Reson.* 14 (1980) 38.
201. A. J. Jones, G. A. Jenkins, and M. L. Hefferman, *Aust. J. Chem.* 33 (1980) 1275.
202. R. Freeman, *J. Chem. Phys.* 43 (1965) 3087.

203. J. L. Marshall, D. E. Miller, S. A. Conn, R. Seiwel, and A. M. Ihrig, *Acc. Chem. Res.* 7 (1974) 333.
204. P. E. Hansen, *Progress in NMR Spectroscopy*, Vol. 14 (eds) J. W. Emsley, J. Feeney, and L. H. Sutcliffe (Pergamon Press, Oxford, 1981) 175.
205. J. W. Emsley, L. Phillips, and V. Wray, *Progress in NMR Spectroscopy*, Vol. 10 (eds) J. W. Emsley, J. Feeney, and L. H. Sutcliffe (Pergamon Press, Oxford, 1977) 83; reprinted in: *Fluorine Coupling Constants* (Pergamon Press, Oxford, 1977).
206. R. E. Wasylishen, *Annual Reports on NMR Spectroscopy*, Vol. 7 (ed) G. A. Webb (Academic, London, 1977) 246.
207. P. E. Hansen, A. Berg, H. J. Jakobsen, A. P. Manzara, and J. Michl. *Org. Magn. Reson.* 10 (1977) 179.
208. P. E. Hansen, *Org. Magn. Reson.* 11 (1978) 215.
209. V. Wray, L. Ernst, T. Lund, and H. J. Jakobsen, *J. Magn. Reson.* 40 (1980) 55.
210. S. L. Smith, *Topics Curr. Chem.* 27 (1972) 117.
211. G. C. Levy and I. R. Peat, *J. Magn. Reson.* 18 (1975) 500.
212. J. H. Noggle and R. E. Schirmer, *The Nuclear Overhauser Effect*. (Academic, New York, 1971).
213. I. D. Campbell and R. Freeman, *J. Magn. Reson.* 11 (1973) 143.
214. R. J. Abraham and E. Bretschneider, in: *Internal Rotation*

- in Molecules. (ed) W. J. Orville-Thomas (Wiley and Sons, London, 1974) Chapter 13.
215. P. Laszlo, Progress in NMR Spectroscopy, Vol. 3 (eds) J. W. Emsley, J. Feeney, and L. H. Sutcliffe (Pergamon Press, Oxford, 1967) 231.
216. W. J. Hehre, L. Radom, and J. A. Pople, J. Am. Chem. Soc. 94 (1972) 1496.
217. J. Catalán and M. Yáñez, J. Am. Chem. Soc. 101 (1979) 3490.
218. A. L. McClellan, Tables of Experimental Dipole Moments. (Rahara Enterprises, El Cerrito, CA, 1974).
219. J. S. Binkley, J. A. Pople, and W. J. Hehre, J. Am. Chem. Soc. 102 (1980) 939.
220. T. Schaefer, T. A. Wildman and R. Sebastian, J. Mol. Struct. (Theochem), in press.
221. V. Bachler and G. Olbrich, Theoret. Chim. Acta 57 (1980) 329.
222. Y. K. Lau and P. Kebarle, J. Am. Chem. Soc. 98 (1976) 7452.
223. D. M. Brouwer, E. L. Mackor, and C. Maclean, Rec. Trav. Chim. 85 (1966) 109.
224. D. M. Brouwer, E. L. Mackor, and C. Maclearn, Rec. Trav. Chim. 85 (1966) 114.
225. M. Barfield and D. M. Grant, Advances in Magnetic Resonance, Vol. 1 (ed) J. S. Waugh (Academic, New York, 1965) 149.
226. M. Barfield and M. Karplus, J. Am. Chem. Soc. 91 (1969) 1.

227. H. M. McConnell, *J. Mol. Spectrosc.* 1 (1957) 11.
228. H. Henry and S. Fliszár, *J. Am. Chem. Soc.* 100 (1978) 3312.
229. L. Ernst, V. Wray, V. A. Chertkov, and N. M. Sergeyev, *J. Magn. Reson.* 25 (1977) 123.
230. M. Barfield, *J. Am. Chem. Soc.* 102 (1980) 1.
231. See D. G. Farnum, in: *Advances in Physical Organic Chemistry*, Vol. 11 (eds) V. Gold and D. Bethell (Academic, New York, 1975) 123.
232. D. F. Ewing, in: *Correlation Analysis in Chemistry*. (eds) N. B. Chapman and J. Shorter (Plenum Press, New York, 1978) 357.
233. W. J. Hehre, R. W. Taft, and R. D. Topsom, in: *Progress in Physical Organic Chemistry*, Vol. 12 (ed) R. W. Taft (Wiley-Interscience, New York, 1976) 159.
234. R. A. Fisher and F. Yates, *Statistical Tables for Biological, Agricultural and Medical Research*. 3 ed (Hafner, New York, 1948) 46.
235. L. Ernst, D. N. Lincoln, and V. Wray, *J. Magn. Reson.* 21 (1976) 115.
236. B. Richardson and T. Schaefer, *Can. J. Chem.* 46 (1968) 2195.
237. M. Hansen and H. J. Jakobsen, *J. Magn. Reson.* 20 (1975) 520.
238. J. W. Emsley, *J. Chem. Soc. A* (1968) 1459.
239. E. Lustig, W. B. Moniz, P. Diehl, and B. Bodmer, *J. Chem. Phys.* 49 (1968) 4550.

240. M. I. Bruce, J. Chem. Soc. A. (1968) 1459.
241. R. J. Abraham, D. B. Macdonald, and E. S. Pepper, J. Am. Chem. Soc. 90 (1968) 147.
242. R. J. Abraham, S. C. M. Fell, and K. M. Smith, Org. Magn. Reson. 9 (1977) 367.
243. L. Penn and F. B. Mallory, J. Magn. Reson. 18 (1975) 6.
244. A. D. Buckingham, Can. J. Chem. 38 (1960) 300.
245. R. H. Contreras, A. R. Engelmann, G. E. Scuseria, and F. C. Facelli, Org. Magn. Reson. 13 (1980) 137.
246. J. Bromilow, R. T. C. Brownlee, D. J. Craik, M. Sadek, and R. W. Taft, J. Org. Chem. 45 (1980) 2429.
247. J. L. Marshall, L. G. Faehl, and R. Kattner, Org. Magn. Reson. 12 (1979) 163.
248. J. L. Marshall, L. G. Faehl, R. Kattner, and P. E. Hansen Org. Magn. Reson. 12 (1979) 169.
249. P. E. Hansen, O. K. Poulsen, and A. Berg, Org. Magn. Reson. 12 (1979) 43.
250. F. J. Weigert and J. D. Roberts, J. Am. Chem. Soc. 93 (1971) 2361.
251. N. Muller and D. T. Carr, J. Phys. Chem. 67 (1963) 112.
252. H. S. Gutowsky, G. G. Belford, and P. E. McMahon, J. Chem. Phys. 36 (1962) 3353.
253. J. C. Schug, P. E. McMahon, and H. S. Gutowsky, J. Chem. Phys. 33 (1960) 843.

254. K. G. R. Pachler and P. L. Wessels, *J. Mol. Struct.* 68 (1980) 145.
255. R. L. Lipnick and E. W. Garbisch, Jr., *J. Am. Chem. Soc.* 95 (1973) 6370.
256. G. Govil and H. J. Bernstein, *J. Chem. Phys.* 47 (1967) 2818.
257. C. T. H. Baker, *The Numerical Treatment of Integral Equations* (Oxford University Press, Oxford, 1977).
258. R. Courant and D. Hilbert, *Methods of Mathematical Physics*, Vol. 1 (Interscience, New York, 1953) Chapter III.
259. R. Laatikainen, THERMO, unpublished.
260. G. H. Golub and C. Reinsch, *Numer. Math.* 14 (1970) 403.
261. S. Fliszár, *Can. J. Chem.* 54 (1976) 2839.
262. R. J. Pugmire and D. M. Grant, *J. Am. Chem. Soc.* 90 (1968) 697.
263. P. S. Hubbard, *Phys. Rev.* 131 (1963) 1155.
264. R. A. Bell and J. K. Saunders, *J. Chem. Soc. Chem. Commun.* (1970) 1078.
265. A. Bax, R. Freeman, and S. P. Kempell, *J. Am. Chem. Soc.* 102 (1980) 4849.
266. A. Bax and R. Freeman, *J. Am. Chem. Soc.* 104 (1982) 1099.

Appendix
Minimal Least-Squares Solution of a Fredholm
Integral Equation of the First Kind by
Singular Value Decomposition

The solution of a Fredholm integral equation of the first kind,

$$\int_a^b K(x,y)f(y)dy = g(x) \quad \text{Eq. (A.1)}$$

is somewhat difficult generally due to ill-conditioning in the sense that many solutions may satisfy exactly an equation which is perturbed slightly from the original. Baker provides a thorough discussion of the existence and uniqueness of solutions.

The present work involves the numerical inversion of an equation

$$J(\beta) = \int_a^b p(\beta, \phi)C(\phi)d\phi \quad \text{Eq. (A.2)}$$

$$\text{where } p(\beta, \phi) = \frac{e^{-\beta V(\phi)}}{\int_a^b e^{-\beta V(\phi)} d\phi} \quad \text{Eq. (A.3)}$$

Since $C(\phi)$ and $V(\phi)$ are periodic in 2π and of even parity, $[a,b] = [0,\pi]$ and the function $C(\phi)$ is approximated by the expansion

$$C(\phi) = \sum_{n=0}^N c_n \cos n\phi \quad \text{Eq. (A.4)}$$

Eq. (A.2) then becomes

$$J(\beta) = \sum_{n=0}^N c_n \int_0^\pi p(\beta, \phi) \cos n\phi d\phi \quad \text{Eq. (A.5)}$$

Discretization of β yields algebraic equations

$$\vec{b} = A \vec{c} \quad \text{Eq. (A.6)}$$

where the elements of A are evaluated by simple numerical

quadrature. (A is $M \times N$)

The linear operator A may be decomposed into a singular system $(\vec{u}_i, \vec{v}_i; \sigma_i)$; $\sigma_i > 0$; $i = 1, 2, 3, \dots$ where

$$A^t A \vec{v}_i = \sigma_i^2 \vec{v}_i \quad \text{and} \quad AA^t \vec{u}_i = \sigma_i^2 \vec{u}_i$$

and A^t is the transpose of A. Formally at least,

$$\vec{c} = \sum_{i=1}^{\infty} \frac{\vec{u}_i^t \cdot \vec{b}}{\sigma_i} \vec{v}_i \quad \text{Eq. (A.7)}$$

Practically, very small singular values σ_i correspond to highly oscillatory singular functions, which are to be excluded from a "smooth" solution. To determine a solution in the least-squares sense, without objection to $M \geq N$, minimize the (Euclidean) norm of the residual, namely $\|\vec{r}\|_2$, where

$$\vec{r} = A\vec{c} - \vec{b} \quad \text{Eq. (A.8)}$$

If this solution is not unique, minimize the (Euclidean) norm of the solution also. The result, called the minimal least-squares solution, is accomplished by the operation of the pseudoinverse of A, denoted A^+ , on \vec{b} . If A is square and non-singular $A^+ = A^{-1}$, the inverse, but if $M > N$ the singular value decomposition is

$$A = UV^t \quad \text{Eq. (A.9)}$$

where

$$\Sigma = \begin{bmatrix} \Sigma_0 \\ 0 \end{bmatrix}$$

and Σ_0 is a square, positive semi-definite, diagonal matrix of

singular values, Σ is $M \times N$, and U, V are orthogonal matrices of order M, N respectively. The pseudoinverse of A is

$$A^+ = V\Sigma^+U^t \quad \text{Eq. (10)}$$

where Σ_{ii}^+ is given by $1/\sigma_{ii}$ if $\sigma_{ii} \neq 0$ and by 0 if $\sigma_{ii} = 0$.

Statistical weighting may be included in the procedure, as Baker describes.

Algorithms which accomplish a singular value decomposition and a minimal least-squares solution based on singular value decomposition are provided by Golub and Reinsch. The latter procedure, translated from the original ALGOL60 to FORTRAN IV for the WATFIV compiler of an Amdahl 470/V7, is incorporated in the program INVERSION which is listed below.

The program AVERAGE evaluates classical expectation values for a given algebraic expression over a one-dimensional, periodic potential by simple numerical quadrature. A listing appears below.

Bibliography

- C. T. H. Baker, L. Fox, D. F. Mayers, and K. Wright, *Comput. J.* 7 (1964) 141.
- C. T. H. Baker, *The Numerical Treatment of Integral Equations*. (Clarendon Press, Oxford, 1977).
- G. H. Golub and C. Reinsch, *Numer. Math.* 14 (1970) 403.
- R. J. Hanson, *SIAM J. Numer. Anal.* 8 (1971) 616.
- G. Peters and J. H. Wilkinson, *Comput. J.* 13 (1970) 309.
- J. Todd, *Basic Numerical Mathematics, Vol. 2: Numerical Algebra* (Birkhäuser Verlag, Basel, 1977) Chapter 12.

C I N V E R S I O N - VERSION 5 - MINIMAL LEAST-SQUARES ANALYSIS
C FOR A FREE ENERGY DISTRIBUTION
C A = E - T * S

C A PROGRAM TO INVERT THE TEMPERATURE DEPENDENCE OF THE CLASSICAL
C CANONICAL AVERAGE OF THE ANGLE-DEPENDENT PROXIMATE COUPLING BETWEEN
C TWO NUCLEI, SUCH AS THE METHYL PROTONS AND FLUORINE IN
C 2-FLUOROACETOPHENONE

C INPUT CONSISTS OF

- C 1) TWO CARDS BEARING A TITLE
- C 2) A CARD BEARING THE INTERVAL (A AND B IN DEGREES), THE
C NUMBER OF PARTITIONS DESIRED IN THE NUMERICAL INTEGRATION,
C THE NUMBER OF COMPONENTS IN THE POTENTIAL, AND

C IOP=0 IF THE POTENTIAL IS GIVEN AS A FOURIER
C COSINE SERIES

C =NON-ZERO IF THE POTENTIAL IS GIVEN AS A SERIES
C OF SIN**2 TEP**S

C IENT=0 IF THE BOLTZMANN DISTRIBUTION IS SELECTED
C =1 IF THE FREE ENERGY DISTRIBUTION IS SELECTED

- C 3) ONE CARD FOR EACH COMPONENT OF THE POTENTIAL.
C EACH CARD BEARS THE FOLDEDNESS (SYMMETRY NUMBER) OF THE
C COMPONENT, THE HEIGHT OF THE COMPONENT (KJ/MOLE), AND THE
C PHASE. IF IOP=0 THE PHASE IS USED TO DESIGNATE SINE TERMS.
C 4) ONE CARD FOR EACH TEMPERATURE (K) AND COUPLING CONSTANT (HZ).
C THE LAST OF THESE CARDS SHOULD BEAR A ZERO OR NEGATIVE
C TEMPERATURE

- C 5) A CARD BEARING THE NUMBER OF FUNCTIONS TO BE USED IN THE
C COSINE SERIES EXPANSION OF THE TARGET FUNCTION, THE
C PRECISION REQUIRED FOR CONVERGENCE IN MINFIT (NOT LESS THAN
C 1.0D-15), AND THE MINIMUM AND MAXIMUM NUMBER OF SINGULAR VALUES
C TO BE KEPT AS NOV-ZERO.

C N.B. THE SINGULAR VALUES ARE ORDERED IN MAGNITUDE. SORTING OF
C THE SINGULAR VALUES IS ACCOMPANIED BY REARRANGEMENT OF THE


```

C      COLUMNS OF V, AND OF THE ROWS OF C.
C
C      WRITTEN FOR THE WATFIV COMPILER OF AN AMDAHL 470/V7 BY
C      TIMOTHY A. WILDMAN
C      DEPARTMENT OF CHEMISTRY
C      UNIVERSITY OF MANITOBA
C      THIS PROGRAM WAS LAST REVISED ON JUNE 16, 1982.
C
C      IMPLICIT REAL*8 (A-H,O-Z)
C
C      FOLD - FOLDEDNESS OF COMPONENT OF POTENTIAL
C      VPHI - AMPLITUDE OF COMPONENT
C      PHASE - PHASE OF COMPONENT
C      T - TEMPERATURES
C      CC - MEASURED COUPLING CONSTANTS
C      BETA - RECIPROCAL OF KT IN KJ/MOLE
C      P - MATRIX OF INTEGRALS FOR THE VARIOUS FOURIER COMPONENTS OF THE
C      TARGET FUNCTION EXPANSION
C      V - MATRIX RESULTING FROM MINFIT
C      C - VECTOR RESULTING FROM MINFIT
C      Q - (BOTH V AND C OCCUPY P AFTER MINFIT IS EXECUTED)
C      SIGMA+ - THE PSEUDOINVERSE
C      SIGMAC - THE PRODUCT OF SIGMA+ AND C
C      X - MINIMAL LEAST-SQUARES COEFFICIENTS OF THE TARGET FUNCTION
C      EXPANSION (THE PRODUCT V(SIGMA+)C )
C      E - ERROR VECTOR USED ONLY IN MINFIT BUT INCLUDED HERE TO ENABLE
C      EXECUTION-TIME DIMENSIONING
C
C      DIMENSION FOLD(10),VPHI(10),PHASE(10),T(20),CC(20),BETA(20),
C      & P(20,20),V(20,20),SIGMA(20,20),Q(20),C(20),E(20),SIGMAC(20),X(20)
C      CHARACTER*4 TITLE(40)
C      COMMON/VDATA/FOLD,VPHI,PHASE,NCOMP,IOP
C      COMMON/DATA/ENORM,BETA1,J,IENT
C      EXTERNAL PYORM,PCOS,ANORM

```

```

C
C TO REDIMENSION THIS PROGRAM CHANGE ALL DIMENSIONS AND NDIM
C
NDIM=20
MAXCOM=10
C
C SET CONSTANTS
C
PI=3.141592653589793D0
CONV=PI/180.0000000000000D0
R=8.314300000000000D-3
C
C READ A TITLE FOR THIS RUN
C
1 READ5,(TITLE(I),I=1,18)
5 FORMAT(18A4)
DC 10 I=1,18
IF (TITLE(I).NE.' ') GOTO 15
10 CONTINUE
GOTO 3000
15 READ5,(TITLE(I),I=21,38)
PRINT20,(TITLE(I),I=1,18),(TITLE(I),I=21,38)
20 FORMAT('1'//10X,'INVERSION OF TEMPERATURE DEPENDENCE OF COUPLING C
&ONSTANT'/2(/10X,18A4))
C
C DESCRIPTION OF INTEGRATION INTERVAL, POTENTIAL, AND TYPE OF
C DISTRIBUTION
C
READ,A,B,INTRVL,NCOMP,IOP,IENI
IF (IENT.NE.0) GOTO 22
PRINT21
21 FORMAT(/10X,'BOLTZMANN DISTRIBUTION')
GOTO 24
22 PRINT23
23 FOPMAT(/10X,'A FREE ENERGY DISTRIBUTION: V-T*S')

```

```

24 ARAD=A*CONV
   BRAD=B*CONV
   PRINT5,A,B,INTRVL
25 FORMAT(/10X,'NUMERICAL INTEGRATION ON THE INTERVAL (',F7.2,
   ' ',F7.2,') WITH ',I4,' PARTITIONS')
   IF (NCOMP.LE.MAXCOM) GOTO 30
   PRINT, '*** POTENTIAL HAS TOO MANY COMPONENTS'
   GOTO 3000
30 DO 35 I=1,NCOMP
   READ,FOLD(I),VPHI(I),PHASE(I)
35 CONTINUE
   IF (IOP.NE.0) GOTO 45
   PRINT40
40 FORMAT(/10X,'V(PHI) = V0 + V1*COS(PHI+PS1) + ... + VN*COS(N*PHI+PS
   &N) WHERE PSN = PHASE SHIFT OF THE N-TH COMPONENT')
   GOTO 55
45 PRINT50
50 FORMAT(/10X,'V(PHI) = V1*SIN(PHI/2+PS1)**2 + ... + VN*SIN(N*PHI+PS
   &N)**2 WHERE PSN = PHASE SHIFT OF THE N-TH COMPONENT')
55 PRINT60
60 FORMAT(/10X,'FOLDEDNESS',5X,'V(N) (KJ/MOLE)',5X,'PHASE SHIFT (DEG)
   &/')
   DO 67 I=1,NCOMP
   PRINT65,FOLD(I),VPHI(I),PHASE(I)
65 FORMAT(13X,F4.1,11X,F7.3,14X,F7.2)
   PHASE(I)=PHASE(I)*CONV
67 CONTINUE
C
C INPUT EXPERIMENTAL TEMPERATURE - COUPLING CONSTANT DATA
C
   NUMT=0
70 READ,TI,CCI
   IF (TI.LE.0.0000000000000000) GOTO 75
   NUMT=NUMT+1
   T(NUMT)=TI

```



```

128 CONTINUE
C
C ORDER THE SINGULAR VALUES, AND REARRANGE THE CORRESPONDING
C COLUMNS OF V AND THE ROWS OF C
C
C CALL ORDER(Q,V,C,NUMFCN,NDIM)
C
C PRINT THE RESULTS OF THE SINGULAR VALUE DECOMPOSITION
C
C PRINT115
115 FORMAT(/10X,'ORDERED SINGULAR VALUES'/)
C CALL PRINTV(Q,NUMFCN,1,NDIM)
C PRINT125
125 FORMAT(/10X,'CORRESPONDING MATRIX V')
C CALL PRINT(V,NUMFCN,NUMFCN,1,NDIM,NDIM)
C PRINT116
116 FORMAT(/10X,'COEFFICIENTS C'/)
C CALL PRINTV(C,NUMFCN,1,NDIM)
C DO 140 I=NMIN,NMAX
C
C FORM THE PSEUDOINVERSE OF Q (SIGMA+), KEEPING ONLY THE I LARGEST
C SINGULAR VALUES
C
C CALL PSINVR(Q,SIGMA,I,NUMFCN,NDIM)
C PRINT130,I
130 FORMAT(/10X,'THE ',I2,' LARGEST SINGULAR VALUES ARE KEPT. ALL ',
6 'OTHER DIAGONAL ELEMENTS ARE SET AT ZERO.'/10X,'THE PSEUDOINVERSE
6 (SIGMA+) IS')
C CALL PRINT(SIGMA,NUMFCN,NUMFCN,1,NDIM,NDIM)
C
C FORM THE MINIMAL LEAST-SQUARES SOLUTION
C
C CALL PROD(SIGMA,NUMFCN,NUMFCN,NUMFCN,C,SIGMAC,NDIV)
C CALL PROD(V,NUMFCN,NUMFCN,SIGMAC,X,NDIM)
C PRINT135

```

```

135 FORMAT(/10X,'MINIMAL LEAST-SQUARES COEFFICIENTS'/)
CALL PRINTV(X,NUMFCN,1,NDIM)
140 CONTINUE
    GOTO 1
3000 PRINT3001
3001 FORMAT('10')
STOP
END
SUBROUTINE TRAP(INTRVL,A,B,F,RINTGL)
C
C TRAP APPROXIMATES THE INTEGRAL OF A FUNCTION, F,
C ON THE INTERVAL (A, B) BY A SERIES OF TRAPEZOIDS.
C
    IMPLICIT REAL*8 (A-H,O-Z)
    SUM=0.0D0
    X=A
    DX=(B-A)/INTRVL
    IN=INTRVL-1
    DO 10 I=1,IN
        X=X+DX
        FX=F(X)
        IF (DABS(FX).LT.1.0D-70) GOTO 10
        SUM=SUM+FX*DX
10 CONTINUE
    RINTGL=SUM+(F(A)+F(B))*DX/2.0D0
    RETURN
    END
DOUBLE PRECISION FUNCTION PNORM(X)
C
C PNORM IS THE PROBABILITY DISTRIBUTION
C
    IMPLICIT REAL*8 (A-H,O-Z)

```

```

COMMON/DATA/ENORM,BETAI,J,IENT
THIS IS AN ATTEMPT TO AVOID AN EXPONENT UNDERFLOW.
EXP=POTENT(X)*BETAI
IF (EXP.GE.180.0D0) GOTO 5
PNORM=DEXP(-EXP)
RETURN
5 PNORM=0.0D0
RETURN
END
DOUBLE PRECISION FUNCTION ANORM(X)
ANORM IS THE POPULATION DISTRIBUTION FROM THE FREE ENERGY
IMPLICIT REAL*8 (A-H,O-Z)
COMMON/DATA/ENORM,BETAI,J,IENT
P=ENORM(X)
IF THE FREE ENERGY DISTRIBUTION WAS SELECTED, INCLUDE THE ENTROPY
IF (IENT.EQ.1) GOTO 1
ANORM=P
RETURN
1 PROB=P/ENORM
EXP IS ALWAYS POSITIVE OR ZERO SINCE PROB IS NEVER GREATER THAN
UNITY
EXPS=-PROB*DLOG(PROB)
THIS IS AN ATTEMPT TO AVOID AN EXPONENT UNDERFLOW
IF (EXPS.GE.180.0D0) GOTO 5
ANORM=P*DEXP(EXPS)

```

C
C
CC
C
CC
C
CC
C
C
CC
C
C


```

RETURN
5 ANORM=0.0D0
RETURN
END
DOUBLE PRECISION FUNCTION PCOS(X)
C
C PCOS IS THE FREE ENERGY-WEIGHTED DISTRIBUTION OF COSINE
C
IMPLICIT REAL*8 (A-H,O-Z)
COMMON/DATA/ENORM,BETA1,J,IENT
DNORM=ANORM(X)
DEN=PNORM(X)
IF (DEN.EQ.0.000000000000000D0) GOTO 1
COS=DCOS(DFLOAT(J)*X)
C
C THIS IS AN ATTEMPT TO AVOID AN EXPONENT UNDERFLOW ON MULTIPLICATION.
C THIS DIVISION IS POSSIBLE SINCE DEN IS NEVER GREATER THAN UNITY.
C THE DENOMINATOR SHOULD BE ANORM, BUT ANORM IS NEVER LESS THAN PNORM.
C USING PNORM WILL SET ZERO SOME SMALL PRODUCTS WHICH WILL NOT
C UNDERFLOW AT THE MULTIPLICATION.
C
COSMIN=0.6D-78/DEN
IF (COS.GT.COSMIN) GOTO 2
1 PCOS=0.000000000000000D0
RETURN
C
IF UNDERFLOW WILL NOT OCCUR, PERFORM THE MULTIPLICATION.
C
2 PCOS=COS*DNORM
RETURN
END
DOUBLE PRECISION FUNCTION POTENT(X)
C
C POTENT IS THE POTENTIAL ENERGY EXPRESSION
C

```

```

C
C
C
      IMPLICIT REAL*8 (A-H,O-Z)
      DIMENSION FOLD(10),V(10),PHASE(10)
      COMMON/VDATA/FOLD,V,PHASE,NCOMP,IOP
      IF (IOP.NE.0) GOTO 20

      THE FOURIER SERIES HAS BEEN CHOSEN
C
      POTENT=0.0D0
      DO 10 I=1,NCOMP
      POTENT=POTENT+V(I)*DCOS(FOLD(I)*X+PHASE(I))
10 CONTINUE
      RETURN
C
      THE SIN**2 SERIES HAS BEEN CHOSEN
C
      20 POTENT=0.0D0
      DO 30 I=1,NCOMP
      POTENT=POTENT+V(I)*DSIN(FOLD(I)*X+PHASE(I))**2
30 CONTINUE
      RETURN
      END
      SUBROUTINE PRINT(A,NR,NC,IJK,NDIMR,NDIMC)
C
C
C
      THIS ROUTINE PRINTS A MATRIX IN BLOCKS OF TEN COLUMNS
C
      IMPLICIT REAL*8 (A-H,O-Z)
      DIMENSION A(NDIMR,NDIMC)
      NCT=NC/10
      NCTP1=NCT+1
      NCU=NC-VCT*10
      K=10
      DO 35 I=1,NCTP1
      IF (I.LT.NCTP1) GOTO 5
      K=NCU
      IF (K.EQ.0) GOTO 35

```

```

5 ITEN=(I-1)*10+IJK+1
  ITENPK=ITEN+K-1
C
C L-1 IS THE COLUMN INDEX. IT BEGINS AT ZERO IF IJK IS ZERO,
C AT ONE IF IJK IS UNITY, AND IT IS NOT PRINTED IF IJK IS NEGATIVE
C
  IF (IJK.LT.0) GOTO 15
  PRINT10,(L-1,L=ITEN,ITENPK)
10 FORMAT(/2X,10(9X,I3))
  L=ITEN-IJK
  M=ITENPK-IJK
C
C IF IJK IS NON-NEGATIVE, JPIJK IS THE ROW INDEX.
C IF IJK IS NEGATIVE, J IS THE ROW INDEX.
C
15 DO 30 J=1, NR
C
C IF IJK IS LESS THAN ZERO, A VECTOR IS TO BE PRINTED WITHOUT
C PRINTING A COLUMN INDEX
C
  IF (IJK.LT.0) GOTO 25
  JPIJK=J+IJK-1
  PRINT2J,JPIJK,(A(J,N),N=L,M)
20 FORMAT(' ',I4,3X,10(D11.4,1X))
  GOTO 30
25 PRINT22,J,A(J,1)
22 FOKMAT(' ',I4,3X,D15.8)
30 CONTINUE
35 CONTINUE
  RETURN
  END
  SUBROUTINE PRINTV(A,NR,IJK,NDIMR)
C
C THIS ROUTINE PRINTS A COLUMN VECTOR
C

```



```

DO 90 J=L,N
E(J)=A3(I,J)/H
90 CONTINUE
DO 120 J=L,M
S=0.0000000000000000
DO 100 K=L,N
S=S+AB(J,K)*AB(I,K)
100 CONTINUE
DO 110 K=L,N
AB(J,K)=AB(J,K)+S*E(K)
110 CONTINUE
120 CONTINUE
GOTO 140
130 G=0.0000000000000000
140 Y=DABS(Q(I))+DABS(F(I))
IF (Y>.1) X=Y
150 CONTINUE
C
C ACCUMULATION OF RIGHT-HAND TRANSFORMATIONS
C
DO 210 II=1,N
I=N+1-I
IF (G>.5) G=0.0000000000000000 GOTO 195
H=AB(I,I+1)*G
DO 160 J=L,N
AB(J,I)=AB(I,J)/H
160 CONTINUE
DO 190 J=L,N
S=0.0000000000000000
DO 170 K=L,N
S=S+AB(I,K)*AB(K,J)
170 CONTINUE
DO 180 K=L,N
AB(K,J)=AB(K,J)+S*AE(K,I)
180 CONTINUE

```



```

290 FG=F-G
300 F=((X-Z)*(X+Z)+H*(Y/FG-H))/X
C
C NEXT OF TRANSFORMATION
C
C=1.00000000000000000000
S=1.00000000000000000000
LP1=L+1
DO 330 I=LP1,K
G=E(I)
Y=Q(I)
H=S*G
G=C*G
IM1=I-1
E(IM1)=DSQRT(F*F+H*H)
Z=E(IM1)
C=F/Z
S=H/Z
F=X*C+3*S
G=-X*S+G*C
H=Y*S
Y=Y*C
DO 310 J=1,N
X=AB(J,IM1)
Z=AB(J,I)
AB(J,IM1)=X*C+Z*S
AB(J,I)=-X*S+Z*C
310 CONTINUE
Q(IM1)=DSQRT(F*F+H*H)
Z=Q(IM1)
C=F/Z
S=H/Z
F=C*G+S*Y
X=-S*G+C*Y
DO 320 J=N1,NP

```

```

Y=AB(IM1,J)
Z=AB(I,J)
AB(IM1,J)=C*Y+S*Z
AB(I,J)=-S*Y+C*Z
320 CONTINUE
330 CONTINUE
E(L)=0.0000000000000000
E(K)=F
Q(K)=X
GOTO 235
C
C CONVERGENCE
C Q(K) IS MADE NON-NEGATIVE
C
340 IF (Z.3E-0.0000000000000000) GOTO 360
Q(K)=-Z
DO 350 J=1,N
AB(J,K)=-AB(J,K)
350 CONTINUE
360 CONTINUE
RETURN
END
SUBROUTINE ORDER(Q,V,C,N,NDIM)
C
C THIS ROUTINE PLACES THE SINGULAR VALUES IN DECREASING ORDER
C OF MAGNITUDE, REARRANGES THE CORRESPONDING COLUMNS OF V, AND
C REARRANGES THE CORRESPONDING ROWS OF C.
C
IMPLICIT REAL*8 (A-H,O-Z)
DIMENSION Q(NDIM),V(NDIM,NDIM),C(NDIM)
DO 15 I=1,N
QMAX=Q(I)
JMAX=I
DO 5 J=I,N
IF (Q(J).LE.QMAX) GOTO 5

```

```

QMAX=Q(J)
JMAX=J
5 CONTINUE
IF (JMAX.EQ.I) GOTO 15
Q(JMAX)=Q(I)
Q(I)=QMAX
DO 10 K=1,N
TEMP=V(K,I)
V(K,I)=V(K,JMAX)
V(K,JMAX)=TEMP
10 CONTINUE
TEMP=C(I)
C(I)=C(JMAX)
C(JMAX)=TEMP
15 CONTINUE
RETURN
END
SUBROUTINE PSINVR(Q,SIGMA,NVAL,N,NDIM)
C
C THIS ROUTINE FORMS THE PSEUDOINVERSE OF SIGMA
C
C IMPLICIT REAL*8 (A-H,O-Z)
C DIMENSION Q(NDIM),SIGMA(NDIM,NDIM)
C
C ZERO SIGMA INITIALLY
C
C DO 2 I=1,NDIM
C DO 1 J=1,NDIM
C SIGMA(I,J)=0.00000000000000000000
1 CONTINUE
2 CONTINUE
C
C FORM THE PSEUDOINVERSE
C
C DO 3 I=1,NVAL

```

```

IF (Q(I).EQ.0.0000000000000000) GOTO 3
SIGMA(I,I)=1.0000000000000000/Q(I)
3 CONTINUE
RETURN
END
SUBROUTINE PROD(A,M,N,X,C,NDIM)
C THIS ROUTINE FORMS THE PRODUCT OF MATRIX A AND COLUMN VECTOR X
C AND RETURNS IT IN COLUMN VECTOR C
C
C IMPLICIT REAL*3 (A-H,O-Z)
C DIMENSION A(NDIM,NDIM),X(NDIM),C(NDIM)
C DO 10 I=1,M
C C(I)=0.0000000000000000
C DO 5 J=1,N
C C(I)=C(I)+A(I,J)*X(J)
5 CONTINUE
10 CONTINUE
RETURN
END

```



```

C BE USED TO VARY THE ABSOLUTE TEMPERATURE
C RUNS MAY BE STACKED. THE LAST CARD OF THE DECK MUST BE BLANK
C
C IMPLICIT REAL*8 (A-H,O-Z)
C
C AVG, SQR, PNORM, AND ANORM ARE FUNCTIONS.
C AVG IS THE INTEGRAND IN THE AVERAGE, THAT IS, THE VARIABLE
C MULTIPLIED BY THE DISTRIBUTION FUNCTION.
C SQR IS THE INTEGRAND IN THE AVERAGE SQUARE OF THE VARIABLE.
C PNORM IS THE BOLTZMANN DISTRIBUTION.
C ANORM IS THE FREE ENERGY DISTRIBUTION.
C
C EXTERNAL AVG,SQR,PNORM,ANORM
C DIMENSION V(10),VMIN(10),VMAX(10),VINC(10),FOLD(10),PHASE(10)
C CHARACTER*4 TITLE(40)
C COMMON/DATA/CONV,BETA,ENORM,IENT
C COMMON/VDATA/V,PHASE,FOLD,MAXCOM,IOP
C MAXCOM=10
C CONV=3.141592653589793D0/180.0D0
C
C CALCULATIONS ARE PERFORMED IN KILOJOULES/MOLE
C
C R=8.3143D-3
C
C READ AND PRINT A TITLE
C
1 READ11,(TITLE(I),I=1,18)
11 FORMAT(18A4)
DO 12 I=1,18
IF (TITLE(I).NE.' ') GOTO 13
12 CONTINUE
GOTO 30
13 READ11,(TITLE(I),I=21,38)
PRINT50
50 FORMAT('1'//10X,'CLASSICAL EXPECTATION VALUES'/+0,9X,28(' _ '))

```

```

C
C
C
C
C
PRINT2,(TITLE(I),I=1,18),(TITLE(I),I=21,38)
2  FORMAT(/2(/25X,18A4))
C
C
C
C
C
READ THE INTERVAL, THE NUMBER OF PARTITIONS, THE NUMBER OF
COMPONENTS IN THE POTENTIAL, THE FORM OF THE POTENTIAL, AND
THE TYPE OF DISTRIBUTION DESIRED.
READ,A,B,INTRVL,NUMFCN,IOP,IENT
IF (IENT.EQ.1) GOTO 8
PRINT7
7  FORMAT(/10X,'BOLTZMANN DISTRIBUTION')
GOTO 6
8  PRINT9
9  FORMAT(/10X,'FREE ENERGY DISTRIBUTION')
6  IF (IOP.EQ.1) GOTO 106
PRINT10,A,B,INTRVL
10  FORMAT(/10X,'NUMERICAL INTEGRATION ON THE INTERVAL (',
& F7.2,' ',F7.2,') (IN DEGREES) WITH ',I5,' PARTITIONS'
& //10X,'V(PHI) = V0 + V1*COS(PHI) + . . . + VN*COS(N*PHI)')
GOTO 21
106 PRINT22,A,B,INTRVL
22  FORMAT(/10X,'NUMERICAL INTEGRATION ON THE INTERVAL (',
& F7.2,' ',F7.2,') (IN DEGREES) WITH ',I5,' PARTITIONS'
& //10X,'V(PHI) = V0 + V1*SIN(PHI/2+PS1)**2 + . . . + VN*SIN(N*PHI
&+PSN)**2 WHERE PSN = PHASE SHIFT OF THE N-TH COMPONENT')
21  DO 18 I=1,MAXCOM
FOLD(I)=C.0D0
PHASE(I)=0.0D0
V(I)=0.0D0
VMIN(I)=0.0D0
VMAX(I)=0.0D0
VINC(I)=1.0D0
18  CONTINUE
C
C
C
C
C
READ THE SYMMETRY NUMBER OF THE COMPONENT, THE MINIMUM, THE MAXIMUM

```

```

C AND THE INCREMENT TO BE USED
C
DO 19 N=1,NUMFCN
  READ,FOLD(N),PHASE(N),VMIN(N),VMAX(N),VINC(N)
19 CONTINUE
  PRINT33,(PHASE(N),N=1,NUMFCN)
33 FORMAT(/4X,PHASE SHIFT (DEG) =/4X,10(1X,F7.2))
  PRINT14,(FOLD(I),I=1,NUMFCN)
14 FORMAT(/42X,V(N) (KJ/MOLE),,37X,T (K),,1X,EX EXPECTATION,,
& 5X,RMS/+,+,4X,80(,_,)/5X,N= ,10(F4.1,4X))
  PRINT17
17 FORMAT(,+,+,101X,VALUE,5X,DEVIATION/)

C
C READ THE MINIMUM, THE MAXIMUM, AND THE INCREMENT OF THE ABSOLUTE
C TEMPERATURE
C
  READ,TMIN,TMAX,TINC
  T=TMIN-TINC
60 T=T+TINC
  IF (T.3T.TMAX) GOTO 1
  BETA=1.0D0/(R*T)
  V(10)=VMIN(10)-VINC(10)
61 V(10)=V(10)+VINC(10)
  IF (V(10).GT.VMAX(10)) GOTO 60
  V(9)=VMIN(9)-VINC(9)
62 V(9)=V(9)+VINC(9)
  IF (V(9).GT.VMAX(9)) GOTO 61
  V(8)=VMIN(8)-VINC(8)
63 V(8)=V(8)+VINC(8)
  IF (V(8).GT.VMAX(8)) GOTO 62
  V(7)=VMIN(7)-VINC(7)
64 V(7)=V(7)+VINC(7)
  IF (V(7).GT.VMAX(7)) GOTO 63
  V(6)=VMIN(6)-VINC(6)
65 V(6)=V(6)+VINC(6)

```



```

IF (V(6).GT.VMAX(6)) GOTO 64
V(5)=VMIN(5)-VINC(5)
66 V(5)=V(5)+VINC(5)
IF (V(5).GT.VMAX(5)) GOTO 65
V(4)=VMIN(4)-VINC(4)
67 V(4)=V(4)+VINC(4)
IF (V(4).GT.VMAX(4)) GOTO 66
V(3)=VMIN(3)-VINC(3)
68 V(3)=V(3)+VINC(3)
IF (V(3).GT.VMAX(3)) GOTO 67
V(2)=VMIN(2)-VINC(2)
69 V(2)=V(2)+VINC(2)
IF (V(2).GT.VMAX(2)) GOTO 63
V(1)=VMIN(1)-VINC(1)
70 V(1)=V(1)+VINC(1)
IF (V(1).GT.VMAX(1)) GOTO 69

C
C CALCULATE THE NORM OF THE PROBABILITY DISTRIBUTION
C
CALL TRAP(INTRVL,A,B,PNORM,ENORM)
C
C CALCULATE THE AVERAGE
C
CALL TRAP(INTRVL,A,B,AVG,FAVG)
C
C CALCULATE THE NORM OF THE FREE ENERGY DISTRIBUTION
C
CALL TRAP(INTRVL,A,B,ANORM,FNORM)
EXPECT=FAVG/FNORM
C
C CALCULATE THE AVERAGE SQUARE
C
CALL TRAP(INTRVL,A,B,SQR,FSQR)
EXSQP=FSQR/FNORM
C

```

```

C      CALCULATE THE RMS DEVIATION OF THE AVERAGE
C
      DIFF=EXSOR-EXPECT**2
      IF (DIFF.LT.0.000) GOTO 31
      RMS=DSQRT(DIFF)
C
C      PRINT THE RESULTS
C
      PRINT24,(V(N),N=1,MAXCOM),T,EXPECT,RMS
      FORMAT(' ',4X,10(1X,F7.3),5X,F8.2,1X,F8.3,5X,F8.3)
      GOTO 70
31 PRINT32,(V(N),N=1,MAXCOM),T,EXPECT
32 FORMAT(' ',4X,10(1X,F7.3),5X,F8.2,1X,F8.3,5X, ' ? ')
      GOTO 70
30 PRINT16
16 FORMAT('10')
      STOP
      END
C      DOUBLE PRECISION FUNCTION POTENT(X)
C      POTENT IS THE POTENTIAL ENERGY EXPRESSION
C
      IMPLICIT REAL*8 (A-H,O-Z)
      DIMENSION V(10),FOLD(10),PHASE(10)
      COMMON/DATA/CONV,BETA,ENORM,IENT
      COMMON/VDATA/V,PHASE,FOLD,MAXCOM,IOP
      IF (IOP.EQ.1) GOTO 20
      POTENT=0.000
      DO 10 I=1,MAXCOM
      POTENT=POTENT+V(I)*DCOS(FOLD(I))*X*CONV)
10 CONTINUE
      RETURN
20 POTENT=0.000
      DO 30 I=1,MAXCOM
      POTENT=POTENT+V(I)*DSIN((FOLD(I)*X+PHASE(I))*CONV)**2

```

```

30 CONTINUE
RETURN
END
DOUBLE PRECISION FUNCTION PARAM(X)
C
C   PARAM IS THE PARAMETER OR EXPRESSION WHICH IS TO BE AVERAGED.
C
    IMPLICIT REAL*8 (A-H,O-Z)
    COMMON/DATA/CONV,BETA,ENORM,IENT
    PHI=X*CONV
C*****
    PARAM=DCOS(PHI)
C*****
RETURN
END
DOUBLE PRECISION FUNCTION AVG(X)
C
C   AVG IS THE INTEGRAND IN THE AVERAGE, THAT IS, THE VARIABLE
C   MULTIPLIED BY THE DISTRIBUTION FUNCTION.
C
    IMPLICIT REAL*8 (A-H,O-Z)
C
C   POTENT IS THE POTENTIAL ENERGY FUNCTION AND PARAM IS THE
C   EXPRESSION TO BE AVERAGED.
C
    COMMON/DATA/CONV,BETA,ENORM,IENT
C
C   THIS IS AN ATTEMPT TO AVOID AN EXPONENT UNDERFLOW.
C
    VAR=PARAM(X)
    BOLTZ=ANORM(X)
    IF (VAR.EQ.0.0D0) GOTO 5
    EXPMIN=DABS(1.0D-70/VAR)
    IF (BOLTZ.LT.EXPMIN) GOTO 5
    AVG=VAR*BOLTZ

```

```

RETURN
5  AVG=0.000
RETURN
END
DOUBLE PRECISION FUNCTION PNORM(X)
C
C  PNORM IS THE DISTRIBUTION FUNCTION FOR THE VARIABLE.
C
IMPLICIT REAL*8 (A-H,O-Z)
COMMON/DATA/CONV,BETA,ENORM,IENT
C
C  THIS IS AN ATTEMPT TO AVOID AN EXPONENT UNDERFLOW.
C
EXP=POTENT(X)*BETA
IF (EXP.GE.180.000) GOTO 5
PNORM=DEXP(-EXP)
RETURN
5  PNORM=0.000
RETURN
END
DOUBLE PRECISION FUNCTION ANORM(X)
C
C  ANORM IS THE POPULATION DISTRIBUTION FROM THE FREE ENERGY
C
IMPLICIT REAL*8 (A-H,O-Z)
COMMON/DATA/CONV,BETA,ENORM,IENT
P=PNORM(X)
IF (IENT.EQ.1) GOTO 1
ANORM=P
RETURN
1  PROB=P/ENORM
EXPS=-PROB*DLOG(PROB)
C
C  THIS IS AN ATTEMPT TO AVOID AN EXPONENT UNDERFLOW
C

```

```

IF (EXPS.GE.180.000) GOTO 5
ANORM=P*DEXP(EXPS)
RETURN
5 ANORM=0.000
RETURN
END
DOUBLE PRECISION FUNCTION SQR(X)
C
C SQR IS THE INTEGRAND IN THE AVERAGE SQUARE OF THE VARIABLE.
C
C IMPLICIT REAL*8 (A-H,O-Z)
C
C POTENT IS THE POTENTIAL ENERGY FUNCTION AND PARAM IS THE
C EXPRESSION TO BE AVERAGED.
C
COMMON/DATA/CONV,BETA,ENORM,IENT
C
C THIS IS AN ATTEMPT TO AVOID AN EXPONENT UNDERFLOW.
C
PARAM=PARAM(X)
IF (DABS(PARAM).LE.1.0D-38) GOTO 5
VAR=PARAM**2
BOLTZ=ANORM(X)
IF (VAR.EQ.0.000) GOTO 5
EXPMIN=DABS(1.0D-70/VAR)
IF (BOLTZ.LT.EXPMIN) GOTO 5
SQR=VAR*BOLTZ
RETURN
5 SQR=0.000
RETURN
END
SUBROUTINE TRAP(INTRVL,A,B,F,RINTGL)
C
C TRAP APPROXIMATES THE INTEGRAL OF A FUNCTION, F,
C ON THE INTERVAL (A, B) BY A SERIES OF TRAPEZOIDS.

```

```

C
  IMPLICIT REAL*8 (A-H,O-Z)
  SUM=0.0D0
  X=A
  DX=(B-A)/INTRVL
  IN=INTRVL-1
  DO 10 I=1,IN
    X=X+DX
    FX=F(X)
  C
  C THIS IS AN ATTEMPT TO AVOID AN EXPONENT UNDERFLOW ON MULTIPLICATION.
  C
  IF (DABS(FX).LT.1.0D-70) GOTO 10
  SUM=SUM+FX*DX
  10 CONTINUE
  RINTGL=SUM+(F(A)+F(B))*DX/2.0D0
  RETURN
  END

```

The Moving Finger writes; and, having writ,
Moves on: nor all thy Piety nor Wit
Shall lure it back to cancel half a Line,
Nor all thy Tears wash out a Word of it.

Edward Fitzgerald,
Rubāiyāt of Omar Khayyām
of Naishapur

Hell is truth seen too late.

H. G. Adams